Title

Essays on Cropping Choice, Carbon Sequestration, and the Productivity of Saskatchewan Farms

Permalink

https://escholarship.org/uc/item/3rz4n845

Author

Serfas, Devin Allen

Publication Date

2024

Peer reviewed|Thesis/dissertation

Essays on Cropping Choice, Carbon Sequestration, and the Productivity of Saskatchewan Farms

By

Devin Serfas
DISSERTATION

Submitted in partial satisfaction of the requirements for the degree of

DOCTOR OF PHILOSOPHY

in

Agricultural and Resource Economics

in the

OFFICE OF GRADUATE STUDIES

of the

UNIVERSITY OF CALIFORNIA

DAVIS

Approved:

_____

Julian Alston, Chair

_____

Richard Gray

_____

Aaron Smith

_____

Pierre Mérel

Committee in Charge

2024

i

Dissertation Abstract

In the face of escalating global climate change, the need to mitigate greenhouse gas emissions has never been more pressing. Agriculture is a major source of greenhouse gas emissions, but is also gaining recognition for its potential role to reduce atmospheric carbon dioxide by sequestering carbon in the soil. A recent French initiative called 4 per mille states that if farmers were to increase soil organic carbon (SOC) on their fields by 0.4% per year, that would be enough to offset all annual anthropogenic greenhouse gas emissions and stop further increases in atmospheric carbon dioxide. This initiative highlights that only a small percentage increase in SOC over a large area of land can yield substantial environmental benefits.

Government and industry stakeholders are beginning to recognize the potential for SOC, and are in the early stages of developing carbon markets for SOC. But there are still important scientific and economic questions to be answered. These questions call for further research on how to accurately measure SOC, understand soil capacity for additional carbon sequestration, and how different farm management practices affect SOC and what their associated private and public benefits are. The topic of carbon markets has garnered significant attention due to recent government initiatives promoting climate-smart agriculture and private investment in carbon offset programs. In this dissertation, I bridge the gap between research conducted by soil scientists, who focus on modeling and sampling techniques to better measure SOC, and the work of economists, who concentrate on policy design and the valuation of environmental benefits. My methodology addresses the challenges of accurately measuring soil carbon and examines how these models can be used to inform policy design and efforts to establish sustainable carbon markets in agriculture.

This dissertation examines, in three chapters, the relationship between carbon sequestration, farm management practices, and agri-environmental policy. I analyze the private and public benefits from carbon sequestration on farms in Saskatchewan from 1998 to 2019. To do this, I employ a novel field-level dataset from the Saskatchewan Crop Insurance Corporation (SCIC) that includes

detailed information for each field in Saskatchewan: cropping choice, yield, fertilizer use, crop insurance coverage, and the number of seeded hectares.

In Chapter 1, I develop a novel SOC prediction model that builds on the existing models developed specifically for Saskatchewan soils. I examine the case of carbon sequestration in the Saskatchewan prairies, which have experienced substantial increases in SOC over the past 30 years. I use several SOC prediction models to simulate the stock of SOC on fields over time and compare the results. I then compute the external social benefit from carbon sequestration on all insurable hectares by simulating various counterfactual scenarios in which 25%, 50%, and 75% of canola hectares are replaced by summer fallow, representing a reversion to tillage-based systems, and using various values for the social cost of carbon (SCC) ranging from 14 USD/Mg to 185 USD/Mg. During the period 1998–2019, this external social benefit ranges from 481 million to 6 billion USD. Projecting average carbon inputs 150 years into the future yields an estimated external social benefit ranging from 851 million to 30.2 billion USD for the same counterfactual comparisons.

In Chapter 2, I use the SOC data simulated in Chapter 1 to determine the effects of increased SOC stocks on crop yield, productivity, and on-farm profit. I use a dynamic panel regression to estimate the shadow value of SOC and find that increased SOC stocks have a statistically significant and a positive affect on crop yields. Performing dynamic simulations, I compute the on-farm and external social benefits from carbon sequestration that are attributed to selecting a particular crop rotation, and compare these benefits across rotations. I find that adoption of the Canola-Spring Wheat-Peas-Spring Wheat crop rotation leads to a 27.5%, 8.2%, and 4.4% increase in long-term average profit in the brown, dark brown, and black & gray soil zones attributable to increased SOC over 32 years. On-farm benefits from increased SOC are lower for crop rotations with lower carbon sequestering capabilities, highlighting the long-term effects on farm profitability and productivity from selecting particular crop rotations. I compute the external social benefit from the adoption of Canola-Spring Wheat-Peas-Spring Wheat rotation relative to Spring Wheat-Fallow-Spring Wheat-Fallow on all insurable hectares in Saskatchewan from 2023 to 2055, and find benefits amounting to 108 billion CAD when employing a SCC of 185 USD/Mg. I find that the external social benefits

from crop rotations that include canola rather than pulses or fallow are greater than the associated private benefits. Hence, selecting crop rotations that have greater SOC sequestration potential not only improves on-farm profitability over time, but also generates sizable environmental benefits.

In Chapter 3, I assess the effectiveness of second-best policies aimed at increasing the stock of SOC by examining a hypothetical policy that subsidizes additional canola hectares differently for each soil zone in Saskatchewan. To analyze the effect of these subsidies, I develop a simulation model that includes on-farm acreage responses and a SOC state equation to measure changes in SOC stocks due to alterations in land-use. I find that a policy offering optimal subsidies specific to each soil zone for additional hectares of canola, implemented in 2019 and continuing indefinitely for all insured fields in Saskatchewan, generates an external social benefit worth 15.2 billion CAD when the subsidy is set to maximize the net external social benefit (NESB), and 30.4 billion CAD when it is set to maximize the change in total welfare. These benefits are calculated using acreage responses estimated by a nested logit model with field-level data from the SCIC, and an annual carbon rental rate computed using a SCC of 185 USD/Mg. The NESB is the public benefit from carbon sequestered by increasing canola hectares minus policy costs, while the change in welfare is the NESB plus the change in producer surplus. This chapter quantifies the potential environmental and social benefits from implementing second-best policies that aim to increase SOC stocks by subsidizing changes in cropping choices.

Acknowledgements

Contents

List of Figures

List of Tables

xiv

List of Abbreviations

AAFC	**A**griculture and **A**gri-**F**ood **C**anada
BE	**B**ellman **E**quation
CAD	**Ca**nadian **D**ollars
CD	**C**rop **D**istrict
C.I.	**C**onfidence **I**nterval
CSP	**C**onservation **S**tewardship **P**rogram
DGP	**D**ata **G**enerating **P**rocess
DICE	**D**ynamic **I**ntegrated **C**limate and **E**conomy
EQIP	**E**nvironmental **Q**uality **I**ncentives **P**rogram
ERP	**E**missions **R**eduction **P**lan
ESB	**E**xternal **S**ocial **B**enefit
FAO	**F**ood and **A**gricultural **O**rganization
FUND	Climate **F**amework for **U**ncertainty, **N**egotiation, and **D**istribution
GHG	**G**reen**h**ouse **G**as
GSAT	**G**rowing **S**eason **A**verage **T**emperature
HI	**H**arvest **I**ndex
IAM	**I**ntegrated **A**ssessment **M**odel
ICBM	**I**ntroductory **C**arbon **B**alance **M**odel
IIA	**I**ndependence of **I**rrelevant **A**lternatives
IIC	**I**ndependence of **I**rrelevant **C**rops
IIN	**I**ndependence of **I**rrelevant **N**ests
IPCC	**I**ntergovernmental **P**anel on **C**limate Change
IRA	**I**nflation **R**eduction Act

IWG	Interagency Working Group on the Social Cost of Greenhouse Gases
MNL	Multinomial Logit
NESB	Net External Social Benefit
NL	Nested Logit
NRCS	Natural Resource Conservation Service
PAGE	Policy Analysis of the Greenhouse Gas Effect
PBCI	Plant Biomass Carbon Input
PESB	Perpetual External Social Benefit
PET	Potential Evapotranspiration
PSCB	Pairie Soil Carbon Balance
ODE	Ordinary Differential Equation
OLS	Ordinary Least Squares
OFCAF	On-Farm Climate Action Fund
O.V.B.	Omitted Variable Bias
RM	Rural Municipality
RMSE	Root Mean Squared Error
SCC	Social Cost of Carbon
SCIC	Saskatchewan Crop Insurance Corporation
SCSOC	Social Cost of Soil Organic Carbon
SOC	Soil Organic Carbon
SMP	Sask Management of Plus
SPARC	Semi-Arid Prairie Aagricultural Research Center
SSP	Shared Socioeconomic Pathway
TAP	Total Annual Precipitation
TMSD	Topsoil Moisture Deficit
UNFCCC	United Nations Framework Convention on Climate Change
USD	United States Dollars
USDA	United States Department of Agriculture

WoSIS   **W**orld **S**oil Information **Service**

WWF   **W**orld **W**ildlife **F**und

"Global warming is the most significant of all environmental externalities. It menaces our planet and looms over our future like a Colossus. It is particularly pernicious because it involves so many activities of daily life, affects the entire planet, does so for decades and even centuries, and, most of all, because none of us acting individually can do anything to slow the changes."

William D. Nordhaus

Chapter 1

A New Field-Level Measure of the Stock of Soil Organic Carbon and the Value of Carbon Sequestration

1.1 Introduction

Agricultural sequestration of soil organic carbon (SOC) is considered by many to be a significant means of reducing atmospheric carbon dioxide. Agricultural production contributes roughly 10% to 14% of anthropogenic greenhouse gas (GHG) emissions, predominantly from soil and livestock sources (Paustian et al., 2016). According to Janzen et al. (2022), on a global scale, carbon sequestration within agricultural ecosystems has the capacity to absorb an extra 1.5% of current yearly anthropogenic carbon dioxide emissions, equivalent to 0.14 gigatons of carbon annually into the soil.

Accurately measuring SOC is essential for a better understanding of the role of agriculture in reducing atmospheric carbon, assessing its significance, and comprehending how different land management practices influence SOC stocks. It is both challenging and expensive to directly measure the changes in SOC attributable to changes in agricultural production systems (McConkey

et al., 2020).[1] In these circumstances, models that predict SOC could offer an economical method for understanding the dynamics of SOC stocks. Although they cannot replace actual soil sampling (Le Noë et al., 2023), SOC prediction models can serve as helpful resources for examining relative changes in SOC stocks in response to various land management practices (Bista et al., 2016).

This essay introduces a novel method for quantifying SOC, termed the Augmented Campbell model, which enhances the conventional Campbell model by integrating a humification component (Campbell et al., 2000, 2001, 2005, 2007a,b). Additionally, the Augmented Campbell model is expanded to include weather-induced decomposition rate modifiers outlined in the Intergovernmental Panel on Climate Change (IPCC) Guidelines for National Greenhouse Gas Inventories (Zhongming et al., 2019). Hence, this essay introduces and uses two versions of the Augmented Campbell model, distinguished as the "base" version (without the weather-induced decomposition rate modifiers) and the "weather" version (with the weather-induced decomposition rate modifiers). Unless noted, the "Augmented Campbell model" refers to the weather version.

Employing the Augmented Campbell model, and various alternative models for comparison, I achieve the first extensive field-level measurement of SOC over time across Saskatchewan. This measurement enables exploration into how carbon sequestration differs among various soil types and in response to agricultural production decisions. To estimate SOC stocks with the Augmented Campbell model, I apply carbon input values derived from the Plant Biomass Carbon Input (PBCI) model developed by Maillard et al. (2018). Additionally, I use detailed crop production data from the Saskatchewan Crop Insurance Corporation (SCIC) spanning from 1998 to 2019. The SCIC dataset includes proprietary details on cropping choices, yields, and input usage at the field level for all insured hectares in Saskatchewan.

This essay accomplishes three primary purposes. Firstly, I develop and offer an intricate overview of the Augmented Campbell model, and assess its accuracy compared with other SOC prediction models, using soil sampling data sourced from Swift Current, Saskatchewan. Secondly, I analyze the growth in SOC stocks on Saskatchewan fields between 1998 and 2019 using the

---

[1]White et al. (2021) state that soil sampling prices typically range from $200 to $300 for each field, which can vary in size from 40 to 160 acres. The variation in costs is influenced by the quantity of samples collected from a field.

Campbell and Augmented Campbell models with field-level agricultural production information from the SCIC. Thirdly, I assess the value of SOC stocks relative to different hypothetical scenarios, involving the conversion of a portion of canola hectares to fallow land. Subsequently, I project these scenarios forward 150 years into the future.

I evaluate the predictive performance of both versions of the Augmented Campbell model (base and weather versions) compared with other SOC prediction models (including the original Campbell model, the Introductory Carbon Balance Model (ICBM), ICBM/2, and the Rothamsted Carbon (RothC) model) using soil sampling data from experimental plots managed by Agriculture and Agri-Food Canada (AAFC) in Swift Current, Saskatchewan. AAFC implements two different crop rotation strategies in these plots, termed the "New Rotation" and the "Old Rotation." In the context of both rotations, both versions of the Augmented Campbell model outperform the Campbell model in predicting SOC under either rotation. In the context of the New Rotation, both versions of the Augmented Campbell model predict SOC stocks more accurately than the alternatives. Among the models, the ICBM/2 shows the best performance across both rotations, albeit with a tendency to estimate higher SOC stocks on average, relative to other models.[2] I cannot verify SOC predictions using SCIC data because long-term, precise, and consistent soil sampling records are not available (see Congreves et al. (2015), Fan et al. (2019), Riggers et al. (2019), Farina et al. (2021), He et al. (2021), and Thiagarajan et al. (2022)).[3]

Using the Augmented Campbell model (weather version), I predict a weighted average increase in the SOC stock in Saskatchewan of 6,797 kg/ha from 1998 to 2019. I observe variation in SOC stock changes across soil zones: 4,437 kg/ha in the brown soil zone, 6,048 kg/ha in the dark brown soil zone, and 7,488 kg/ha in the black & gray soil zone. This difference among soil zones is attributed to heterogeneity in their cropping choices, farming practices, climate conditions, and crop yields. In the brown soil zone, characterized by a drier climate compared to the dark brown

---

[2]Despite the ICBM/2's overall superior performance in SOC stock predictions, Riggers et al. (2019) indicate that, relative to other SOC prediction models, it may overestimate SOC levels more when initial SOC stocks are high.

[3]For consideration for use in model validation, I further examine the Prairie Soil Carbon Balance (PSCB) project, which collected soil samples from 90 fields across Saskatchewan on five occasions between 1996 and 2018 (McConkey et al., 2020). However, inconsistencies in these data pose challenges for their use in validating predicted SOC stock changes over time. (Paustian et al., 2019). Despite its limitations for validation, the PSCB project still offers researchers valuable insights into the internal dynamics of SOC within sampled fields throughout Saskatchewan.

and black & gray soil zones (Marchildon and Sauchyn, 2009), farmers grow a higher proportion of crops suitable for arid conditions. Consequently, farmers in the brown soil zone plant a lower proportion of their land to crops with substantial carbon inputs (e.g., canola) and a higher proportion to pulse crops (e.g., lentils and peas) and fallow. The simulated SOC stock change from 1998 to 2019 corresponds to an average annual change of 309 kg/ha/yr across Saskatchewan.

The estimated annual SOC change of 309 kg/ha/yr from the Augmented Campbell model (weather version) aligns with the range of benchmarks for validating SOC predictions in the Canadian GHG National Inventory Report (see VandenBygaart et al. (2003), VandenBygaart et al. (2008), Liang et al. (2020), and Environment and Climate Change Canada (2022)). According to a meta-analysis by Liang et al. (2020), SOC stocks from no-till systems in western Canada exhibit an annual change of 300 kg/ha/yr in medium-textured soils (such as silt, silt loam, loam, or sandy clay loam) and 430 kg/ha/yr in fine-textured soils (including sandy clay, clay loam, silty clay loam, silty clay, or clay). Given that a significant portion of Saskatchewan's soils fall within the medium- and fine-textured categories,[4] the annual change in SOC projected by the Augmented Campbell model in Saskatchewan falls comfortably within the range of SOC stock changes observed under no-till practices in the meta-analysis conducted by Liang et al. (2020).

To value the change in SOC from 1998 to 2019 in Saskatchewan as predicted by the Augmented Campbell model (weather version), I introduce a more sensible method for estimating the external social benefits of carbon sequestration compared with approaches that calculate these benefits as though new sequestrations will be sustained in perpetuity. This method employs a rental rate for carbon derived from the social cost of carbon (SCC) and its related discount rate applied to the annual change in the stock of SOC implied by a specific counterfactual comparison over time. The benefit calculation depends on the choice of a counterfactual scenario against which to compare actual agricultural production choices. Each counterfactual scenario entails a switch of a certain percentage of canola hectares to summer fallow, which I simulate field by field based on draws from a binomial distribution. The counterfactual scenarios proposed in this essay

---

[4]Please refer to Saskatchewan Soil Information System for a detailed overview of soil textures across soil zones and types in Saskatchewan (University of Saskatchewan, 2023).

envision lower adoption rates of zero-tillage and continuous cropping practices, which have been widely implemented across Saskatchewan since the 1990s and are known to sequester SOC unlike the practices they have replaced (Awada et al., 2016). In what follows, in this chapter all monetary figures are reported in 2023 United States dollars and are adjusted for inflation using the GDP Deflator from the Federal Reserve Bank of St. Louis (U.S. Bureau of Economic Analysis, 2024).

I estimate that the adoption of zero-tillage and continuous cropping, particularly in relation to canola cultivation, yielded external social benefits over the period 1998 to 2019 ranging from $481 million to $6 billion. This range reflects variation in both the assumed Social Cost of Carbon (SCC) and the percentage of canola hectares that were converted to summer fallow. Specifically, the lower estimate of $481 million is derived from an SCC of $14/Mg (14 dollars per metric ton), with 25% of canola hectares converted to summer fallow, and using the lowest value drawn from the binomial distribution. Conversely, the higher estimate of $6 billion results from an SCC of $185/Mg, with 75% of canola hectares converted to summer fallow, and employing the highest value drawn from the binomial distribution. When these changes in management practices are valued indefinitely into the future, generating a perpetual stream of benefits, the range expands further, from $766 million to $29.1 billion in external social benefits, depending on the SCC and the specific counterfactual scenario considered.

In this essay, I also extend the projection of SOC stocks 150 years into the future employing the Augmented Campbell model (weather version). This projection reveals an external social benefit ranging from as low as $856 million, based on a SCC of $14/Mg and the scenario where 25% of canola hectares revert to summer fallow, to as high as $30.2 billion, with an SCC of $185/Mg and the scenario where 75% of current canola hectares revert to summer fallow. This forward-looking projection accounts for additional dynamics in SOC, resulting in a broader range in predicted SOC stocks compared with the counterfactual scenarios over the long term. The projected benefits per year range from roughly 0.03% to 1% of the $20 billion annual value of cereals, oilseeds, and pulse exports from Saskatchewan (Government of Saskatchewan, 2022).

If SOC prediction models are to be used in policy guidance, there are several economic and biogeochemical factors that need to be considered. The impermanence of carbon storage in the

5

soil means that SOC can be released back into the atmosphere with changes in farming practices. This feature necessitates a careful approach to estimating the value of SOC over time. Instead of presuming indefinite carbon storage, a more nuanced valuation employs the concept of an annual rental rate for SOC. This rate depends on the prevailing SCC and adjusts for the conversion factor between SOC and CO_2, which is applied to yearly changes in SOC attributable to sequestration efforts. Such an approach ensures that the valuation of SOC aligns with the actual duration of policy effects. Yet, given the enduring challenge posed by climate change, valuing carbon sequestration from specific management practices as a perpetual asset may also be warranted.

The remainder of the essay unfolds as follows: sections 1.2 and 1.3 provide background on crop production in Saskatchewan and on SOC prediction models; sections 1.4 and 1.5 describe the PBCI model and the Augmented Campbell model; sections 1.6 and 1.7 describe the data and the sample selection procedure; sections 1.8 and 1.9 evaluate the models, comparing their predictions to the observed stock of SOC using the soil sampling data from AAFC and field-level data from the SCIC confidential dataset; section 1.10 provides a brief overview of the PSCB project; section 1.11 describes the method used to compute the external social benefit from changes in the stock of SOC and proposes potential counterfactuals to be used to estimate the external social benefits from changes in farming practices and cropping choices; sections 1.12 and 1.13 provide the results from estimating the historical and forward projected external social benefits from carbon sequestration by crop farmers in Saskatchewan; and section 1.14 concludes the essay.

1.2   Saskatchewan Crop Production and Carbon Sequestration

Agricultural carbon sequestration involves capturing and storing carbon dioxide from the atmosphere, a process that can occur naturally in forests and soils through biological means, or be facilitated by human-made systems, as a strategy to mitigate climate change. Illustrated in Figure 1.1, this concept is exemplified by the carbon sequestration cycle of wheat, canola, and summer fallow. The diagram details how carbon flows in and out of these systems, with the width and color of the lines indicating the magnitude and direction of carbon movement. Plants like wheat and canola absorb CO_2, integrating carbon into their biomass as they grow. This carbon is partly

transferred to the soil by plant residues and becomes part of the soil humus, though some is later released back to the atmosphere as it decomposes. Additionally, carbon is stored in the seeds produced by these plants, which are then harvested. The practice of tillage influences how quickly soil organic carbon (SOC) breaks down, with Figure 1.1 highlighting that traditional tillage methods accelerate CO_2 release into the atmosphere compared with no-till practices.

FIGURE 1.1: Agricultural Carbon Sequestration Cycle
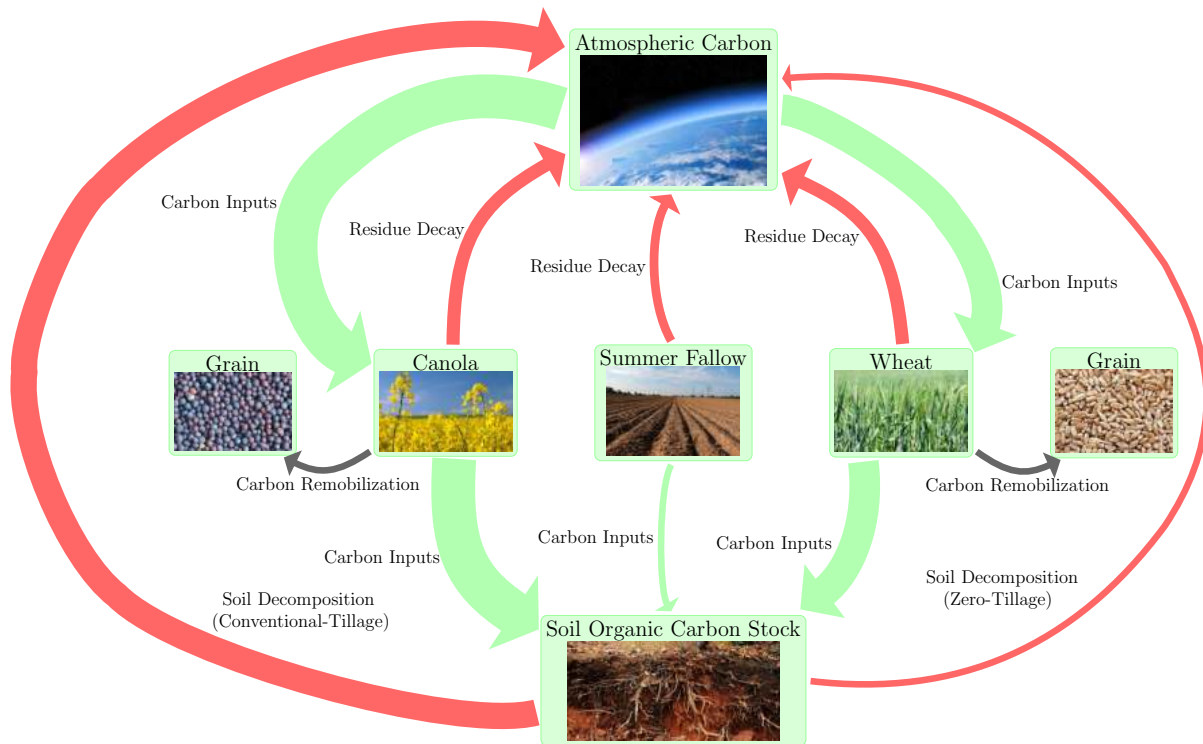
Note: Arrow Thickness represents Rate of Carbon Transfer

Source: Author.

In 1980, cereals dominated the harvested landscape of Saskatchewan, encompassing 89.5% of the total harvested area, while oilseeds occupied 10.4%, and pulses a mere 0.01%. Between 1980 and 2021, the crop mix was significantly transformed, with cereals declining to 47.2%, oilseeds rising to 36.3%, and pulses expanding to 16.5% (refer to Figure 1.2). Over the same period, Saskatchewan witnessed a remarkable increase in its total harvested area, expanding by 4.7 million hectares, or by 47.6%. The growth in harvested acres primarily resulted from a reduction

in summer fallow. Between 1976 and 2016, the extent of summer fallow in Canada dwindled by 7.5 million hectares, or decrease of 92% (Weersink et al., 2019). Saskatchewan contributed significantly to this trend, with an average annual conversion of 150 thousand hectares of summer fallow land into production each year during this period (Statistics Canada, 2021).

FIGURE 1.2: Total Harvested Hectares for Pulses, Cereals, and Oilseeds in Saskatchewan from 1980 to 2021
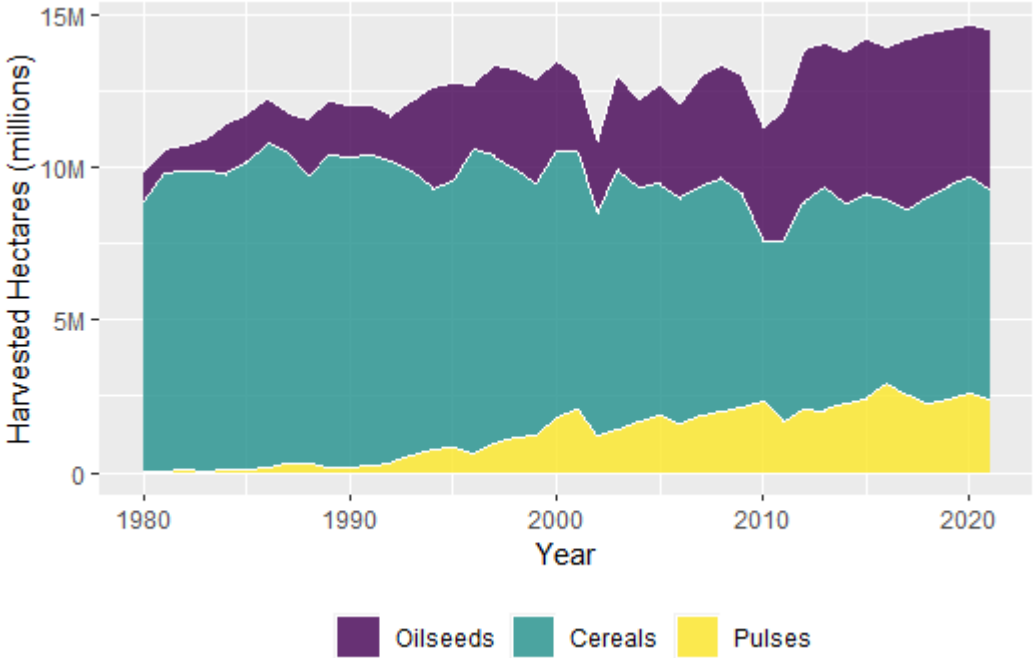
Source: Created using data from Statistics Canada (2021).

Prior to the widespread adoption of zero-tillage systems, many farmers allocated their land using a half-and-half rotation method, reserving half of their land for fallow each year. The introduction of advanced farming equipment, such as air seeders in the late 1980s, propelled the uptake of zero-tillage practices. Over just two decades, from 1991 to 2011, zero tillage in Saskatchewan grew from 10% to 70% (Awada et al., 2016). Awada et al. (2016) attribute much of this shift to outreach initiatives and knowledge dissemination efforts targeting farmers, facilitated by government reports aimed at addressing soil erosion in the prairies and highlighting the economic advantages

of zero-tillage methods.[5] Both Zentner et al. (1990) and Lafond et al. (1993) agree that transitioning away from fallow-based rotations mitigates soil erosion while simultaneously enhancing soil productivity and farm profitability across Saskatchewan.

Since 1990, advances in crop breeding, agricultural machinery, and pesticides have significantly influenced the adoption of zero-tillage and continuous cropping practices. Factors such as the decreased cost of glyphosate, the introduction of herbicide-tolerant canola varieties, the availability of legume inoculants, the invention of air seeders, the use of flexible harvest headers and straw choppers on combines, the implementation of land rollers for pulse crops, increased quotas from the Canadian Wheat Board, and lower interest rates have all contributed to the decline of traditional tillage methods across the Canadian prairies (Awada et al., 2016). Nowadays, the majority of farmers plant crops on all of their cropland each year.

1.3   Soil Organic Carbon Prediction Models

In this section, I provide a brief overview of the various SOC prediction models in use today, examining their strengths and weaknesses. SOC prediction models fall into two categories: process-based models and empirical models. Process-based models are more complex, simulating SOC stocks on either a daily or monthly basis, while empirical models operate on an annual basis. Empirical models use data on crop yield and carbon inputs to estimate SOC stocks, whereas process-based models also factor in soil type and weather. Empirical models can be categorized further as either (1) models based on differential equations that describe the behavior of soil carbon, nitrogen, or microbial biomass, or (2) models that are derived from regression analyses applied to soil sampling data. Process-based models are solely based on the former.

Numerous process-based models are capable of predicting crop yields, enhancing their ability to more accurately project SOC stocks by integrating forecasted crop yields (and thus carbon

---

[5]In 1983, the Prairie Farm Rehabilitation Administration (PFRA), a branch of AAFC, released a seminal report titled "Land Degradation and Soil Conservation Issues on the Canadian Prairies," shedding light on soil erosion and loss associated with conventional tillage systems (Awada et al., 2016).

inputs) with projected weather conditions (Bista et al., 2016). These models often include inter-actions among SOC measures, nitrogen, nitrous oxide, ammonia, or methane (greenhouse gases), employing mathematical formulations to simulate the biological and chemical processes influ-enced by plant life cycles, soil nutrient levels, water and temperature fluctuations, and solar ex-posure (Necpálová et al., 2015). Notable examples of process-based models include Century, Day-Cent, and RothC. Both Century and RothC models operate on a monthly basis, while DayCent offers a more granular, daily time-step analysis, building upon the framework of the Century model (Chang et al., 2013).

Extensive research has been conducted to evaluate the effectiveness of various SOC predic-tion models (see Bolinder et al. (2006), Campbell et al. (2007a,b), Lemke et al. (2010), Smith et al. (2012), Congreves et al. (2015), He et al. (2021), and Thiagarajan et al. (2022)). Bolinder et al. (2006) find that process-based models do not significantly outperform empirical models. Bolinder et al. (2006), Congreves et al. (2015), and Thiagarajan et al. (2022) indicate that enhancing the parame-terization of empirical models such as the Campbell model and the ICBM could elevate their pre-dictive accuracy, making them more competitive with some process-based models. Specifically, Campbell et al. (2007a,b) revise the parameters within the ICBM to better reflect the characteris-tics of chernozemic soils found in Saskatchewan. Improvements to the original ICBM have led to variants like the ICBM/2, which boast enhanced predictive capabilities (Kätterer and Andrén, 2001; Poeplau et al., 2015; Kröbel et al., 2016). The Augmented Campbell model represents the first effort to advance the original Campbell model, offering a refined approach to SOC prediction.

A significant critique of the Campbell model is that the time-path to the steady-state equi-librium is too short. Congreves et al. (2015) show that the Campbell model often underpredicts SOC in the initial years and attains steady-state equilibrium more quickly than both the ICBM and DayCent models. This is attributed to the Campbell model employing residue decomposi-tion parameters from the Voroney equation, which is derived from a study with only ten years of residue decomposition data (Voroney et al., 1989). Such a duration is insufficient to capture the complex dynamics of plant residue decomposition, which varies among different plant parts and

takes longer to achieve a steady-state. To remedy this, the Augmented Campbell model developed in this essay introduces a humification process, which not only increases carbon inputs but also extends the time taken to reach steady-state equilibrium.[6] In this essay, I concentrate on the Campbell and Augmented Campbell models due to their manageable data requirements and their parameters' suitable representation of soil dynamics in Saskatchewan.

1.4   Plant Biomass Carbon Input Model

The Plant Biomass Carbon Input (PBCI) model computes carbon inputs based on crop yields, considering yield variations due to changes in weather conditions, cropping selections, and farming practices. To calculate annual carbon inputs, the PBCI model employs conversion formulas that consider specific plant traits (Bolinder et al., 2007; Maillard et al., 2018; Fan et al., 2019; He et al., 2021; Zhang et al., 2021; Thiagarajan et al., 2022). These conversions require information on crop yield, moisture content, the shoot-to-root ratios, and the harvest index for each type of crop.

To simulate SOC stocks, carbon inputs are essential. Following the method used by Fan et al. (2019), I apply estimated annual carbon inputs derived from the PBCI model across all SOC prediction models discussed in this essay. Leveraging crop production data to estimate carbon inputs presents a significant advantage, as directly measuring carbon inputs is both challenging and costly.

The harvest index—defined as the ratio of grain to total shoot dry-matter (i.e., plant residue) (Porker et al., 2020)—is a measure of reproductive efficiency determined by genotypes, environment, and crop management, that influences biomass accumulation and grain yield potential. Values of the harvest index can be calculated using data on grain and straw yields. Equation (1.1) shows the formula for the harvest index, which is equal to the amount of dry-matter yield of grain divided by the total amount of above-ground biomass (i.e., dry-matter yield of grain and dry-matter yield of straw).

$$HI_c = \frac{Y_{grain,c}}{Y_{grain,c} + Y_{straw,c}} = \frac{Y_{grain,c}}{Y_{abovegroundbiomass,c}}, \tag{1.1}$$

---

[6]Humification involves the transformation of organic matter into humus.

where, for crop c, HI_c is the harvest index, $Y_{grain,c}$ is the dry-matter yield of grain (kg/ha/yr), $Y_{straw,c}$ is the dry-matter yield of straw, and $Y_{abovegroundbiomass,c}$ is the total above-ground dry matter yield (i.e., grain plus straw).

Because information is not readily available on dry-matter yields of straw by crop, I follow Fan et al. (2017) and calculate the harvest index from data on dry-matter grain yields (equation (1.2)):[7]

$$HI_c = \alpha_c + \beta_c Y_{grain,c} \tag{1.2}$$

where α_c and β_c are coefficients, unique for crop c, that determine the Harvest Index.

In the PBCI model, carbon inputs originate from the straw and roots of plants as they decompose, and rhizodeposition from the plants as they are growing, at rates that differ among crops.[8] These sources of carbon are characterized in equations (1.3) to (1.5). The quantities of carbon inputs from roots are calculated using the shoot-to-root ratio by crop.[9] Plant biomass is zero for summer fallow and 5% of the carbon inputs from the previous year's crop for chemical fallow (Campbell et al., 2001; Maillard et al., 2018). The SCIC data do not make a distinction between chemical and summer fallow; hence, in the absence of specific information, it is presumed that all idle land is considered summer fallow.

$$A_{straw,n,c} = Y_{grain,n,c} \times \left(\frac{1 - HI_c}{HI_c} \right) \times 0.45, \tag{1.3}$$

$$A_{root,n,c} = \left(Y_{grain,n,c} / \left(HI_c \times S/R_c \right) \right) \times 0.45, \tag{1.4}$$

$$A_{rhizodep,n,c} = A_{root,n,c} \times 0.65, \tag{1.5}$$

---

[7]Yields in Equation (1.2) are measured as dry-matter grain yields. I use the percentage of moisture content for grain by crop to convert observed yield to dry-matter yield. Moisture content by crop is based on marketing, harvest, and storage standards in Saskatchewan (Government of Saskatchewan, 2020).

[8]Rhizodeposition is the excretion of inorganic and organic elemental solution from living roots (Bolinder et al., 2007).

[9]Gill et al. (2002) find that the proportion of roots that die annually in a year (i.e., rhizodeposition) is equal to 0.65.

where for crop c in year n, $A_{straw,n,c}$, $A_{root,n,c}$, and $A_{rhizodep,n,c}$ are the quantities of plant carbon input from straw, roots, and rhizodeposition, respectively, and S/R_c is the shoot-to-root ratio.

Carbon inputs from equations (1.3) to (1.5) make up the total carbon inputs for each crop. Hence, for a representative crop c, the total quantity of carbon inputs is,

$$A_{n,c} = Y_{grain,c} \times \left(\frac{1 - HI_c}{HI_c} \right) \times 0.45 + \left(\frac{Y_{grain,c}}{S/R_c \times HI_c} \right) \times 0.7425, \qquad (1.6)$$

where $A_{n,c}$ is the plant carbon input from straw, roots, and rhizodeposition in year n.

Table 1.1 presents the parameter values for estimating the harvest index of each crop (α_c and β_c in equation (1.2)), listed in column (1), as determined by Fan et al. (2017). To derive these parameters, Fan et al. (2017) used harvest index data and grain yields from 91 studies conducted across Canada. Additionally, the table includes data on shoot-to-root ratios by crop and soil profile depth, sourced from Thiagarajan et al. (2018) and displayed in column (2) for soil depths of 0–20cm and 0–100cm. Thiagarajan et al. (2018) determines the shoot-to-root ratios based on findings from 58 Canadian studies.

Fan et al. (2019) find that across Canada 90% of the root system and rhizodeposition occur within the 0–20cm profile depth, with nearly all distribution existing within the 0–100cm profile depth. Bolinder et al. (2007) suggest that the shoot-to-root ratio for specific crops may differ between western and eastern Canada. To approximate the shoot-to-root ratios at the required 0–15cm profile depth, I use data from Thiagarajan et al. (2018), focusing on shoot-to-root ratios at the 0–20cm profile depth. This approximation is crucial for inputting into SOC prediction models. Estimates of site-specific initial SOC stocks are derived from observations at six sites in Saskatchewan, categorized by soil type, and measured at the 0–15cm profile depth (McConkey et al., 2003), which is significantly influenced by tillage, plant roots, and residue incorporation (Campbell et al., 2000). Crop yields are standardized to dry-matter yields by considering the moisture content percentage for each crop, as detailed in column (3) of Table 1.1, based on established standards for marketing, harvesting, and storage in Saskatchewan (Government of Saskatchewan, 2020).

TABLE 1.1: Harvest Index Coefficients, Shoot-to-Root Ratios, and Moisture Content
by Crop

	(1)		(2)		(3)
	Harvest Index Coefficients[a]		Shoot-to-Root Ratio		Moisture Content[b]
Crop	Intercept (α_c)	Slope (β_c)	0–20cm	0–100cm	%
Barley	0.373	0.028	7.35	5.00	13.5
Canary seed	0.336	0.020	6.94	4.22	13.0
Canola	0.180	0.046	4.24	2.71	9.5
Chick peas	0.301	0.063	8.47	4.59	14.0
Flaxseed	0.171	0.110	12.66	5.18	8.5
Lentils	0.305	0.059	6.45	4.18	13.5
Mustard seed	0.197	0.078	7.63	4.20	9.5
Oats	0.357	0.029	3.72	2.39	12.5
Peas, dry[b]	0.323	0.067	8.70	4.74	16.0
Wheat, durum	0.344	0.015	7.81	4.61	13.5
Wheat, spring	0.344	0.015	7.81	4.61	13.5
Wheat, winter	0.344	0.015	7.81	4.61	13.5

Source: Fan et al. (2017); Thiagarajan et al. (2018); Government of Saskatchewan (2020).

Notes: The Harvest Index Coefficients sourced from Fan et al. (2017), the Shoot-to-Root Ratios provided by Thiagarajan et al. (2018), and the Moisture Content is obtained from the Government of Saskatchewan (2020).

[a] The Harvest Index Coefficients for dry peas are sourced from the upper 95% confidence interval of pulse crop estimates provided by Fan et al. (2017). These coefficients ensure that carbon inputs for peas remain non-negative.

[b] Moisture contents by crop are based on marketing, harvest, and storage standards published by the Government of Saskatchewan (2020).

I now demonstrate how the PBCI model is used to estimate the average annual carbon inputs from plant biomass by crop and year, employing equation (1.6) and data on average annual crop yields in Saskatchewan sourced from Statistics Canada (2021). Figure 1.3 shows the average annual carbon input values per hectare for various crops in Saskatchewan between 1980 and 2021. These total carbon input values per hectare as shown in Figure 1.3 align closely with the carbon input amounts measured by Gan et al. (2009), who determined carbon contributions from straw, roots, and rhizodeposition by sampling seven crops in western Canada during 2006 and 2007.[10]

---

[10]Plant samples were collected from the Agriculture and Agri-Food Canada's Semiarid Prairie Agricultural Research Centre, located near Swift Current, Saskatchewan (Gan et al., 2009).

FIGURE 1.3: Plant Biomass Carbon Inputs per Hectare by Crop in Saskatchewan from 1980 to 2021
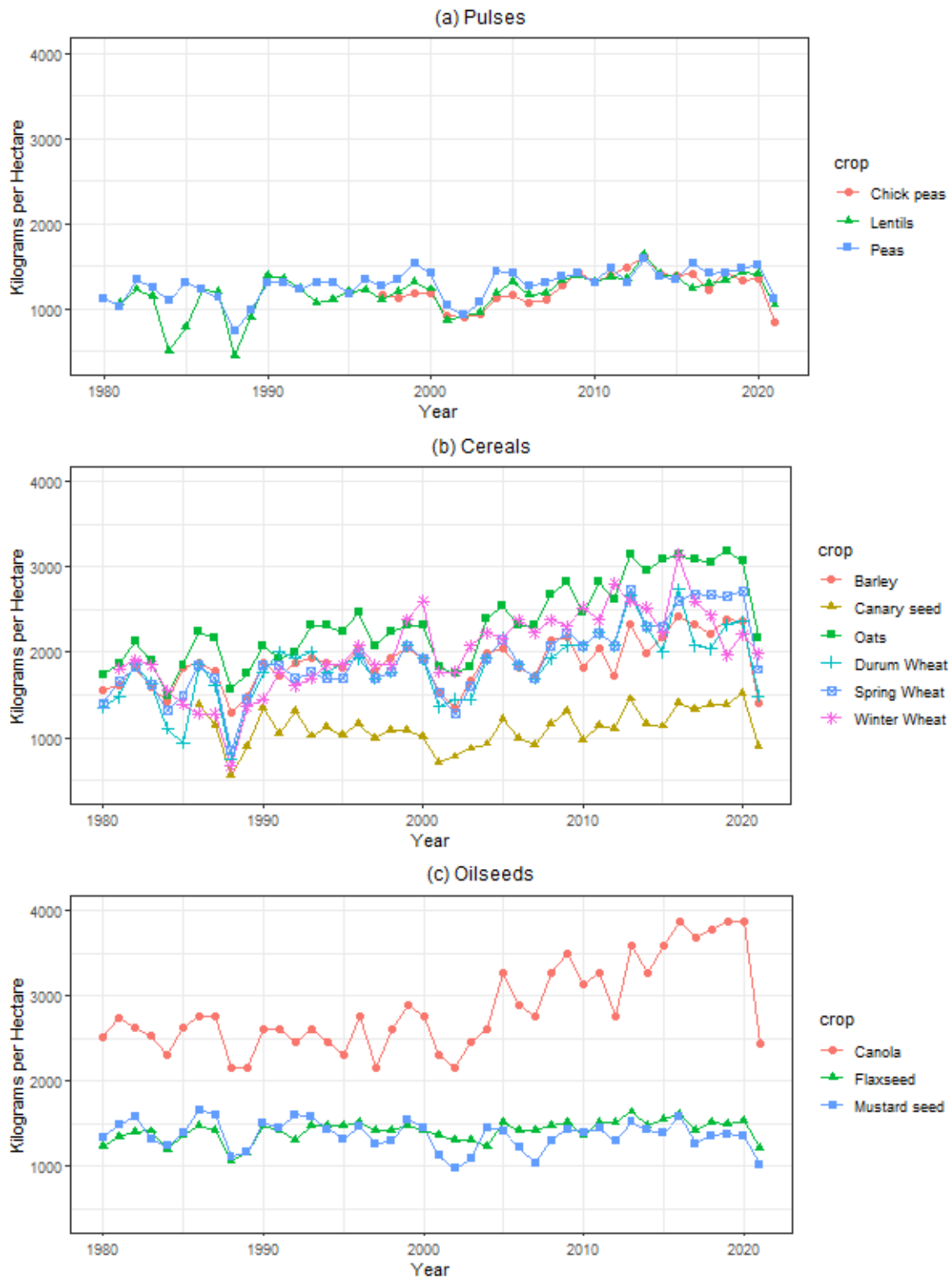
Source: Author's Estimates

Typically, crops that produce more biomass, meaning larger plants with more plant material, contribute to greater quantities of carbon inputs. This is evident from Figure 1.3, where canola, being a relatively large plant, leads in carbon input yields among all the crops analyzed. Cereals also produce more carbon inputs compared to pulses; meanwhile, specialty crops like mustard, chickpeas, and canary seed generate comparatively smaller quantities of carbon inputs. This illustration offers insight into which types of crops and crop rotations are likely to enhance carbon sequestration and boost SOC stocks more effectively.

1.5 Augmented Campbell Model

In this section, I describe the development of the Augmented Campbell model by integrating the Campbell model with the humification process from the ICBM. The Campbell and Augmented Campbell models stand out for their simplicity and minimal initial stock information requirements. The setup of the Campbell model is based on assumptions regarding the allocation of initial carbon stocks into labile and stable carbon categories,[11] without having to initialize the distribution of the initial stocks across different carbon pools. To derive the Augmented Campbell model, I assume that a fraction of annual outflux from plant residue to soil carbon occurs through a humification process, specifically, the same humification process as in the ICBM.

The complete derivation of the Augmented Campbell model is shown in Appendix 1A. The derivation involves the following sequential steps:

1. solve for a system of differential equations using the Campbell model,

2. add the humification terms from the ICBM to the system,

3. solve the differential equations using the variable coefficients initial value problem,

4. approximate the solutions back to discrete-time using the Euler-Maclaurin formula, and

5. combine the discrete-time solutions to obtain the Augmented Campbell model.

---

[11]Labile carbon and refractory carbon decompose at different rates and originate in both plant residue and soil humus. Labile carbon decomposes more rapidly through microbially or photochemically mediated processes, whereas refractory carbon is more resistant to degradation (Kätterer and Andrén, 2001).

Relative to the Campbell model, the Augmented Campbell model predicts higher SOC stocks across all years, and it requires a longer period for SOC stocks to achieve a steady-state equilibrium. This adjustment effectively addresses the primary critiques of the original Campbell model. Throughout this essay, I calculate SOC stocks using both the Augmented Campbell model and the Campbell model for every scenario presented. This approach demonstrates the affect of including the humification process on the time path of predicts SOC stocks.

The Campbell model uniquely processes recent additions of carbon inputs from plant residues and the existing carbon in the soil separately,[12] with the proportion of carbon directed towards each pool (labile and refractory fractions of plant residues and soil humus) being strictly determined by its parameter values. Consequently, neither the Campbell model nor the Augmented Campbell model require initialization for distributing the initial SOC stock among the different pools, as these distributions are inherently fixed by the parameters established within the Campbell model (Thiagarajan et al., 2022).

The calculation of SOC stocks in the Augmented Campbell model (base version), as outlined in equation (1.7), simplifies notation by excluding the crop-specific subscript from the plant biomass carbon input variable, A_n, for readability. This formula embeds the original Campbell model within the Augmented version, with its initial component representing the traditional Campbell calculation and the subsequent term accounting for SOC accumulation through the humification of plant residues. The Augmented Campbell model (base version) consistently predicts a higher SOC stock than its Campbell counterpart in all periods. This is because the humification process in the Augmented model decomposes at a slower rate compared to the rapid decomposition of plant residues in the Campbell model. As a result, the added term in the Augmented model accumulates over time, diverging from the static nature of the Campbell model, thereby extending the time taken to achieve a steady-state equilibrium.

In the Campbell model, the portions of the SOC stock (i.e., labile and refractory) within plant residue and soil humus decompose at different rates. The Campbell model has two pools

---

[12]In the Campbell model, treating carbon from plant residue and pre-existing carbon in the soil separately is a method developed by Woodruff (1950).

that represent different portions of the SOC stock that decompose at different rates, whereas the base and weather versions of the Augmented Campbell model both have three pools. To adjust the decay rates of plant residue humification, I incorporate a scaling parameter γ on the decomposition rates for the plant residue humification term in the Augmented Campbell model (base and weather versions). When γ exceeds 10, the Augmented Campbell model closely aligns with the Campbell model. The calibration of the scaling factor for the humification process leverages soil sampling data from the same AAFC-operated Experimental Research Station in Swift Current, Saskatchewan, which also provided the foundational data for developing and calibrating the Campbell model (Campbell et al., 2000).

$$
SOC_t = \underbrace{C_0(q_1 e^{-k_1 t} + q_2 e^{-k_2 t}) + \sum_{n=0}^{t} A_n(p_1 e^{-r_1(t-n)} + p_2 e^{-r_2(t-n)})}_{\text{Campbell Model}}
$$
$$
+ \underbrace{\sum_{s=1}^{t} \sum_{n=0}^{t} A_n h(r_1 p_1 e^{-\gamma(r_1(t-n)+k_1(t-s))} + r_2 p_2 e^{-\gamma(r_2(t-n)+k_2(t-s))})}_{\text{Plant Residue Humification}}
$$

(1.7)

Subscripts 1 and 2 in equation (1.7) refer to labile and refractory carbon, respectively. Labile carbon decomposes more rapidly, whereas refractory carbon decomposes more slowly (Kätterer and Andrén, 2001). In equation (1.7), SOC_t is the total SOC per soil unit mass in year t (this does not include current year plant residue), C_0 is the initial carbon stock, $q_1 + q_2$ are the proportions of labile and refractory soil humus carbon ($q_1 + q_2 = 1$), k_1 and k_2 are the annual rates of soil humus decomposition, A_n is the quantity of carbon inputs in year n (kg/ha/yr) derived from the PBCI model, p_1 and p_2 are the proportions of plant residue carbon ($p_1 + p_2 = 1$), r_1 and r_2 are the annual rates of plant residue decomposition, and h is a humification coefficient.

Table 1.2 shows the values of all the parameters used in the model for predicting the stock of SOC, including concise descriptions for each parameter.

TABLE 1.2: Parameter Values in the Augmented Campbell Model

Soil Decomposition Rates	
Proportion of old labile soil carbon – q_1	0.2
Proportion of old refractory soil carbon – q_2	0.8
Rates of labile soil decomposition:	
Continuous cropping – k_1	0.001
Fallow within 6 years and more that every 3rd year – k_1	0.0015
Fallow every 3rd year – k_1	0.01
Fallow every other year – k_1	0.02
Rate of refractory soil decomposition – k_2	0.00066
Plant Decomposition Rates	
Proportion of labile plant residue carbon – p_1	0.72
Proportion of refractory plant residue carbon – p_2	0.28
Rate of labile plant residue decomposition – r_1	1.4
Rate of refractory plant residue decomposition – r_2	0.081
Humification coefficient – h	0.125
Humification scaling parameter[a] – γ	0.10
	0.20
Weather modifier calibration parameter – ε	1.5

Source: Andrén and Kätterer (1997), Congreves et al. (2015), and Lemke et al. (2010).
Notes: All parameter values are set as in Congreves et al. (2015) and Lemke et al. (2010) except the humification rate, which is set as in Andrén and Kätterer (1997). The humification scaling parameter and weather modifier calibration parameter are calibrated using soil sampling data from the Experimental Research Stations operated by Agriculture and Agri-Food Canada located in Swift Current, Saskatchewan.
[a] The humification scaling parameter is set to 0.1 in the base version of the Augmented Campbell model, whereas it is set to 0.2 in the weather version of the Augmented Campbell model.

Values for the parameters q, k, p, and r are estimated by Campbell et al. (2000, 2001, 2007a,b) and Lemke et al. (2010) for different cropping systems on chernozemic soils, the broad soil type in Saskatchewan. In the Campbell model, for soil humus, values of q_1 and q_2 are 0.20 and 0.80, and k_2 is 0.00066 which is suited for chernozemic soils (Campbell et al., 2000). Values for k_1 vary by cropping system and if rotations incorporate summer fallow. As done by Congreves et al. (2015), I assume values of 0.001 for continuous cropping (fallow less than once every five years), 0.0015 for rotations including fallow once every four or five years, 0.01 for rotations with fallow every third year, and 0.02 for rotations with fallow every other year. Hence, tillage increases the

decomposition rate of SOC in both the Campbell model and Augmented Campbell model (base and weather versions), which lowers the stock of SOC relative to zero-tillage. In the Campbell model, the decomposition rate varies with tillage only in the humus portion of the stock of SOC, whereas in the Augmented Campbell model, it also varies with decomposition rate in the plant residue humification term. The humification coefficient, h, determines the fraction of plant residue that enters as soil carbon. I assume a rate of 0.125 for h as done by Andrén and Kätterer (1997) and Campbell et al. (2007a,b), assuming no farmyard manure or sewage sludge is added to the field.

The Augmented Campbell model (weather version) incorporates weather modifiers on decomposition rates based on the 2019 refinement to the 2006 Intergovernmental Panel on Climate Change (IPCC) guidelines for national GHG inventories (Zhongming et al., 2019). Equation (1.8) presents the formulation of the weather version of the Augmented Campbell model. These modifiers are determined through calibration, with ε set to 1.5 and the scaling parameter adjusted to 0.2, ensuring optimal alignment with soil sampling data from the AAFC-operated experimental research station in Swift Current, Saskatchewan. While capturing essential aspects of process-based models, the weather version of the Augmented Campbell model maintains a level of simplicity and ease of implementation that sets it apart from more complex process-based models.

$$
\begin{aligned}
SOC_t = C_0 &\left(q_1 e^{-\frac{t_{fac} w_{fac}}{\varepsilon} k_1 t} + q_2 e^{-\frac{t_{fac} w_{fac}}{\varepsilon} k_2 t} \right) \\
&+ \sum_{n=0}^{t} \left[A_n \left(p_1 e^{-\frac{t_{fac} w_{fac}}{\varepsilon} r_1(t-n)} + p_2 e^{-\frac{t_{fac} w_{fac}}{\varepsilon} r_2(t-n)} \right) \right] \\
&+ \sum_{s=1}^{t} \sum_{n=0}^{t} \left[A_n \left(h r_1 p_1 e^{-\gamma \frac{t_{fac} w_{fac}}{\varepsilon} (r_1(t-n)+k_1(t-s))} + h r_2 p_2 e^{-\gamma \frac{t_{fac} w_{fac}}{\varepsilon} (r_2(t-n)+k_2(t-s))} \right) \right].
\end{aligned}
\tag{1.8}
$$

The temperature modifier represents how decomposition rates vary with temperature, and is equal to:

$$t_{fac} = \frac{1}{12} \sum_{i=1}^{12} T_i$$

and   (1.9)

$$T_i = \left(\frac{t_{max} - temp_i}{t_{max} - t_{opt}} \right)^{0.2} - \exp\left(0.0076 * \left(1 - \left(\frac{t_{max} - temp_i}{t_{max} - t_{opt}} \right)^{2.63} \right) \right),$$

where t_{fac} is the annual average air temperature effect on soil carbon decomposition, T_i is the monthly average air temperature effect on decomposition, t_{max} is the maximum monthly air temperature for decomposition (set to 45 °C), $temp_i$ is the monthly air temperature in degrees Celsius, t_{opt} is the optimum air temperature for decomposition (set to 33.69 °C).

The water modifier represents how decomposition rates vary with respect to precipitation and is equal to:

$$w_{fac} = 1.5 * \left(\frac{1}{12} \sum_{i=1}^{12} w_i \right),$$

$$w_i = 0.2129 + (w_s * mappet_i) - (0.2413 * mappet_i^2),$$ (1.10)

and

$$mappet_i = \min\left(1.25, \frac{precip_i}{PET_i} \right),$$

where w_{fac} is the annual effect of water on soil carbon decomposition, w_i is the monthly effect of water on soil carbon decomposition, w_s is the modifier for $mappet_i$ (set to 1.331), $precip_i$ is the total precipitation for month i in millimeters, and PET_i is the total potential evapotranspiration (PET) for month i in millimeters.

I employ the adjusted PET formulation provided by Willmott et al. (1985), which builds upon the Thornthwaite and Mather approach.[13] Willmott et al. (1985) adjusts the Thornthwaite and Mather formula to account for the specific number of days per month and sunlight hours on

---

[13]In contrast to the Thornwaite and Mather formula for PET, the Hargreaves-Samani and Penman-Monteith equations provide alternate methodologies for PET calculation, adjusting for daily sunlight hours to yield daily PET estimates. Notably, the Penman-Monteith equation demands further data on daily wind speed (Cai et al., 2007). Both the Hargreaves-Samani and Penman-Monteith equations, compared to Willmott's adaptation of the Thornthwaite and Mather formula, necessitate additional data and subsequent aggregation to derive monthly PET values.

21

the 15th day of each month for each observation. As done by Thornthwaite and Mather (1955), I specify the monthly unadjusted PET for month m as equal to,

$$PET_m = \begin{cases} 16 * \left(\frac{10 * T_m}{I}\right)^a & if\, T_m < 27°C \\ -0.43 * T_m^2 + 32.24 * T_m - 415.85 & if\, T_m \geq 27°C \end{cases},$$

(1.11)

$$\text{where} \begin{cases} a = (0.000000675 * I^3) - (0.0000771 * I^2) + (0.01792 * I) + 0.49239, \\ \text{and } I = \sum_{m=1}^{12} (0.2 * T_m)^{1.514} \end{cases}.$$

In equation (1.11), PET_m is the monthly potential evapotranspiration in millimeters per month, T_m is the mean monthly temperature in °C, and a is a coefficient that depends on the annual heat index I, which depends on the monthly temperature. If the monthly mean temperature (T) is less than 0 °C, then PET is equal to 0. The PET is adjusted by the hours of sunlight on the 15th day of each month and the number of days within a month, such that

$$\widetilde{PET} = PET * [(\theta/30)(h/12)],$$

(1.12)

where θ is the number of days in the month and h is the duration of daylight that varies by the latitude and longitude of a field (Willmott et al., 1985).

In addition to the Augmented Campbell model (base and weather versions) and Campbell model, I also employ the ICBM, ICBM/2, and the Rothamsted Carbon (RothC) model. The ICBM and ICBM/2 are empirical models that use annual time-steps to predict SOC stocks, whereas the RothC model is a process-based model that uses monthly time-steps. Appendix 1B includes further explanation of the ICBM and ICBM/2; likewise, Appendix 1C for the RothC model.

1.6 Data Collection

To calculate SOC stocks for the province of Saskatchewan at the field level, I employ innovative, field-specific crop yield and cropping choice data from the SCIC. Most of the past research examining the agronomic and economic determinants of SOC, farm profitability, or farm productivity has relied on aggregate data or results from field trials and plot experiments. Previous studies on the agronomic and economic factors influencing SOC, with farm profitability and productivity, have predominantly used broad aggregate data or findings from controlled field trials and experiments. Such aggregate data fail to account for the variation among different fields, and overlook critical details regarding historical cropping choices and yields for specific plots of land. Meanwhile, data from field trials have their limitations in assessing the broader effects that necessitate acknowledging the diversity of field conditions throughout Saskatchewan.

The SCIC dataset spans the years 1998 to 2019 and encompasses a wide array of information for each field and year, including the legal land description, municipality, risk zone for insurance, soil classification, land utilization, insurance status (indicated by a variable), level of insurance coverage, planted acreage, type of crop, crop variety, yield, and fertilizer application. Notably, detailed field-level data on crop yield and fertilizer use are only provided by farmers participating in the Sask Management Plus (SMP) program at SCIC. For farmers not in the SMP program, reported crop yields reflect the average yield for a specific crop on a farm across all fields with that crop. Nonetheless, all farmers report their crop choices at the field level. This reporting structure enables SOC changes at the field level to be estimated using information on the field-specific crop choices and the farm's average annual yield (as a proxy for field-specific yield) for those not participating in the SMP program.

FIGURE 1.4: Field-Level Map of Soil Zones in Saskatchewan
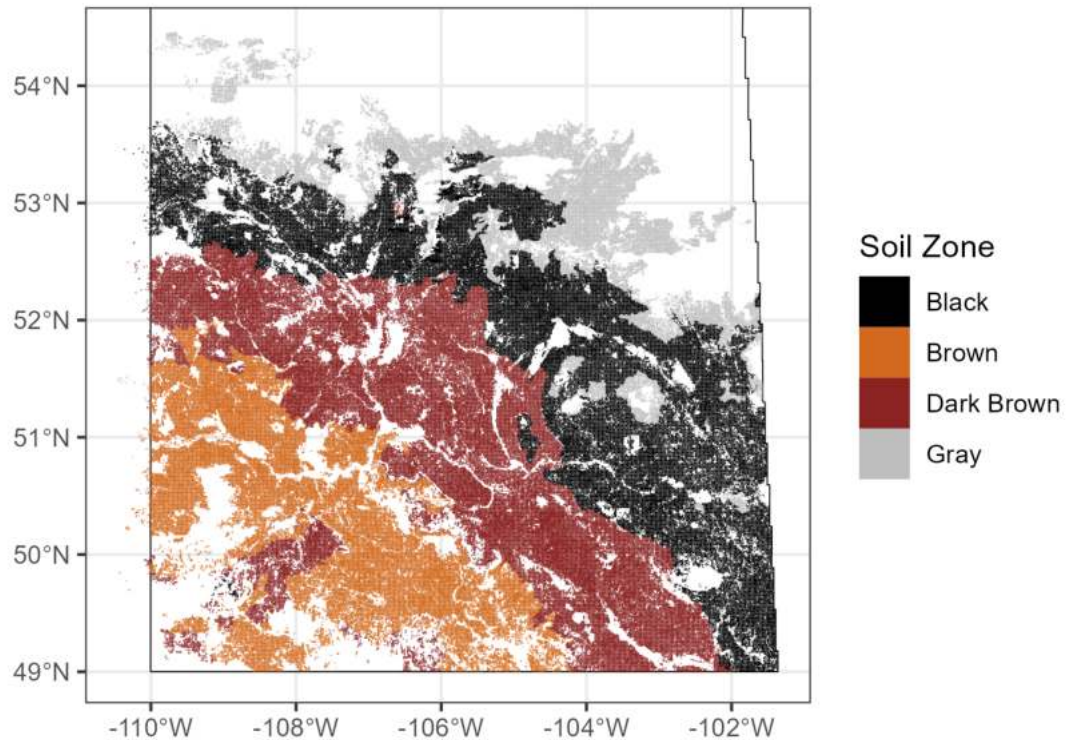
Source: Generated from ISC land titles registry polygons and soil characteristics from the Canadian National Soils Database (Agriculture and Agri-Food Canada, 2022; ISC, 2022).

I use the land title dataset provided by ISC, the primary source of land titles registry information in Saskatchewan (ISC, 2022). This dataset contains detailed field-level polygons across the province, and I incorporate soil attributes sourced from both the Saskatchewan Detailed Soil Survey and the Canadian National Soil Database (Agriculture and Agri-Food Canada, 2022).[14] Figure 1.4 illustrates the spatial distribution of fields in Saskatchewan, classified according to distinct soil zones. Throughout this essay, I aggregate my research results to the brown, dark brown, and black & gray soil zones. This allows for an examination of the variations in SOC influenced by diverse farm management practices, soil attributes, and agronomic factors that differ across these soil zones.

---

[14]Soil attributes encompass a range of factors such as clay, sand, and silt percentages, slope, bulk density, organic carbon content, water retention capacity, cation exchange capacity, and other pertinent characteristics. For further details, please refer to the Canadian National Soil Database (Agriculture and Agri-Food Canada, 2022).

I match soil characteristics from the Canadian National Soil Database to all the fields in Figure 1.4. As an illustration, Figure 1.5 displays the distribution of clay content percentages across Saskatchewan fields, derived from the same database (Agriculture and Agri-Food Canada, 2022). The clay percentage plays a specific role solely within the RothC model, where it influences decomposition rates and the carbon storage capacity of each field. Notably, fields with the highest clay percentages are predominantly clustered in two regions within the brown and dark brown soil zones. These regions feature vertisolic soils, situated within the former glacial lake basins of the Regina and Rosetown plains in Saskatchewan (Brierley et al., 2011).

I obtain weather data from stations managed by Environment and Climate Change Canada (2023b) and I transform the daily temperature and precipitation records into monthly values. My analysis incorporates data from 56 weather stations strategically positioned across the agricultural regions of Saskatchewan, as well as a few stations in Alberta and Manitoba near the provincial boundaries of Saskatchewan. I employ inverse distance weighting from the five closest weather stations to interpolate weather data directly to the field level.[15] Equation 1.13 presents the inverse distance weighting formula for weather $W_{m,n}$ in month m for pixel n. The weather observed at station i is weighted by its inverse distance $1/d_{i,n}$ to pixel n, ensuring the sum of all weights equals one.

$$W_{m,n} = \frac{\sum_{i=1}^{5} \left(\frac{w_{m,i}}{d_{i,n}} \right)}{\sum_{i=1}^{5} \left(\frac{1}{d_{i,n}} \right)} \tag{1.13}$$

I match temperature and precipitation to all fields in Saskatchewan. Figure 1.6 shows the spatial variation in precipitation for June 2007. In any given year and month, precipitation and temperature vary considerably across the province of Saskatchewan.

---

[15]I use around one million spatial pixels throughout Saskatchewan, and employ the inverse distance weather calculation with respect to each spatial pixel. For generating field-level data, I computed the average of the measurements from spatial pixels situated within each field. This method significantly enhances the efficiency of computing interpolated spatial data compared to other spatial techniques available in R.

FIGURE 1.5: Saskatchewan Field-Level Clay Content in Percentage by Field
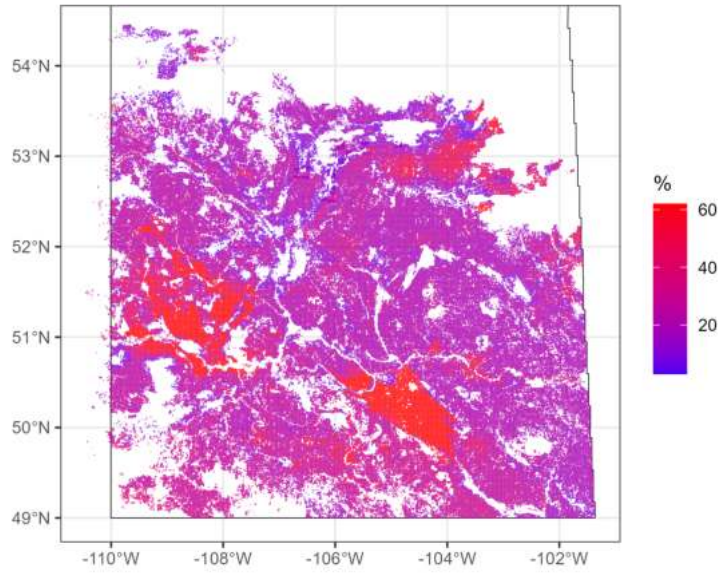
Source: Generated using data from the Canadian National Soils Database (Agriculture and Agri-Food Canada, 2022).

FIGURE 1.6: Environment Canada Weather Station interpolated data in Saskatchewan – Precipitation for June 2007
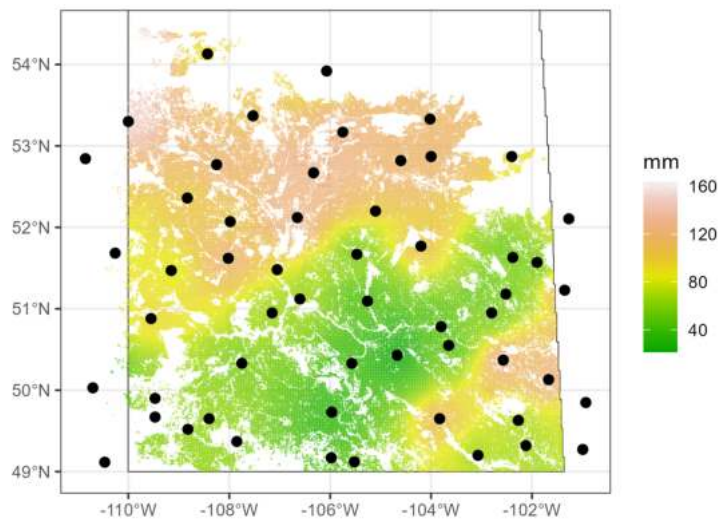
Source: Generated from weather station data collected by Environment and Climate Change Canada (2023b).

Notes: The black dots represent the location of weather stations.

The initial stocks of SOC are determined using soil sampling data sourced from the Saskatchewan Detailed Soil Survey within the Canadian National Soil Database (Agriculture and Agri-Food Canada, 2022), as well as data from McConkey et al. (2003). The Saskatchewan Detailed Survey provides SOC stocks for a soil profile depth of 0–20cm in 1971 across the entire province, which I match to each field in Saskatchewan. Employing measures of bulk density and organic carbon concentration from the survey, I apply the fixed-depth calculation method, as outlined in Ellert et al. (1995), to estimate SOC stocks in 1971. Although the fixed-depth method does not account for changes in bulk density and soil horizons, I refine the 1971 SOC stocks using soil sampling data from McConkey et al. (2003), which are measured and computed based on an equivalent mass basis. McConkey et al. (2003) provide data on SOC stocks at a depth of 0-15cm for certain locations across the province in 1994 and 1995 as shown in Table 1.3. Soil samples were collected from various plots near different towns, such as Hatton, Swinton, Sceptre, Elstow, Melfort, and Indian Head during specific periods.[16] I make the assumption that there was minimal change in SOC stocks between 1995 and 1998. Therefore, I estimate the initial SOC stocks in 1998 at a soil profile depth of 0-15cm, as the SOC stock values updated using samples from 1995 as given in Table 1.3 are reported at this depth.

To determine the initial SOC stock, I employ the inverse-distance-squared weighting technique, using it to interpolate the percentage change in SOC stocks across fields between the soil sampling data from McConkey et al. (2003) and the area-wide average SOC stock from the Saskatchewan Detailed Soil Survey. This process is performed in three stages: (1) calculate the percentage change in SOC from 1971 to 1998 at test sites from McConkey et al. (2003), (2) extrapolate these changes to yield a specific percentage change for each field across Saskatchewan through inverse-distance-squared weighting, and (3) apply this interpolated percentage change to the field-specific baseline SOC stock (1971) to compute specific SOC estimates for 1998 at a 0-15cm soil profile depth.

---

[16]Soil samples were collected from 30 plots near the towns of Hatton, Swinton, and Sceptre in the spring of 1994, from eight plots near Elstow in the fall of 1995, and from 39 plots near Melfort and Indian Head in the fall of 1994 (McConkey et al., 2003).

TABLE 1.3: Tillage Effects on Bulk Density and Soil Organic Carbon

Soil Type	(1) Tillage[a]	(2) Bulk Density[b] Mg/m^3	(3) Soil Organic Carbon Mg/ha
Elstow clay loam	CT	1.14	52.2
	NT	1.16	56.6
Meflort silty clay loam	CT	1.03	77.2
	MT	1.08	84.3
	NT	1.14	89.2
Indian Head clay	CT	1.17	39.5
	MT	1.15	43.6
	NT	1.21	43.6
Hatton fine sandy loam	MT	1.43	17.4
	NT	1.45	19.4
Swinton silt loam	MT	1.28	27.9
	NT	1.3	28.7
Sceptre clay	MT	1.21	25.9
	NT	1.27	28.4

Source: McConkey et al. (2003)
Notes: In the spring of 1994, soil samples were collected from 30 plots near the towns of Hatton, Swinton, and Sceptre, and from 8 plots near Elstow in the fall of 1995. In the fall of 1994, soil samples were collected from 39 plots near Melfort and Indian Head. All plots experienced different tillage systems by crop rotation. Please refer to McConkey et al. (2003) for more information on the crop rotations and tillage systems employed at each site.
[a] CT: cultivator (full) tillage, MT: minimum tillage, NT: no-tillage
[b] Bulk Densities are based on soil sample depths of 0-15cm.

Figure 1.7 shows the interpolated changes by field in Saskatchewan between 1971 and 1998, where the black dots are locations where the soil sampling data originate in McConkey et al. (2003). These interpolated changes reveal a decrease in SOC stocks on the western side of the province and an increase on the eastern side. I attribute this primarily to inter-regional differences between farming practices; canola production and no-till techniques were adopted earlier in eastern Saskatchewan while farmers in the western regions continued tillage-intensive practices until the 2000s.

FIGURE 1.7: Interpolated Difference in Soil Organic Carbon Stocks by Field in
Saskatchewan from 1971 to 1998
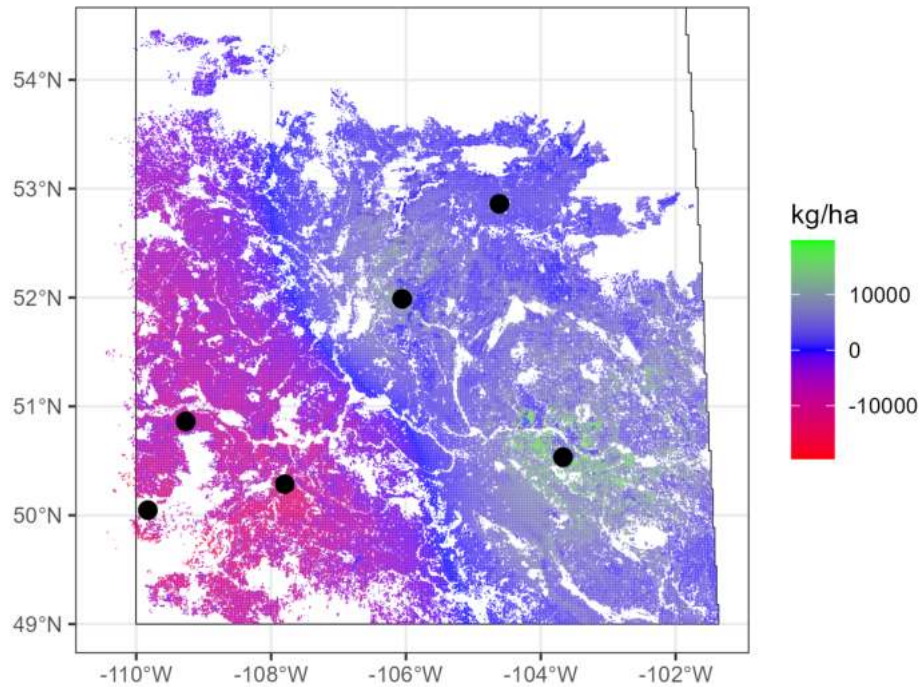
Source: Generated from regional soil sampling data from McConkey et al. (2003)
and soil sampling data from the Canadian National Soil Database (Agriculture and
Agri-Food Canada, 2022).

Notes: Black dots represent the soil sampling locations from McConkey et al. (2003).

Figure 1.8 presents the calculated SOC stock at the field level in Saskatchewan for the year
1998. This calculation is obtained by applying the interpolated percentage change in SOC stock
from 1971 to 1998 to the initial field-level SOC stock data from 1971, as recorded in the Saskatchewan
Detailed Soil Survey and the Canadian National Soil Database.

FIGURE 1.8: Field-Level Stock of Soil Organic Carbon in Saskatchewan in ~1998
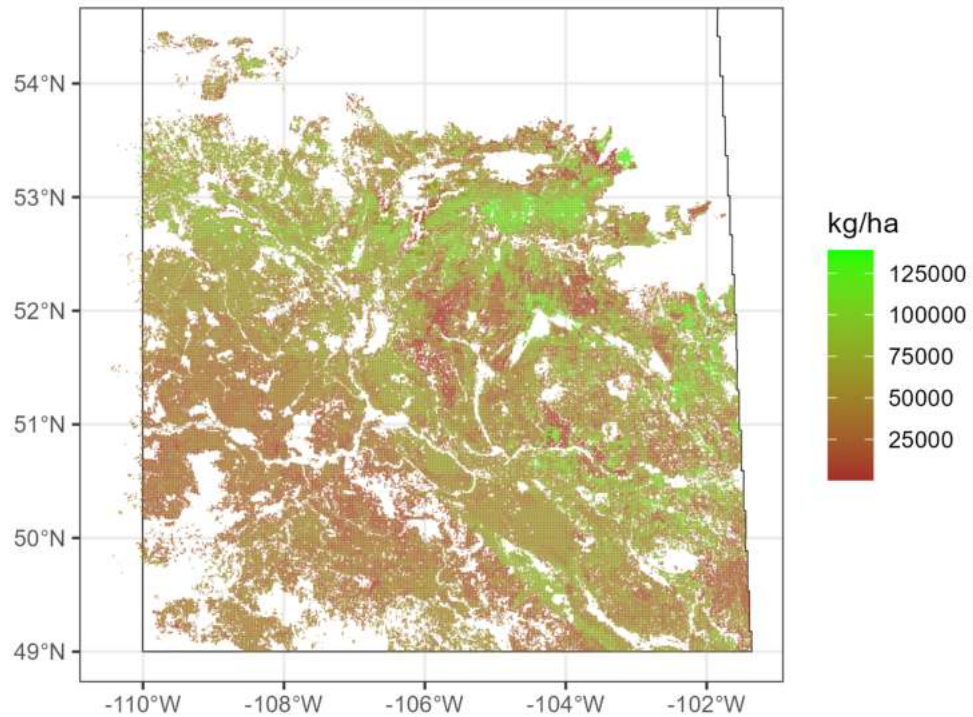
Source: Generated from regional soil sampling data from McConkey et al. (2003)
and soil sampling data from the Canadian National Soil Database (Agriculture and
Agri-Food Canada, 2022).

To validate the measures of the initial SOC stock values across the province, I benchmark the

SOC stock depicted in Figure 1.8 against data from soil samples collected in 1996 and 1999 as part

of the Prairie Soil Carbon Balance (PSCB) project. Funded by the Saskatchewan Soil Conservation

Association, the PSCB project conducted soil sampling on fields throughout Saskatchewan from

1996 to 2018 to track changes in SOC stocks on commercial farms (McConkey et al., 2020). Ini-

tially, the project sampled 136 fields in 1996. However, due to alterations in sampling methods,

changes in land ownership and in land management practices, some fields were not re-sampled

in subsequent years, leading to a decrease in the number of fields available for longitudinal anal-

ysis (Paustian et al., 2019). To estimate the SOC stock for 1998, I assume a linear change in SOC

between 1996 and 1999 and calculate the interpolated value for 1998. In Table 1.4, SOC stock measurements from the PSCB project are summarized by province, as well as by the brown, dark brown, and black & gray soil zones.

TABLE 1.4: Initial Stocks of Soil Organic Carbon for Saskatchewan in 1998 by Soil Zone

	(1)		(2)	
Source:	Prairie Soil Carbon Balance Project[a]		Saskatchewan Detailed Soil Survey and McConkey et al. (2003)[b]	
Soil Zone	SOC (kg/ha)	# of Sites	SOC (kg/ha)	# of Sites
All	43,513	136	53,771	36,443
Brown & Dark Brown	33,780	61	43,989	13,674
Brown	-	0	34,332	3,644
Dark Brown	-	0	47,497	10,030
Black & Gray	55,732	75	59,646	22,769

Source: McConkey et al. (2003, 2020) and Agriculture and Agri-Food Canada (2022).
[a] Prairie Soil Carbon Balance Project values of SOC are based on interpolating 1996 and 1999 measured soil samples to the year of 1998.
[b] To calculate the SOC stock by field in 1998, I use the inverse-distance-squared weighting technique to interpolate the percentage change in SOC stock across all field in Saskatchewan, based on the comparison between soil sampling data retrieved by McConkey et al. (2003) and the area average SOC stock values from the Saskatchewan Detailed Soil Survey and Canadian National Soil Database (Agriculture and Agri-Food Canada, 2022).

Column (1) of Table 1.4 shows the SOC stocks obtained from the PSCB project alongside the corresponding number of sites, while column (2) shows the calculated initial SOC stocks for all of Saskatchewan and the number of fields. In the black & gray soil zone, these two measures are similar, with only a 7% difference. However, in the brown and dark brown soil zones, the difference is larger, with the value in column (2) being almost one-third larger than the measure from the PSCB project. Notably, the SOC stock for both the brown and dark brown soil zones from the PSCB project in column (1) closely aligns with the SOC stock of the brown soil zone in column (2), differing by only 1.6%. In column (2), the average SOC stock in the dark brown soil zone is similar to the combined average stock in the brown and black & gray soil zones. Specifically, the average SOC stock across the brown and black & gray soil zones is 43,989 kg/ha, while the SOC stock for the dark brown soil zone is 47,497 kg/ha. The spatial correlation of SOC

stocks across fields in Saskatchewan is clear, with the dark brown soil zone showing a higher SOC stock than the brown soil zone, but lower than the black & gray soil zone. The PSCB project does not fully reveal the spatial diversity in the SOC stock across soil zones, as it combines the brown and dark brown soil zones into a single region. The verification process provided in this section shows that the initial SOC stocks estimated in column (2) are within the range of SOC stock measurements calculated on an equivalent mass basis, as derived from soil sampling data throughout Saskatchewan, as depicted in column (1) of Table 1.4.

1.7   Sample Selection

To predict the stock of SOC by field, I need a balanced panel dataset encompassing data for every field in each year. However, the SCIC only gathers data on fields eligible for insurance, excluding those under summer fallow since farmers do not insure these. To identify fields potentially used for summer fallow, I incorporated every field that was at least once insured within specific time blocks: 1998–2001, 2002–2005, 2006–2009, 2010–2013, 2014–2017, and 2018–2019. These intervals are set at four-year spans, accommodating up to three years of consecutive summer fallow within a single block and up to six years across two blocks. The final block, covering the last two years, is shorter and deemed less critical due to the declining use of summer fallow in this period. This structure ensures each block is of sufficient length to identify a substantial number of fields. Any field not present in every time block is removed, leaving a dataset of 36,443 fields. This method mitigates the risk of incorrectly assuming a field is under summer fallow if it does not appear in the SCIC data. Fields divided among various crops are also excluded, as it is challenging to determine the specific crop coverage within each field over time. As a result, the dataset is reduced to 36,443 fields spanning from 1998 to 2019, with 22,769 (62.5%) in the black & gray soil zone, 10,030 (27.5%) in the dark brown soil zone, and 3,644 (10%) in the brown soil zone, culminating in a comprehensive panel dataset of 801,746 field-year observations.

Figure 1.9 illustrates the temporal variation of summer fallow acres within the selected sample compared with the estimates of summer fallow hectares reported by Statistics Canada (Statistics Canada, 2022). The two datasets display similar trends in summer fallow hectares across

the observed period. From 1998 to 2019, the proportion of summer fallow hectares in the SCIC sub-sample is, on average, 6.3 percentage points greater than that reported by Statistics Canada. This discrepancy becomes most noticeable between the years of 2012 and 2019. In these years, Statistics Canada data display a summer fallow share of 4.7 percent, in contrast to the 12.4 percent observed in the SCIC sub-sample. The figures for summer fallow (and other crops) provided by Statistics Canada are derived from a field crop reporting series, which compiles data through farm questionnaires and surveys, in addition to model-based estimates (Statistics Canada, 2022).

FIGURE 1.9: Comparison of the Summer Fallow Hectares Index (1998=100) in Saskatchewan
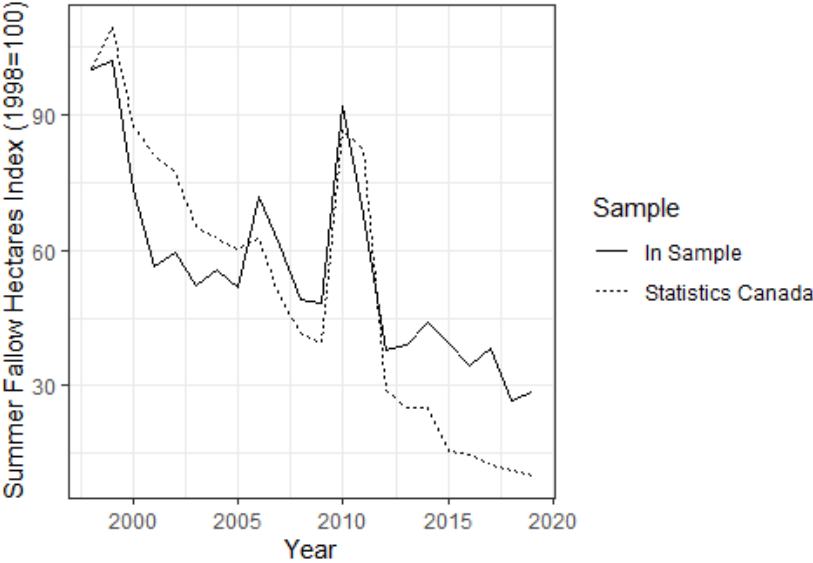
Source: Constructed from SCIC confidential data and (Statistics Canada, 2022).
Notes: "In Sample" denotes the summer fallow hectares from fields selected from the SCIC dataset for carbon prediction, while "Statistics Canada" pertains to their estimated summer fallow hectares in Saskatchewan.

Reflecting crop rotation practices, the extent of summer fallow hectares fluctuates over time and varies across different soil zones. Figure 1.10 shows the shares of summer fallow hectares in the brown, dark brown, and black & gray soil zones from 1998 to 2019. The highest proportion of summer fallow is found in the brown soil zone, reflecting this area's slower uptake of canola and certain agricultural techniques, such as no-till farming. Since 1999, summer fallow decreased sharply across all soil zones, with a continuing downward trend over the years. Notably, the

33

years 2010 and 2011 saw a spike in summer fallow hectares in the dark brown and black & gray zones, owing to flooding in these areas. Given the consistently lower percentage of summer fallow hectares in the dark brown and black & gray zones, I anticipate that the average changes in SOC stocks from 1998 to 2019 in these zones were greater compared with the brown soil zone.

FIGURE 1.10: SCIC Selected Sample – Share of Summer Fallow Hectares relative to all Crops by Soil Zone in Saskatchewan
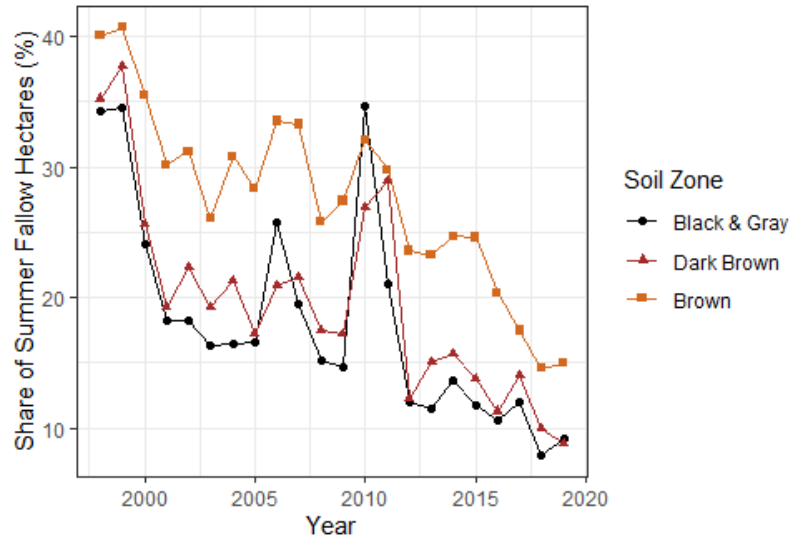
Source: Constructed using SCIC confidential data.

Table 1.5 presents comprehensive information on the crop choices across the three soil zones within two segments of the total SCIC sample: the analysis dataset and the fields that were excluded. The columns in Table 1.5 show hectares of crops for different soil zones, with column (1) for the brown soil zone, column (2) for the dark brown soil zone, column (3) for the black & gray soil zone, and column (4) for the province as a whole. Panel (A) shows the area (thousand hectares) sown to each crop for the sample chosen for analysis (selected sample), panel (B) for the fields that were excluded but still insured, and panel (C) for all fields recorded in the SCIC dataset. The hectare figures represent the cumulative total from 1998 to 2019 within each soil zone.

34

TABLE 1.5: Saskatchewan Crop Insurance Corporation Insured Hectares by Sample Selection, Crop Type, and Soil Zone for 1998 to 2019

	(1)		(2)		(3)		(4)	
Soil Zone:	Brown		Dark Brown		Black & Gray		All	
(A) Selected Sample								
	(000s ha)	*(%)*	*(000s ha)*	*(%)*	*(000s ha)*	*(%)*	*(000s ha)*	*(%)*
Barley	113	4.3	727	7.9	2,375	11.2	3,216	9.7
Canola	257	9.8	2,629	28.6	9,060	42.8	11,947	36.2
Flaxseed	38	1.5	457	5.0	606	2.9	1,101	3.3
Lentils	402	15.4	887	9.7	119	0.6	1,408	4.3
Oats	8	0.3	110	1.2	1,048	4.9	1,166	3.5
Peas, dry	215	8.2	757	8.2	1,304	6.2	2,276	6.9
Wheat	1,577	60.4	3,622	39.4	6,676	31.5	11,874	36.0
Sub-Total	2,609	100.0	9,189	100.0	21,188	100.0	32,987	100.0
Summer Fallow	975		2,231		4,668		7,873	
Total	3,584		11,420		25,856		40,860	
(B) Out of Sample Insured								
	(000s ha)	*(%)*	*(000s ha)*	*(%)*	*(000s ha)*	*(%)*	*(000s ha)*	*(%)*
Barley	1,986	5.2	4,924	7.7	8,656	12.7	15,565	9.1
Canola	3,287	8.6	14,922	23.2	27,905	41.1	46,114	27.0
Flaxseed	628	1.6	3,184	4.9	2,133	3.1	5,945	3.5
Lentils	5,780	15.1	8,107	12.6	453	0.7	14,340	8.4
Oats	237	0.6	970	1.5	4,428	6.5	5,636	3.3
Peas, dry	3,588	9.3	5,069	7.9	3,839	5.7	12,495	7.3
Wheat	22,876	59.6	27,161	42.2	20,512	30.2	70,549	41.3
Total	38,381	100.0	64,338	100.0	67,924	100.0	170,644	100.0
(C) All Insured								
	(000s ha)	*(%)*	*(000s ha)*	*(%)*	*(000s ha)*	*(%)*	*(000s ha)*	*(%)*
Barley	2,099	5.1	5,651	7.7	11,031	12.4	18,781	9.2
Canola	3,543	8.6	17,552	23.9	36,965	41.5	58,060	28.5
Flaxseed	666	1.6	3,641	5.0	2,739	3.1	7,046	3.5
Lentils	6,182	15.1	8,994	12.2	572	0.6	15,748	7.7
Oats	245	0.6	1,080	1.5	5,476	6.1	6,801	3.3
Peas, dry	3,802	9.3	5,826	7.9	5,143	5.8	14,772	7.3
Wheat	24,453	59.7	30,783	41.9	27,187	30.5	82,423	40.5
Total	40,991	100.0	73,528	100.0	89,113	100.0	203,631	100.0

Source: Author's Estimates and constructed using SCIC confidential data.

Notes: Summer fallow hectares are determined by selecting fields within the SCIC database that insured in all time period segments: 1998-2001; 2002-2005; 2006-2009; 2010-2013; 2014-2017; 2018-2019.

FIGURE 1.11: Share of Insured Hectares by Crop from 1998 to 2019 in Saskatchewan
for Selected SCIC Field-level data for Soil Organic Carbon Prediction
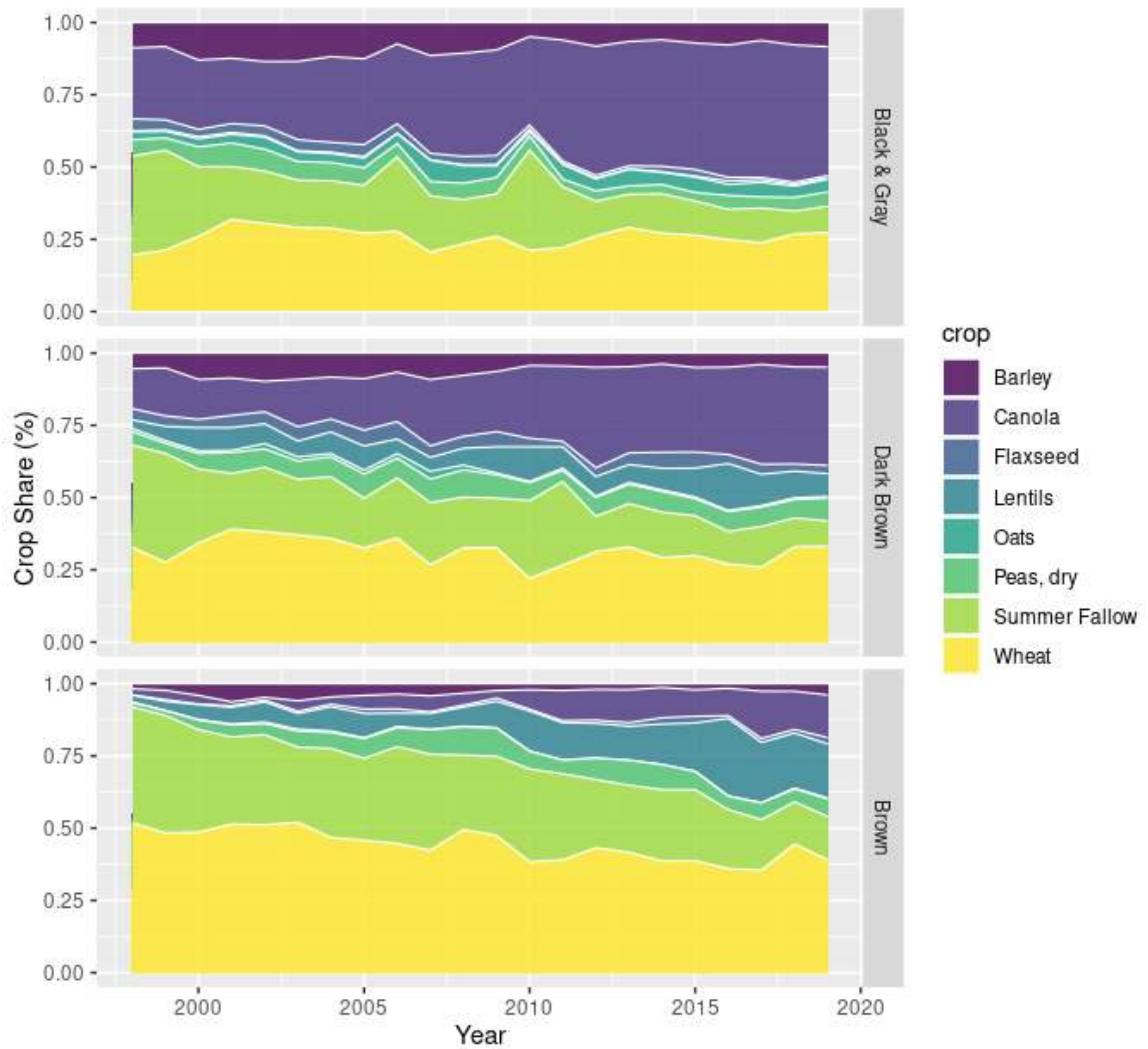
Source: Constructed using SCIC confidential data.

Within the selected sample, the black & gray soil zone accounts for 25.8 million hectares, significantly larger than the 11.4 million hectares in the dark brown soil zone and the 3.6 million hectares in the brown soil zone. Relative to the overall hectares recorded in the SCIC dataset, a greater proportion of the hectares selected for carbon prediction is found in the black & gray soil zone. This indicates that farmers within this zone are more inclined to consistently secure insurance and less likely to allocate fields to multiple crops compared to those in the dark brown and

brown soil zones. Regarding the crop distribution, wheat constitutes a major portion of the agricultural land across the province, with canola and barley primarily planted within the dark brown and black & gray soil zones. Conversely, the brown soil zone has a notably higher percentage of lentil hectares compared with the other two zones.

Figure 1.11 illustrates the shares of crops for the selected sample from the SCIC dataset spanning 1998 to 2019. Over time, there is a noticeable increase in the proportion of canola, especially within the black & gray and dark brown soil zones. Wheat remains a dominant crop across all soil zones. The decline in summer fallow coincides with an expansion of canola production in the black & gray and dark brown zones, along with a rise in both canola and lentil production within the brown soil zone.

From the examination of Table 1.5 and Figure E.1 in Appendix E,[17] I find that the selected sample closely resembles the excluded fields concerning crop-specific shares and yields. Given this similarity in attributes between the two samples, it is reasonable to extend certain findings on a per-hectare basis to derive provincial-level changes in carbon sequestration.

1.8 Validation of Soil Organic Carbon Prediction Models

In this section, I calibrate both versions of the Augmented Campbell model and validate all nine SOC prediction models using soil sampling data from the Experimental Research Station operated by AAFC in Swift Current, Saskatchewan. The Campbell Model was originally developed and parameterized using soil sampling data from the South Farm of the Semi-Arid Prairie Agricultural Research Centre (SPARC) also operated by AAFC at Swift Current (Campbell et al., 2000). Presently, SPARC remains under the operation of AAFC in Swift Current. I evaluate the accuracy of both versions of the Augmented Campbell model (base and weather), alongside the Campbell model, ICBM, ICBM/2, and RothC model, by simulating their performance using agricultural production data derived from the long-term crop rotation experiments conducted at SPARC.

---

[17]For a more detailed examination of field-level characteristics between the in-sample data and the out-of-sample insured data, Appendix 1E offers additional summary statistics.

The data provided by AAFC at Swift Current comprises two distinct crop rotation experiments: the "Old Rotation" and the "New Rotation." The Old Rotation experiment encompasses soil sampling data collected at a 0–30cm soil profile depth spanning 1976–2003. It includes rotations such as fallow-wheat, fallow-wheat-wheat, and continuous wheat (cont-wheat). On the other hand, the New Rotation involves soil sampling data obtained at the 0–15cm soil profile depth spanning 1990-2003 and incorporates rotations such as fallow-wheat-wheat, fallow-wheat-wheat-wheat, and continuous wheat (cont-wheat). In both cases, adjustments to the coefficients for the shoot-to-root ratio within the PBCI model are made to accommodate the variation in soil profile depth.

In both the Old Rotation and New Rotation experiments, each crop rotation consists of multiple plots, with each phase of the rotation occurring annually throughout the duration of the experiment. For instance, in the fallow-wheat rotation, two plots are typically planted where one plot is left fallow while the other is planted to wheat. These datasets from the Old and New Rotation experiments conducted at Swift Current are also used by Thiagarajan et al. (2022), who investigate the predictive capabilities of models including the Campbell model, ICBM, RothC model, and the IPCC Steady State Tier 2 model (modified Century model).

To evaluate the predictive accuracy of the Campbell model, Augmented Campbell model, ICBM, ICBM/2, and RothC model, I employ two widely used statistics for measuring deviations: the root mean squared error (RMSE) and the index of agreement (d-index) (Congreves et al., 2015; He et al., 2021; Thiagarajan et al., 2022). The RMSE quantifies prediction errors and facilitates accuracy comparison among various models, whereas the d-index employs a specific ranking criterion to assess the deviation of predictions from observed data for a particular model (Willmott, 1981). The performance of a model is considered moderate when the d-index ranges from 0.7 to 0.8, good between 0.8 and 0.9, and excellent with a d-index above 0.9 (Willmott, 1981). A d-index value below 0.5 indicates a high level of inconsistency and diversity in model predictions, reflecting poor model performance (Attia et al., 2016; Banger et al., 2019). It is important to note that the thresholds used to judge model performance based on the d-index can be somewhat subjective, leading some studies to simply state that a d-index of 0 reflects an absence of agreement between

the model predictions and observed data (Farina et al., 2021).

Equation (1.14) shows the formula for RMSE and equation (1.15) shows the d-index formula.

$$RMSE = \sqrt{\frac{\sum_{t=1}^{T}(SOC_{t,predicted} - SOC_{t,sampled})^2}{N}},$$ (1.14)

$$d = 1 - \frac{\sum_{t=1}^{T}(SOC_{t,predicted} - SOC_{t,sampled})^2}{\sum_{t=1}^{T}(|SOC_{t,predicted} - \overline{SOC}_{sampled}| + |SOC_{t,sampled} - \overline{SOC}_{sampled}|)^2},$$ (1.15)

where d is the d-index, $SOC_{t,predicted}$ is the simulated or predicted SOC in year t, $SOC_{t,sampled}$ is the measured SOC (soil sampled), and $\overline{SOC}_{sampled}$ is the average of the measured SOC stocks over T years (sampling period).

Figures 1.12 and 1.13 show the SOC prediction outcomes generated by the Augmented Campbell model (both base and weather versions), Campbell model, ICBM, ICBM/2, and RothC model. Here, the base version of the Augmented Campbell model is calibrated using the fitting parameter $\gamma = 0.1$, while the weather version is calibrated with $\gamma = 0.2$ and $\varepsilon = 1.5$. Each panel in either Figures 1.12 or 1.13 represents a specific crop rotation and its phase. For example, "f-w-W*" denotes the fallow-wheat-wheat rotation, with the uppercase "W*" indicating that wheat was planted in the first year of the experiment. Across both the Old Rotation and New Rotation, all SOC prediction models initially predict similar measures of SOC stocks in the earlier years but diverge gradually over time. Notably, the SOC stock predictions from both the base and weather versions of the Augmented Campbell model and ICBM fall within the range defined by the maximum and minimum values projected by other models (Campbell model, ICBM/2, RothC model).

FIGURE 1.12: Prediction of Soil Organic Carbon stocks by Prediction model at Agriculture and Agri-Food Canada for "Old Rotation" Crop Rotation Experiment in Swift Current, Saskatchewan
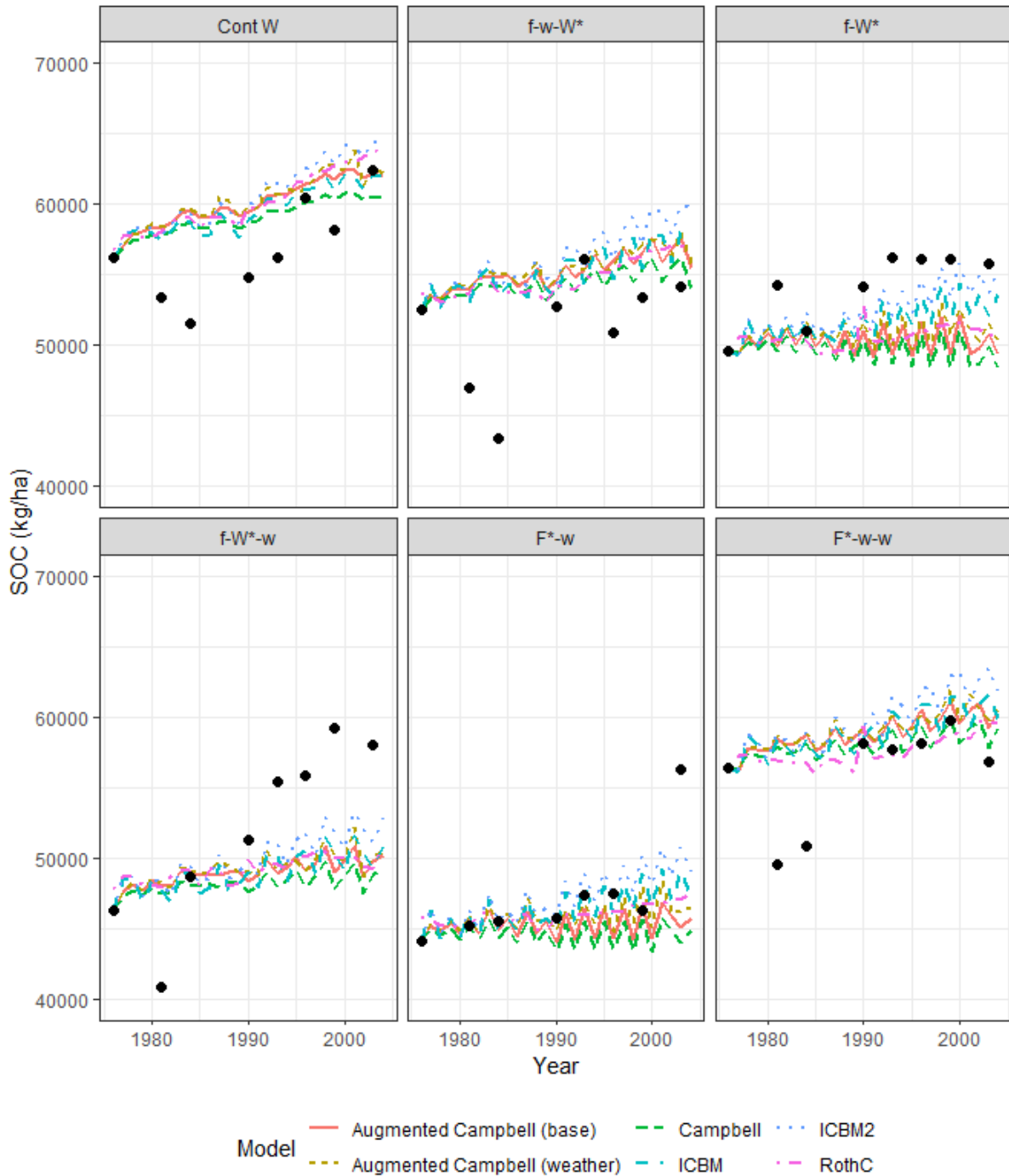
Source: Author's Estimates and created using data from the Experimental Research Station operated by Agriculture and Agri-Food Canada in Swift Current, Saskatchewan.

Notes: Black dots represent the measured SOC from soil samples.

FIGURE 1.13: Prediction of Soil Organic Carbon stocks by Prediction model at Agriculture and Agri-Food Canada for "New Rotation" Crop Rotation Experiment in Swift Current, Saskatchewan
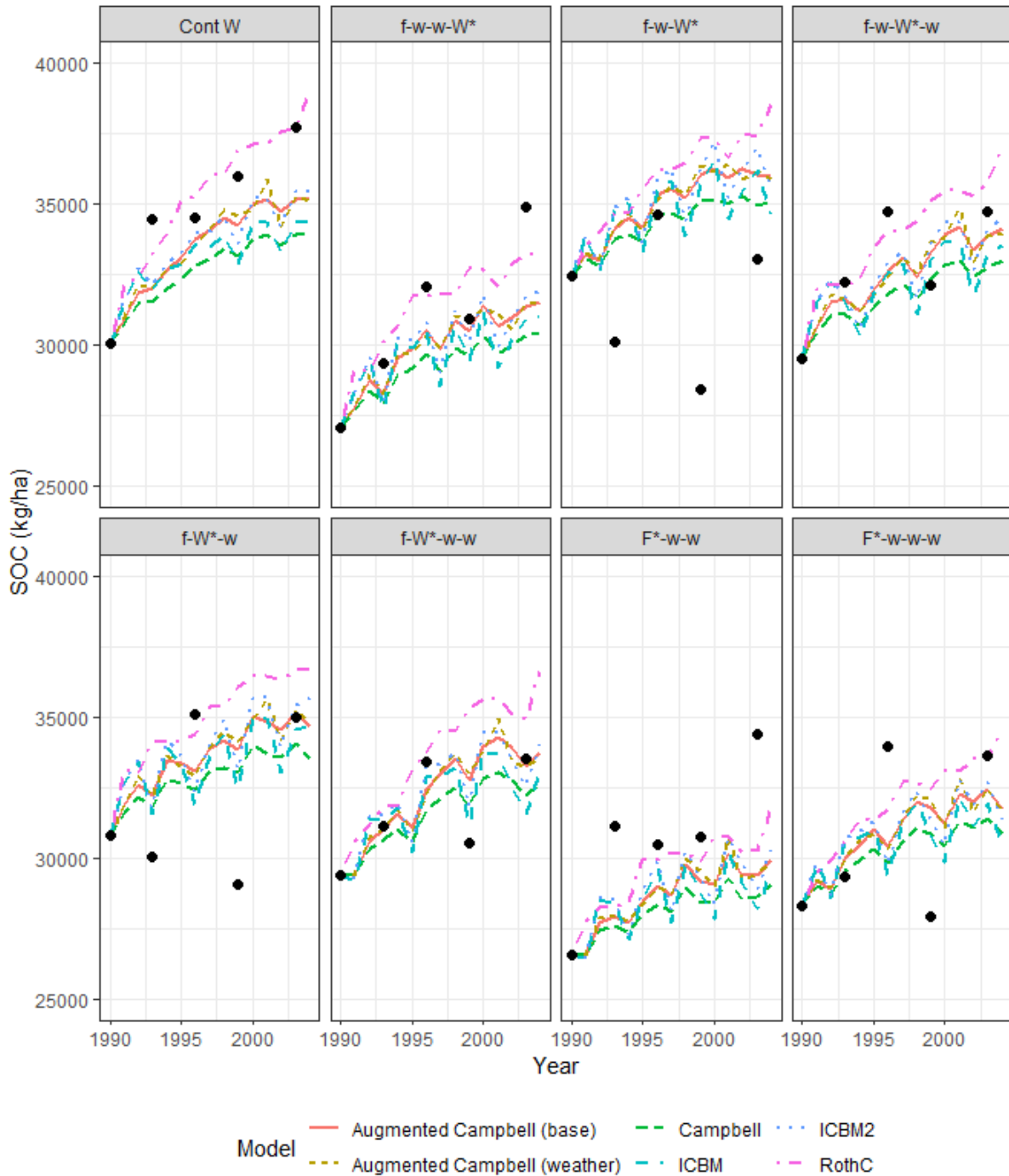
Source: Author's Estimates and created using data from the Experimental Research Station operated by Agriculture and Agri-Food Canada in Swift Current, Saskatchewan.

Notes: Black dots represent the measured SOC from soil samples.

Among the models, the predicted SOC stocks exhibit notable similarities. The primary difference lies in the consistent tendency of one model to predict either higher or lower stocks compared to another model. This often results in a model consistently either overestimating or underestimating the SOC stock relative to the sampled measurements. For example, in Figure 1.13, all models underestimate the stock for Cont W, f-w-w-W*, and F*-w-w, while they overestimate the stock for Cont W, f-w-W*, and F*-w-w in Figure 1.12. According to Riggers et al. (2019), the ICBM/2 model tends to overestimate the SOC stock, particularly when the initial SOC stock is relatively high compared to other prediction models such as C-TOOL, CCB, Century, RothC, and YASSO07.

Among SOC prediction models, they struggle to promptly adapt to significant changes in measured SOC stocks in the short term, as evident by scenarios such as cont-w, f-W*-w, Fw-w, and F-w in Figure 1.12, and f-w-W* in Figure 1.13. However, these models demonstrate greater proficiency in predicting long-term trends in SOC stocks.

In Figure 1.12, the SOC predictions for the Old Rotation demonstrate poor alignment with the soil sampling data across various rotations for all models, particularly evident in panels for cont-w, f-w-W*, and f-W*-w. In contrast, Figure 1.13 illustrates that SOC predictions for the New Rotation are generally more accurate across all models. The varied performance of SOC prediction models on the Swift Current experimental plots highlights the difficulty of accurately predicting cumulative changes in SOC stocks over both short and long periods of time. While the prediction in Figures 1.12 and 1.13 reasonably capture the trends in SOC stock, they fail to capture the variance observed in measured SOC stocks.

Table 1.6 shows the calibration outcomes for various values of the humification scaling parameter γ in the base version of the Augmented Campbell model, as well as different combinations of γ and the weather modifier calibration parameter ε in the weather version. I conduct separate calibrations for each version of the Augmented Campbell model based on the RMSE and d-index, specifically for both the Old Rotation and New Rotation (see columns (3) and (4) in Table 1.6). The calibration parameters for both versions are chosen to minimize the cumulative rank across the RMSE and d-index metrics for both rotations. This process yields a humification scaling parameter of $\gamma = 0.1$ for the base version and $\gamma = 0.2$ along with $\varepsilon = 1.5$ for the weather version

of the Augmented Campbell model. Further calibration with additional SOC data is needed for the Augmented Campbell model to increase the performance of SOC prediction. Out-of-sample predictions are also necessary in understanding the Augmented Campbell's performance relative to the other SOC prediction models used for model validation in this section.

Table 1.6 additionally presents the RMSE and d-index values, along with their rankings, for the Campbell model, Augmented Campbell model, ICBM, ICBM/2, and RothC model. According to the d-index, all models exhibit poor performance on the Old Rotation and moderate performance on the New Rotation. Since all d-index measures surpass 0.5 (refer to column (2)), there is no indication of increased inconsistency or diversity in model predictions (Attia et al., 2016; Banger et al., 2019).

In Table 1.6, column (5) ranks the models according to their RMSE performance. With respect to the Old Rotation, the ICBM, ICBM/2, and RothC models yield the most accurate predictions, while for the New Rotation, the Augmented Campbell model (both base and weather versions) and ICBM/2 are most precise. The Campbell model shows the poorest performance for the Old Rotation, with both the Campbell and RothC models performing equally as bad for the New Rotation. Comparing RMSE values, the Augmented Campbell model (base and weather versions) demonstrates superior accuracy over the Campbell model for both rotations, indicating that the integration of the humification process into the Campbell model—the augmentation—significantly enhances its SOC stock prediction capability.

If SOC prediction models at best predict the trend in the stock of SOC, their ability to provide precise measures of SOC stocks is questionable. This emphasizes the necessity for re-evaluating or improving the calibration and validation of SOC prediction models. Future research in Saskatchewan should focus on better calibration and regional validation of these models if they are to serve as reliable alternatives to soil sampling for accurately quantifying SOC stocks. While SOC prediction models remain valuable for understanding SOC dynamics and trends relative to changes in farm management practices, for cases requiring precise SOC stock measurements, soil sampling remains the preferred method.

TABLE 1.6: Deviation Statistics for Crop Rotation Experiments in Swift Current, Saskatchewan by SOC Prediction Model

	(1)	(2)	(3)	(4)	(5)	(6)
(A) Old Rotation						
Model:	RMSE	d-index	Calibration Rank (RMSE)	Calibration Rank (d-index)	Rank (RMSE)	Rank (d-index)
Augmented Campbell (base)						
$\gamma = 0.01$	4,980	0.590	1	1	5	5
$\gamma = 0.1$	5,153	0.584	2	2		
$\gamma = 0.2$	5,301	0.576	3	3		
$\gamma = 0.3$	5,370	0.572	4	4		
Augmented Campbell (weather)						
$\gamma = 0.01$ & $\varepsilon = 1$	5,531	0.547	9	9		
$\gamma = 0.01$ & $\varepsilon = 1.5$	4,922	0.589	6	6		
$\gamma = 0.01$ & $\varepsilon = 2$	4,937	0.591	5	5		
$\gamma = 0.1$ & $\varepsilon = 1$	4,871	0.591	4	4		
$\gamma = 0.1$ & $\varepsilon = 1.5$	4,764	0.604	2	2		
$\gamma = 0.1$ & $\varepsilon = 2$	5,283	0.576	7	7		
$\gamma = 0.2$ & $\varepsilon = 1$	4,678	0.606	1	1		
$\gamma = 0.2$ & $\varepsilon = 1.5$	4,827	0.601	3	3	4	4
$\gamma = 0.2$ & $\varepsilon = 2$	5,457	0.567	8	8		
Campbell	5,532	0.564			6	6
ICBM	4,265	0.641			2	1
ICBM/2	4,235	0.634			1	2
RothC	4,609	0.616			3	3
(B) New Rotation						
Model:	RMSE	d-index	Calibration Rank (RMSE)	Calibration Rank (d-index)	Rank (RMSE)	Rank (d-index)
Augmented Campbell (base)						
$\gamma = 0.01$	2,708	0.719	2	4		
$\gamma = 0.1$	2,679	0.744	1	1	1	1
$\gamma = 0.2$	2,720	0.743	3	2		
$\gamma = 0.3$	2,753	0.740	4	3		
Augmented Campbell (weather)						
$\gamma = 0.01$ & $\varepsilon = 1$	3,175	0.661	9	9		
$\gamma = 0.01$ & $\varepsilon = 1.5$	2,853	0.704	6	7		
$\gamma = 0.01$ & $\varepsilon = 2$	2,740	0.725	1	5		
$\gamma = 0.1$ & $\varepsilon = 1$	2,988	0.694	8	8		
$\gamma = 0.1$ & $\varepsilon = 1.5$	2,762	0.733	3	4		
$\gamma = 0.1$ & $\varepsilon = 2$	2,778	0.742	4	1		
$\gamma = 0.2$ & $\varepsilon = 1$	2,893	0.712	7	6		
$\gamma = 0.2$ & $\varepsilon = 1.5$	2,759	0.741	2	2	3	2
$\gamma = 0.2$ & $\varepsilon = 2$	2,841	0.736	5	3		
Campbell	2,849	0.724			5	5
ICBM	2,845	0.727			4	4
ICBM/2	2,745	0.730			2	3
RothC	3,019	0.691			6	6

Source: Author's Estimates and created using data from the Experimental Research Station operated by Agriculture and Agri-Food Canada in Swift Current, Saskatchewan.

Notes: The calibrating parameters for the base and weather version of the Augmented Campbell model are selected by choosing the calibrated model which has the highest cumulative rank for both RMSE and d-index statistics across both the Old Rotation and New Rotation.

An emerging body of literature aims to develop improved and more precise SOC prediction models. Riggers et al. (2019), Farina et al. (2021), He et al. (2021), and Thiagarajan et al. (2022) employ an ensemble approach, combining multiple models rather than using a single model, to predict SOC stocks. In this case, different weights are assigned to individual SOC prediction models as a way to calibrate the ensemble of models with soil sampling data.

Researchers are increasingly turning to machine learning techniques to predict SOC stocks, likely due to the constrained calibration flexibility in traditional SOC prediction models. These machine learning-based models incorporate satellite data alongside field-level attributes like soil texture, vegetation characteristics, and crop yield data (see Sothe et al. (2022), St. Luce et al. (2022), and Taneja et al. (2022)). By making use of machine learning algorithms, these models can make more adaptable predictions that are unrestricted by the dynamic parameterization inherent in systems of differential equations.

1.9   Soil Organic Carbon Prediction Results

In this section, the results of SOC stock predictions across 36,443 fields in Saskatchewan from 1998 to 2019 are presented, using six different prediction models. Figure 1.14 shows box and whiskers plots for the field-specific changes in SOC stocks over the 22-year study period for each prediction model, within each of the three soil zones, and across the entire province.[18] Each plot shows 801,746 field-year data points across all soil zones, where the box indicates the interquartile range, the median is denoted by the central line, and the whiskers extend to the minimum and maximum values, excluding outliers. Outliers, identified by Tukey's Method, are plotted as dots, defined as values more than 1.5 times the interquartile range below the first quartile or above the third quartile (Tukey, 1970).

---

[18]All SOC prediction models were executed on a high-performance computing (HPC) cluster at the University of Saskatchewan, using the PLATO server, which is equipped with a SLURM workload manager for batch job management. This server boasts 120 nodes, 7.4 TB of RAM, and 2,000 CPU cores. The SOC prediction tasks were programmed for parallel processing to leverage the multi-core capabilities. The empirical models (Campbell, ICBM, and Augmented Campbell) each completed in roughly 7 hours. In contrast, the RothC model, requiring 40 CPU cores and 128GB of RAM, took between 3 to 4 days to run. Counterfactual scenarios were processed using 30 CPU cores, all running concurrently, with a total runtime of about 7 hours.

FIGURE 1.14: Field-Specific Predicted Change in the Stock of Soil Organic Carbon from 1998 to 2019 by Carbon Prediction model and Soil Zone in Saskatchewan
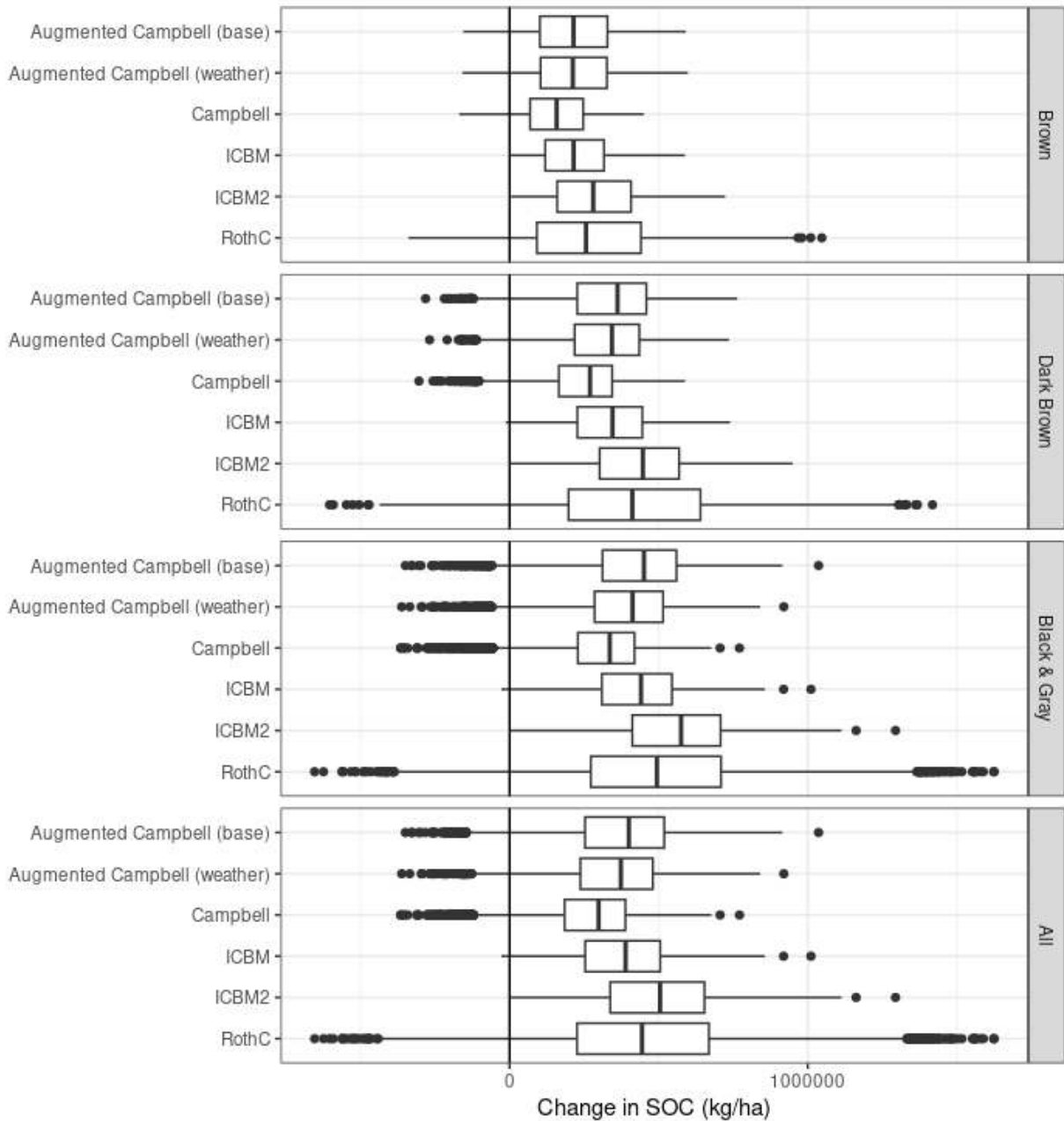
Source: Author's Estimates.

Notes: The box represents the range between the 1st and 3rd quartiles, and the line in the middle of the box represents the median value. The ends of the whiskers are the minimum and maximum values, excluding ouliers represented by dots. Outliers are chosen using Tukey's Method where an outlier is selected if the observation is 1.5 times the interquartile range beyond either the first or third quartiles (Tukey, 1970). This is often referred to as a "fence" boundary where data beyond the fences are outliers.

Figure 1.14 shows that the majority of SOC prediction models predict comparable changes in SOC stocks, with subtle variations. All models yield closely aligned predictions, with the Campbell model indicating the least change in SOC stock, ICBM/2 forecasting the greatest change, and the RothC model exhibiting the broadest range of predictions (widest distribution across fields). These findings align with earlier SOC predictions validated against soil sampling data from long-term crop rotation experiments at Swift Current, Saskatchewan.

In Figure 1.14, the two versions of the Augmented Campbell model produce nearly identical outcomes, albeit with the base version predicting slightly larger SOC stocks. Notably, the weather version of the Augmented Campbell model incorporates weather modifiers affecting decomposition rates, directly affecting the predicted SOC stock. [19]

Among SOC prediction models, the findings shown in Figure 1.14 reveal a consistent pattern: the simulated changes in SOC stock increases from the brown soil zone to the dark brown soil zone, and further to the black & gray soil zone. These changes in simulated SOC stocks are attributed to evolving cropping patterns, crop yields, and weather conditions over time within each soil zone, coupled with reductions in summer fallow hectares. Notably, in the brown soil zone, pulse crops such as lentils and peas constitute a larger proportion of the crop rotation compared to the dark brown and black & gray soil zones. While pulse crops are well-suited to the semi-arid climate of the brown soil zone,[20] they tend to yield lower carbon inputs and consequently result in less carbon sequestration relative to other crops with higher biomass.

Table 1.7 presents statistical summaries of the simulated changes in SOC stock from 1998 to various years (2005, 2011, 2019) across different soil zones and SOC prediction model. These summaries include the mean changes and the bounds of the 90% confidence interval (5% and 95% limits). According to the Augmented Campbell model (weather version), the mean increase in SOC stock from 1998 to 2019 is recorded at 4,437 kg/ha in the brown soil zone (see column (2), Table 1.7), 6,048 kg/ha in the dark brown soil zone, and 7,488 kg/ha in the black & gray soil

---

[19]For a detailed comparison of SOC stock predictions over time between the base and weather versions of the Augmented Campbell model, please refer to Figure 1G.1 in Appendix 1G, which showcases results across six randomly selected fields in Saskatchewan.

[20]The brown soil zone is often referred to as the Palliser Triangle and upon colonization was deemed unsuitable for crop production, owing to its drought-prone semi-arid climate (Marchildon and Sauchyn, 2009).

zone. A sizable share of the SOC stock changes across all zones was observed post-2011, though significant changes began earlier. Specifically, in the brown (dark brown, black & gray) soil zone, 55% (64%, 63%) of the increase occurred between 2005 and 2019, with 34% (36%, 37%) occurring after 2011. Table 1.7 displays the SOC stock changes at the 5% and 95% confidence interval limits for each soil zone, indicating broad confidence intervals. This variation reflects the significant effect of farm management practices and crop selection on carbon sequestration, and is suggestive of the potential for considerable variation in SOC stocks within a soil zone due to differences in field-level management.

Currently, there is a lack of publicly accessible long-term soil sampling data available for validation purposes throughout Saskatchewan. Soil sampling data collected on farms are typically privately owned by both the farmers themselves and the private companies conducting the soil sampling, such as Cargill, Richardson Pioneer, Bayer, and others. Due to the unavailability of soil sampling data for additional validation, I have validated my findings using the same source material that is used to validate SOC predictions in the 2021 GHG National Inventory Report (Environment and Climate Change Canada, 2022). Additionally, in Appendix 1D, I have conducted a comparison of my SOC predictions with those made by Sothe et al. (2022), who employ remote sensing data and machine learning algorithms to predict the average SOC stock from 2015 to 2019 at a spatial resolution of $250m^2$ across Canada. Sothe et al. (2022) develop the first-ever carbon map of Canada at a $250m^2$ spatial grid.

The validation of SOC predictions in the GHG National Inventory Report is conducted by comparing them with regional soil carbon factor changes derived from a Century-based model using the IPCC Tier 1 methodology, as calculated by VandenBygaart et al. (2008). These regional soil carbon factor changes represent the average annual variation in SOC stocks compared to a counterfactual scenario. They are subsequently validated against sampled measurements of SOC stocks obtained by VandenBygaart et al. (2003).

TABLE 1.7: Distribution of Change in the Stock of Soil Organic Carbon per Hectare from 1998 to 2005/2011/2019 by Soil Zone and Prediction Model in Saskatchewan

	(1)	(2)	(3)	(4)	(5)	(6)
	Change in SOC					
	Augmented Campbell (base)	Augmented Campbell (weather)	Campbell	ICBM	ICBM/2	RothC
	(kg/ha)					
A. Brown Soil Zone	1998 - 2005					
Mean	1,917	2,003	1,352	1,934	2,278	1,773
Standard Deviation	1,285	1,271	1,042	1,278	1,355	1,967
5% C.I. Limit	−224	−77	−445	49	247	−1,615
95% C.I. Limit	3,910	4,003	2,921	3,916	4,419	4,759
	1998 - 2011					
Mean	2,875	2,918	2,034	2,781	3,471	2,870
Standard Deviation	1,792	1,716	1,473	1,491	1,665	2,922
5% C.I. Limit	−263	−50	−639	415	789	−2,131
95% C.I. Limit	5,587	5,524	4,179	5,163	6,130	7,342
	1998 - 2019					
Mean	4,422	4,437	3,220	4,543	5,857	5,700
Standard Deviation	2,185	2,111	1,809	1,734	2,069	3,881
5% C.I. Limit	307	545	−296	1,573	2,298	−898
95% C.I. Limit	7,458	7,431	5,619	7,287	9,061	11,753
B. Dark Brown Soil Zone	1998 - 2005					
Mean	2,210	2,154	1,569	2,058	2,489	1,657
Standard Deviation	1,333	1,260	1,084	1,270	1,364	2,418
5% C.I. Limit	−230	−120	−496	19	278	−2,469
95% C.I. Limit	4,173	4,023	3,122	4,127	4,708	5,517
	1998 - 2011					
Mean	3,937	3,883	2,824	3,516	4,463	3,359
Standard Deviation	2,076	1,992	1,702	1,778	2,007	3,775
5% C.I. Limit	−81	74	−585	560	1,059	−3,165
95% C.I. Limit	6,805	6,669	5,097	6,299	7,629	9,409
	1998 - 2019					
Mean	6,338	6,048	4,673	6,281	8,132	7,976
Standard Deviation	2,480	2,305	2,041	2,101	2,544	5,049
5% C.I. Limit	1,302	1,440	437	2,471	3,544	−707
95% C.I. Limit	9,619	9,160	7,293	9,446	12,034	15,791

	(1)	(2)	(3)	(4)	(5)	(6)
	Change in SOC					
	Augmented Campbell (base)	Augmented Campbell (weather)	Campbell	ICBM	ICBM/2	RothC
	(kg/ha)					
C. Black & Gray Soil Zone	1998 - 2005					
Mean	2,954	2,774	2,112	2,690	3,293	2,371
Standard Deviation	1,543	1,459	1,254	1,389	1,508	2,666
5% C.I. Limit	−77	−74	−416	173	542	−2,364
95% C.I. Limit	5,089	4,806	3,781	4,710	5,501	6,352
	1998 - 2011					
Mean	5,027	4,702	3,627	4,174	5,492	4,002
Standard Deviation	2,215	2,091	1,813	1,927	2,158	3,976
5% C.I. Limit	606	547	−68	950	1,765	−3,130
95% C.I. Limit	8,002	7,480	5,978	7,152	8,849	9,928
	1998 - 2019					
Mean	8,155	7,488	6,041	8,076	10,579	9,505
Standard Deviation	2,525	2,370	2,080	2,114	2,588	5,052
5% C.I. Limit	3,184	2,837	1,864	3,988	5,752	556
95% C.I. Limit	11,361	10,529	8,586	11,067	14,382	17,162
D. All Soil Zones	1998 - 2005					
Mean	2,648	2,527	1,888	2,442	2,972	2,115
Standard Deviation	1,517	1,424	1,225	1,383	1,512	2,556
5% C.I. Limit	−154	−88	−453	87	382	−2,322
95% C.I. Limit	4,850	4,600	3,610	4,545	5,297	6,047
	1998 - 2011					
Mean	4,519	4,304	3,252	3,859	5,013	3,715
Standard Deviation	2,255	2,110	1,829	1,905	2,182	3,847
5% C.I. Limit	187	275	−356	739	1,331	−3,002
95% C.I. Limit	7,681	7,253	5,732	6,884	8,499	9,652
	1998 - 2019					
Mean	7,295	6,797	5,392	7,240	9,449	8,719
Standard Deviation	2,766	2,529	2,242	2,387	2,986	5,087
5% C.I. Limit	1,842	1,837	869	2,862	4,047	−93
95% C.I. Limit	10,976	10,186	8,286	10,698	13,856	16,648

Source: Author's Estimates

VandenBygaart et al. (2003) conduct a meta-analysis, compiling annual changes in SOC stocks per hectare in Canada following a land management change to no-till practices from either conventional tillage or summer fallow. Liang et al. (2020) update this review by incorporating an additional 16 peer-reviewed studies, bringing the total to 37. This updated meta-analysis revealed that in western Canada, the adoption of no-till practices led to an average annual increase in SOC stocks of 740 kg/ha/yr ($\pm$ 220 kg/ha/yr) after 10 years, and 260 kg/ha/yr ($\pm$ 50 kg/ha/yr) in the subsequent decade. No-till systems in western Canada exhibit an average SOC stock increase of 300 kg/ha/yr in medium-textured soils and 430 kg/ha/yr in fine-textured soils.[21]

The weather version of the Augmented Campbell model, the SOC stock in Saskatchewan increased by 309 kg/ha/yr ($\pm$ 115 kg/ha/yr) between 1998 and 2019. This growth varied across soil zones, with the black & gray zone seeing an increase of 340 kg/ha/yr, the dark brown zone 274 kg/ha/year, and the brown soil zone 201 kg/ha/year. Given that a significant portion of soils in Saskatchewan are either medium-textured (such as silt, silt loam, loam, or sandy clay loam) or fine-textured (including sandy clay, clay loam, silty clay loam, silty clay, or clay),[22] the annual SOC stock changes in Saskatchewan as predicted by the Augmented Campbell model align closely with the range of annual SOC stock changes under no-till practices reported in meta-analysis done by Liang et al. (2020).

The results presented in this section offer insights into the geographical distribution of carbon sequestration within Saskatchewan, highlighting areas of significant growth of SOC stocks. Notably, there are additional environmental factors beyond those considered in this analysis, such as the reduction in atmospheric carbon equivalent through albedo radiative forcing resulting from practices like no-till, continuous cropping, and the planting of reflective crops like canola, peas, and lentils (Liu et al., 2022). Research by Liu et al. (2022) suggest that these additional albedo changes have led to a drawdown of 179.9 Tg of carbon dioxide equivalent from no-till practices and 101.6 Tg from continuous cropping in the Canadian Prairies between 1990 and 2019. Given that the SOC stock is influenced by carbon inputs that are linked to crop yields, it is pertinent for

---

[21]In western Canada, 62% of the data analyzed in this meta-assessment were derived from medium-textured soils.

[22]The Saskatchewan Soil Information System provides in-depth information by location on soil type, texture, and soil characteristics for all agricultural land in Saskatchewan (University of Saskatchewan, 2023).

crop-breeding efforts to consider the implications for carbon sequestration, including the development of higher-yielding, drought-tolerant varieties.

1.10   Soil Sampling Data for Model Validation and Limitations

In Saskatchewan, the Prairie Soil Carbon Balance (PSCB) project conducted soil sampling across the province from 1996 to 2018 to monitor changes in SOC stocks (McConkey et al., 2020). Initially encompassing a network of 136 fields operated by commercial farms in 1996, the project's scope reduced to 90 fields by its final year in 2018. Throughout the duration of the project, there were variations in sampling methods, technology, and laboratory analysis techniques.[23]   SOC stock changes were calculated on an equivalent mass basis, employing six cores at each site sampled at 40cm depth intervals with 10cm increments.[24] Sampling in 1996, 1999, 2005, and 2011 occurred in the fall post-harvest, while in 2018, sampling took place in the spring, with some samples collected before and after seeding.

Aggregate findings of the PSCB project are detailed in a report to the Saskatchewan Soil Conservation Association (see McConkey et al. (2020)). Comparing these aggregated findings with the results presented in this essay, it appears that the changes in SOC stocks documented by the PSCB project from 1996 to 2018 align more closely with the lower 5% interval of the 90% confidence interval for the changes in SOC stocks from 1998 to 2019 within Saskatchewan predicted by the Augmented Campbell model.

The management data in the PSCB project are limited and described as "spotty" in the 2020 report (McConkey et al., 2020). Only 56 sites had management data with nine years of information. Because the management information in the PSCB project is limited, it is difficult to compare the SOC predictions made using SCIC data with the measured changes from the PSCB project. Because of the large variation in SOC stocks in Saskatchewan, the small sample size in the PSCB project makes it impossible to conduct any meaningful validation. The entire PSCB project makes

---

[23]Verified with personal communication with Dr. Mervin St. Luce, a project leader of the PSCB project.

[24]Ellert and Bettany (1995) and Rovira et al. (2022) advocate for the equivalent mass approach as the preferred method for SOC stock calculation, which adjusts for changes in soil mass at fixed depths.

up 0.25% of the fields used to predict SOC stocks from the SCIC database. Hence, without any management information, using data from the PSCB project will entail a sizable risk of sample selection bias for validation.

Paustian et al. (2019) also note technical discrepancies with the PSCB project. Reflecting on the period before the 2018 sampling in the PSCB project, Paustian et al. (2019, p. 580) state: "this 15-year study illustrates some of the logistical challenges of direct sampling of SOC through time. During the study, there were numerous changes in ownership or land management at the study sites and some sites were lost to attrition. In 2005, 121 of the original 137 sites were sampled, and at the last sampling in 2011, only 82 sites has the required management data and manager authorization for inclusion in the project. Additionally, because of the heterogeneity of SOC within fields (30–65 ha), it was prohibitively expensive to collect enough samples to estimate the average stock across the field."

The lack of comprehensive farm management and production data, and an adequate sample size, contribute to uncertainty on how well the sites in the PSCB project and their observed changes in SOC stocks correspond with the simulated SOC stocks in this analysis. This highlights the importance of gathering comprehensive farm management and production data, with consistent soil sampling methods and methodologies. Doing so is crucial for accurately validating SOC prediction models.

1.11   The External Social Benefit from Changes in Soil Organic Carbon

In this section, I describe the approach used to calculate the annual external social benefits of SOC sequestered on Saskatchewan farms over the period 1998–2019. These benefits may be determined as the avoided social cost of carbon emissions, compared with a counterfactual alternative in which the entire stock of SOC would have been emitted into the atmosphere. However, it is improbable all SOC would be released from the soil in any reasonable scenario. To measure the

external social benefits from any particular action affecting the stock of SOC, and hence atmospheric carbon, the crucial step is to define and appropriately quantify the corresponding counterfactual scenario. Here, the relevant counterfactuals are defined and quantified in terms of changes in the SOC stocks that would have resulted from hypothetical partial reversals of past changes in agricultural practices or transitions to different land uses.

Mikhailova et al. (2019) pose a methodology for assessing the value of SOC stocks making use of a conversion factor of SOC to carbon dioxide and available estimates of the social cost of atmospheric carbon. They use a conversion factor of 44 Mg CO_2 per 12 Mg SOC and a social cost of carbon (SCC) of 42 U.S. dollars per incremental Mg (metric ton) of carbon dioxide permanently added to the atmosphere, calculated using a real discount rate of 3% per year (Environmental Protection Agency, 2016).

In 2021, President Biden made an Executive Order 13990 for the Interagency Working Group on Social Cost of Greenhouse Gases (IWG) to estimate and publish an interim SCC value (Interagency Working Group on Social Cost of Greenhouse Gases, 2021).[25] Using a real discount rate of 3% per year the IWG (2021) computed an SCC of 51 U.S. dollars (in 2020 dollars) per Mg of CO_2 in February 2021. The IWG's SCC ranges from $14 per Mg of carbon dioxide using a discount rate of 5% per year to $76 per Mg of carbon dioxide using a discount rate of 2.5% per year. Alternatively, Rennert et al. (2022) estimates a SCC that is greater than the IWG's SCC, equal to $185/Mg of CO_2. Rennert et al. (2022) uses several damage functions and discount rates to estimate the SCC, and calculate their preferred SCC of $185/Mg using the Greenhouse Gas Impact Value Estimator

---

[25]IWG uses three integrated assessment models (i.e., DICE, PAGE, and FUND) from peer-reviewed research to determine the SCC. These estimates are to be upheld in courts for government policy and regulation, are updated on a continual basis, and undergo several rounds of review by the peer reviewers, analysts, and stakeholders (Interagency Working Group on Social Cost of Greenhouse Gases, 2021).

(GIVE) damage function with a 2% near-term risk-free discount rate.[26, 27]

I employ SCC values of \$14/Mg, \$51/Mg, and \$76/Mg from the IWG, and \$185/Mg from Rennert et al. (2022) to compute a range of estimates for the external social benefits of carbon sequestration in Saskatchewan from 1998 to 2019. These values are expressed in real 2023 dollars, using the GDP Deflator from the Federal Reserve Bank of St. Louis (U.S. Bureau of Economic Analysis, 2024).

The standard formula for the present value in the current year, t of a stream of annual social benefits over an indefinite future horizon is:

$$PV_t = \sum_{n=1}^{\infty} SB_{t+n}(1+r)^{-n}, \tag{1.16}$$

where PV_t is in constant, inflation-adjusted dollars in year t, r is the corresponding real discount rate, and SB_{t+n} is the social benefit in year $t+n$. In this application, SB_{t+n} is the benefit from the introduction of a policy aiming to increase the stock of SOC over time, defined as

$$SB_{t+n} = P_t(SOC_{t+n}^A - SOC_{t+n}^C)$$

(1.17)

$$\text{where } P_t = r \times SCC_t \times \frac{44 \text{ Mg CO}_2}{12 \text{ Mg SOC}},$$

---

[26]The near-term discount rate used by Rennert et al. (2022) is equal to the average risk-free discount rate over the first decade of the time horizon, and incorporates a Ramsey-like framework to value the marginal damages from CO_2 to account for the risk and uncertainty in future payoffs. The discount rate is determined by the Ramsey-like equation: $r_t = \rho + \eta g_t$. The variable g_t is the average rate of consumption growth from the year of the emission pulse (a 0.1 Mt pulse of CO_2 emissions), whereas parameter ρ represents the rate of pure time preference and η reflects how much the marginal value of consumption decreases as consumption increases. At a 2% near-term risk-free discount rate, the discounting parameters are $\rho = 0.2\%$ and $\eta = 1.24$. In this essay, I use the framework employed by the IWG and assume a constant, deterministic discount rate with the SCC provided by Rennert et al. (2022). This means that the environmental benefits computed in this analysis are considered to be a lower-bound in comparison to applying Ramsey-like discounting as done by Rennert et al. (2022).

[27]Russell et al. (2022) find that depending on the Representative Concentration Pathways (RCPs) in temperature projections and Shared Socioeconomic Pathways (SSPs), the SCC could be as low as \$2.35/Mg of CO_2 as high as \$258.40/Mg of CO_2.

P_t is the annual rental price in 2023 U.S. dollars for an additional unit of SOC reflecting the value of atmospheric carbon and the conversion rate from SOC to atmospheric carbon,[28] and SOC_{t+n}^i is the stock of SOC in year $t+n$ under scenario i, where $i = A$ refers to the "actual" or with-policy scenario and $i = C$ refers to the "counterfactual" or without-policy scenario, such that the term in parentheses is the policy-induced change in the SOC stock. Benefits start to accrue in the following year ($n = 1$) because the initial stock of SOC for both the actual and counterfactual scenarios in year t are equal, and results in an social benefit in year t equal to zero.

Combining equations (1.16) and (1.17), equation (1.18) represents the present value of the external social benefit from the policy-induced changes in the stock of SOC over the indefinite future, and provides a money-metric measure of the future external benefits to society from policy-induced changes in sequestered carbon emissions.

$$PV_t = \sum_{n=1}^{\infty} P_t(SOC_{t+n}^A - SOC_{t+n}^C)(1+r)^{-n}. \tag{1.18}$$

An equivalent approach for a backwards-looking assessment of social benefits from a policy-induced change in farming practices introduced N years in the past yields:

$$PV_t = \sum_{n=1}^{N} P_t(SOC_{t-n-1}^A - SOC_{t-n-1}^C)(1+r)^{(n-1)}. \tag{1.19}$$

Let r be the real discount rate used to calculate the respective SCC. To ensure the SCC accurately reflects the present value of all future welfare effects resulting from a marginal increase in atmospheric CO_2 in the present context, the discount rate applied to compute the present value of policy-induced changes in SOC stocks should be the same as the discount rate used to estimate the SCC. Pearce (2003) provides further details on the SCC. Appendix 1F provides a mathematical derivation and proof, illustrating how the discount rate, as derived from the SCC, quantifies the effect of an additional unit of CO_2 emitted into the atmosphere over a definite time horizon.

---

[28]If this annual flow of social benefits is constant forever, then the value of the perpetuity per ton, $/Mg is given by $V = P/r$, where r is the IWG's real discount rate for the social cost of atmospheric carbon. For example, if $V = \$51/Mg$, then the equivalent annual rental price is $P = 0.03 * V = \$1.53/Mg$.

I define counterfactual scenarios with lower adoption rates of zero-tillage and continuous cropping on Saskatchewan farms compared with the observed rates. Using two carbon prediction models (specifically, the Campbell model and Augmented Campbell model (weather version)), I simulate counterfactual scenarios in which a certain percentage of canola or lentil hectares is instead set to summer fallow each year. This percentage is determined using random draws from a binomial distribution. Equation (1.20) is the equation for the binomial distribution, where $P(Canola^C | Canola^A = 1)$ represents the probability of seeding canola on a field given it was actually sown with canola, n is the number of trials or experiments, x is the number of times canola is not switched to summer fallow within a trial, p is the probability of canola fields that are not switched to summer fallow in a trial, and q is the probability of switching canola to summer fallow in a trail. Each field is subjected to a Bernoulli trial (i.e., one trial per field per year), where the probability of switching canola to summer fallow corresponds to the desired counterfactual scenario (e.g., 25%, 50%, or 75% of canola hectares converted to summer fallow). This procedure remains constant throughout the simulation model, with a draw from the binomial distribution followed by application of the Campbell and Augmented Campbell model (weather version).

$$P(Canola^C | Canola^A = 1) = \binom{n}{x} p^x q^{n-x} = \frac{n!}{x!(n-x)!} p^x q^{n-x} \tag{1.20}$$

I perform thirty simulations for each counterfactual scenario across all fields in the selected sample, totaling 1,093,290 fields. These simulations are conducted using the same seed of the random number generator in R for subsequent draws for a specific counterfactual scenario.[29] Subsequently, I predict the SOC stocks for all counterfactual scenarios to generate a distribution of multiple time-paths for each field. These distributions represent the counterfactual SOC stocks for each field from 1998 to 2019.

---

[29]By employing the same seed for subsequent draws from the binomial distribution in R, I ensure that different random outcomes are generated for separate counterfactual draws on the same field.

FIGURE 1.15: Soil Organic Carbon Stock per Hectare for a Randomly Selected Field in the Black & Gray Soil Zone with respect to the Counterfactual draws from the Binomial Distribution

Source: Author's Estimates.

Notes: In every panel, the solid black line depicts the simulated actual SOC stock in the base-line scenario for a field chosen at random. In the left column, all lines other than the solid black one show the simulated SOC stocks from various draws of the binomial distribution for a particular counterfactual scenario, each draw randomly converting a percentage of canola hectares to summer fallow. On the right column, the red dashed line illustrates the average simulated SOC stock derived from 30 binomial draws (representing the mean of all SOC stocks shown in the left panel, excluding the solid black line).

Figure 1.15 displays the predicted SOC stocks derived from the Augmented Campbell model (weather version) for a single field chosen at random within the black & gray soil zone,[30] illustrating variation among random selections from the binomial distribution. The figure is organized into three rows, each corresponding to different probabilities of converting canola fields back to fallow land. On the left column of each row, various lines indicate individual outcomes from the binomial distribution, with the solid black line marking the actual SOC stock in the baseline simulation, with actual cropping patterns. On the right column of each row, the figure displays the average SOC stocks across all binomial draws for each counterfactual scenario of converting canola to summer fallow (indicated by a red dashed line) compared with the original simulated SOC stock (depicted by a solid black line).

Employing these measures, I assess the differences between the counterfactual mean SOC stocks and the actual SOC stocks in the baseline simulation for each field. Figure 1.16 illustrates the divergence in the trajectory of the mean SOC per hectare across different soil zones (weighted by hectares) for each counterfactual scenario. The SOC stocks depicted in Figure 1.16 are predicted using the weather version of the Augmented Campbell model. Each plot depicts weighted average stock of SOC from 1998 to 2019 in Saskatchewan for each counterfactual scenario, resulting from switching a certain percentage of canola to summer fallow (25%, 50%, and 75%).

Figure 1.16 highlights the differences in SOC stocks for each time path for each counterfactual scenario and soil zone. The differences between the actual SOC stock and the counterfactual scenarios are more pronounced in the black & gray soil zone. Disparity arises due to the higher proportion of canola hectares in the black & gray soil zone compared with the brown and dark brown soil zones. Hence, switching a set percentage of canola hectares to summer fallow has a more substantial affect on SOC stocks within the black & gray soil zone compared to the dark brown and brown soil zones.

---

[30]Due to the confidentiality of field location and identity within the SCIC dataset, I refrain from disclosing any details about this particular field, except for the fact that it was chosen randomly to illustrate the effect of various binomial outcomes for different hypothetical scenarios of converting canola hectares to summer fallow.

Weighted Average Soil Organic Carbon Stock per Hectare by Soil Zone and Counterfactual Scenario in Saskatchewan from 1998 to 2019
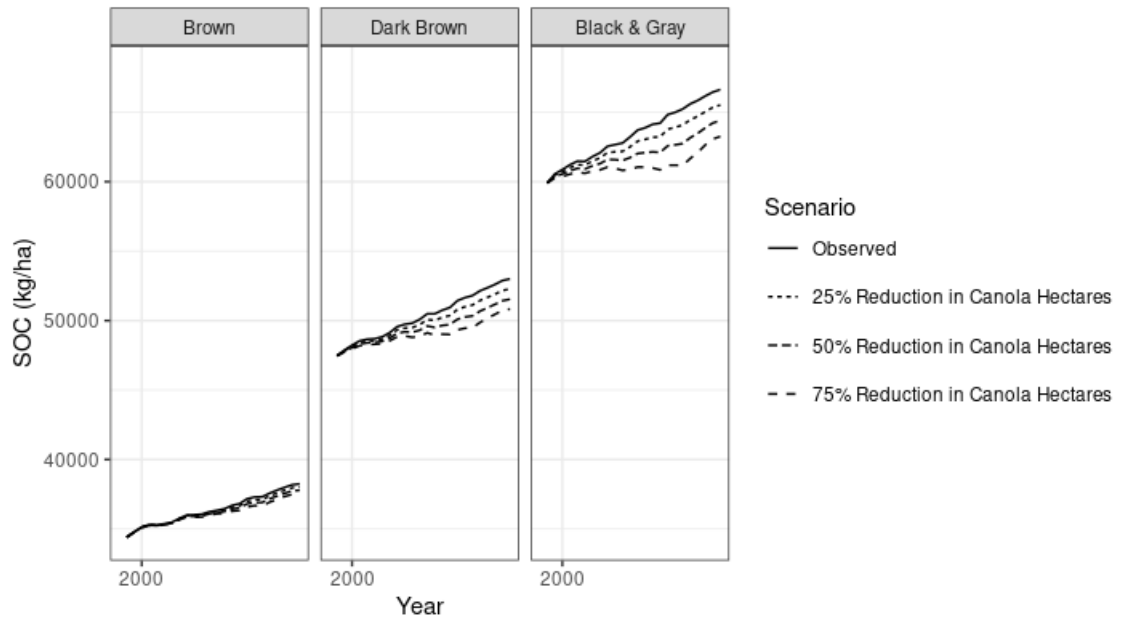
Source: Author's Estimates.

FIGURE 1.17: Weighted Average Soil Organic Stock per Hectare by Draw from the Binomial Distribution in the Black & Gray Soil Zone from 1998 to 2019
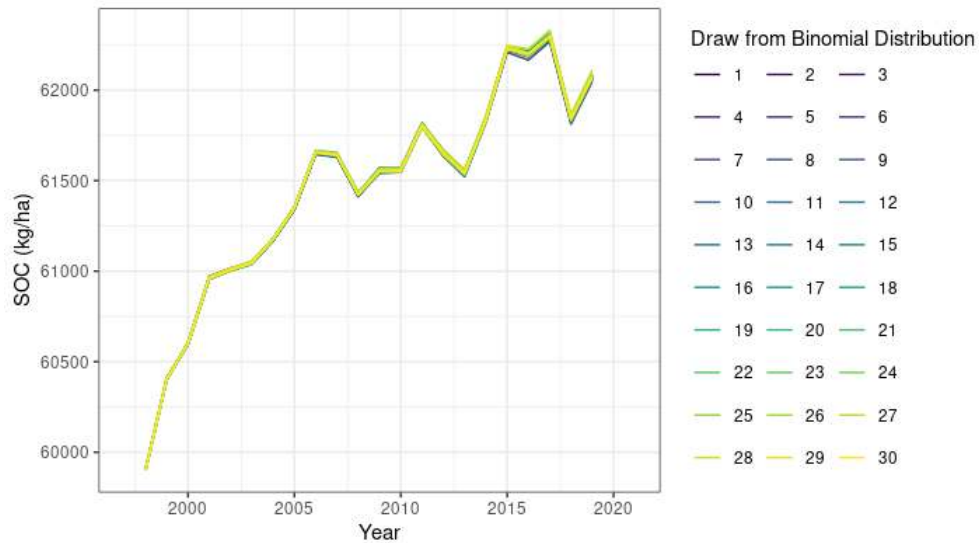
Source: Author's Estimates.

Notes: Draws from the binomial distribution are based on the counterfactual scenario of switching 75% of canola hectares to summer fallow.

Figure 1.17 illustrates the range of outcomes in the time path of the weighted average SOC stock per hectare when 75% of the provincial canola hectares transition to summer fallow in the black & gray soil zone. Variability in the weighted average SOC stock per hectare among binomial draws tends to become larger in later years (i.e., 2015–2019), as SOC stocks undergo dynamic adjustments reflecting historical changes in canola hectares. Nevertheless, the disparity in the aggregate change of SOC stocks across binomial draws remains relatively minor compared to the variance observed at the individual field level. This is primarily because the effects of switching canola from one field to another are largely consistent, differing primarily based on the seeding year and canola yield. Consequently, when aggregated, the disparities across binomial draws in the weighted average change in SOC stocks become negligible.

1.12 External Social Benefit from Carbon Sequestration Results

In this section, I provide the results from computing the external social benefits for each year between 1998 and 2019 by applying a rental rate to the annual difference between the simulated SOC stocks associated with actual production and the simulated SOC stocks associated with the respective counterfactual scenario, summarized as a present value. This approach assesses the societal benefits derived from actual adoption and use of practices such as zero-tillage and continuous cropping, compared with counterfactual scenarios involving less canola adoption, more summer fallow, and more tillage. The calculations for the external social benefits are initially performed for each field within the selected SOC prediction sample. These values are then normalized on a per-hectare basis and scaled up to encompass all hectares insured by SCIC in Saskatchewan. This process yields a comprehensive provincial-level estimate of the external benefits associated with enhanced carbon sequestration under each counterfactual scenario. The approximation is deemed suitable, given the comparable crop yields and crop shares between the samples, as illustrated in Figures 1E.1 and 1E.2 in Appendix 1E.

Figures 1.18 to 1.20 present the per-field distribution of the external social benefits derived from increased carbon sequestration between 1998 and 2019, compared with the a counterfactual scenario in which canola hectares revert to summer fallow. This analysis does not account for the

potential dynamic effects of carbon sequestration on crop yield which would feed back into SOC. Therefore, the findings here should be viewed as conservative estimates regarding how carbon sequestration affects SOC. The calculations of external social benefits follows equation (1.16), using a value for the SCC expressed in 2020 U.S. dollars. The estimates of benefits are adjusted to 2023 dollars using a GDP Deflator provided by the Federal Reserve Bank of St. Louis (U.S. Bureau of Economic Analysis, 2024). Each distribution in Figures 1.18 to 1.21 represents the present value of external social benefits per hectare in the period from 1998 to 2019 for 36,443 fields, including 30 draws from the binomial distribution for each counterfactual scenario. Specifically, Figure 1.18 illustrates the benefits at a $14/Mg SCC, while Figures 1.19, 1.20, and 1.21 apply SCC values of $51/Mg, $76/Mg, and $185/Mg, respectively.

Across soil zones, the benefits vary considerably, reflecting differences in the external social benefits per hectare, the total number of fields, and the proportion of land planted to canola. The external social benefits per hectare are notably less in the brown soil zone, than in the other zones. This is largely because not all fields are planted with canola or undergo the counterfactual treatment where canola is replaced with summer fallow, leading to a concentration of benefits at zero in the brown soil zone. This phenomenon is more pronounced in scenarios in which a smaller percentage of canola hectares are converted to summer fallow, resulting in fewer fields being subject to this counterfactual treatment. As anticipated, the benefits per hectare increase with a higher SCC. Over the period from 1998 to 2019, the weighted average benefit per hectare across the analyses in Figures 1.18 to 1.21 varies, showing a range from $0.51/ha to $5.44/ha in the brown soil zone, from $1.94/ha to $22.78/ha in the dark brown soil zone, and from $3.36/ha to $40.97/ha in the black & gray soil zones.

I also calculate external social benefits per hectare using the Campbell model, yielding slightly lower estimates than those obtained from the Augmented Campbell model. Please refer to Figures 1G.2 to 1G.5 in Appendix 1G to view the computed field-level external social benefits per hectare derived using the Campbell model. Figures 1G.6 and 1G.7 in Appendix 1G present findings for a scenario in which 25% of lentil hectares are counterfactually converted to summer fallow. In this case, the weighted average benefit per hectare varies, ranging from $0.42/ha to $1.49/ha in

the brown soil zone, $0.35/ha to $1.21/ha in the dark brown soil zone, and $0.02/ha to $0.07/ha in the black & gray soil zones. The greatest benefits are observed in the brown soil zone, which is the predominant area for lentils. Because lentils have less carbon sequestration capacity than canola, the external social benefits foregone by reverting 25% of lentil acres to summer fallow are significantly less than those foregone by similar reversions of canola hectares.

Figure 1G.8 in Appendix 1G shows the variability in external social benefits for a single randomly selected field within the black & gray soil zone, as depicted in Figure 1.15, across different binomial distribution draws. This figure highlights how the external social benefit per hectare for this particular field can significantly vary depending on the specific draw from the binomial distribution, the counterfactual scenario considered, and the SCC applied. While Figure 1G.8 focuses on the external social benefits for all fields from just one binomial distribution draw, Figure 1G.9 compares the distribution of external social benefits per hectare for a single draw against the distribution from all draws in Figure 1.19, both employing a SCC of $51/Mg. This comparison demonstrates that while there is notable variation in benefits for a single field across different binomial draws, the overall distribution of benefits across all fields remains consistent across different binomial draws.

FIGURE 1.18: Field-level Distribution of External Social Benefit per Hectare by Draw of the Binomial Distribution, Counterfactual Scenario and Soil Zone in Saskatchewan using the Augmented Campbell Model (weather) and a Social Cost of Carbon of $14/Mg
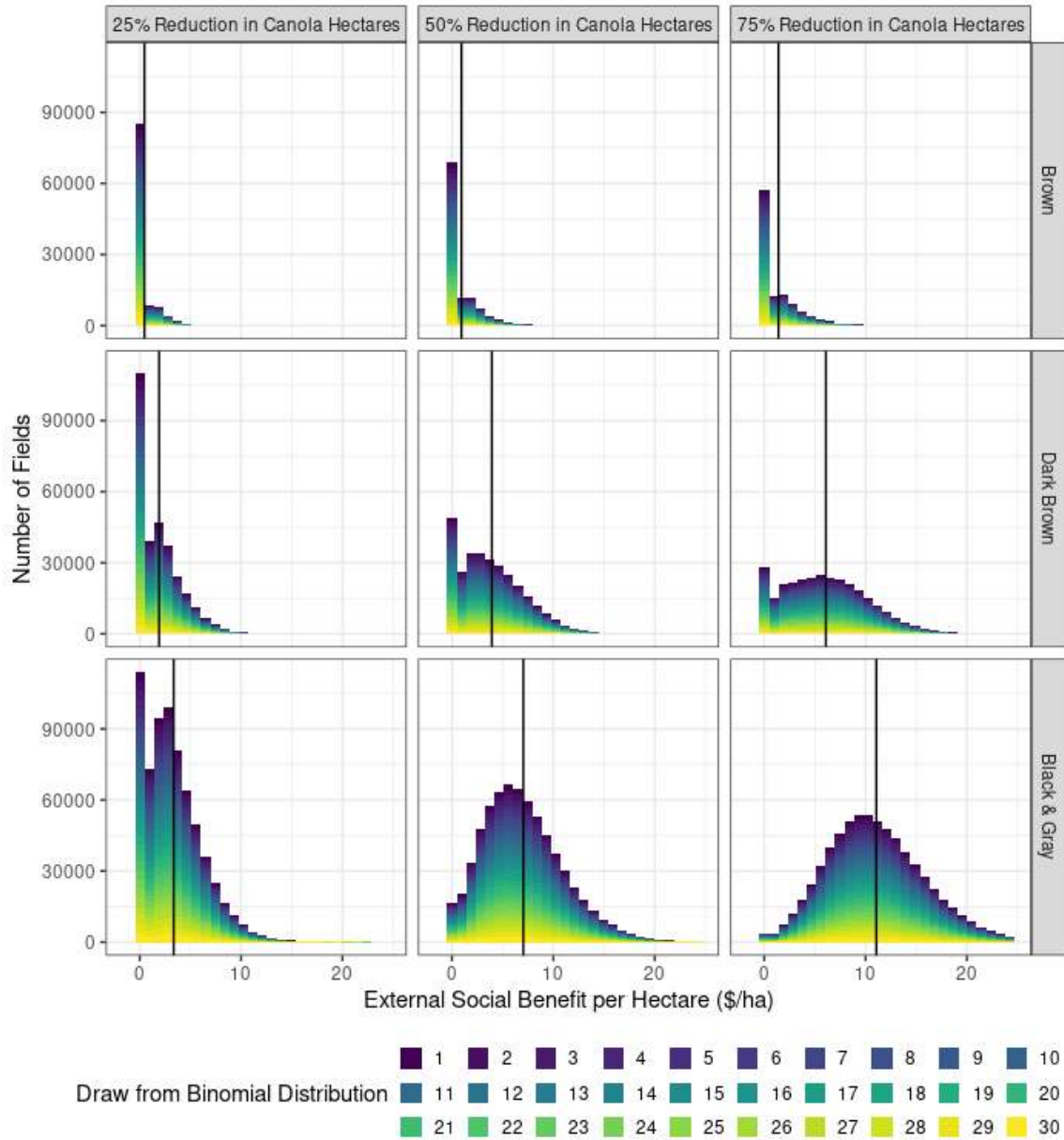
Source: Author's Estimates.

Notes: All soil organic carbon predictions in the above graph are computed using the Augmented Campbell model. The columns of panels refer to the counterfactual shares of canola switched to summer fallow (25%, 50%, and 75%) of insured hectares in Saskatchewan, whereas the rows of panels refer to different soil zones.

FIGURE 1.19: Field-level Distribution of External Social Benefit per Hectare by Draw of the Binomial Distribution, Counterfactual Scenario and Soil Zone in Saskatchewan using the Augmented Campbell Model (weather) and a Social Cost of Carbon of $51/Mg

Source: Author's Estimates.

Notes: All soil organic carbon predictions in the above graph are computed using the Augmented Campbell model. The columns of panels refer to the counterfactual shares of canola switched to summer fallow (25%, 50%, and 75%) of insured hectares in Saskatchewan, whereas the rows of panels refer to different soil zones.

65
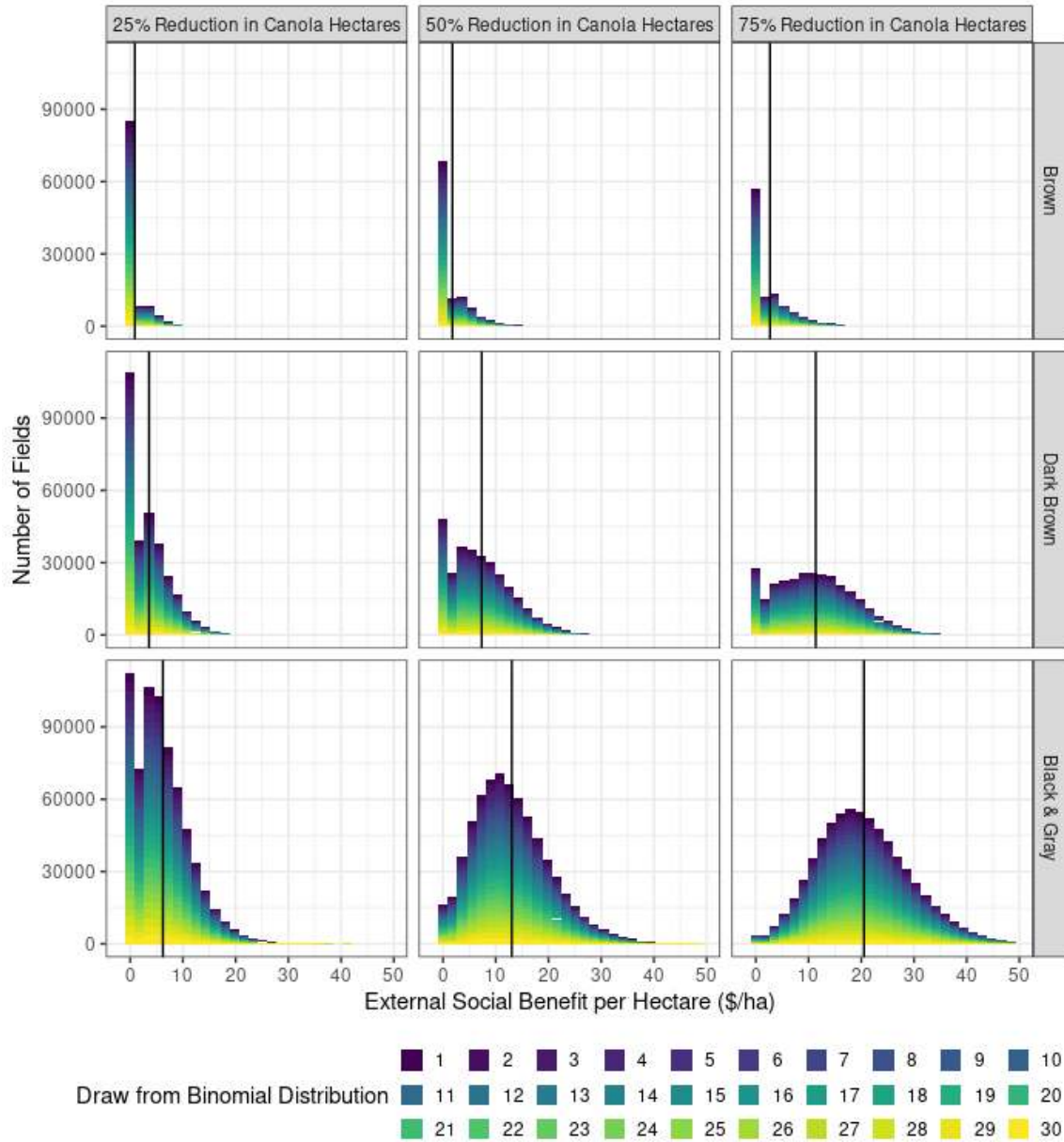
FIGURE 1.20: Field-level Distribution of External Social Benefit per Hectare by Draw of the Binomial Distribution, Counterfactual Scenario and Soil Zone in Saskatchewan using the Augmented Campbell Model (weather) and a Social Cost of Carbon of $76/Mg
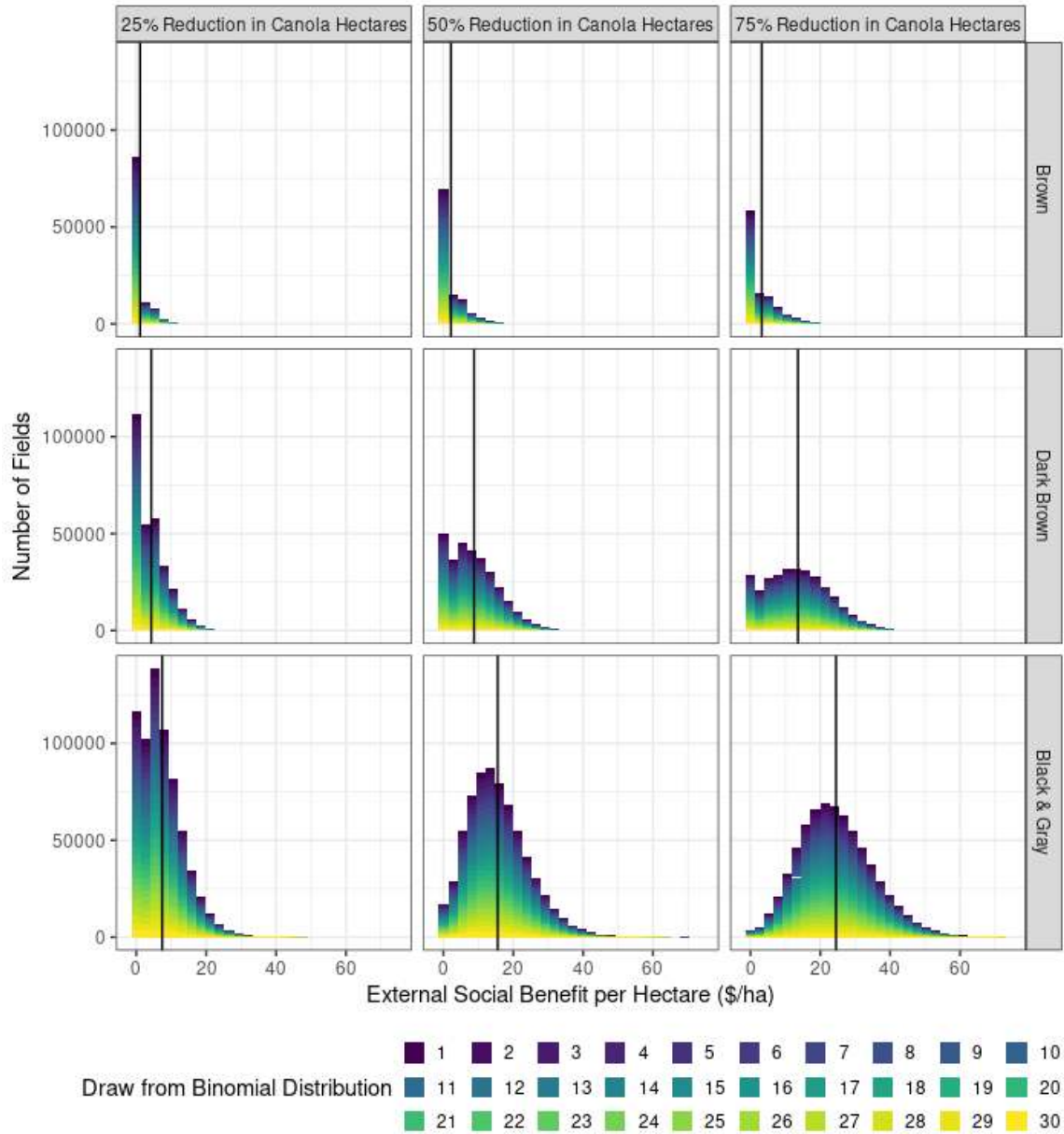
Source: Author's Estimates.

Notes: All soil organic carbon predictions in the above graph are computed using the Augmented Campbell model. The columns of panels refer to the counterfactual shares of canola switched to summer fallow (25%, 50%, and 75%) of insured hectares in Saskatchewan, whereas the rows of panels refer to different soil zones.

FIGURE 1.21: Field-level Distribution of External Social Benefit per Hectare by Draw of the Binomial Distribution, Counterfactual Scenario and Soil Zone in Saskatchewan using the Augmented Campbell Model (weather) and a Social Cost of Carbon of $185/Mg
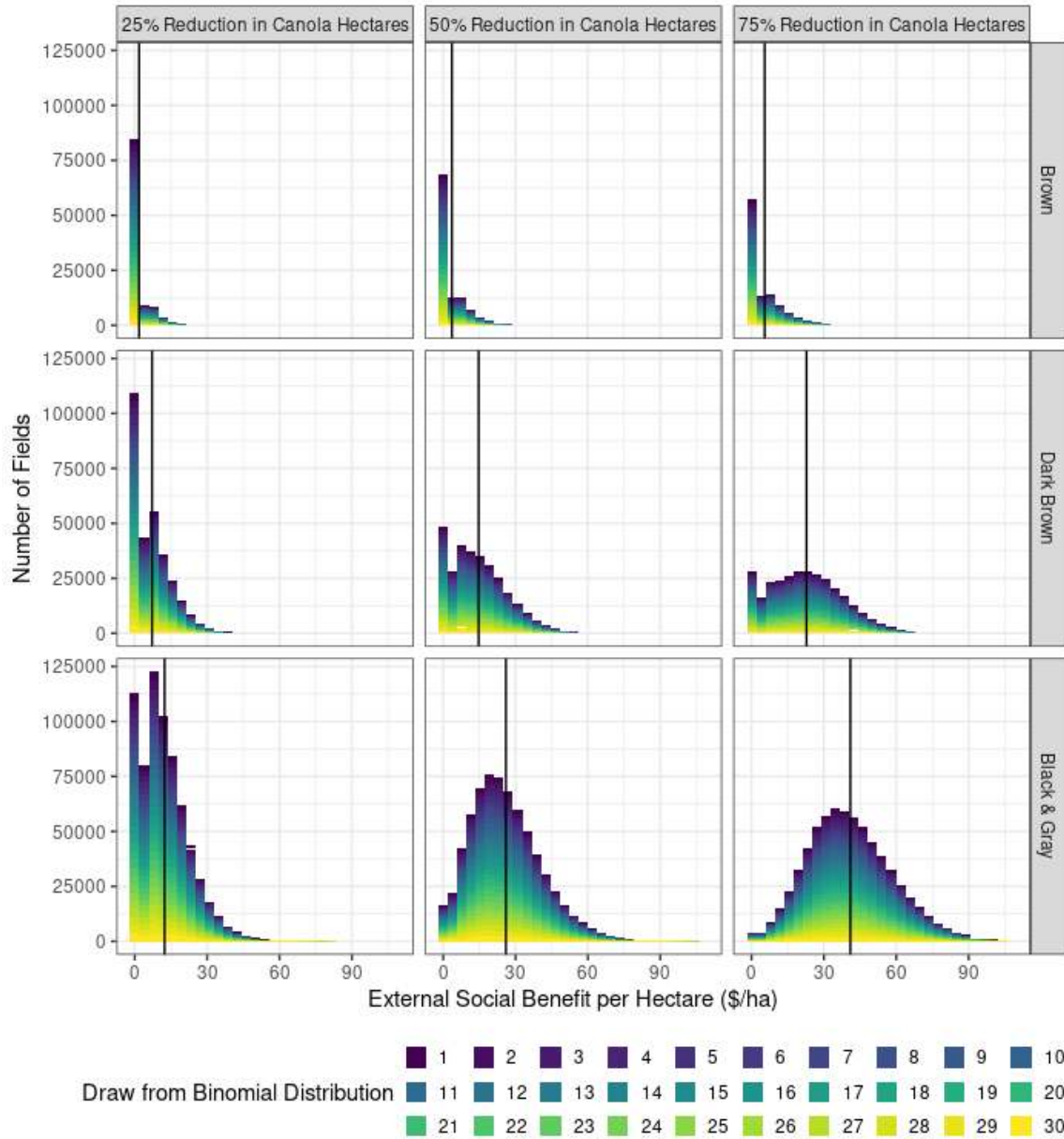
Source: Author's Estimates.

Notes: All soil organic carbon predictions in the above graph are computed using the Augmented Campbell model. The columns of panels refer to the counterfactual shares of canola switched to summer fallow (25%, 50%, and 75%) of insured hectares in Saskatchewan, whereas the rows of panels refer to different soil zones.

Table 1.8 shows the cumulative external social benefits estimated for each counterfactual scenario across various soil zones and SCC rates, using the weather version of the Augmented Campbell model to simulate SOC stocks. Meanwhile, in Appendix 1G, Table 1G.1 shows the external benefits computed using the Campbell model to predict all SOC stocks. To compute the total external social benefit for each counterfactual scenario across Saskatchewan, I use the total insurable hectares from the SCIC database spanning from 1998 to 2019, along with the weighted average external social benefits per hectare extracted from Figures 1.18 to 1.21. Table 1.8 provides insights into the range of estimated external social benefits, including the minimum, mean, and maximum values, corresponding to different draws from the binomial distribution, considering each SCC, counterfactual scenario, and soil zone. Because the computed external social benefits depend on the dynamics of SOC stocks, the benefits in Table 1.8 are not proportional to the share of canola reverted to summer fallow as a result of differences in crop yields and crops shares across soil zones. The external social benefits are also not proportional to the SCC employed because benefits are computed using a different discount rate for each SCC.

I estimate that, compared with a counterfactual scenario in which some fraction of canola hectares reverted to summer fallow, the adoption of zero-tillage and continuous cropping in Saskatchewan yielded external social benefits over the period 1998 to 2019 ranging (in 2023 present value terms) from $481 million to $6 billion. The range of values depends up the draw from the binomial distribution, the chosen counterfacual scenario, and the SCC employed. The mean benefit across binomial draws is equal to $5.9 billion when a SCC of $185/Mg of CO_2 is applied, as proposed by Rennert et al. (2022).[31]

 With the counterfactual scenario of converting lentil hectares to summer fallow, the estimated benefits span from $44 million to $182 million. Broadly speaking, compared to counterfactual scenarios featuring reduced canola hectares and increased summer fallow and tillage from 1998 to 2019, the adoption of zero-tillage and continuous cropping practices represents a value in the billions of dollars in terms of external social benefits.

---

[31]The computed external social benefit exhibits relative consistency across various draws from the binomial distribution, fluctuating by a maximum of $75 million across different draws within a given counterfactual scenario.

TABLE 1.8: Distribution of External Social Benefits from 1998 to 2019 by Counterfactual Scenario, Soil Zone, and Social Cost of Carbon in Saskatchewan using the Augmented Campbell model (weather)

	(1)	(2)	(3)	(4)
	External Social Benefit			
Counterfactual:	Share of Canola Hectares reverted to Summer Fallow			Share of Lentil Hectares reverted to Summer Fallow
	25%	50%	75%	25%
	(i) Brown Soil Zone			
Social Cost of Carbon:	*(millions of dollars)*			
$14/Mg				
Mean	21	43	65	18
Minimum	20	41	64	17
Maximum	23	44	66	19
$51/Mg				
Mean	41	83	124	34
Minimum	39	79	122	32
Maximum	43	85	126	37
$76/Mg				
Mean	49	99	150	41
Minimum	47	95	147	39
Maximum	52	102	152	44
$185/Mg				
Mean	83	168	252	69
Minimum	79	160	247	66
Maximum	87	172	256	74
	(ii) Dark Brown Soil Zone			
$14/Mg				
Mean	149	305	472	26
Minimum	146	302	469	25
Maximum	151	308	475	28
$51/Mg				
Mean	277	570	883	49
Minimum	273	565	877	47
Maximum	282	576	888	51
$76/Mg				
Mean	332	682	1,055	58
Minimum	326	675	1,048	56
Maximum	337	689	1,062	61
$185/Mg				
Mean	555	1,142	1,768	97
Minimum	546	1,131	1,757	93
Maximum	565	1,155	1,780	101

TABLE 1.8: Distribution of External Social Benefits from 1998 to 2019 by Counterfactual Scenario, Soil Zone, and Social Cost of Carbon in Saskatchewan using the Augmented Campbell model (weather) *(continued)*

Counterfactual:	(1)	(2)	(3)	(4)
	External Social Benefit			
	Share of Canola Hectares reverted to Summer Fallow			Share of Lentil Hectares reverted to Summer Fallow
	25%	50%	75%	25%
	(iii) Black & Gray Soil Zone			
Social Cost of Carbon:	*(millions of dollars)*			
$14/Mg				
Mean	318	669	1,052	2
Minimum	314	664	1,047	2
Maximum	322	674	1,057	2
$51/Mg				
Mean	589	1,239	1,952	3
Minimum	581	1,229	1,942	3
Maximum	596	1,249	1,962	4
$76/Mg				
Mean	702	1,479	2,330	4
Minimum	693	1,467	2,318	4
Maximum	711	1,490	2,342	4
$185/Mg				
Mean	1,173	2,473	3,898	7
Minimum	1,159	2,452	3,877	6
Maximum	1,188	2,491	3,917	7
	(iv) Saskatchewan (All Soil Zones)			
$14/Mg				
Mean	488	1,018	1,589	46
Minimum	481	1,007	1,579	44
Maximum	496	1,027	1,598	49
$51/Mg				
Mean	907	1,893	2,959	87
Minimum	893	1,873	2,941	82
Maximum	921	1,910	2,976	91
$76/Mg				
Mean	1,083	2,260	3,535	103
Minimum	1,066	2,237	3,513	99
Maximum	1,100	2,281	3,556	109
$185/Mg				
Mean	1,811	3,783	5,918	173
Minimum	1,784	3,743	5,881	165
Maximum	1,840	3,818	5,952	182

Source: Author's Estimates

1.13 Forward Projection of External Social Benefit from Carbon Sequestration in Perpetuity

In this section, I calculate the external social benefits stemming from carbon sequestration in perpetuity, under the assumption that the change in SOC stocks in 2019 as simulated by the Augmented Campbell model (weather version), relative to each counterfactual scenario, represents a permanent alteration in SOC. Additionally, I offer a forward-looking projection of the external social benefits arising from carbon sequestration by modeling future SOC stocks using the Augmented Campbell model (base version) and assuming constant carbon inputs for each field based on their average from 2015 to 2019.

To compute the external social benefit in perpetuity, I assume that the difference between the actual and counterfactual SOC stocks attributable to changes in production practices observed in 2019 is sustained forever afterwards. The external social benefit from permanent carbon sequestration is then computed as follows:

$$PESB_{2019} = \left[SCC_{2019} \times \frac{44 \, \text{Mg CO}_2}{12 \, \text{Mg SOC}} \right] (SOC_{2019}^A - SOC_{2019}^C),$$

where PESB represents the present value of the external social benefit from a permanent change in SOC stocks equal to the change relative to the counterfactual stock of SOC in 2019.

Table 1.9 presents the estimates of external social benefit for a permanent increase in the stock of SOC. Estimates are presented for each counterfactual scenario, SCC, and soil zone, based on corresponding measures of changes in SOC in 2019 simulated using the the Augmented Campbell model (weather version).[32] The largest external social benefit from a permanent change in SOC stock is observed in the black & gray soil zone, amounting to $17.9 billion for a 75% reduction in canola hectares and an SCC of $185/Mg. This constitutes approximately 61% of the total external social benefit projected for Saskatchewan under this scenario, totaling $29.1 billion for

---

[32]To see the computed external social benefits from a permanent change in SOC stocks using the Campbell model, please refer to Table 1G.2 in Appendix G.

the entire province. Notably, the external social benefit from a permanent change in SOC stock is anticipated to be less than the external social benefit from a permanent change in production projected forward from 2019 to 2169 with the Augmented Campbell model (base version). This discrepancy arises because the forward projection accounts for ongoing dynamics between actual and counterfactual SOC stocks until they reach a steady-state equilibrium under constant carbon inputs, whereas benefits from a permanent change in SOC stocks do not consider further changes in SOC stocks beyond the initial difference observed in 2019.

TABLE 1.9: External Social Benefits from a Permanent Change in SOC Stocks in 2019
by Counterfactual Scenario, Soil Zone, and Social Cost of Carbon in Saskatchewan
using the Augmented Campbell Model (weather)

	(1)	(2)	(3)
	External Social Benefit		
	Share of Canola Hectares reverted to Summer Fallow		
Counterfactual:	25%	50%	75%
	(i) Brown Soil Zone		
Social Cost of Carbon:	*(millions of dollars)*		
$14/Mg	75	151	228
$51/Mg	267	538	812
$76/Mg	396	798	1,204
$185/Mg	857	1,728	2,607
	(ii) Dark Brown Soil Zone		
$14/Mg	233	483	753
$51/Mg	832	1,723	2,685
$76/Mg	1,234	2,556	3,982
$185/Mg	2,672	5,533	8,621
	(iii) Black & Gray Soil Zone		
$14/Mg	458	977	1,562
$51/Mg	1,633	3,485	5,571
$76/Mg	2,422	5,168	8,262
$185/Mg	5,242	11,188	17,885
	(iv) Saskatchewan (All Soil Zones)		
$14/Mg	766	1,611	2,542
$51/Mg	2,732	5,757	9,068
$76/Mg	4,052	8,522	13,448
$185/Mg	8,771	18,449	29,113

Source: Author's Estimates

To calculate the forward projection of external social benefits in Saskatchewan, I proceed under the assumption that the average carbon inputs on fields, as observed during the final five years of the dataset from 2015 to 2019, will continue unchanged for the next 150 years, up to the

year 2169. Since weather forecasts are not available, I use the base version of the Augmented Campbell model to predict the forward-projected SOC stocks. For comparison, I also employ the Campbell model, where the results can be seen in Table 1G.3 in Appendix G.

The projected estimates should not be seen as reflecting predictions of the future measures of SOC stocks. The Augmented Campbell model, along with the Campbell model, are not calibrated for out-of-sample forecasting purposes. The soil humus component in both the Augmented Campbell and Campbell model converges to zero in a steady-state equilibrium owing to the way carbon pools are compartmentalized as developed by Woodruff (1950). Hence, using the Augmented Campbell model and the Campbell model to forward project SOC stocks over extended periods (beyond 30 years) is not advisable for predicting SOC stocks. Nonetheless, this limitation does not completely invalidate the analysis. Comparative analysis using differences in projections from SOC prediction models can still offer valuable insights into the effects of adopting different agricultural management practices on SOC stocks, as demonstrated by (Bista et al., 2016). Bista et al. (2016) use the DayCent model, coupled with weather data from 1930 to 2013, to predict yields from 2011 to 2080 and to analyze differences in SOC stocks between wheat rotations with no-till and tillage systems in Pendleton, Oregon. Similarly, Lychuk et al. (2019) apply the EPIC model to assess the effect of various climate scenarios on SOC stocks at the AAFC's Experimental Research Station in Scott, Saskatchewan. Importantly, both the Bista et al. (2016) and Lychuk et al. (2019) studies make comparisons across different counterfactual scenarios rather than providing standalone forecasts of SOC stocks. This approach acknowledges that while SOC prediction models are fairly reliable for comparing the effects of various management practices and climate scenarios on SOC stocks, they are not suited for predicting steady-state equilibria. Confirming a steady-state equilibrium would necessitate data spanning hundreds of years, under consistent management and climatic conditions, which is practically unobtainable.

The analysis in this section sheds light on the prospective external social benefits from maintaining current land management practices well into the future, referred to as the baseline scenario, compared with various counterfactual scenarios. The baseline scenario assumes that the extent of canola hectares remains unchanged going into the future. For each of these scenarios, including

the baseline, I project the evolution of SOC stocks, assuming production patterns consistent with the average carbon inputs recorded from 2015 to 2019. To simplify the simulation, I select only a single draw from the binomial distribution for each scenario. This decision is based on findings in the previous section, that the measures of external social benefits aggregated over fields did not significantly depend on the specific draws from the binomial distribution.

FIGURE 1.22: Projected Weighted Average Soil Organic Carbon Stock per Hectare by Counterfactual Scenario, Model, Soil Zone in Saskatchewan from 2020 to 2169
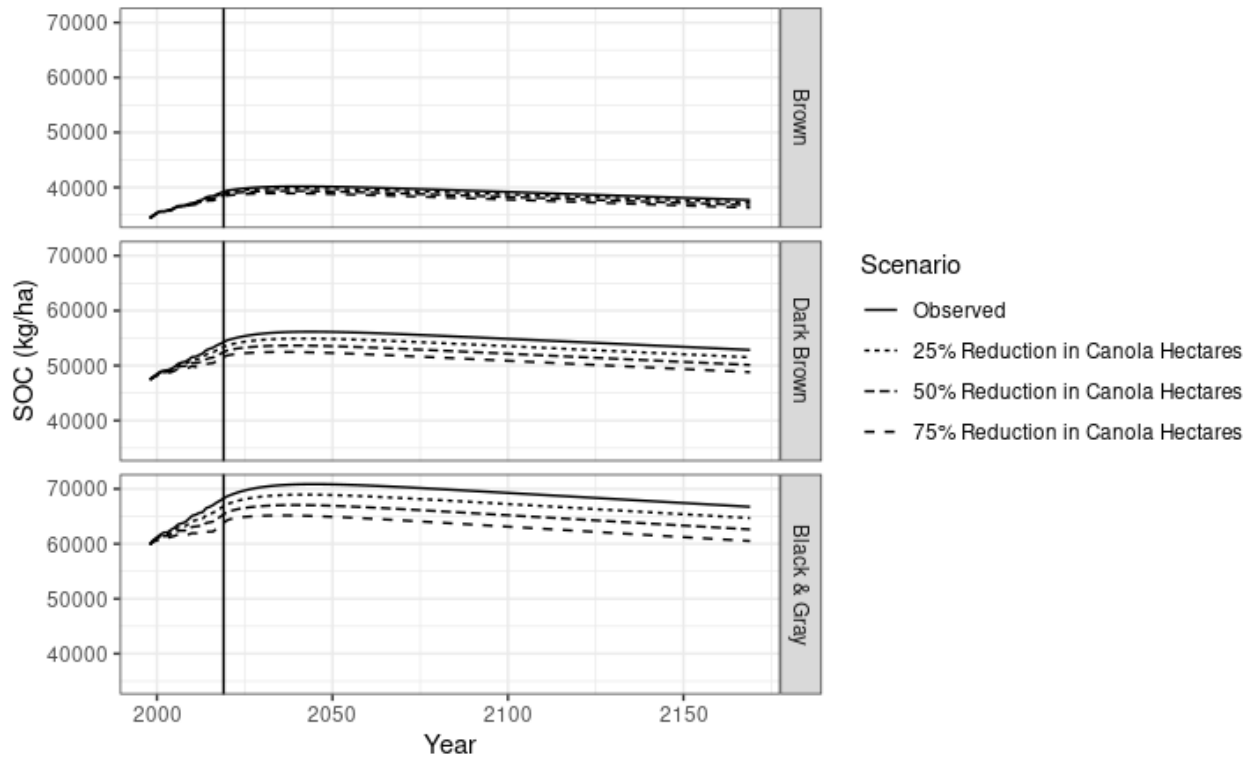
Source: Author's Estimates.

Figure 1.22 displays the projected weighted average SOC stock per hectare across different scenarios, soil zones, and prediction models up to the year 2169. In both the Campbell and Augmented Campbell models, the compartmentalization procedure developed by Woodruff (1950) results in a steady-state equilibrium where the soil humus component reverts to zero. Consequently, the external social benefit arises from the difference in carbon inputs between the observed scenario and the hypothetical counterfactual scenarios. This difference in SOC stocks between the

observed and counterfactual scenarios between time paths is precisely what the external social benefit is calculated from, as depicted in Figure 1.22.

Table 1.10 shows the forward-projected external social benefits across different counterfactual scenarios, soil zones, and social costs of carbon (SCC) from 2020 to 2169, using the base version of the Augmented Campbell model. The companion table, Table 1G.3 in Appendix 1G, presents similar forecasts using the Campbell model. The external social benefits range from $851 million to $30.2 billion, depending on the SCC and the specific counterfactual scenario considered.

TABLE 1.10: Projected External Social Benefits from 2020 to 2169 by Counterfactual Scenario, Soil Zone, and Social Cost of Carbon in Saskatchewan using the Augmented Campbell Model (base)

	(1)	(2)	(3)
	External Social Benefit		
	Share of Canola Hectares reverted to Summer Fallow		
Counterfactual:	25%	50%	75%
		(i) Brown Soil Zone	
Social Cost of Carbon:		*(millions of dollars)*	
$14/Mg	51	108	165
$51/Mg	190	400	610
$76/Mg	282	594	906
$185/Mg	603	1,269	1,935
		(ii) Dark Brown Soil Zone	
$14/Mg	278	564	833
$51/Mg	1,023	2,076	3,068
$76/Mg	1,516	3,076	4,546
$185/Mg	3,231	6,555	9,687
		(iii) Black & Gray Soil Zone	
$14/Mg	527	1,058	1,599
$51/Mg	1,938	3,890	5,882
$76/Mg	2,870	5,761	8,712
$185/Mg	6,114	12,273	18,559
		(iv) Saskatchewan (All Soil Zones)	
$14/Mg	856	1,729	2,597
$51/Mg	3,151	6,365	9,560
$76/Mg	4,669	9,431	14,164
$185/Mg	9,948	20,097	30,181

Source: Author's Estimates

The results presented in Tables 1.9 and 1.10 shed light on the potential external social benefits arising from maintaining current land management practices in Saskatchewan, characterized by zero-tillage, continuous cropping, and crop rotations that include more canola than in past decades. Table 1.9 shows the benefits resulting from a permanent change in SOC stocks, without accounting for future dynamic processes in SOC stocks beyond 2019. In contrast, Table 1.10 shows the benefits implied by a forward projection of SOC stocks for each scenario, 150 years into the future. Allowing for future dynamics in SOC stocks results in larger differences between the actual and counterfactual scenarios over time, and hence greater estimates of external social benefits relative to the benefits from a permanent change in SOC stocks equal to that estimated for 2019. However, assuming that the difference between the actual and counterfactual SOC stocks attributable to changes in production practices observed in 2019 are permanent results in external social benefits in perpetuity that are comparable to those computed from the forward projection. It is apparent that these two differing methods for valuing future SOC relative to a counterfactual scenario, as presented in this section, each have their own set of advantages and disadvantages.

1.14   Conclusion

In this essay, I introduce an new way to predict SOC stocks on farms across Saskatchewan. Using the newly developed Augmented Campbell model combined with an exclusive, confidential dataset at the field level from SCIC, I simulate annual SOC stocks across Saskatchewan farmlands from 1998 to 2019. Additionally, I calculate the external social benefits derived from agricultural management practices implemented over the 22 year period, compared with a range of hypothetical counterfactual alternative scenarios and using various estimates of the social cost associated with atmospheric carbon.

Using the weather version of the Augmented Campbell Model, my analysis shows that, on average, SOC stocks across Saskatchewan rose by approximately 6,797 kg/ha between 1998 and 2019. This effect is heterogeneous by soil zone, with SOC stocks growing by 4,437 kg/ha in the brown soil zone, 6,048 kg/ha in the dark brown soil zone, and 7,488 kg/ha in the black & gray

soil zone. It translates into an annual average change in SOC stocks across Saskatchewan of 309 kg/ha/yr.

To calculate the external social benefit, I simulate the actual past compared with various counterfactual scenarios in Saskatchewan, where a percentage of canola hectares revert to summer fallow (i.e., 25%, 50%, and 75%). I apply a rental rate for SOC implied by an assumed value for the SCC, representing the marginal social cost of increasing atmospheric carbon stocks. The estimated external social benefits resulting from canola adoption in Saskatchewan vary depending on the assumed SCC value and the proportion of canola hectares that would otherwise have reverted to summer fallow, ranging from $481 million to $6 billion. These estimates refer to benefits accruing between 1998 and 2019. If the additional SOC storage accomplished in 2019 is permanent from 2019 forward, an additional $766 million to $29.1 billion in external social benefits will accrue.

Furthermore, I project SOC stocks 150 years into the future using the most recent five-year average carbon inputs for each field. I compute the external social benefit using projections for a baseline scenario (maintaining current farming practices) and three alternative scenarios (25%, 50%, and 75% of canola hectares converted to summer fallow). I find that the projected external social benefit from increased SOC stocks—resulting from the continuation of current farming practices, relative to alternative practices involving reduced canola, increased summer fallow, and more tillage—could potentially reach up to $30.2 billion, depending on the SCC and the chosen counterfactual scenario.

The external social benefits, both per hectare and in total, are most significant in the black & gray soil zone, where canola predominates, and lowest in the brown soil zone, where summer fallow is more common. My analysis indicates that the estimated external social benefits from the adoption of lentils are considerably smaller, amounting to approximately 3% of the benefits observed from canola adoption under similar scenarios. These benefits are primarily concentrated in the brown and dark brown soil zones, where lentils are predominantly grown.

Overall, the estimated external social benefits observed over the past 22 years can be largely attributed to the reduction in tillage and summer fallow, as well as increased adoption of canola.

This is primarily because canola sequesters significantly more carbon in the soil compared to other crops because it is physically larger. While canola is typically less common in the brown soil zone because of higher drought risk and limited moisture (Marchildon and Sauchyn, 2009), integrating more canola into wheat-lentil rotations in this zone could potentially benefit society by storing additional carbon. Furthermore, Lafond et al. (2011), Oldfield et al. (2019), Rubio et al. (2021), Kane et al. (2021), and Wu and Congreves (2021) find that increased SOC improves soil health, crop yield, and overall crop productivity, further highlighting the potential societal benefits of carbon sequestration through agricultural practices. In conclusion, the results in this essay show that the carbon sequestration achieved in Saskatchewan over the past 22 years through practices like zero-tillage, continuous cropping, and canola adoption is worth billions of dollars.

Appendix 1A: Derivation of the Augmented Campbell Model

In this appendix, I derive the Augmented Campbell model using the Campbell model and a humi-fication process that originates from the Introductory Carbon Balance Model (ICBM). The formula for SOC from the Campbell model is,

$$SOC_t = C_0(q_1 e^{-k_1 t} + q_2 e^{-k_2 t}) + \sum_{n=0}^{t} [A_n(p_1 e^{-r_1(t-n)} + p_2 e^{-r_2(t-n)})]. \qquad (1A.1)$$

The first-order differential equation that represents the dynamics of the Campbell model is shown in equation (1A.2). The Campbell model implicitly assumes there are four types of carbon stocks, comprising two types for each of both young and old carbon stocks, with different decay rates (k_1, k_2, r_1, and r_2). These two types of carbon are labile (i.e., with shares q_1 and p_1) and refractory (i.e., with shares q_2 and p_2). In the essay, I refer to the carbon pools as plant residue and soil carbon. Throughout Appendix 1A, I instead refer to the carbon pools as young (i.e., plant residue) and old (i.e., soil carbon) to be consistent with the ICBM terminology.

$$\frac{dSOC_t}{dt} = \underbrace{A_t p_1 + A_t p_2}_{\text{Plant Residue}} - \underbrace{r_1 SOC_t^{Y_1} - r_2 SOC_t^{Y_2}}_{\text{Residue Decay}} - \underbrace{k_1 SOC_t^{O_1} - k_2 SOC_t^{O_2}}_{\text{Humus Decay}} \qquad (1A.2)$$

I now provde the derivation for equation (1A.2). Expanding the summation over planting years in equation (1A.1) results in

$$SOC_t = C_0(q_1 e^{-k_1 t} + q_2 e^{-k_2 t}) + A_0(p_1 e^{-r_1 t} + p_2 e^{-r_2 t}) + \cdots + A_t(p_1 + p_2). \qquad (1A.3)$$

To solve for the first-order differential equation, differentiate equation (1A.3) with respect to time, t. Equation (1A.4) represents the state equation of the Campbell model. Now,

$$\frac{dSOC}{dt} = -C_0(k_1 q_1 e^{-k_1 t} + k_2 q_2 e^{-k_2 t}) - A_0(r_1 p_1 e^{-r_1 t} + r_2 p_2 e^{-r_2 t})$$
$$- A_1(r_1 p_1 e^{-r_1(t-1)} + r_2 p_2 e^{-r_2(t-1)}) - \cdots .$$
(1A.4)

Expanding terms in equation (1A.4) gives,

$$\frac{dSOC}{dt} = -C_0 k_1 q_1 e^{-k_1 t} - C_0 k_2 q_2 e^{-k_2 t} - A_0 r_1 p_1 e^{-r_1 t} - A_0 r_2 p_2 e^{-r_2 t} - \cdots .$$
(1A.5)

I derive equations (1A.6) – (1A.9) by separating equation (1A.5) into four types of SOC stocks. Following this system of differential equations, I add a humification term to account for the conversion of young to old carbon stocks in equations (1A.10) and (1A.11). Before adding the humification process, I verify the solutions to the system of differential equation with the Campbell model.[33]

Old Labile Carbon Stocks:
$$\frac{dSOC_t^{O_1}}{dt} = -k_1 SOC_t^{O_1}$$
(1A.6)

Old Refractory Carbon Stocks:
$$\frac{dSOC_t^{O_2}}{dt} = -k_2 SOC_t^{O_2}$$
(1A.7)

Young Labile Carbon Stocks:
$$\frac{dSOC_t^{Y_1}}{dt} = A_t p_1 - r_1 SOC_t^{Y_1}$$
(1A.8)

---

[33]The differential equations (1A.6) – (1A.9) come from the variable coefficients initial value problem. These differential equations include a plant residue input and a decay rate on SOC stocks as depicted in the ICBM. Please refer to Andrén and Kätterer (1997) for more details on the structure of SOC differential equations.

Young Refractory Carbon Stocks:

$$\frac{dSOC_t^{Y_2}}{dt} = A_t p_2 - r_2 SOC_t^{Y_2} \tag{1A.9}$$

The Campbell model does not allow for a proportion of plant residue (i.e., young carbon stocks) to convert into old carbon stocks. I propose a change in the differential equations to allow for feedback from young to old carbon stocks through plant residue humification. The Augmented Campbell model is characterized by the system of ordinary differential equations (1A.10) – (1A.13).

$$\frac{dSOC_t^{O_1}}{dt} = hr_1 SOC_t^{Y_1} - k_1 SOC_t^{O_1} \tag{1A.10}$$

$$\frac{dSOC_t^{O_2}}{dt} = hr_2 SOC_t^{Y_2} - k_2 SOC_t^{O_2} \tag{1A.11}$$

$$\frac{dSOC_t^{Y_1}}{dt} = A_t p_1 - r_1 SOC_t^{Y_1} \tag{1A.12}$$

$$\frac{dSOC_t^{Y_2}}{dt} = A_t p_2 - r_2 SOC_t^{Y_2} \tag{1A.13}$$

Summing these terms, equation (1A.14) characterizes the change in SOC over time in the Augmented Campbell Model.

$$\frac{dSOC_t}{dt} = \underbrace{A_t p_1 + A_t p_2}_{Plant\,Residue} - \underbrace{r_1 SOC_t^{Y_1} - r_2 SOC_t^{Y_2}}_{Residue\,Decay} + \underbrace{hr_1 SOC_t^{Y_1} + hr_2 SOC_t^{Y_2}}_{Humification} - \underbrace{k_1 SOC_t^{O_1} - k_2 SOC_t^{O_2}}_{Humus\,Decay}$$
$$\tag{1A.14}$$

Solving the differential equations (1A.10) – (1A.13) and using the Euler-Maclaurin formula to approximate the integral as a summation transforms the ordinary differential equation back into

the Campbell model's summation form.

For young stocks, the particular solution is the same as the Campbell model,

$$SOC_t^{Y_1} = A_0 p_1 e^{-r_1 t} + e^{-r_1 t} \int_0^t A_s p_1 e^{r_1 s} ds. \tag{1A.15}$$

The integral in equation (1A.15) is approximated as a sum by use of the Euler-Maclaurin formula. Equations (1A.16) – (1A.18) provide the results for young labile carbon stocks, which is identical to the Campbell Model.

$$\int_0^t A_s p_1 e^{r_1 s} ds = A_1 p_1 e^{r_1} + \cdots + A_{t-1} p_1 e^{r_1(t-1)} + A_t p_1 e^{r_1 t} \tag{1A.16}$$

$$SOC_t^{Y_1} = A_0 p_1 e^{-r_1 t} + A_1 p_1 e^{-r_1(t-1)} + \cdots + A_{t-1} p_1 e^{-r_1} + A_t p_1 \tag{1A.17}$$

$$SOC_t^{Y_1} = \sum_{n=0}^t A_n p_1 e^{-r_1(t-n)} \tag{1A.18}$$

The equation for refractory young SOC stocks can also be calculated similarly. The result is shown in equation (1A.19).

$$SOC_t^{Y_2} = \sum_{n=0}^t A_n p_2 e^{-r_2(t-n)} \tag{1A.19}$$

The solution for labile old stock is different from the Campbell model because it now includes a humification process which is linked to the young stocks. Equation (1A.20) shows the solution to the first-order differential equation (1A.10).

$$SOC_t^{O_1} = C_0 q_1 e^{-k_1 t} + e^{-k_1 t} \int_0^t \sum_{n=0}^s h r_1 A_n p_1 e^{-r_1(s-n)} e^{k_1 s} ds \tag{1A.20}$$

Equations (1A.21) – (1A.23) approximate the sum of the integral by the Euler-Maclaurin formula.

$$\int_0^t \sum_{n=0}^s A_n p_1 e^{-r_1(s-n)} e^{k_1 s} ds = \sum_{n=0}^t A_n p_1 e^{-r_1(t-n)} e^{k_1} + \cdots$$
$$+ \sum_{n=0}^t A_n p_1 e^{-r_1(t-n)} e^{k_1(t-1)} + \sum_{n=0}^t A_n p_1 e^{-r_1(t-n)} e^{k_1 t} \tag{1A.21}$$

$$e^{-k_1 t} hr_1 \int_0^t \sum_{n=0}^s A_n p_1 e^{-r_1(s-n)} e^{k_1 s} ds = \sum_{n=0}^t A_n hr_1 p_1 e^{-r_1(t-n)} e^{-k_1(t-1)} + \cdots$$
$$+ \sum_{n=0}^t A_n hr_1 p_1 e^{-r_1(t-n)} e^{-k_1} + \sum_{n=0}^t A_n hr_1 p_1 e^{-r_1(t-n)} \tag{1A.22}$$

$$e^{-k_1 t} hr_1 \int_0^t \sum_{n=0}^s A_n p_1 e^{-r_1(s-n)} e^{k_1 s} ds = \sum_{s=1}^t \sum_{n=0}^t A_n hr_1 p_1 e^{-r_1(t-n)} e^{-k_1(t-s)} \tag{1A.23}$$

This gives the equation for labile carbon stocks for the Augmented Campbell model as shown in equation (1A.24).

$$SOC_t^{O_1} = C_0 q_1 e^{-k_1 t} + \sum_{s=1}^t \sum_{n=0}^t A_n hr_1 p_1 e^{-r_1(t-n)} e^{-k_1(t-s)} \tag{1A.24}$$

With the same derivation, I obtain the refractory old carbon stocks depicted in equation (1A.25).

$$SOC_t^{O_2} = C_0 q_2 e^{-k_2 t} + \sum_{s=1}^t \sum_{n=0}^t A_n hr_2 p_2 e^{-r_2(t-n)} e^{-k_2(t-s)} \tag{1A.25}$$

Combining equations (1A.18), (1A.19), (1A.24), and (1A.25) results in the Augmented Campbell model:

$$SOC_t = C_0(q_1 e^{-k_1 t} + q_2 e^{-k_2 t}) + \sum_{n=0}^{t} [A_n(p_1 e^{-r_1(t-n)} + p_2 e^{-r_2(t-n)})] +$$

$$\sum_{s=1}^{t} \sum_{n=0}^{t} [A_n(hr_1 p_1 e^{-r_1(t-n)-k_1(t-s)} + hr_2 p_2 e^{-r_2(t-n)-k_2(t-s)})]. \tag{1A.26}$$

The last modification to the Augmented Campbell model involves introducing a scalar parameter, γ, to the plant residue decomposition rates. Specifically, the decomposition rate for plant residue humification should be lower than that for plant residue but higher than for soil humus. The equation representing the Augmented Campbell model is then adjusted as follows,

$$SOC_t = C_0(q_1 e^{-k_1 t} + q_2 e^{-k_2 t}) + \sum_{n=0}^{t} [A_n(p_1 e^{-r_1(t-n)} + p_2 e^{-r_2(t-n)})] +$$

$$\sum_{s=1}^{t} \sum_{n=0}^{t} [A_n(hr_1 p_1 e^{\gamma(-r_1(t-n)-k_1(t-s))} + hr_2 p_2 e^{\gamma(-r_2(t-n)-k_2(t-s))})]. \tag{1A.27}$$

The Augmented Campbell model incorporates the Campbell model in the initial two terms of equation (1A.27). The third term introduces an extra pool of SOC, prolonging the time required to achieve a steady-state equilibrium compared to the Campbell model. With each time period, the Augmented Campbell model yields a higher SOC stock compared to the Campbell model, thereby minimizing prediction errors and mitigating the underestimation of SOC stocks observed in the Campbell model.

Appendix 1B: Introductory Carbon Balance Model

The ICBM shares a comparable structure with the Campbell model, featuring distinct pools for young (labile) and old (refractory) carbon. However, the key difference is in the ICBM's segmentation of carbon into two distinct pools, namely young and old carbon stocks, which are connected by a humification process (Andrén and Kätterer, 1997). In Saskatchewan, the decomposition and humification rates for the ICBM are parameterized by Campbell et al. (2007a,b) and Lemke et al. (2010).

In Figure 1B.1, Y and O represent the stocks of young and old carbon. Equations inside the square representing each stock are the steady states for SOC whereas the arrows represent the inflows and outflows for the SOC system.

FIGURE 1B.1: ICBM Structure of Soil Organic Carbon System
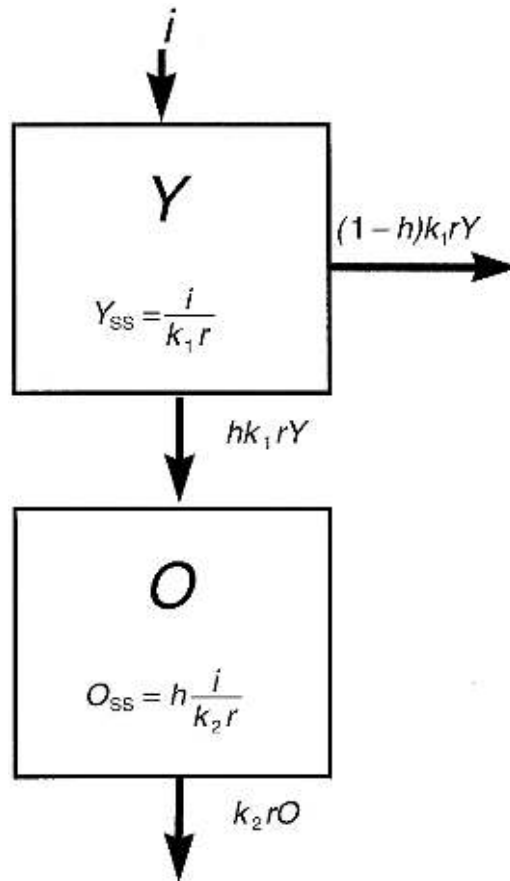
Source: Andrén and Kätterer (1997).

The ICBM's system of differential equations is solved analytically to derive the steady-state equations for each pool. By employing the average carbon inputs for each system and determining the percentage allocations based on these steady-state equations, I initialize the model by distributing the initial SOC stock into the young and old pools. Following the approach of Lemke et al. (2010), I employ the average carbon inputs for each field to compute the steady-state equilibria for the young and old pools of SOC. I will now present the solutions for the steady-state equations that are needed for initializing the ICBM model.

The differential equations that represent the state variable dynamics for the system in Figure 1B.1 can be represented by the system of differential equations shown equations (1B.1) and (1B.2).

$$\frac{dY}{dt} = i - k_1 r Y, \tag{1B.1}$$

$$\frac{dO}{dt} = h k_1 r Y - k_2 r O, \tag{1B.2}$$

where i is the annual carbon input, k_1 is the decomposition rate for young carbon, k_2 is the decomposition rate of old carbon, and h is the humification rate. All decomposition and humification rates are values are based are parameterized for Saskatchewan (see Campbell et al. (2007a,b) and Lemke et al. (2010)).

The first-order differential equations can be solved through two main approaches: the integrating factor method or the Laplace transform technique. Andrén and Kätterer (1997) employ the integrating factor method, incorporating an initial value to address the system. In this work, I confirm their findings by applying the Laplace transform. These differential equations are formalized in equations (1B.3) and (1B.4), with the ICBM system's initial value condition specified as $Y(t = 0) = Y_0$ where $a, c, b, d \in R$ and $a, b, d \neq 0$.

$$\frac{dY}{dt} + aY = c, \tag{1B.3}$$

$$\frac{dO}{dt} + bO = dY, \qquad (1B.4)$$

where $a = k_1 r$, $c = i$, $b = k_2 r$ and $d = hk_1 r$. The Laplace transform for equations (1B.1) and (1B.2) are shown in equations (1B.5) to (1B.12). The variable s represents a common value that corresponds the variables shown in equations (1B.5) and (1B.6).

$$\mathcal{L}\left\{\frac{dY}{dt}\right\} + \mathcal{L}\{aY\} = \mathcal{L}\{c\} \qquad (1B.5)$$

$$\mathcal{L}\left\{\frac{dO}{dt}\right\} + \mathcal{L}\{bO\} = \mathcal{L}\{d\} \qquad (1B.6)$$

Where:

$$\mathcal{L}\{s\} = \int_0^\infty f(t)e^{-st}dt \qquad (1B.7)$$

$$\mathcal{L}\left\{\frac{dY}{dt}\right\} = \int_0^\infty \frac{dY}{dt}e^{-st}dt = -\int_0^\infty Y(t)(-se^{-st}dt) + [e^{-st}Y(t)]_0^\infty = s\mathcal{L}\{Y\} - Y_0 \qquad (1B.8)$$

$$\mathcal{L}\left\{\frac{dO}{dt}\right\} = \int_0^\infty \frac{dO}{dt}e^{-st}dt = -\int_0^\infty O(t)(-se^{-st}dt) + [e^{-st}O(t)]_0^\infty = s\mathcal{L}\{O\} - O_0 \qquad (1B.9)$$

$$\mathcal{L}\{Y\} = \int_0^\infty Y(t)e^{-st}dt \qquad (1B.10)$$

$$\mathcal{L}\{O\} = \int_0^\infty O(t)e^{-st}dt \qquad (1B.11)$$

$$\mathcal{L}\{c\} = \int_0^\infty ce^{-st}dt = c\left[-\frac{e^{-st}}{s}\right]_0^\infty = \frac{c}{s} \tag{1B.12}$$

Using the Laplace identities in equations (1B.7) to (1B.12), the Laplace transforms for young and old carbon stocks are:

$$s\mathcal{L}\{Y\} - Y_0 + a\mathcal{L}\{Y\} = \frac{c}{s}, \tag{1B.13}$$

and

$$s\mathcal{L}\{O\} - O_0 + b\mathcal{L}\{O\} = d\mathcal{L}\{Y\}. \tag{1B.14}$$

Equations (1B.13) and (1B.14) reduce to:

$$\mathcal{L}\{Y\} = \frac{ca}{as(s+a)} + \frac{aY_0}{a(s+a)}, \tag{1B.15}$$

$$\mathcal{L}\{O\} = \frac{d}{s+b}\left[\frac{c}{s(s+a)} + \frac{Y_0}{s+a}\right] + \frac{O_0}{s+b}. \tag{1B.16}$$

Employing partial fraction expansion, the first and second terms in equation (1B.16) are:

$$\frac{c}{s(s+a)(s+b)} = \frac{A_1}{s} + \frac{A_2}{s+a} + \frac{A_3}{s+b} \quad \text{and} \quad \frac{Y_0}{(s+a)(s+b)} = \frac{B_1}{s+a} + \frac{B_2}{s+b}. \tag{1B.17}$$

Solving for A_1, A_2, and A_3:

$$\left[\frac{c}{(s+a)(s+b)}\right]_{s=0} = \left[A_1 + s\frac{A_2}{s+a} + s\frac{A_3}{s+b}\right]_{s=0} \implies A_1 = \frac{c}{ab}, \tag{1B.18}$$

88

$$\left[\frac{c}{s(s+b)}\right]_{s=-a} = \left[(s+a)\frac{A_1}{s} + A_2 + (s+a)\frac{A_3}{s+b}\right]_{s=-a} \implies A_2 = -\frac{c}{a(b-a)}, \quad \text{(1B.19)}$$

$$\left[\frac{c}{s(s+a)}\right]_{s=-b} = \left[(s+b)\frac{A_1}{s} + (s+b)\frac{A_2}{s+a} + A_3\right]_{s=-b} \implies A_3 = \frac{c}{b(b-a)}. \quad \text{(1B.20)}$$

Solving for B_1 and B_2:

$$\left[\frac{Y_0}{s+b}\right]_{s=-a} = \left[B_1 + (s+a)\frac{B_2}{s+b}\right]_{s=-a} \implies B_1 = \frac{Y_0}{b-a}, \quad \text{(1B.21)}$$

$$\left[\frac{Y_0}{s+a}\right]_{s=-b} = \left[(s+b)\frac{B_1}{s+a} + B_2\right]_{s=-b} \implies B_2 = -\frac{Y_0}{b-a}. \quad \text{(1B.22)}$$

Substituting equations (1B.18) to (1B.22) into equation (1B.15) and (1B.16) leads to the Laplace transform identity for the old carbon stock:

$$\mathcal{L}\{O\} = d\left[\frac{c}{sab} - \frac{c}{a(s+a)(b-a)} + \frac{c}{b(s+b)(b-a)} + \frac{Y_0}{(s+a)(b-a)} - \frac{Y_0}{(s+b)(b-a)}\right] + \frac{O_0}{s+b}. \quad \text{(1B.23)}$$

I now use formulas from the table of Laplace transforms to convert $\mathcal{L}\{Y\}$ and $\mathcal{L}\{O\}$ to Y and O. These formulas describe the relationships between the Laplace transform and the first-order differential form to obtain a solution. The solutions to the system of differential equations in the ICBM are,

$$\mathcal{L}\{Y\} = \frac{i}{k_1 r}(1 - e^{-k_1 rt}) + Y_0 e^{-k_1 rt}, \quad \text{(1B.24)}$$

89

$$\mathcal{L}\{O\} = hk_1 r \left[\frac{i}{k_1 r k_2 r} - \frac{i}{k_1 rr(k_2 - k_1)} e^{-k_1 rt} + \frac{i}{k_2 rr(k_2 - k_1)} e^{-k_2 rt} \right.$$
$$\left. + \frac{Y_0}{r(k_2 - k_1)} e^{-k_1 rt} - \frac{Y_0}{r(k_1 - k_2)} e^{-k_2 rt} \right] + O_0 e^{-k_2 rt}. \tag{1B.25}$$

Rearranging terms in equations (1B.24) and (1B.25) provides the solution to the first-order differential equations:

$$Y = \frac{i}{k_1 r} + \left(Y_0 - \frac{i}{k_1 r} \right) e^{-k_1 rt}, \tag{1B.26}$$

$$O = h\frac{i}{k_2 r} + \left(O_0 - h\frac{k_2 r k_1 r Y_0 - k_1 ri}{k_2 rr(k_2 - k_1)} \right) e^{-k_2 rt} + \left(h\frac{k_1 r Y_0 - i}{r(k_2 - k_1)} \right) e^{-k_1 rt}$$
$$+ h\frac{r(k_2 - k_1)i}{k_2 rr(k_2 - k_1)} e^{-k_2 rt} - h\frac{i}{k_2 r} e^{-k_2 rt}. \tag{1B.27}$$

The last two terms in equation (1B.27) are added and subtracted to provide a more concise equation. This is shown in equation (1B.28).

$$O = h\frac{i}{k_2 r} + \left(O_0 - h\frac{i}{k_2 r} + h\frac{k_1 r Y_0 - i}{r(k_2 - k_1)} \right) e^{-k_2 rt} + \left(h\frac{k_1 r Y_0 - i}{r(k_2 - k_1)} \right) e^{-k_1 rt} \tag{1B.28}$$

The steady states for young and old carbon stocks exist when $t \to \infty$. Equations (1B.29) and (1B.30) display the steady-state carbon stocks for young and old soil carbon pools.

$$Y_{SS} = \frac{i}{k_1 r} \tag{1B.29}$$

$$O_{SS} = h\frac{i}{k_2 r} \tag{1B.30}$$

Equations (1B.29) and (1B.30) are required for initializing the ICBM. The share of the initial SOC stock that is allocated to each pool by field is based on the average carbon input over the sample period found in equations (1B.29) and (1B.30).

The initial stocks of SOC for each pool using the steady-state equations are as follows:

$$Y_0 = \frac{Y_{SS}}{Y_{SS} + O_{SS}} \times C_0, \text{ and} \tag{1B.31}$$

$$O_0 = \frac{O_{SS}}{Y_{SS} + O_{SS}} \times C_0. \tag{1B.32}$$

Where Y_0 is the initial stock of SOC in the young carbon pool, O_0 is the initial SOC stock in the old carbon pool, and C_0 in the initial stock of SOC by field based on soil sampling data.

ICBM/2

In addition to the ICBM, the ICBM/2 model is also employed to predict SOC stocks in this essay. Originally developed by Kätterer and Andrén (2001), the ICBM/2 splits the young pool into aboveground and belowground components, each with distinct decomposition rates. Poeplau et al. (2015) later modified the ICBM/2 to incorporate different humification rates for these aboveground and belowground pools, instead of varying decomposition rates as in version constructed by Kätterer and Andrén (2001). For this analysis, I employ the version of the ICBM/2 that is updated by Poeplau et al. (2015). The model parameters are calibrated for chernozemic soils in Saskatchewan by Congreves et al. (2015) and Kröbel et al. (2016), who evaluate its performance using soil sampling data from the AAFC Experimental Research Station in Swift Current, Saskatchewan. Both the ICBM and ICBM/2 models consider tillage effects through a "rate modifier" parameter, which adjusts the decomposition rates of young and old carbon pools (Congreves et al., 2015). Additionally, some studies introduce an extra pool for manure, resulting in the ICBM/3 (see Fortin et al. (2011) Kröbel et al. (2016), and Thiagarajan et al. (2022)). Figure 1B.2 illustrates the flow diagram for the modified ICBM/2 model.

FIGURE 1B.2: ICBM/2 Flow Diagram including Above Ground and Below Ground
Pools with distinct Humification Rates.

$$i_l \qquad i_r$$

$$k_y r_e(1-h_l)Y_l \leftarrow \boxed{Y_l} \ \boxed{Y_r} \rightarrow k_r r_e(1-h_r)Y_r$$

$$h_l k_y r_e Y_l \qquad h_r k_y r_e Y_r$$

$$\boxed{O} \rightarrow k_O r_e O$$
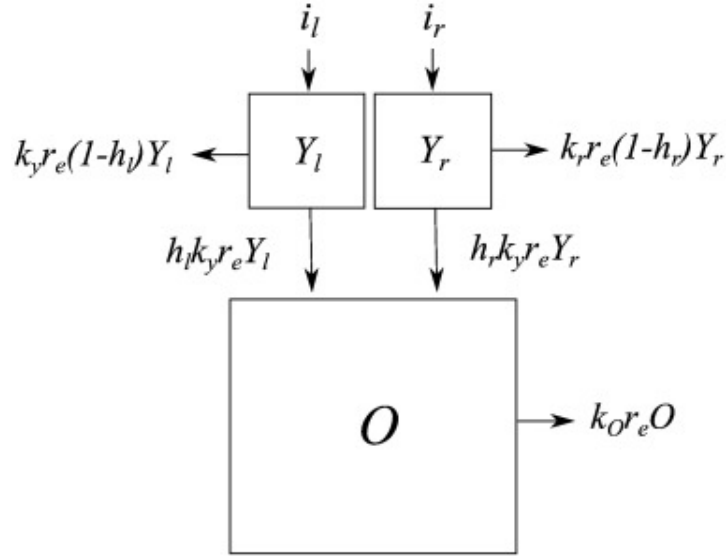
Source: Poeplau et al. (2015).

The system of first-order differential equations describing the ICBM/2 are,

$$\frac{dY_l}{dt} = i_l - k_1 r Y_l, \tag{1B.33}$$

$$\frac{dY_r}{dt} = i_r - k_1 r Y_r, \tag{1B.34}$$

$$\frac{dO}{dt} = h_l k_1 r Y_l + h_r k_1 r Y_r - k_2 r O, \tag{1B.35}$$

where Y_l is the labile young carbon pool representing the aboveground plant residue, and Y_r is the resistant young carbon pool representing the belowground plant residue, i_l and i_r are the respective carbon inputs (i.e., separated using the PBCI model), and h_l and h_r are the respective humification rates.

Solving the model either by the initial value problem or the Laplace transform provides the solutions to the steady-state equations. The steady-state equations for each carbon pool for the ICBM/2 are shown in equations (1B.37) to (1B.39).

$$Y_{l,SS} = \frac{i_l}{k_1 r} \tag{1B.36}$$

$$Y_{r,SS} = \frac{i_r}{k_1 r} \tag{1B.37}$$

$$O_{SS} = h_l \frac{i_l}{k_2 r} + h_r \frac{i_r}{k_2 r} \tag{1B.38}$$

where $Y_{l,SS}$ is the steady-state SOC stock for the young carbon pool for the stock of aboveground SOC, $Y_{r,SS}$ is the steady-state SOC stock for the young carbon pool for the stock of belowground SOC. The initial SOC stock values for each carbon pool are equal to:

$$Y_{l,0} = \frac{Y_{l,SS}}{Y_{l,SS} + Y_{r,SS} + O_{SS}} \times C_0, \tag{1B.39}$$

$$Y_{r,0} = \frac{Y_{r,SS}}{Y_{l,SS} + Y_{r,SS} + O_{SS}} \times C_0, \tag{1B.40}$$

$$O_0 = \frac{O_{SS}}{Y_{l,SS} + Y_{r,SS} + O_{SS}} \times C_0. \tag{1B.41}$$

where $Y_{l,0}$ is the initial stock of SOC for the aboveground young carbon pool, and $Y_{r,0}$ is the initial stock of SOC for the belowground young carbon pool.

Appendix 1C: Rothamsted Carbon Model

The version of the RothC model used in this essay is 26.3, developed by Coleman and Jenkinson (1996). This model integrates biogeochemical data across five distinct carbon pools and applies short, monthly time-steps to accurately depict the dynamics of SOC. It consists of four active soil organic matter pools: Decomposable Plant Material (DPM), Resistant Plant Material (RPM), Microbial Biomass (BIO), and Humified Organic Matter (HUM), alongside a fifth pool, Inert Organic Matter (IOM), which is not subject to decomposition. The RothC model's comprehensive system of differential equations is used to simulate SOC dynamics across these five pools. As such, the model employs numerical methods to determine the steady-state equilibrium for each pool at initialization, allocating specific portions of the initial SOC stock to each pool, in contrast to the analytical approach to steady-state equations found in the ICBM and ICBM/2 models.

In this essay, I present a derivation of the RothC model that incorporates variable carbon inputs and makes use of a system of discrete difference equations established by Parshotam (1996, 2001). These equations have undergone rigorous testing and validation against version 26.3 of the RothC model, ensuring their reliability and accuracy (Parshotam, 1996, 2001). They are derived directly from the exponential state equations governing each carbon pool, as described by Coleman and Jenkinson (1996).

I employ the forward Euler method to simulate SOC stocks within the RothC model. Due to uncertainties regarding the accuracy of solutions derived from certain dynamic solvers for ordinary differential equations in the RothC model (see Martin et al. (2009) and Diele et al. (2021)), I also address discrete solutions obtained from continuous solutions, as outlined by Martin et al. (2009) in this Appendix. The discrete solutions provided by Parshotam (1996, 2001) align with the continuous solutions presented by Martin et al. (2009) when applying the forward Euler method to solve the system of differential equations, which is the standard solver employed in the SoilR package.[34]

---

[34]For a comprehensive list of models solved using the Euler Method in the SoilR package, please refer to the documentation available at `https://cran.r-project.org/web/packages/SoilR/SoilR.pdf`.

Figure 1C.1 illustrates a flow diagram depicting the RothC model's process of transitioning plant residues into various carbon compartments. The abbreviation FYM denotes farmyard manure, which is not a significant factor in this context. Plant material enters each compartment in accordance with the parameters outlined in the figure below and undergoes decomposition across successive stages, progressing from left to right (i.e., time-steps).

Several guides are available for initializing and executing the RothC model version 26.3. The conventional approach is outlined by Coleman and Jenkinson (1996), while an updated version is included in the Food and Agriculture Organization (FAO) guidelines for predicting global soil carbon sequestration (Food and Agricultural Organization, 2020). For this analysis, I adopt the latest initialization procedure offered by the FAO.

Rothamsted Carbon Model Setup

In the RothC model used for systems of agricultural crops, 59% of plant material goes to DPM (γ), and the remaining 41% goes to RPM ($1 - \gamma$) (i.e., a DPM/RPM ratio of 1.44).[35] The ratio of CO_2 to BIO+HUM is

$$x = 1.67(1.85 + 1.60e^{-0.0786*pclay}), \tag{1C.1}$$

where *pclay* is the percentage of clay in the soil by field. The amount going to CO_2 is equal to $x/(x+1)$ and the amount going to BIO+HUM is $1/(x+1)$. Roughly 46% of the carbon going to BIO+HUM goes to BIO and the remaining 54% goes to HUM. Hence, the coefficients in Figure 1C.1 are $\alpha = \frac{0.46}{1+1.67(1.85+1.60e^{-0.0786*pclay})}$ and $\beta = \frac{0.54}{1+1.67(1.85+1.60e^{-0.0786*pclay})}$. The IOM compartment is based on the Falloon method, $IOM = 0.049 * C_0^{1.139}$ where C_0 is the initial stock of organic carbon in Mg/ha (Falloon et al., 1998).

---

[35]Refer to Figure 1C.1 for the corresponding parameters.

FIGURE 1C.1: Flow diagram of the Rothamsted Carbon model.
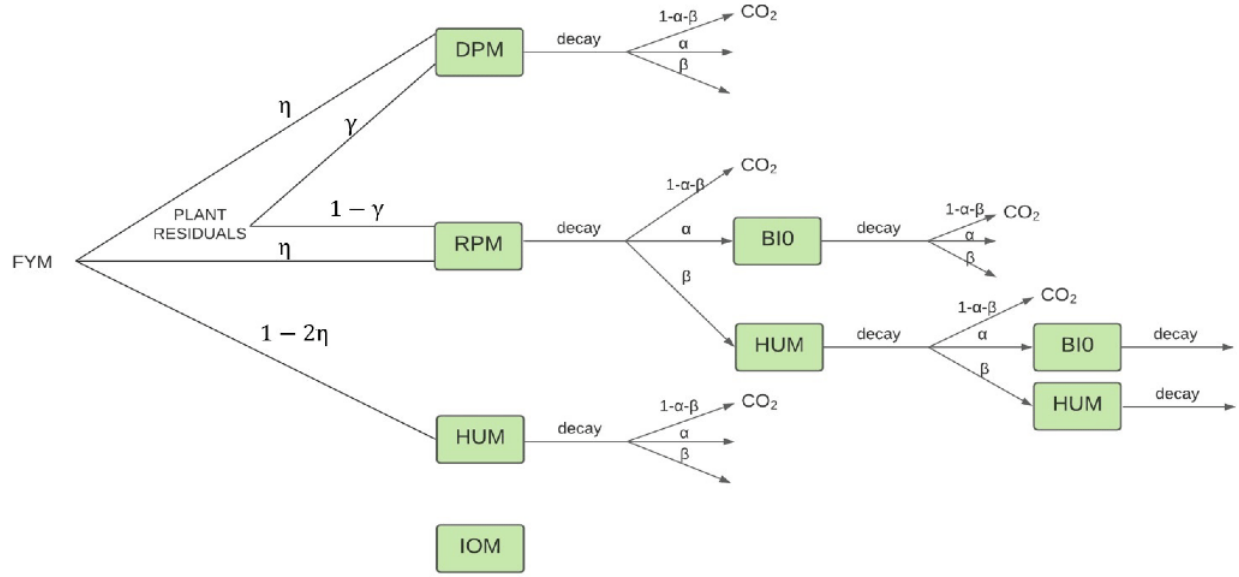
Source: Diele et al. (2021).

Notes: FYM is Farmyard Manure, DPM is Decomposable Plant Material, RPM is Resistant Plant Material, BIO is microbial Biomass, HUM is Humified organic matter, and IOM is Inert Organic Matter

Building on the soil carbon dynamics illustrated in Figure 1C.1, the RothC model is represented by a system of first-order differential equations is,

$$\dot{\mathbf{c}} = \rho(t) \underbrace{\begin{bmatrix} k_{dpm} & 0 & 0 & 0 \\ 0 & k_{rpm} & 0 & 0 \\ \alpha k_{dpm} & \alpha k_{rpm} & (\alpha-1)k_{bio} & \alpha k_{hum} \\ \beta k_{dpm} & \beta k_{rpm} & \beta k_{bio} & (\beta-1)k_{hum} \end{bmatrix}}_{=\mathbf{A}} \mathbf{c}(t) + \mathbf{b}(t), \text{ such that } \mathbf{c}(t_0) = \mathbf{c}_0 \geq 0. \text{ (1C.2)}$$

where $\mathbf{c}(t) = \begin{bmatrix} c_{dpm}(t) & c_{rpm}(t) & c_{bio}(t) & c_{hum}(t) \end{bmatrix}^T$ denotes the vector of initial concentrations,

and $b(t) = g(t) \begin{bmatrix} \gamma & 1-\gamma & 0 & 0 \end{bmatrix}^T$ represents the carbon inputs entering the system at time t

96

such that $0 \leq \gamma \leq 1$ are the fraction of inputs that sum to one. The decomposition rate for each respective compartment is k_i, where $i \in (dpm, rpm, bio, hum)$. The RothC model has rate modifiers that are "compartment" dependent. I will explain these modifiers in further detail after deriving the discrete system of differential equations for the RothC model. Here, the carbon inputs from plant biomass enter the soil only through DPM and RPM compartments.

Expanding the system in equation (1C.2) provides the system of first-order differential equations for the RothC model provided in equation (1C.3) to (1C.6).

Decomposable Plant Material (DPM):

$$\frac{dc_{dpm}(t)}{dt} = -\rho(t)k_{dpm}c_{dpm}(t) + g(t)\gamma \tag{1C.3}$$

Resistant Plant Material (RPM):

$$\frac{dc_{rpm}(t)}{dt} = -\rho(t)k_{rpm}c_{rpm}(t) + g(t)(1 - \gamma) \tag{1C.4}$$

Microbial Biomass (BIO):

$$\frac{dc_{bio}(t)}{dt} = \rho(t)[\alpha k_{dpm}c_{dpm}(t) + \alpha k_{rpm}c_{rpm}(t) + (\alpha - 1)k_{bio}c_{bio}(t) + \alpha k_{hum}c_{hum}(t)] \tag{1C.5}$$

Humified Organic Matter (HUM):

$$\frac{dc_{hum}(t)}{dt} = \rho(t)[\beta k_{dpm}c_{dpm}(t) + \beta k_{rpm}c_{rpm}(t) + \beta k_{bio}c_{bio}(t) + (\beta - 1)k_{hum}c_{hum}(t)] \tag{1C.6}$$

Let the system of equations be represented in vector form,

$$\dot{\mathbf{c}} = \rho(t)\mathbf{A}\mathbf{c} + \mathbf{b}(t). \tag{1C.7}$$

The solution to this problem is characterized by,

$$\mathbf{c} = \mathbf{c}_0 e^{\mathbf{A}\int_0^t \rho(t)dt} + e^{\mathbf{A}\int_0^t \rho(t)dt}\int_0^t \mathbf{b}(t)e^{-\mathbf{A}\int_0^s \rho(t)ds}ds. \tag{1C.8}$$

Based on the initial value problem represented in equation (1C.8), the solution to this discrete system is characterized as,

$$\mathbf{c}_{(n+1)} = \mathbf{c}_n e^{\mathbf{A}\rho(t_n)\Delta t} + \Delta t\mathbf{b}(t). \tag{1C.9}$$

Martin et al. (2009) suggests that equation (1C.9) provides an approximation of the discrete-form RothC model. To address this discretization issue, they propose a Fourier transformation to estimate the discrete RothC model. Employing the continuous form in software like MATLAB offers adaptable numerical integration techniques facilitated by program functions designed to solve systems of ordinary differential equations (ODEs), such as ODE45. Alternatively, Diele et al. (2021) proposes using the Exponential Rosenbrock-Euler model to discretize the continuous RothC model, which is expected to decrease the estimation time required for calculating SOC stocks. They evaluate this numerical integration method using dynamic solvers within MATLAB.

Discretization of the Rothamsted Carbon model

In this section, I present the explicit solutions for the discrete RothC model by discretizing the continuous RothC system using the Euler method (specifically, the forward Euler method) with a time-step procedure defined as $t_{n+1} = t_0 + n\Delta t$ where $\Delta t = 1$. Parshotam (1996, 2001) provides the discrete form solutions for the RothC model, but there exists some uncertainty when choosing between the continuous and discrete models and their corresponding solvers for ordinary differential equations. Despite this, the simplicity of the forward Euler method allows for intuitive analytical solutions, unlike the more complex numerical integration methods as stated above or other collocation methods. The SoilR package in R predominantly uses the forward Euler method to solve the ordinary differential equations for the RothC, Century, ICBM, and many other models.

This approach follows the same discrete temporal grid outlined by Diele et al. (2021), illustrating the time-step scheme from the original discrete RothC model.

Applying the Euler scheme with steps defined as $t_{n+1} = t_0 + n\Delta t$ where $\Delta t = 1$, and using equations (1C.3) to (1C.6) for integrating over time on the discretized equation, yields the discrete form solutions for the DPM and RPM compartments (equations (1C.10) and (1C.11)).

DPM:

$$\frac{dc_{dpm}(t)}{dt} = -\rho(t)k_{dpm}c_{dpm}(t) + g(t)\gamma \implies$$

$$c_{dpm,n+1} = c_{dpm}(t_n)e^{-\rho(t_n)k_{dpm}\Delta t} + e^{-\rho(t_n)k_{dpm}\Delta t} \int_{t_0}^{t_0+\Delta t} g(s)\gamma e^{\rho(t_n)k_{dpm}\Delta t}ds \implies \qquad (1C.10)$$

$$c_{dpm,n+1} = c_{dpm,n}e^{-\rho(t_n)k_{dpm}\Delta t} + \Delta t g_n \gamma$$

RPM:

$$\frac{dc_{rpm}(t)}{dt} = -\rho(t)k_{rpm}c_{rpm}(t) + g(t)(1-\gamma) \implies$$

$$c_{rpm,n+1} = c_{rpm}(t_n)e^{-\rho(t_n)k_{rpm}\Delta t} + e^{-\rho(t_n)k_{rpm}\Delta t} \int_{t_0}^{t_0+\Delta t} g(s)\gamma e^{\rho(t_n)k_{rpm}\Delta t}ds \implies \qquad (1C.11)$$

$$c_{rpm,n+1} = c_{rpm,n}e^{-\rho(t_n)k_{rpm}\Delta t} + \Delta t g_n(1-\gamma)$$

The solutions for DPM and RPM first-order differential equations are the same solutions to the discrete RothC model as in Parshotam (1996, 2001). The discrete RothC model is derived from the exponential terms in Coleman and Jenkinson (1996), using discrete time intervals to obtain the system of difference equations with a matrix of coefficients and the sum of exponentials.

To simplify the BIO and HUM first-order differential equations, I solve for the connecting stocks of carbon pools using the initial value problem. These terms reflect past biological input processes and are used to obtain the exact solution to the discrete-time RothC model.

Let the general initial value problem for the associated biological carbon input stocks be

$$c_{i,t} = c_i e^Y + e^Y \int_0^x (s) e^{-Y} ds \rightarrow c_{i,t} = c_0 e^Y - \frac{x(t)}{Y} (e^Y - 1). \qquad (1C.12)$$

Substituting equation (1C.12) into equation (1C.5) results in

$$\frac{dc_{bio}(t)}{dt} = \rho(t) k_{bio} c_{bio}(t) + \rho(t) \alpha \sum_{i \in dpm,rpm,bio,hum} k_i \left(c_{0,i} e^Y - \frac{x(t)}{Y} (e^Y - 1) \right). \qquad (1C.13)$$

Now using the forward Euler method to solve the discrete form for the biological pool implies,

$$c_{bio,n+1} = c_{bio}(t_n) e^{-\rho(t_n) k_{bio} \Delta t}$$
$$- e^{-\rho(t_n) k_{bio} \Delta t} \int_{t_0}^{t_0 + \Delta t} \left(\rho(t) \alpha \sum_{i \in dpm,rpm,bio,hum} k_i \left(c_{0,i} e^Y - \frac{x(s)}{Y} (e^Y - 1) \right) \right) e^{\rho(t_n) k_{bio} \Delta t} ds.$$

$$(1C.14)$$

The solution to the integral in equation (1C.14) is,

$$c_{bio,n+1} = c_{bio}(t_n) e^{-\rho(t_n) k_{bio} \Delta t} - \Delta t \rho(t) \alpha \sum_{i \in \{dpm,rpm,bio,hum\}} k_i \left(c_{0,i} e^Y - \frac{x(t_n)}{Y} (e^Y - 1) \right). \qquad (1C.15)$$

To solve for the exact solution as the discrete-time RothC model, it is evident that the general form initial value problem parameters are equal to $c_0 = 0, Y = -\rho(t_n) k_i \Delta t$ and $x(t_n) = c_{i,n}$. This implies,

$$c_{bio,n+1} = c_{bio,n} e^{-\rho(t_n) k_{bio} \Delta t} + \sum_{i \in \{dpm,rpm,bio,hum\}} \alpha c_{i,n} (1 - e^{\rho(t_n) k_i \Delta t}), \qquad (1C.16)$$

and by symmetry the discrete solution for the HUM compartment is

100

$$c_{hum,n+1} = c_{hum,n}e^{-\rho(t_n)k_{hum}\Delta t} + \sum_{i\in\{dpm,rpm,bio,hum\}} \beta(c_{i,n}(1 - e^{\rho(t_n)k_i\Delta t})). \qquad \text{(1C.17)}$$

This provides the solution for the discrete-time version of the RothC model, aligning with the solutions proposed by Parshotam (1996, 2001), which have undergone testing and validation against the computational implementation of RothC model version 26.3.

Rothamsted Carbon Rate Modifiers

In this section, I explain the rate modifying decompositions rates shows in equation (1C.2) as $\rho(t)$. In Coleman and Jenkinson (1996), within each compartment the decomposition rate is

$$Y_{m+1} = Y_m(1 - e^{-abckt}), \qquad \text{(1C.18)}$$

where Y is a compartment such as DPM, RPM, BIO, and HUM, a is the rate modifying factor for temperature, b is the rate modifying factor for moisture, c is the soil cover rate modifying factor, k is the decomposition rate constant for that compartment, and t is equal to $1/12$, since k is based on a yearly decomposition rate. Corresponding to the notation in equation (1C.2), I assume that $\rho(t) = abc$.

Decomposition rate constant (k) is $k_{dpm} = 10$ for DPM, $k_{rpm} = 0.3$ for RPM, $k_{bio} = 0.66$ for BIO, and $k_{hum} = 0.02$ for HUM. This corresponds to the parameters shown in equation (1C.2).

Temperature Modifier

The rate modifying factor for temperature (a) is equal to

$$a = \frac{47.91}{1 + e^{\left(\frac{106.06}{T_m + 18.27}\right)}}, \qquad \text{(1C.19)}$$

where T_m is average monthly air temperature in degrees Celsius.

Soil Moisture Modifier

The rate modifying factor for soil moisture is based on the topsoil moisture deficit (TSMD) index. The maximum TSMD for 0–23cm soil profile depth is

$$TSMD_{max} = -(20 + 1.3(\%clay) - 0.01(\%clay)^2), \tag{1C.20}$$

and to change soil thickness simply divide by 23cm and multiply by actual thickness. Calculating Accumulated TSMD is obtained from the first month $PET = 0.75 * OPE$ (open pan evaporation) that is greater than the rainfall (mm) (i.e., $TSMD_{acc} = \sum(Precip_m - 0.75 * OPE_m)$) until it reaches its maximum TSMD value. For fields with fallow, the maximum TSMD is divided by 1.8. I chose to use non-fallow maximum TSMD for all observations because I cannot tell whether the soil is tilled when a farmer uses summer fallow.

The modifying factor for moisture (b) is

$$b = \begin{cases} 1.0 & \text{if } TSMD_{acc} < 0.444 * TSMD_{max} \\ 0.2 + (1.0 - 0.2) * \frac{TSMD_{max} - TSMD_{acc}}{TSMD_{max} - 0.444 * TSMD_{max}} & \text{otherwise} \end{cases} \tag{1C.21}$$

Soil Cover Factor Modifier

If plants are present on the soil, then $c = 0.6$, and if the soil is bare, $c = 1.0$.

Rothamsted Carbon Initialization Procedure

Following the Food and Agricultural Organization (2020) recommendations for initializing the RothC model, I compute the concentrations in each SOC compartment using two spin-up phases. In the first phase, I run the model for a 500 year period using constant climatic conditions and carbon inputs of $1 \, \text{t C ha}^{-1} \, \text{yr}^{-1}$. The initial allocation of the compartments in the first spin-up phase are based on pedotransfer functions from Weihermüller et al. (2013), which are specifically derived for the RothC model. These equations are equal to

$$RPM = (0.1847 \times C_0 + 0.1555)(\%clay + 1.2750)^{-0.1158}, \tag{1C.22}$$

$$HUM = (0.7148 \times C_0 + 0.5069)(\%clay + 0.3421)^{0.0184}, \tag{1C.23}$$

$$BIO = (0.0140 \times C_0 + 0.0075)(\%clay + 8.8473)^{0.0567}, and \tag{1C.24}$$

$$DPM = C_0 - IOM - RPM - HUM - BIO. \tag{1C.25}$$

The second phase of the initialization procedure uses the simulated SOC stocks from the first stage and adjusts carbon inputs using a factor from Smith et al. (2005). I then use these carbon inputs running the model until the SOC stock is approximately equal to my initial observed SOC stock. I set a very low tolerance level of 0.00001 kg C ha^{-1} in the function for the second phase of the initialization procedure. The formula for the carbon input adjusts in the second phase to

$$C_{eq} = \frac{C_0 - IOM}{C_{sim} - IOM}, \tag{1C.26}$$

where C_{eq} is the adjusted carbon input for the second spin-up phase and C_{sim} is the simulated SOC stock from the first spin-up phase after running the model for 500 years with constant climatic conditions and carbon inputs of 1 t C ha^{-1} yr^{-1}. Once the initialization procedure is complete, the corresponding percentages for each compartment can used to allocate the initial SOC stock accordingly and proceed using the prediction model with measures of carbon inputs over time.

Appendix 1D: Satellite- versus Crop Production-based Predictions of Soil Organic Carbon Stocks

In this Appendix, I assess the accuracy of SOC predictions made by the Augmented Campbell model, Campbell model, ICBM, ICBM/2, and RothC model against Canada's first ever carbon map produced by Sothe et al. (2022). Sothe et al. (2022) employed satellite data alongside machine learning techniques to predict average SOC levels spanning from 2015 to 2019, achieving a spatial resolution of 250m^2 across Canada. Collaborating with the World Wildlife Fund (WWF) Canada, Sothe et al. (2022) use a random forest algorithm and 3D modeling methods to estimate SOC stocks at both 30cm and 1m soil profile depths. I extend the SOC estimations from 30cm to 15cm depths and adjust them based on the average bulk density ratio and organic carbon percentage at various soil depths in Saskatchewan sourced from the Canadian National Soil Database (Agriculture and Agri-Food Canada, 2022).

Sothe et al. (2022) used satellite data, including NDVI from Landsat-8 and MODIS, to predict plant carbon biomass. They incorporated various additional factors such as precipitation, temperature, and spectral bands from Landsat-8, including red, red-edge near infrared, and short-wave infrared regions. Moreover, their analysis involved slope and topographic indices, canopy height percentiles, and Synthetic Aperture Radar data, sourced from satellites like LiDAR, Sentinel-1, ALOS-2, and ICESat-2. These diverse datasets were integrated into a random forest algorithm and 3D machine learning techniques to estimate SOC stocks across different soil depths. To validate their SOC prediction model, Sothe et al. (2022) compared their results with soil sampling data from the World Soil Information Service (WoSIS_latest) database, focusing on non-forested areas. They also employ data from Lehigh University datasets, primarily applicable to forested areas, which are not extensively discussed in this essay. The WoSIS database contains soil samples from 2,157 sites gathered between 1952 and 1985, including data from the Canadian National Soil Database (Agriculture and Agri-Food Canada, 2022). To align SOC stocks with fields selected for SOC prediction from the SCIC database to the data provided by Sothe et al. (2022), each field's SOC values were weighted based on the area of each raster cell within the field polygon.

Figures 1D.1 and 1D.2 depict the carbon distribution maps of Canada and southern Saskatchewan, focusing on soil organic carbon (SOC) stocks at a 15cm depth, derived from data provided by Sothe et al. (2022). While Figure 1D.1 presents a comprehensive view of carbon distribution across Canada, Figure 1D.2 zooms in on the prairie region of Saskatchewan. This carbon map illustrates that the majority of carbon storage in Canada is concentrated in forested regions, with particularly dense concentrations around Lake Winnipeg in Manitoba (refer to Figure 1D.1). On the other hand, Figure 1D.2 reveals that Saskatchewan's carbon reserves are predominantly situated in forested areas closer to the Canadian shield, which lies farther north. To enhance the visual representation and capture a wider range of SOC variation in cropland areas of southern Saskatchewan, I censor the upper limit of SOC stocks at 100,000 kg/ha. Although no formal analysis has been conducted, the SOC prediction outcomes from the previous section appear consistent with carbon map shown in Figure 1D.2, showcasing higher SOC stocks in the black & gray soil zone, gradually declining as one moves spatially into the dark brown soil zone and further into the brown soil zone.

FIGURE 1D.1: World Wildlife Fund, Average Soil Organic Carbon Map of Canada from 2015 to 2019
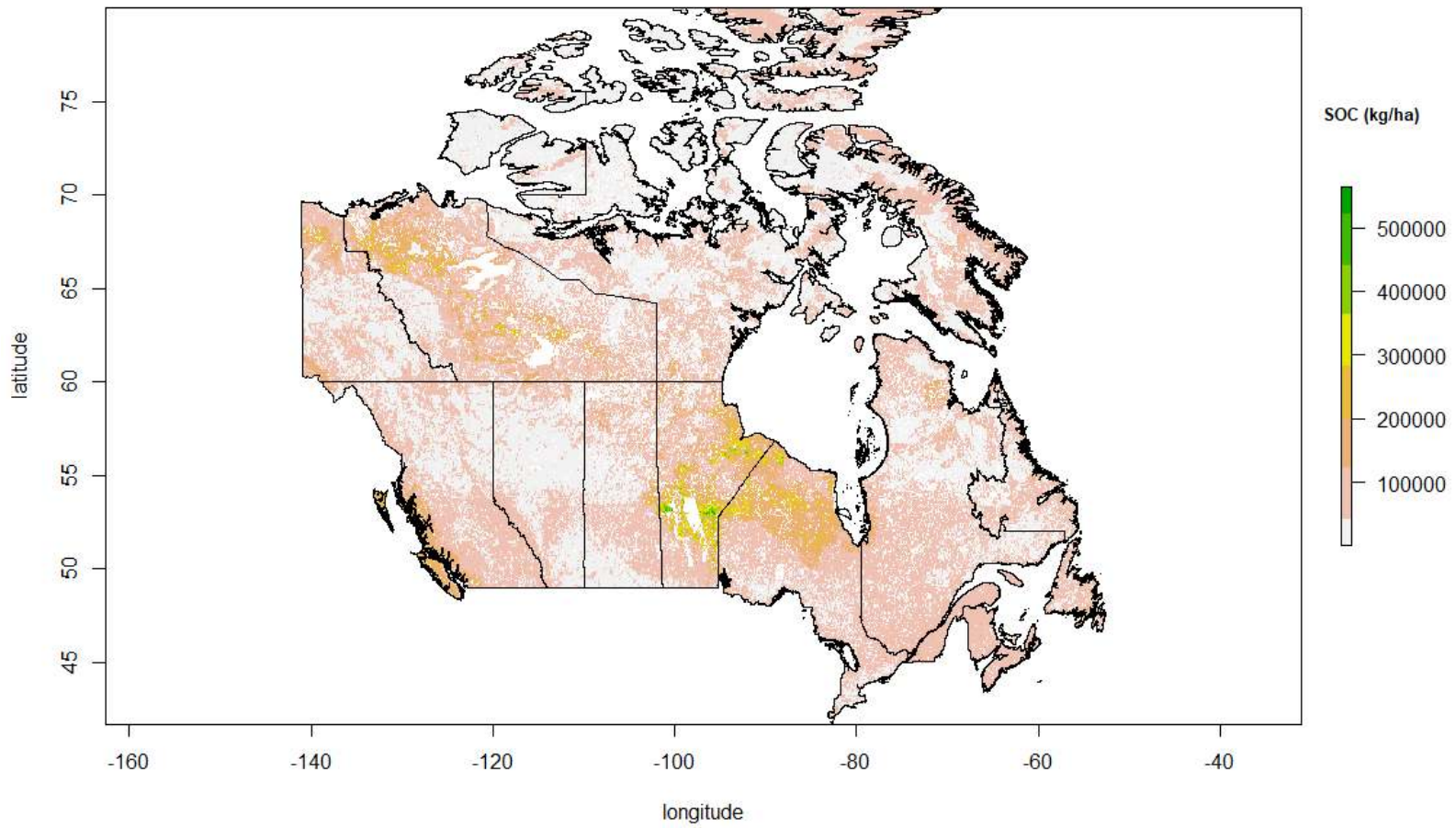
Source: Created using data from Sothe et al. (2022).

FIGURE 1D.2: World Wildlife Fund, Average Soil Organic Carbon Map of Southern
Saskatchewan from 2015 to 2019
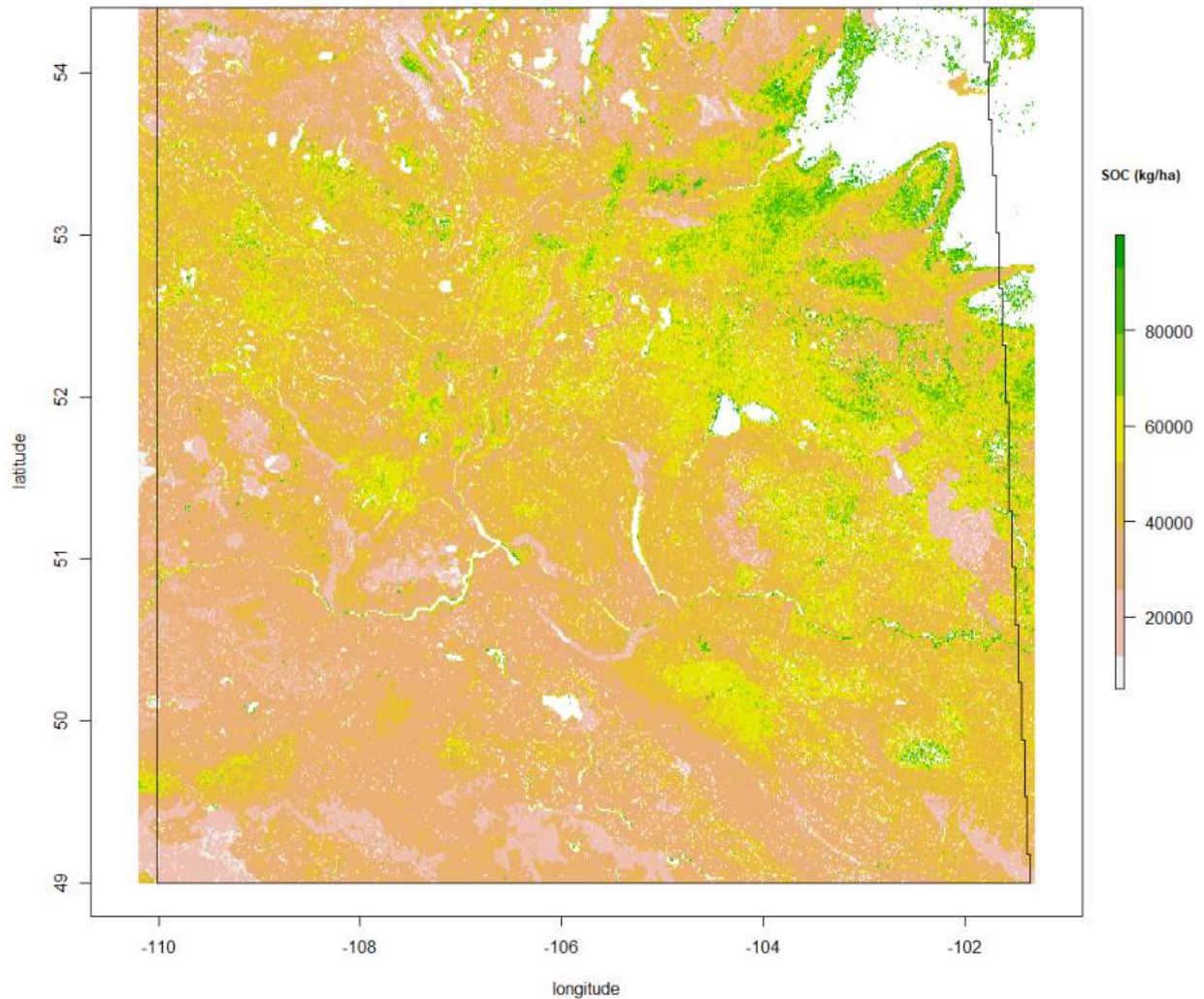
Source: Created using data from Sothe et al. (2022).

Notes: Soil Organic Carbon values are censored at 100,000 kg/ha to better illustrate the variation in soil organic carbon across the prairies.

I match the carbon map data from Sothe et al. (2022) with fields designated for SOC prediction within the SCIC dataset. The carbon map from Sothe et al. (2022), structured as a raster dataset, encompasses individual cells corresponding to locations within each field. Figure 1D.3 illustrates the alignment of SOC stock predictions for each field, according to various SOC prediction models, with the estimations derived from the WWF carbon map (displayed across panels (a)

to (f)). A diagonal line in Figure 1D.3, present in every panel, indicates instances where the predictions from both the SOC models and the WWF carbon map align perfectly for SOC stocks on a field basis. To address extreme values, I apply a filter to the SOC stocks, considering only those between 20,000 kg/ha and 150,000 kg/ha as indicated by the WWF carbon map, thereby excluding outlier cells within each field. These outliers often arise from inaccuracies in remote sensing data, including cells that capture trees, buildings, roads, bodies of water, and other elements that can distort satellite imagery. The comparison in Figure 1D.3 reveals significant discrepancies at the field level between SOC stock measures predicted by SOC models and those from the WWF carbon map, indicating considerable variance in SOC stock data across different fields. This results in instances of over prediction by SOC prediction models (or under prediction in the WWF carbon map) at higher SOC stock values, and under prediction by SOC prediction models (or over prediction in the WWF carbon map) at lower SOC stock values.

Figures 1D.4 to 1D.6 depict the effect of aggregating SOC predictions at different levels: Rural Municipality (RM), crop district, and soil zone. In Figures 1D.4 to 1D.6, prediction variances that deviate from the 45-degree line indicate discrepancies between the two SOC prediction methodologies. Through this aggregation process, the predictions of SOC stocks from each model and the WWF carbon map converge.

FIGURE 1D.3: Soil Organic Carbon Prediction Model results by Field in Saskatchewan compared to Satellite Prediction Results from the World Wildlife Fund Carbon Map of Canada
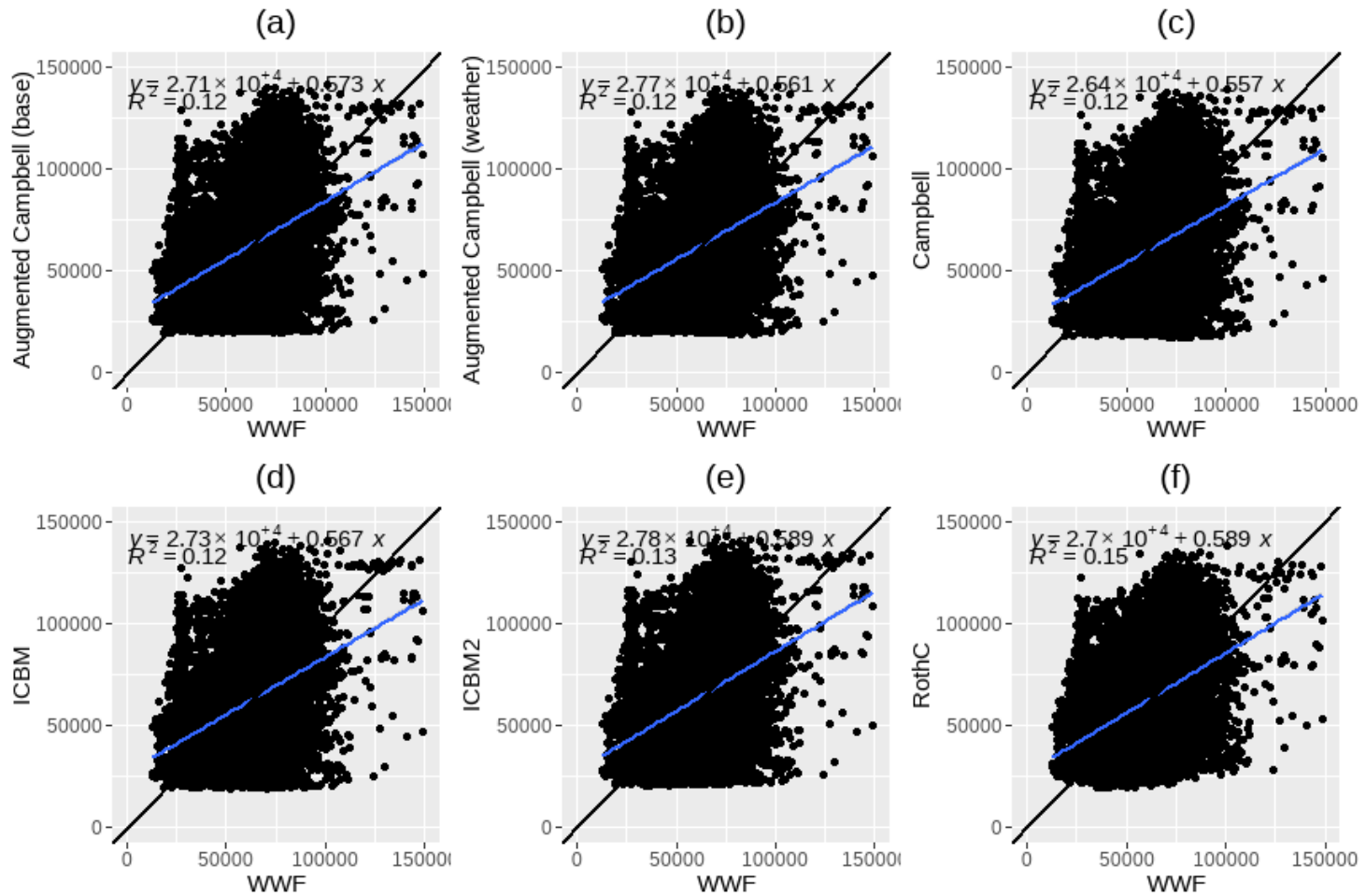
Source: Author's Estimates and created using data from Sothe et al. (2022).
Notes: All units on the y-axis and x-axis in each panel are in kg/ha. The y-axis of each panel shows the predicted SOC for each prediction model using the SCIC data, whereas the x-axis includes the matched SOC data using the World Wildlife Fund Carbon map created by Sothe et al. (2022).

FIGURE 1D.4: Soil Organic Carbon Prediction Model results by Rural Municipality in Saskatchewan compared to Satellite Prediction Results from the World Wildlife Fund Carbon Map of Canada
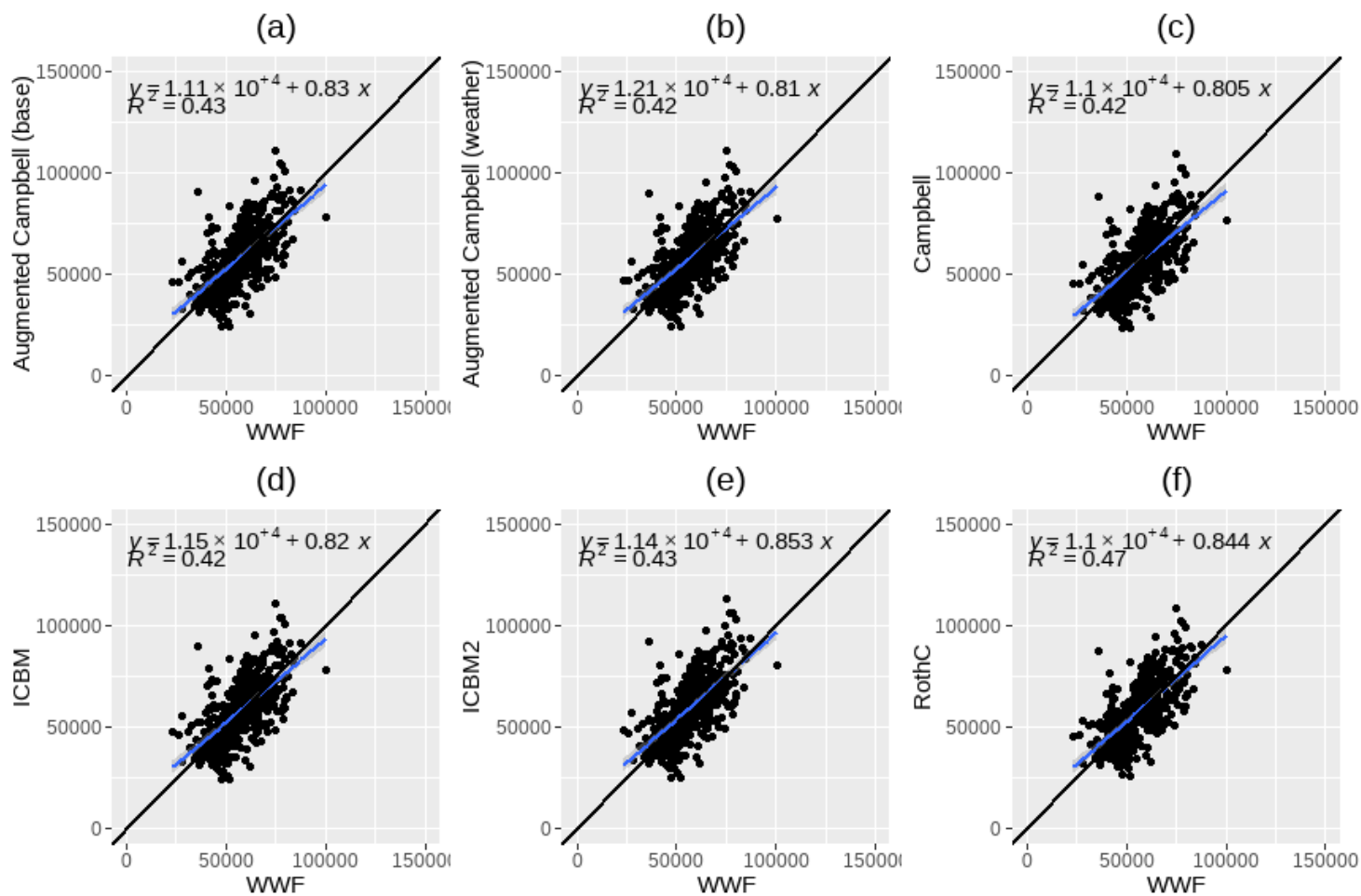
Source: Author's Estimates and created using data from Sothe et al. (2022).

Notes: All estimates of SOC stocks are aggregated from fields to Rural Municipalities. All units on the y-axis and x-axis in each panel are in kg/ha. The y-axis of each panel shows the predicted SOC for each prediction model using the SCIC data, whereas the x-axis includes the matched SOC data using the World Wildlife Fund Carbon map created by Sothe et al. (2022).

FIGURE 1D.5: Soil Organic Carbon Prediction Model results by Crop District in Saskatchewan compared to Satellite Prediction Results from the World Wildlife Fund Carbon Map of Canada

(a)

$y = -1.15 \times 10^{+4} + 1.21\ x$
$R^2 = 0.73$

(b)

$y = -1.02 \times 10^{+4} + 1.18\ x$
$R^2 = 0.72$

(c)

$y = -1.12 \times 10^{+4} + 1.17\ x$
$R^2 = 0.72$

(d)

$y = -1.07 \times 10^{+4} + 1.19\ x$
$R^2 = 0.72$

(e)

$y = -1.14 \times 10^{+4} + 1.23\ x$
$R^2 = 0.73$

(f)

$y = -1.17 \times 10^{+4} + 1.22\ x$
$R^2 = 0.76$
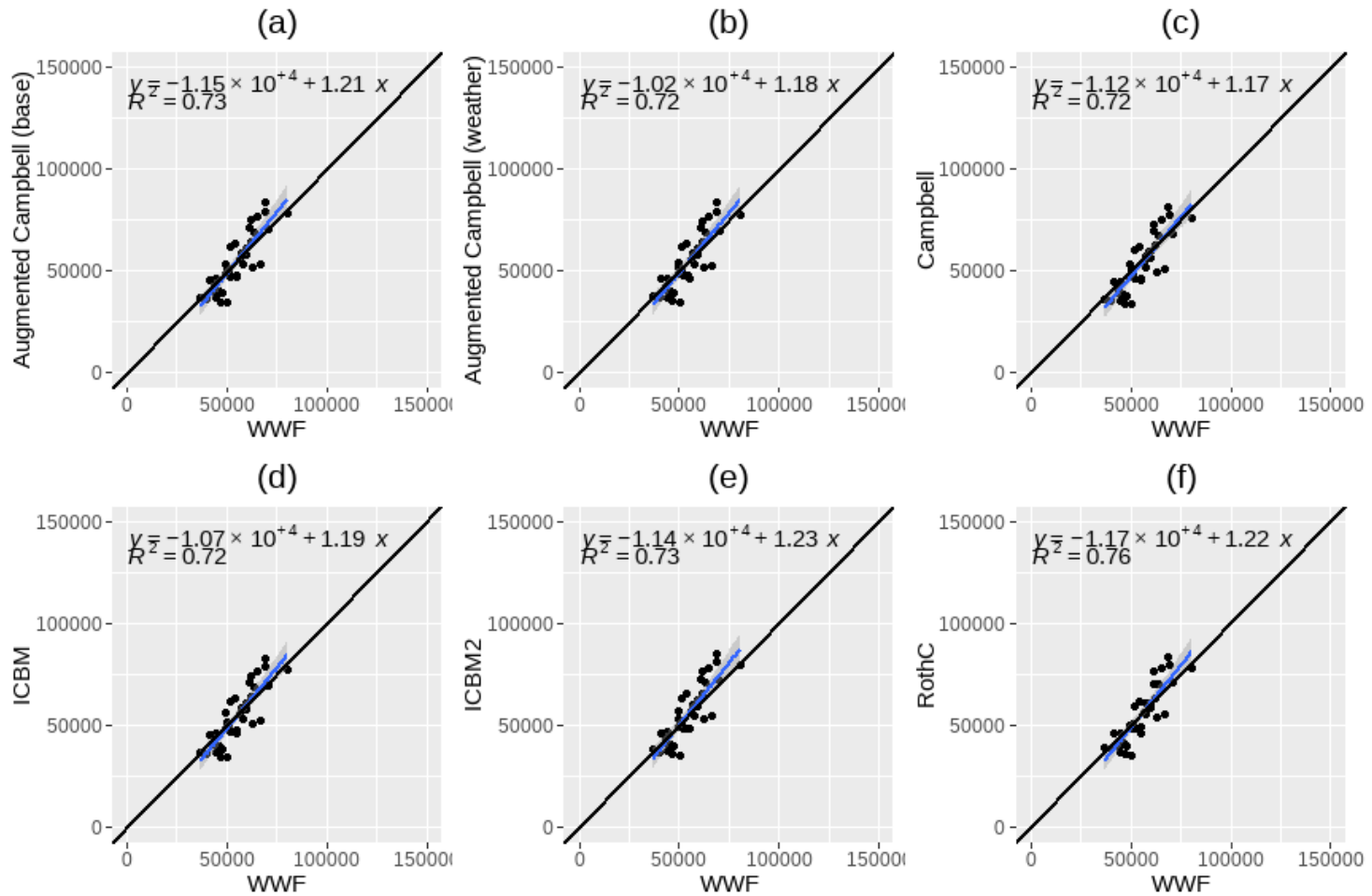
Source: Author's Estimates and created using data from Sothe et al. (2022).
Notes: All estimates of SOC stocks are aggregated from fields to crop districts. All units on the y-axis and x-axis in each panel are in kg/ha. The y-axis of each panel shows the predicted SOC for each prediction model using the SCIC data, whereas the x-axis includes the matched SOC data using the World Wildlife Fund Carbon map created by Sothe et al. (2022).

FIGURE 1D.6: Soil Organic Carbon Prediction Model results by Soil Zone in Saskatchewan compared to Satellite Prediction Results from the World Wildlife Fund Carbon Map of Canada
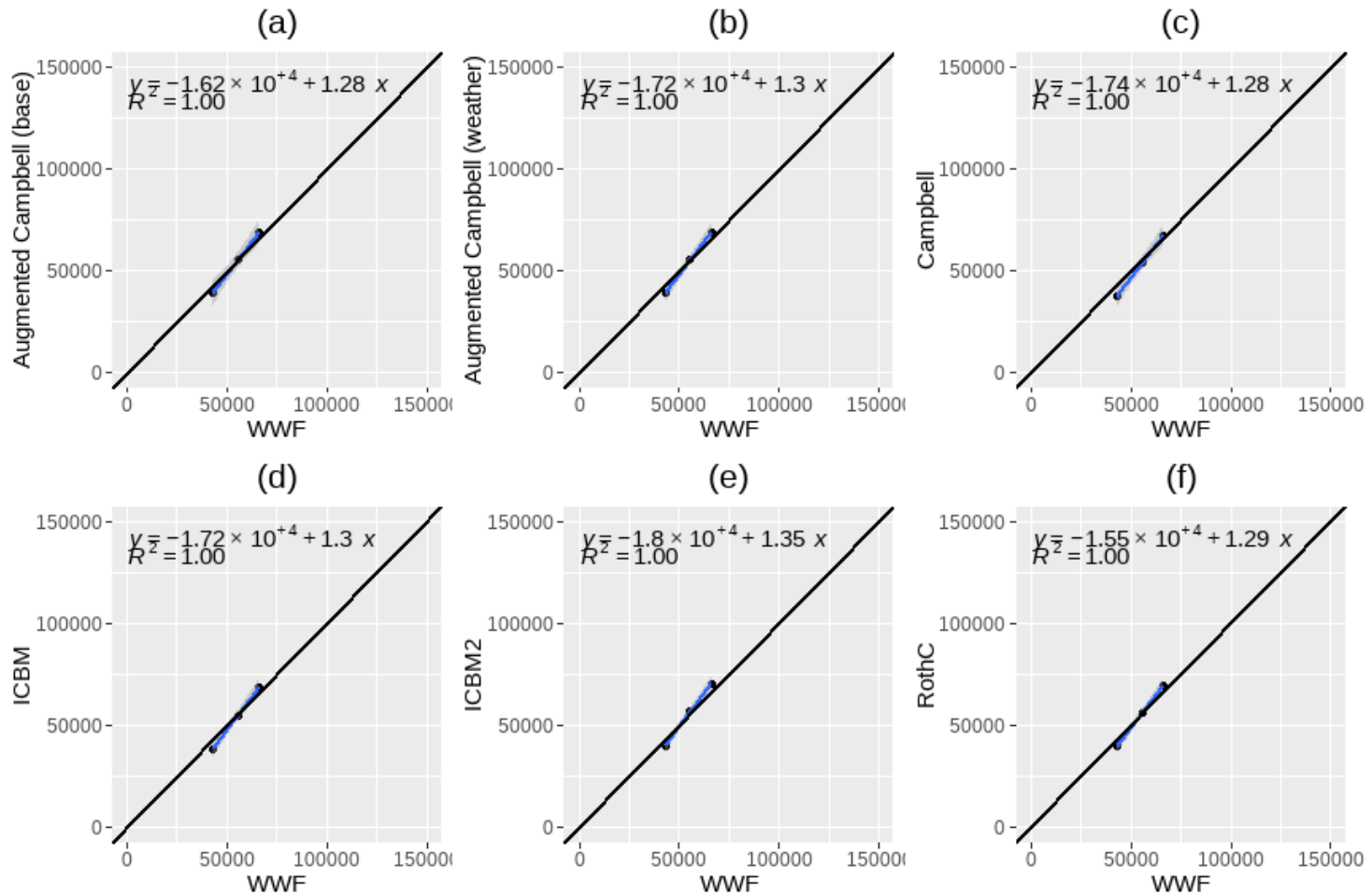
Source: Author's Estimates and created using data from Sothe et al. (2022).
Notes: All estimates of SOC stocks are aggregated from fields to soil zones. All units on the y-axis and x-axis in each panel are in kg/ha. The y-axis of each panel shows the predicted SOC for each prediction model using the SCIC data, whereas the x-axis includes the matched SOC data using the World Wildlife Fund Carbon map created by Sothe et al. (2022).

In Figure 1D.4, although some discrepancies persists in SOC stocks at the RM level, aggregating to the crop district level in Figure 1D.5 results in more comparable simulated SOC stocks across the prediction models and predictions from the WWF carbon map. Figure 1D.6 presents the weighted average SOC stocks for each soil zone. Notably, the SOC prediction models predict higher SOC stocks in the black & gray soil zone (with the highest observations) and lower SOC stocks in the brown soil zone (with the lowest observations) compared to the WWF carbon map SOC stocks. Consequently, the weighted average SOC stocks by crop district from 2015 to 2019 exhibit similarity across both prediction methods: SOC prediction models based on soil science and soil carbon dynamics, and machine learning algorithms employing satellite data.

The objective of this appendix is to compare the SOC stock predictions made in this study with those from other published research predicting SOC stocks in Saskatchewan. The findings offer insights into the apparent differences between SOC prediction models grounded in SOC dynamic processes with crop production data and those employing machine-learning algorithms that incorporate satellite data. Machine-learning algorithms deliver more computationally efficient SOC stock predictions and are easier to scale up compared to models like the Augmented Campbell model or RothC model. These algorithms are typically modeled using cross-validation techniques, incorporating both training and testing data for prediction. In contrast, SOC prediction models such as ICBM, DayCent, and RothC simulate SOC stocks over a time series for individual observations, fields, or plots. However, machine learning-based SOC prediction models often do not integrate SOC dynamics, relying instead on statistical methods to predict SOC stocks.

Appendix 1E: Saskatchewan Crop Insurance Sample Selection for Soil Organic Carbon Prediction

In this appendix, I describe the difference between the SCIC insured sample used for SOC prediction and the observed SCIC insured sample not used for SOC prediction. The primary distinctions lie in the distribution of seeded crops and crop yield across each sample. Additionally, there are differences in the field size, measured in hectares per field. However, both samples exhibit remarkable similarity in terms of crop distribution, yield, and field size. This alignment suggests that extrapolating the predicted SOC stock per hectare from the sampled fields to all SCIC insured hectares is justified. This assertion is supported by the comparable nature of prediction outcomes for fields not included in the sample, given the identical crop distribution and yields across both sample sets.

Figure 1E.1 shows the distribution of crop shares within and outside the SOC prediction sample from 1998 to 2019, categorized by soil zone. Across the timeline, the proportion of hectares dedicated to each crop type remains consistent between the two samples. Notable distinctions include a slightly higher proportion of canola hectares within the sample compared to outside the sample in the dark brown soil zone, and conversely, a slightly lower proportion of durum wheat hectares within the sample in the same soil zone compared to its representation outside the sample.

Figure 1E.2 shows that crop yields over time, as well as by crop type and soil zone, are similarly distributed between the samples selected for SOC prediction and those not selected. Yields within the selected sample are slightly higher for certain crops and soil zones compared to the yields in the out-of-sample group. While density plots and histograms for each crop and soil zone across all years were generated for both samples, they are not displayed here due to the excessive number of graphs such an inclusion would necessitate. The analysis reveals no significant statistical difference in the yield distributions between the samples for each crop covered in this essay and soil zone annually. The most notable variance in yield is observed with oats, which represent a minor portion of the total hectares recorded in the SCIC database.

Figure 1E.3 shows the trend in average field size over time, distinguishing between the fields chosen for SOC prediction (selected sample) and those not chosen (out of sample), further distinguished by fields seeding a single crop and those with multiple crops. The field sizes within the selected sample remain relatively consistent over time, in contrast to the out-of-sample fields, which exhibit a gradual increase in size for both single and multiple crop scenarios. In the initial years covered by the study, fields not included in the sample and growing only one crop were typically smaller in size, as a portion of the land was left fallow.

Figure 1E.4 illustrates a declining trend in the proportion of fields growing multiple crops across all soil zones within the SCIC dataset over time. This trend suggests that differences in field size between fields selected for SOC prediction (in sample) and those not selected (out of sample) are unlikely to introduce significant selection bias, especially when crop shares and yields are consistent between the two groups. Nevertheless, the observed changes in field size reflect broader agricultural trends toward larger farm operations and going towards economies of scale in grain production. As a result, with the adoption of larger farming equipment and a reduction in the number of farmers, the average field size is converging towards the conventional legal land parcel of 65 hectares (160 acres).

FIGURE E.1: SCIC Insured Share of Crop Hectares in Saskatchewan In- and Out-of-Sample for Soil Organic Carbon Prediction
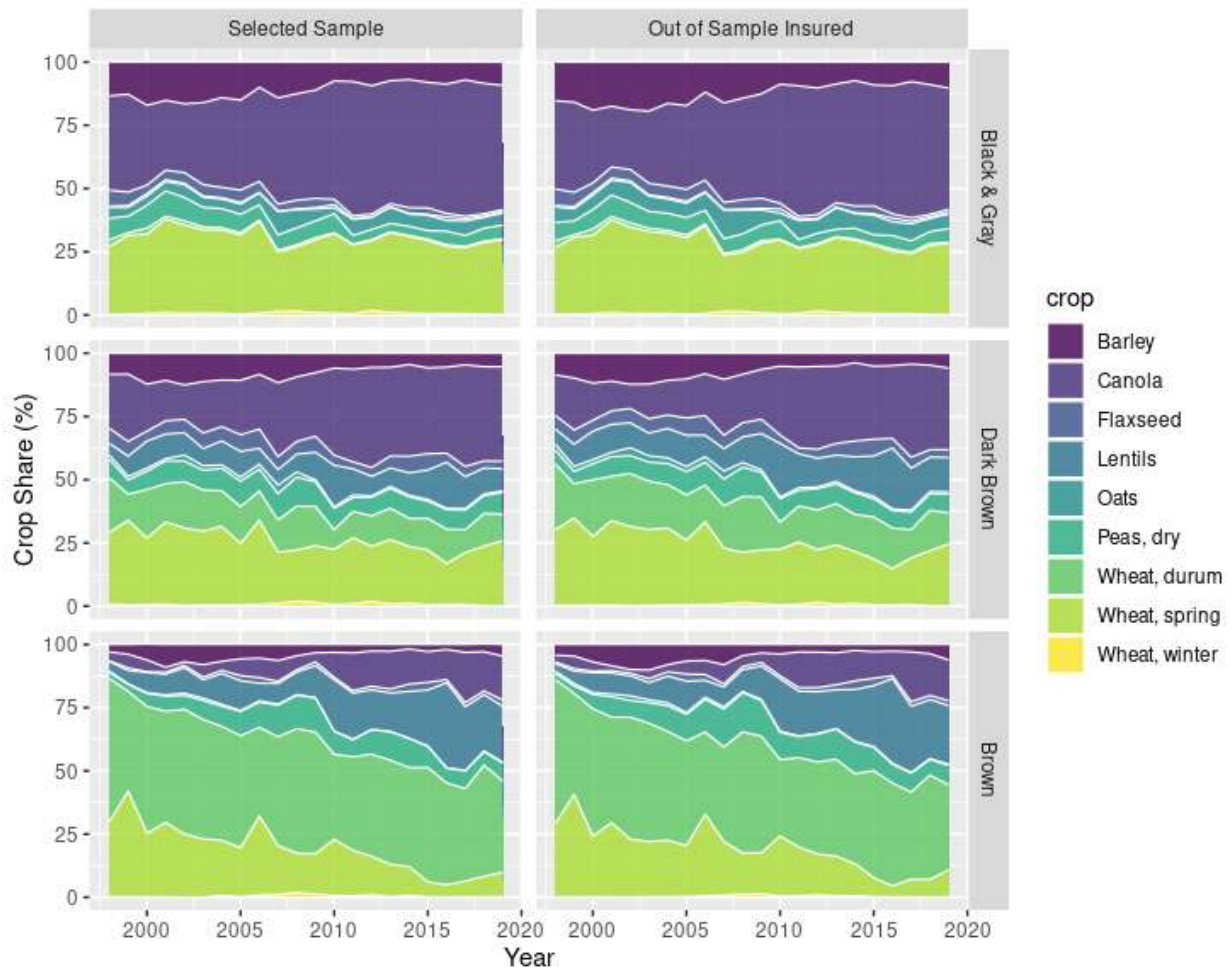
Source: Constructed using SCIC confidential data.

FIGURE E.2: SCIC Insured Mean Crop Yield in Saskatchewan In- and Out-of-Sample for Soil Organic Carbon Prediction
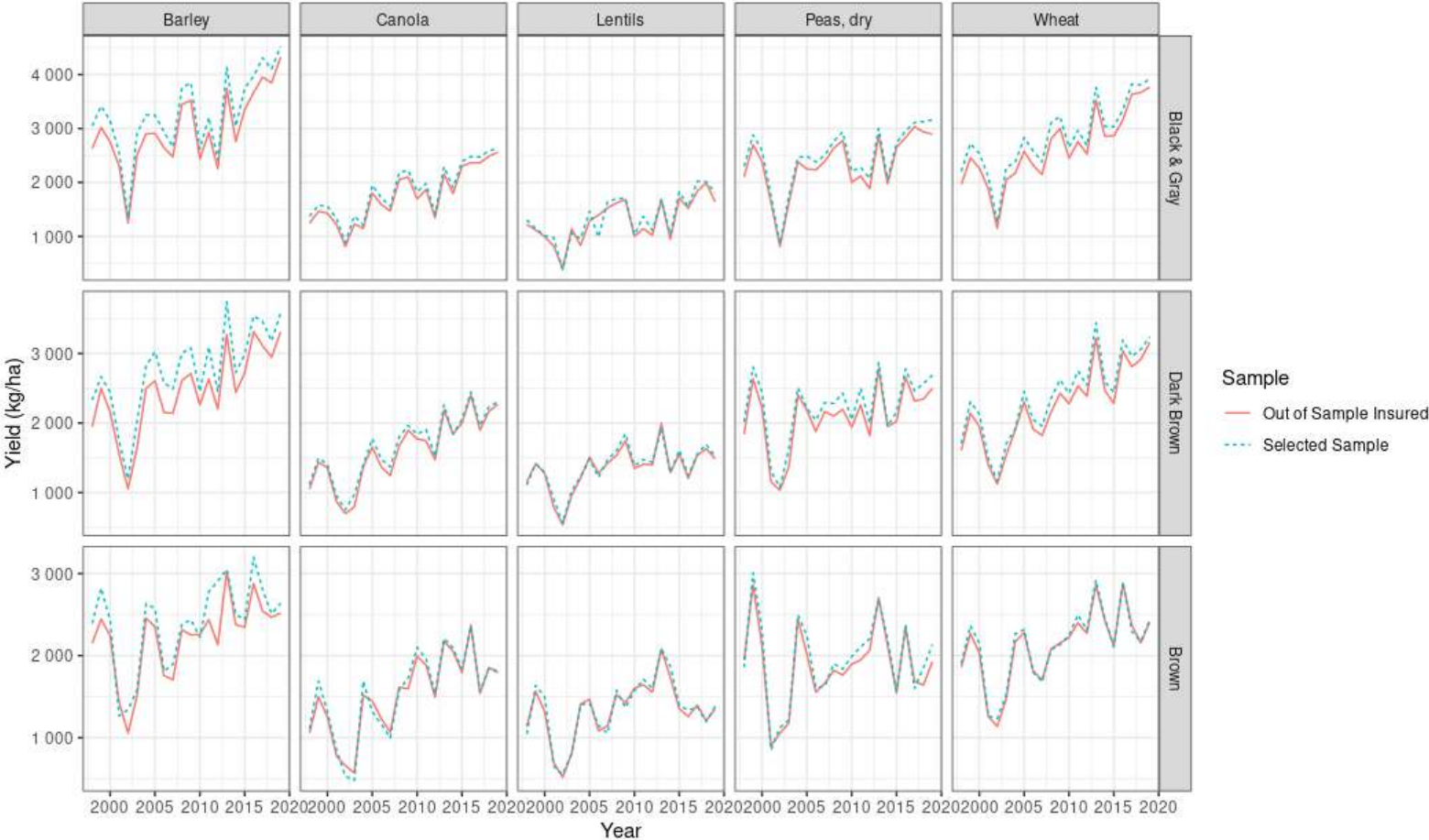
Source: Constructed using SCIC confidential data.

FIGURE E.3: SCIC Insured Mean Field Hectares in Saskatchewan In- and Out-of-Sample for Soil Organic Carbon Prediction
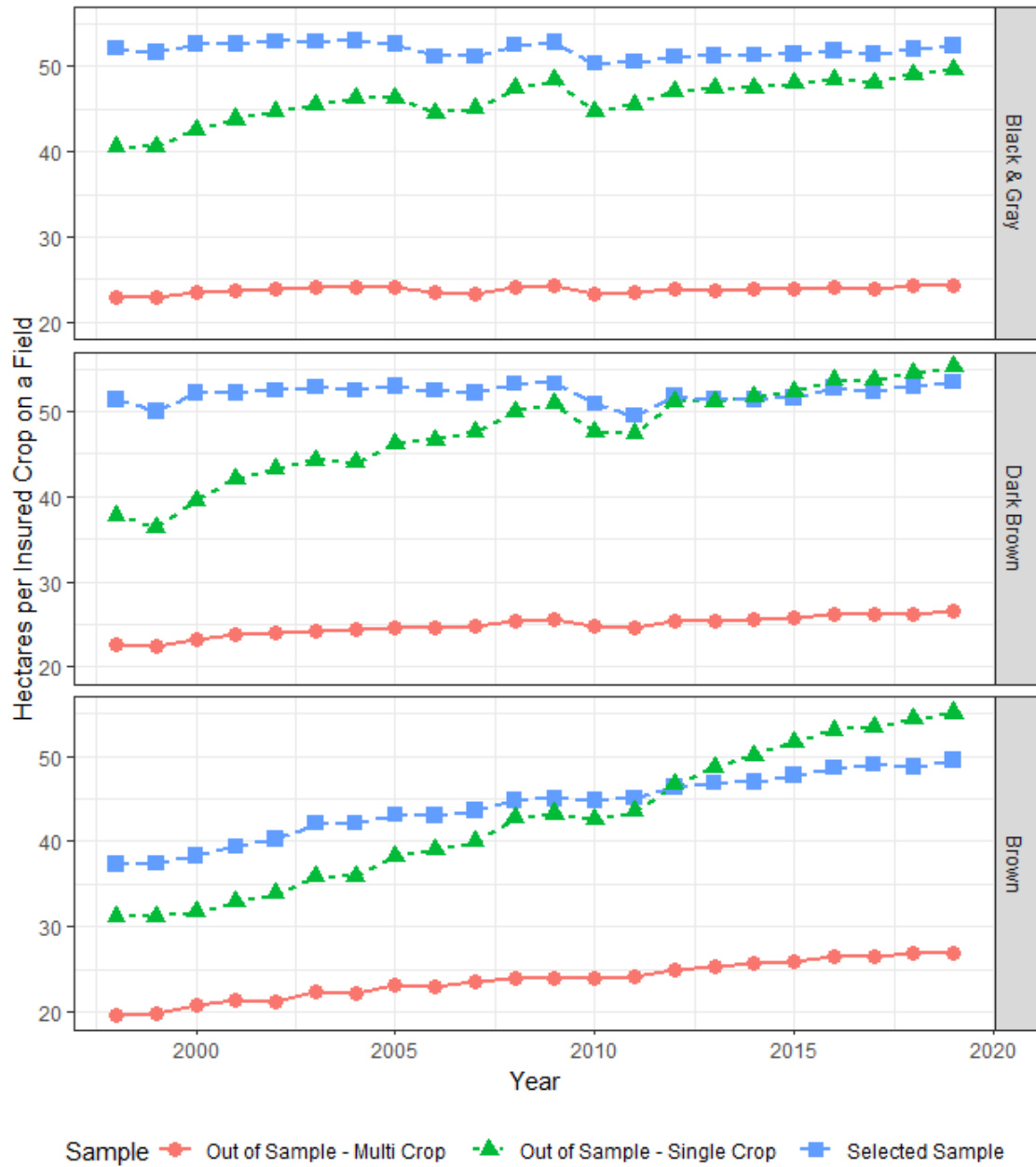
Source: Constructed using SCIC confidential data.

FIGURE E.4: SCIC Percentage of Insured Fields that Seed Multiple Crops in Saskatchewan
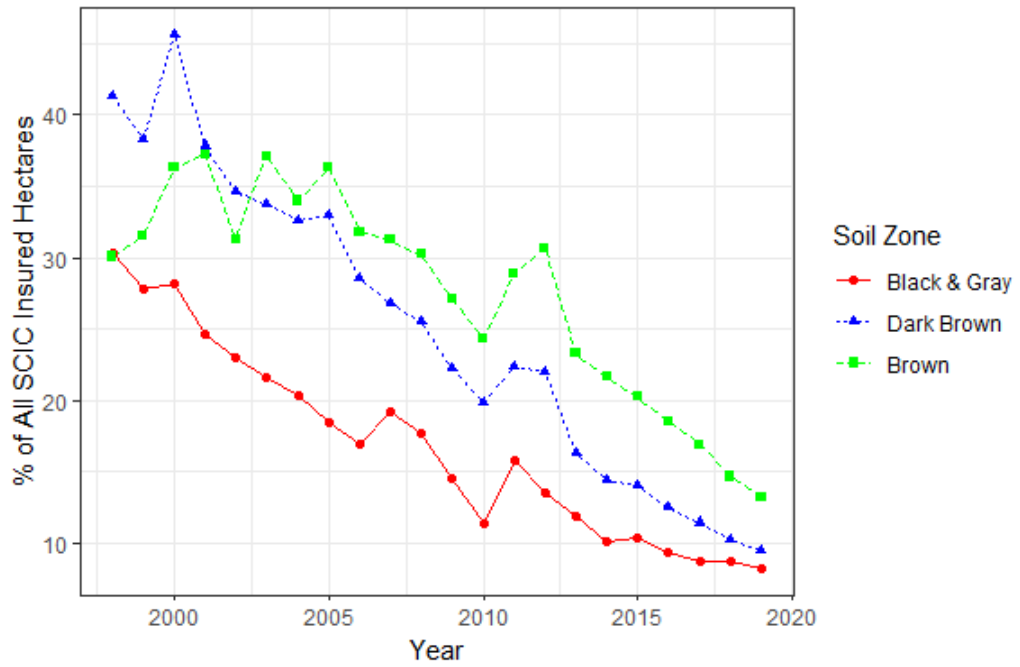
Source: Constructed using SCIC confidential data.

Appendix 1F: Calculating the Present Value of Carbon Sequestration using the Social Cost of Carbon

The economic impact of increasing atmospheric carbon dioxide endures for many decades into the future, due to the prolonged presence of carbon dioxide in the atmosphere (Greenestone et al., 2013). Pearce (2003) defines the social cost of carbon (SCC) as the present value of all future incremental damages resulting from the release of an additional unit of carbon dioxide into the atmosphere, which is an estimate of the marginal cost of permanent change. Presently, determining the SCC relies on integrated assessment models (IAMs), which simulate how human behaviors and consumption choices influence climate change. IAMs are "integrated" because they merge economic and societal behaviors with specific Earth's physical systems, connecting economic and geophysical stocks and flows.

In 2021, President Biden issued Executive Order 13990, directing the Interagency Working Group on Social Cost of Greenhouse Gases (IWG) to release an interim estimate for the social cost of carbon (SCC) (Interagency Working Group on Social Cost of Greenhouse Gases, 2021). By February 2021, the IWG had computed the SCC at 51 U.S. dollars per Mg of carbon dioxide, employing a real discount rate of 3% per annum (in 2020 dollars). Depending on the chosen discount rate, the SCC varied from $14 per Mg of carbon dioxide with a 5% annual discount rate to $76 per Mg of carbon dioxide with a 2.5% annual discount rate. Numerous other studies use IAMs to estimate the SCC. Rennert et al. (2022) propose a more precise SCC estimate of $185 per Mg of CO_2 with a 2% near-term risk-free discount rate, whereas Russell et al. (2022) demonstrate that depending on the Representative Concentration Pathways (RCPs) in temperature projections and Shared Socioeconomic Pathways (SSPs), the SCC might range from as low as $2.35 per Mg of CO_2 to as high as $258.40 per Mg ton of CO_2.

The interim values for the SCC released by the IWG derive from the an ensemble of three IAMs to evaluate the economic damages of releasing an additional unit of carbon dioxide into the atmosphere. The three IAMs are the Dynamic Integrated Climate and Economy (DICE) 2010, the

Climate Framework for Uncertainty, Negotiation, and Distribution (FUND), and the Policy Analysis of the Greenhouse Gas Effect (PAGE). These models project future policy scenarios through dynamic processes that incorporate data on economic development and climatic changes.

In this appendix, I demonstrate how to use the SCC to calculate the external social benefits from carbon sequestration. Given that a unit of carbon sequestered in the soil does not equate to a unit of atmospheric carbon dioxide, I adjust the SCC to reflect the social cost of sequestering soil organic carbon (SCSOC). The SCSOC represents the worth of capturing an additional unit of soil organic carbon (SOC) indefinitely. However, since SOC is not retained in the soil indefinitely, it is necessary to translate the SCSOC into an annual rental value. This value represents the benefit from sequestering SOC for one year.

To convert the SCC to SCSOC, Mikhailova et al. (2019) employ a conversion factor of 44 Mg of carbon dioxide per 12 Mg of SOC. The SCSOC is equal to,

$$SCSOC_t = SCC_t * \frac{44 \text{ Mg CO}_2}{12 \text{ Mg SOC}}. \tag{1F.1}$$

This represents the value of storing an additional ton of SOC forever rather than releasing it into the atmosphere.

In equation (1F.2), the annual rental rate of the SCSOC (P_t) is equal to the SCSOC multiplied by the discount rate (r) that correspond to the discount rate used to calculate the SCC.

$$P_t = r * SCSOC_t. \tag{1F.2}$$

Using equation (1F.2), by applying the rental rate to the existing SOC stock, I estimate the external societal benefits of the carbon stored in the soil relative to a hypothetical scenario where this carbon would be emitted into the atmosphere. To assess the external benefits of changes in carbon sequestration against a baseline SOC stock, it is essential to establish a specific counterfactual SOC stock level. This hypothetical SOC stock can either be determined directly or modeled to

evaluate the effect of certain carbon sequestration policies. For instance, the baseline SOC stock might be set equal to the steady-state equilibrium stock for native prairie lands or another land management practice, such as zero tillage.

Equation (1F.3) shows a formula for calculating the external social benefit from carbon sequestered in year $t + n$ for the "actual" or with-policy stock of SOC (SOC_{t+n}^A) relative to a "counterfactual" or with-out policy stock of SOC (SOC_{t+n}^C). The term in parentheses is the policy-induced change in the stock of SOC.

$$SB_{t+n} = P_t(SOC_{t+n}^A - SOC_{t+n}^C) \tag{1F.3}$$

Consider a policy change made in year t, such that changes in the stock of SOC occurs in the following year. The present value of the external social benefit that originates from the policy-induced change in the stock of SOC over the indefinite future, and using a real discount rate equal to δ, is equal to:

$$PV_t = \sum_{n=1}^{\infty} SB_{t+n}(1 + \delta)^{-n}. \tag{1F.4}$$

If the SCSOC indicates the marginal effect of raising the SOC stock by one unit indefinitely, then the discount rate in equation (1F.4) should match the discount rate in equation (1F.2).

For instance, suppose that the difference between the stock of SOC with and without a policy remains unchanged over time. By adopting this assumption, the variable for external social benefit (SB) no longer requires a time index. Under this condition, equation (1F.4) simplifies to the following form:

$$PV_t = SB \sum_{n=1}^{\infty} (1 + \delta)^{-n}. \tag{1F.5}$$

The closed form solution to the geometric series in equation (1F.5) is,

122

$$PV_t = \frac{SB/(1+\delta)}{1 - 1/(1+\delta)}. \tag{1F.6}$$

Substituting equation (1F.3) that includes the constant external social benefit into equation (1F.6) implies,

$$PV_t = \frac{P_t}{\delta}(SOC^A - SOC^C). \tag{1F.7}$$

Substituting r for δ in equation (1F.7) implies,

$$PV_t = \frac{P_t}{r}(SOC^A - SOC^C) = SCC_t * \frac{44 \, \text{Mg CO}_2}{12 \, \text{Mg SOC}}(SOC^A - SOC^C). \tag{1F.8}$$

When the discount rate applied to determine the present value of the policy-induced variation in the SOC stock matches the discount rate used for computing the SCC ($\delta = r$), the SCC reflects the present value of all future welfare effects resulting from a unit increase in carbon dioxide emissions into the atmosphere.

Appendix 1G: Supplementary Graphs and Tables

This appendix includes the supplementary graphs and tables referenced throughout the essay.

FIGURE 1G.1: Comparison of SOC Prediction using Base and Weather Versions of the Augmented Campbell model on six Randomly Selected Fields in Saskatchewan from 1998 to 2019
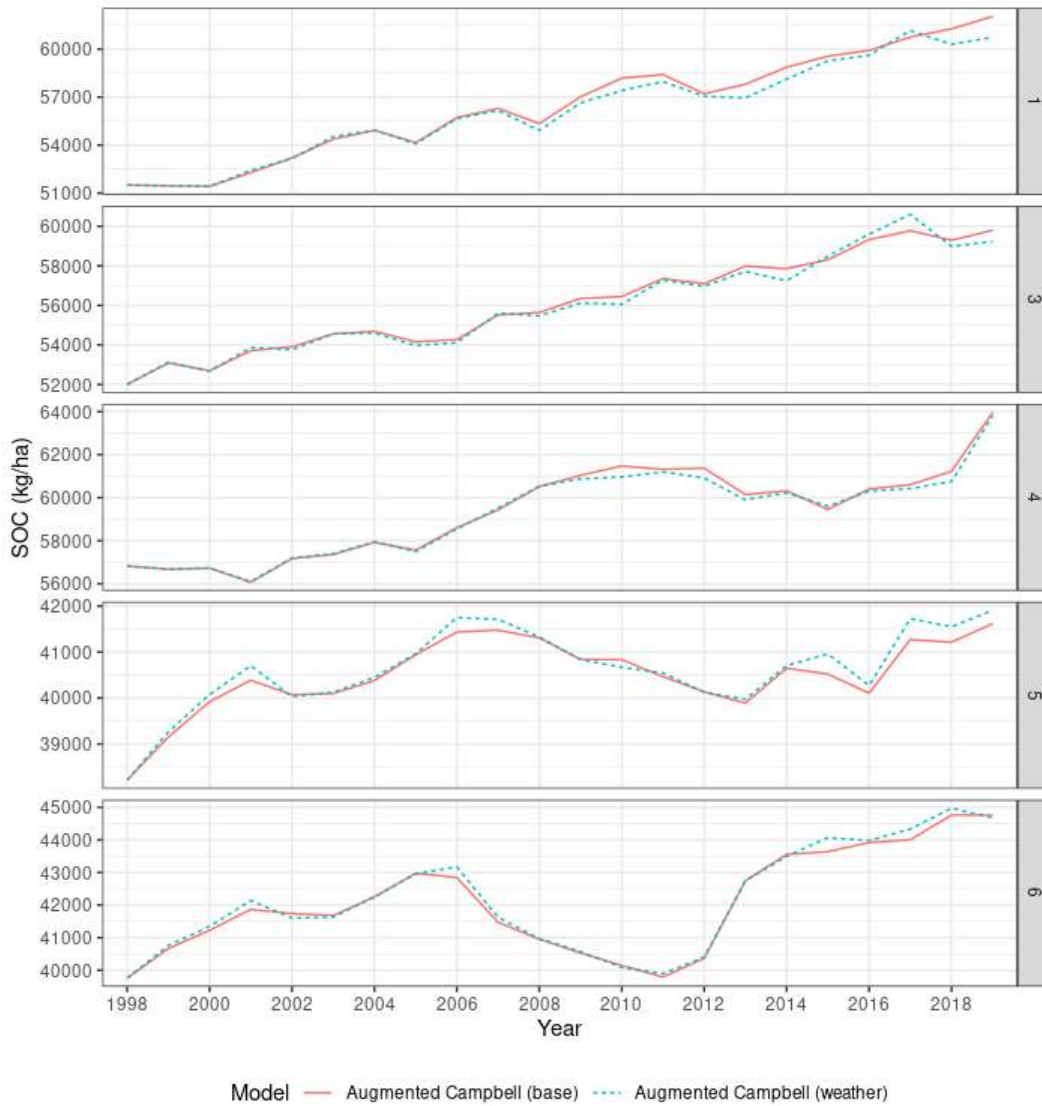
Source: Author's Estimates.

Notes: Each panel refers to an individual field that is randomly selected in Saskatchewan.

FIGURE 1G.2: Field-level Distribution of External Social Benefit per Hectare by Draw of the Binomial Distribution, Counterfactual Scenario, and Soil Zone in Saskatchewan using the Campbell Model and a Social Cost of Carbon of $14/Mg
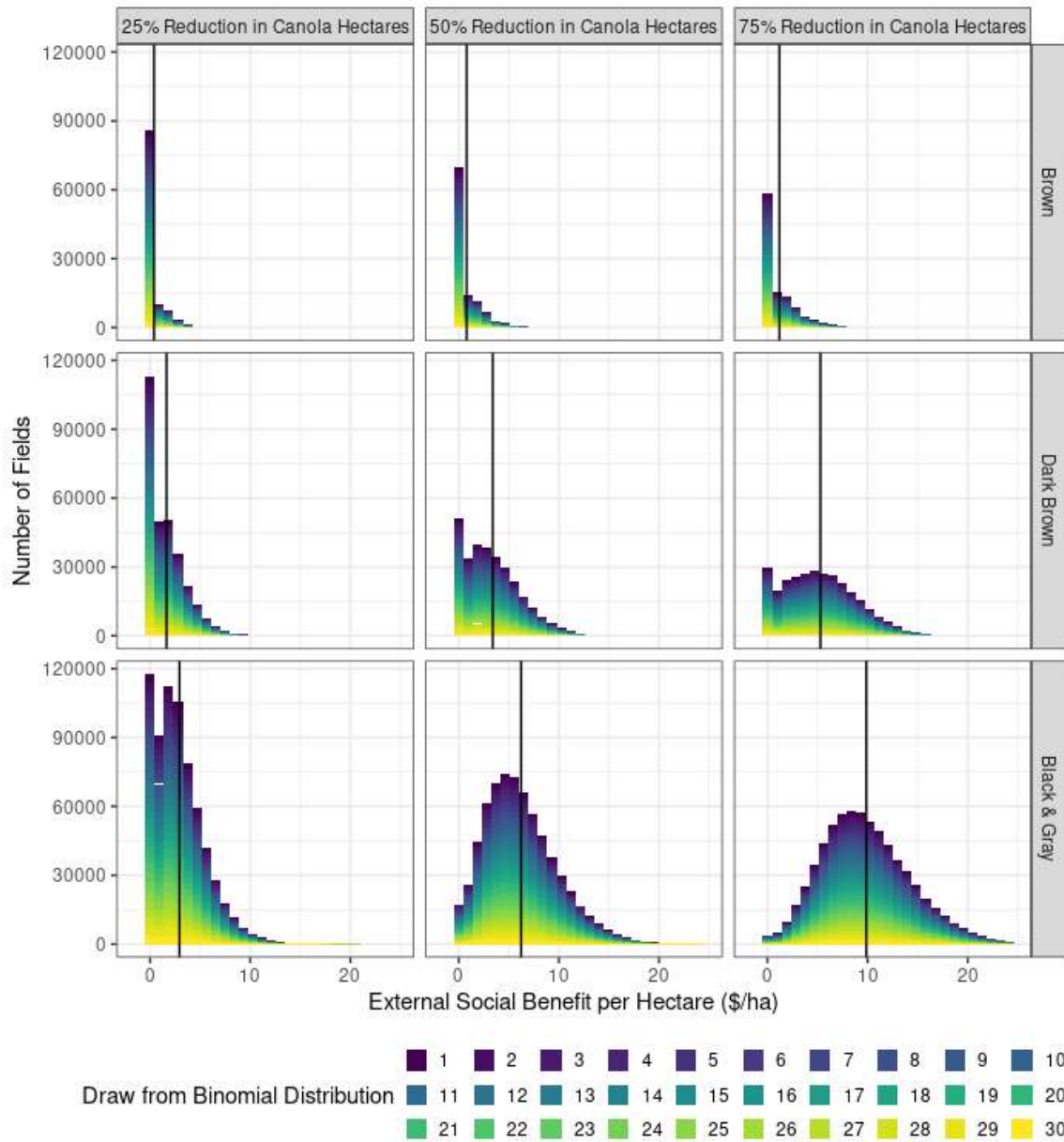
Source: Author's Estimates.

Notes: All soil organic carbon predictions in the above graph are computed using the Campbell model. The columns of panels refer to the counterfactual shares of canola switched to summer fallow (25%, 50%, and 75%) of insured hectares in Saskatchewan, whereas the rows of panels refer to different soil zones.

FIGURE 1G.3: Field-level Distribution of External Social Benefit per Hectare by Draw of the Binomial Distribution, Counterfactual Scenario, and Soil Zone in Saskatchewan using the Campbell Model and a Social Cost of Carbon of $51/Mg
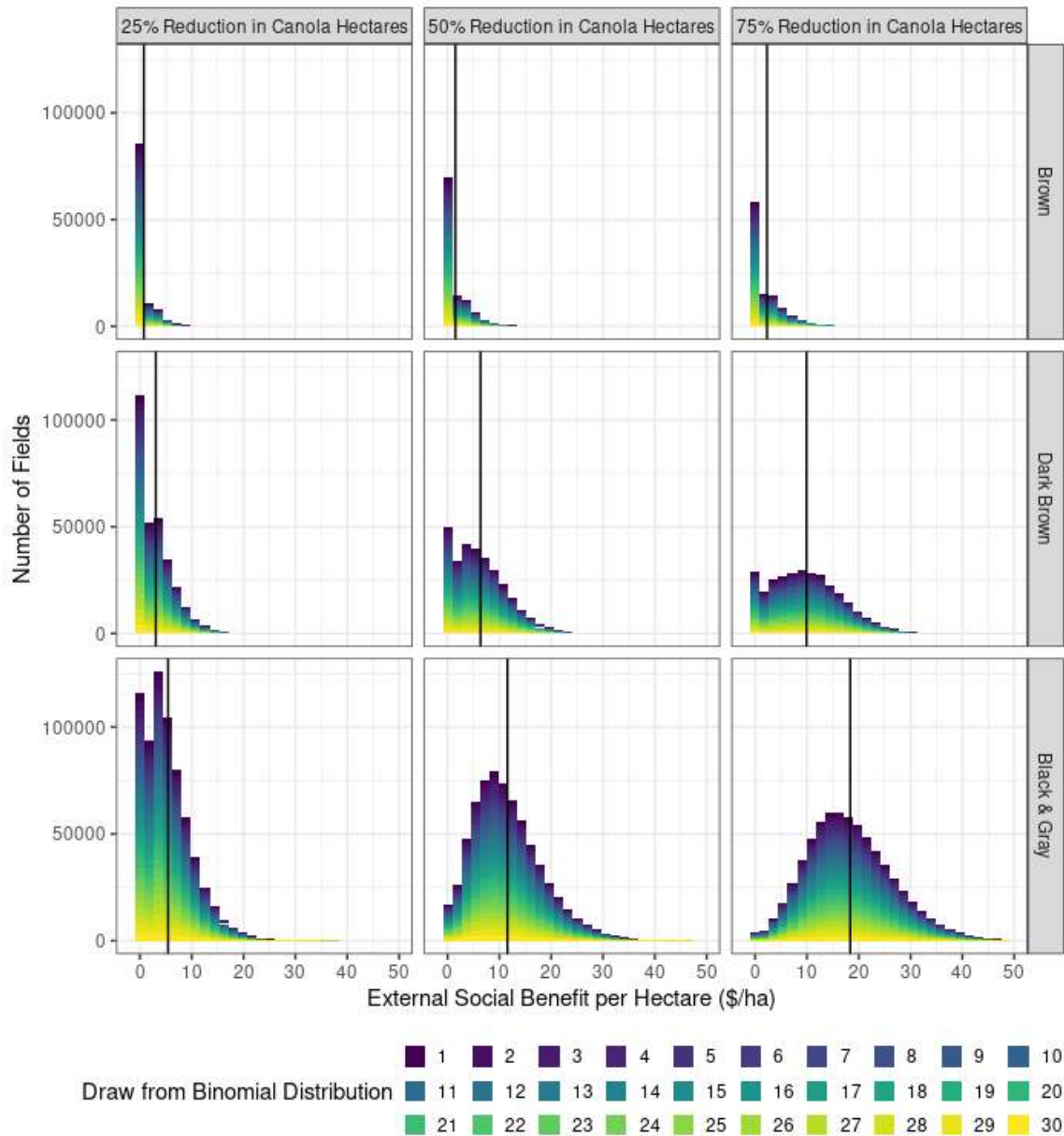
Source: Author's Estimates.

Notes: All soil organic carbon predictions in the above graph are computed using the Campbell model. The columns of panels refer to the counterfactual shares of canola switched to summer fallow (25%, 50%, and 75%) of insured hectares in Saskatchewan, whereas the rows of panels refer to different soil zones.

FIGURE 1G.4: Field-level Distribution of External Social Benefit per Hectare by Draw of the Binomial Distribution, Counterfactual Scenario, and Soil Zone in Saskatchewan using the Campbell Model and a Social Cost of Carbon of $76/Mg
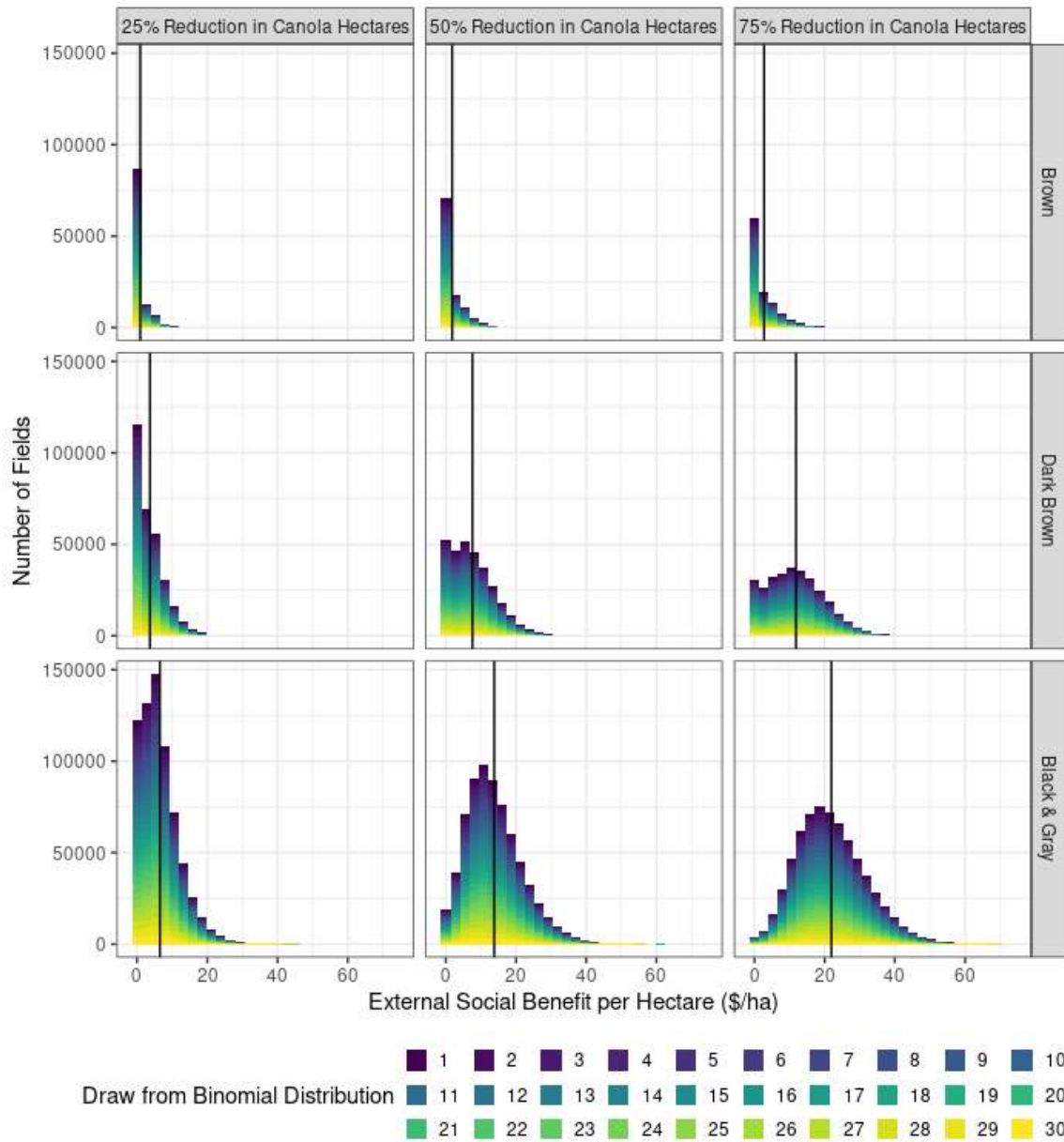
Source: Author's Estimates.

Notes: All soil organic carbon predictions in the above graph are computed using the Campbell model. The columns of panels refer to the counterfactual shares of canola switched to summer fallow (25%, 50%, and 75%) of insured hectares in Saskatchewan, whereas the rows of panels refer to different soil zones.

FIGURE 1G.5: Field-level Distribution of External Social Benefit per Hectare by Draw of the Binomial Distribution, Counterfactual Scenario, and Soil Zone in Saskatchewan using the Campbell Model and a Social Cost of Carbon of $185/Mg
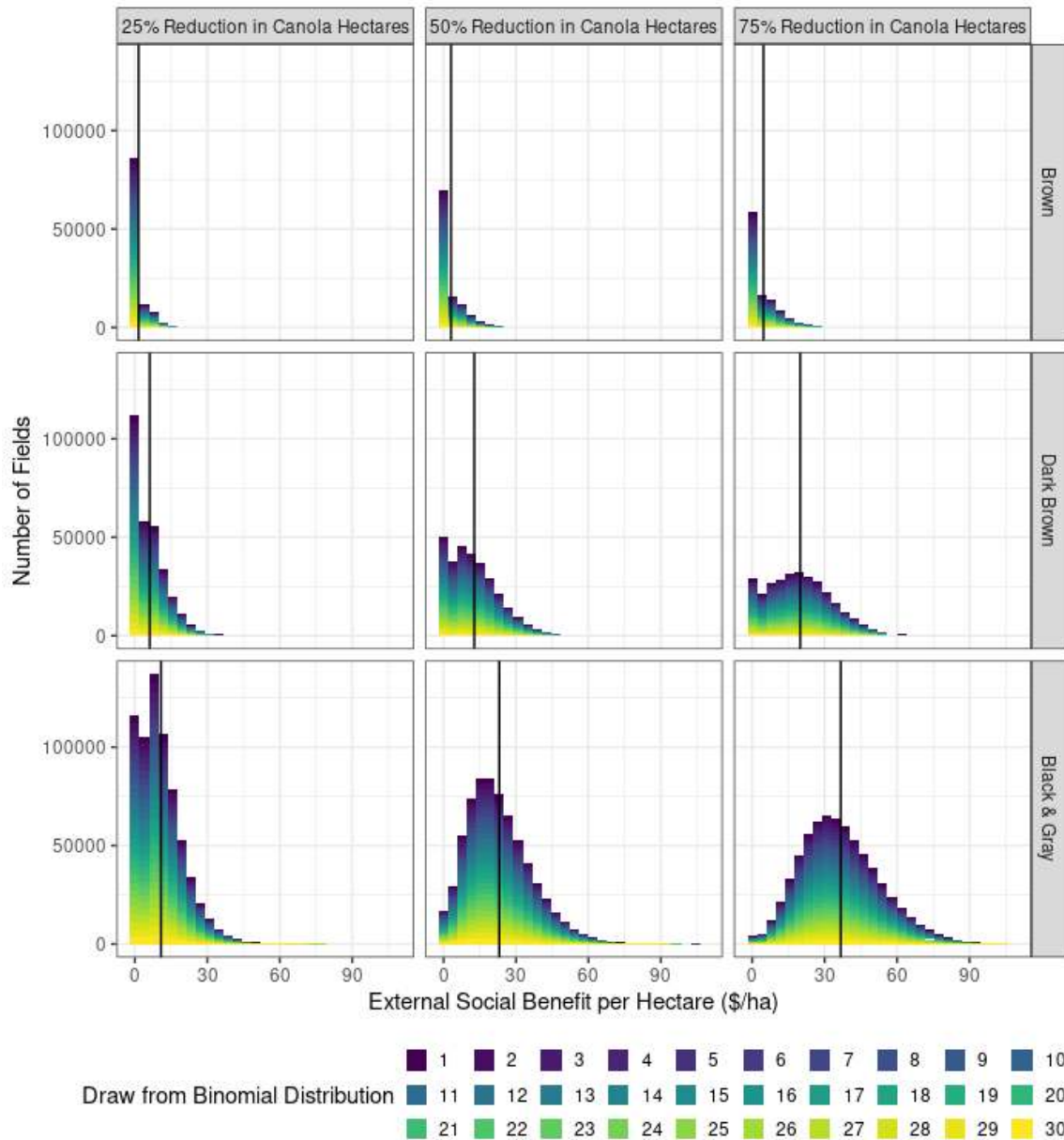
Source: Author's Estimates.

Notes: All soil organic carbon predictions in the above graph are computed using the Campbell model. The columns of panels refer to the counterfactual shares of canola switched to summer fallow (25%, 50%, and 75%) of insured hectares in Saskatchewan, whereas the rows of panels refer to different soil zones.

FIGURE 1G.6: Field-level Distribution of External Social Benefit per Hectare by Draw of the Binomial Distribution, Model, and Soil Zone in Saskatchewan using a Social Cost of Carbon of $51/Mg

Notes: The columns of panels refer to SOC prediction model employed, whereas the rows of panels refer to different soil zones. In all panels, I use the counterfactual share of 25% of lentil hectares switched to summer fallow of insured hectares in Saskatchewan.

FIGURE 1G.7: Censored Field-level Distribution of External Social Benefit per Hectare by Draw of the Binomial Distribution, Model, and Soil Zone in Saskatchewan using a Social Cost of Carbon of $51/Mg
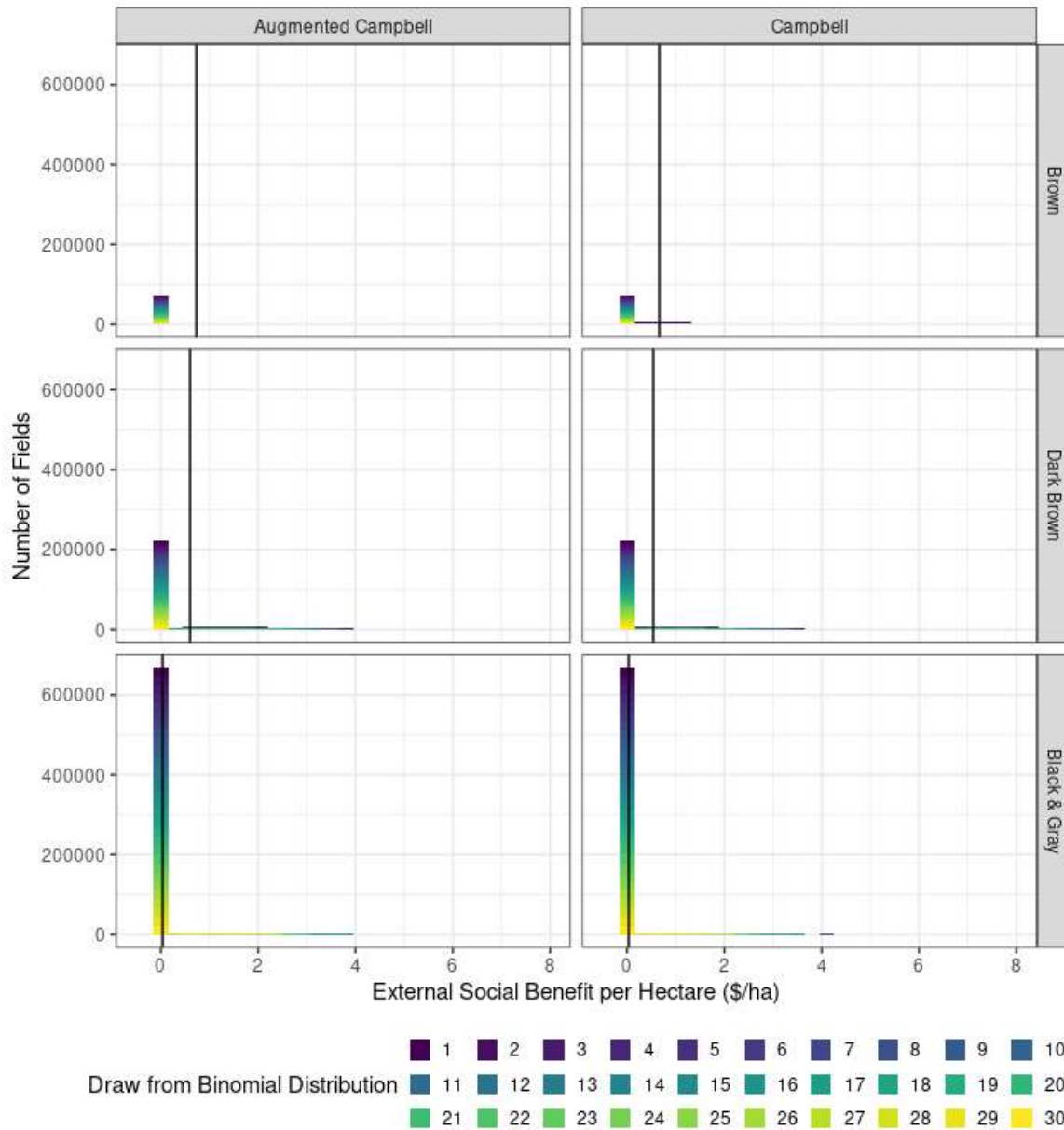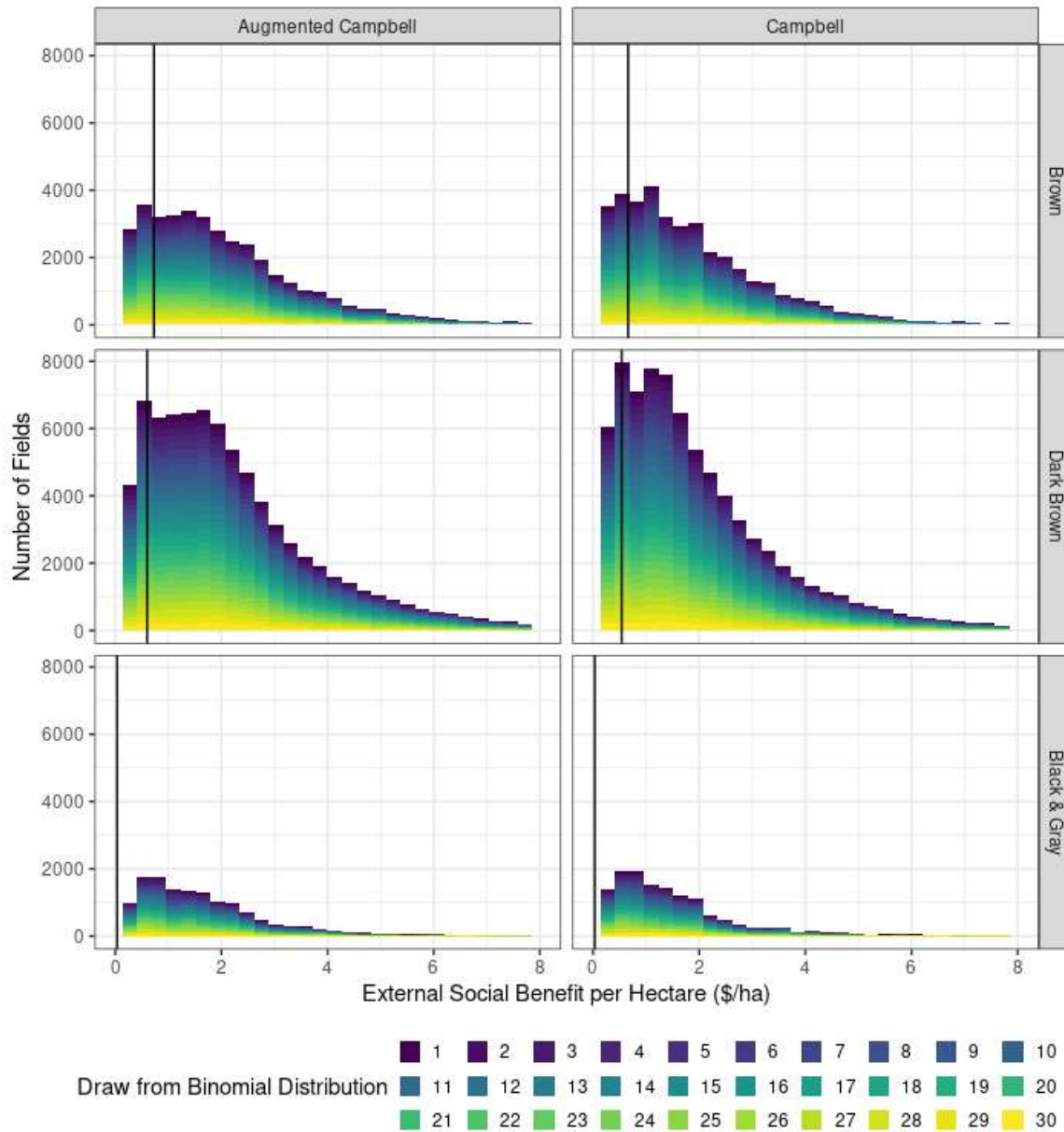
Source: Author's Estimates.

Notes: The columns of panels refer to SOC prediction model employed, whereas the rows of panels refer to different soil zones. In all panels, I use the counterfactual share of 25% of lentil hectares switched to summer fallow of insured hectares in Saskatchewan. The external social benefit per hectare are censored at zero, which means the figure above only includes benefits only positive dollars per hectare.

FIGURE 1G.8: Distribution of External Social Benefit per Hectare by Draw of the Binomial Distribution, Social Cost of Carbon, and Counterfactual Scenario using the the Augmented Campbell Model (weather) for a Randomly Selected Field in the Black & Gray Soil Zone in Saskatchewan
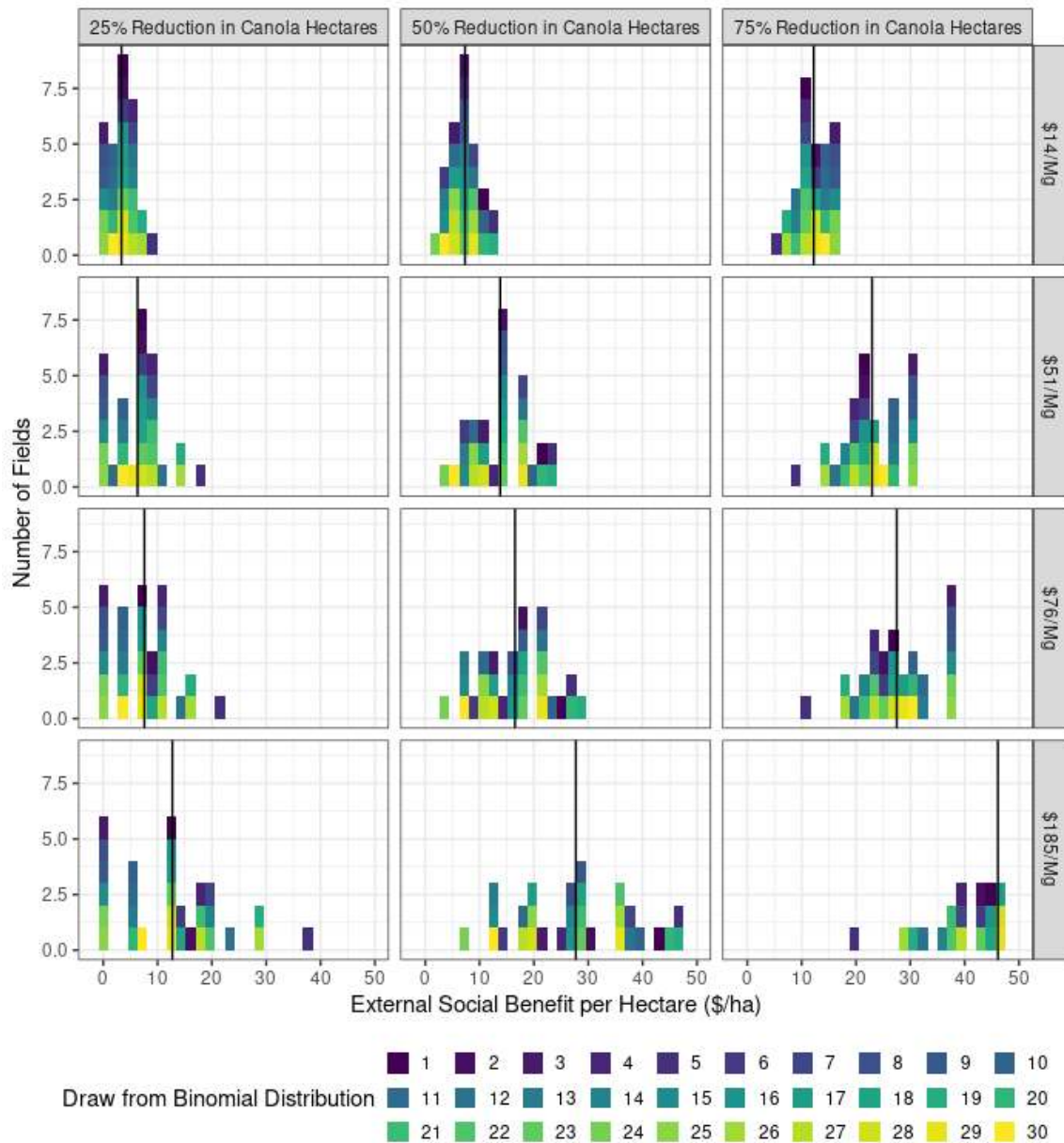
Source: Author's Estimates.

Notes: All soil organic carbon predictions in the above graph are computed using the Augmented Campbell model. The columns of panels refer to the counterfactual shares of insured hectares of canola in Saskatchewan switched to summer fallow (25%, 50%, and 75%), whereas the rows of panels refer to different soil zones.

FIGURE 1G.9: Field-level Distribution of External Social Benefit per Hectare for a single Draw from the Binomial Distribution by Counterfactual Scenario and Soil Zone in Saskatchewan using the Augmented Campbell Model (weather) and a Social Cost of Carbon of $51/Mg
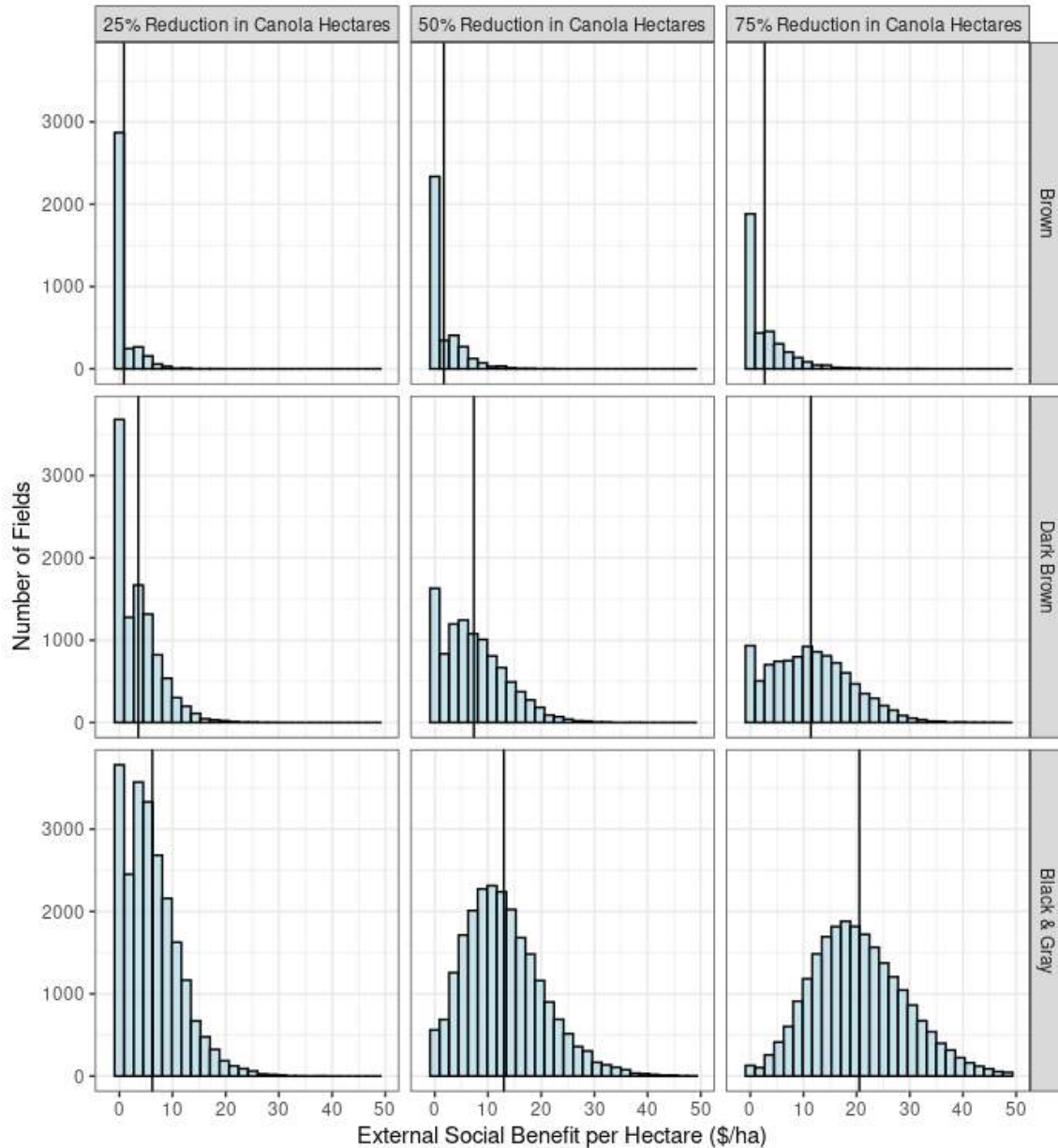
Source: Author's Estimates.

Notes: All soil organic carbon predictions in the above graph are computed using the Augmented Campbell model. The columns of panels refer to the counterfactual shares of canola switched to summer fallow (25%, 50%, and 75%) of insured hectares in Saskatchewan, whereas the rows of panels refer to different soil zones.

TABLE 1G.1: Distribution of External Social Benefits from 1998 to 2019 by Counter-factual Scenario, Soil Zone, and Social Cost of Carbon in Saskatchewan using the Campbell Model

	(1)	(2)	(3)	(4)
	External Social Benefit			
Counterfactual:	Share of Canola Hectares reverted to Summer Fallow			Share of Lentil Hectares reverted to Summer Fallow
	25%	50%	75%	25%
	(i) Brown Soil Zone			
Social Cost of Carbon:	*(millions of dollars)*			
$14/Mg				
Mean	18	37	56	16
Minimum	17	35	54	15
Maximum	19	38	56	17
$51/Mg				
Mean	35	70	106	31
Minimum	33	67	104	29
Maximum	37	73	108	33
$76/Mg				
Mean	42	85	128	37
Minimum	40	81	125	35
Maximum	44	87	130	40
$185/Mg				
Mean	70	143	216	63
Minimum	67	136	211	59
Maximum	75	147	219	67
	(ii) Dark Brown Soil Zone			
$14/Mg				
Mean	127	264	411	24
Minimum	125	261	408	23
Maximum	130	267	414	25
$51/Mg				
Mean	238	493	769	44
Minimum	234	488	764	42
Maximum	242	499	774	46
$76/Mg				
Mean	284	589	920	52
Minimum	279	583	914	50
Maximum	289	596	926	54
$185/Mg				
Mean	476	988	1,542	87
Minimum	468	977	1,531	84
Maximum	485	999	1,552	91

TABLE 1G.1: Distribution of External Social Benefits from 1998 to 2019 by Counterfactual Scenario, Soil Zone, and Social Cost of Carbon in Saskatchewan using the Campbell Model *(continued)*

	(1)	(2)	(3)	(4)
	External Social Benefit			
Counterfactual:	Share of Canola Hectares reverted to Summer Fallow			Share of Lentil Hectares reverted to Summer Fallow
	25%	50%	75%	25%
	(iii) Black & Gray Soil Zone			
Social Cost of Carbon:	*(millions of dollars)*			
$14/Mg				
Mean	279	592	939	2
Minimum	275	587	934	2
Maximum	282	596	944	2
$51/Mg				
Mean	516	1,098	1,745	3
Minimum	510	1,089	1,736	3
Maximum	523	1,106	1,754	3
$76/Mg				
Mean	616	1,311	2,084	4
Minimum	608	1,299	2,073	3
Maximum	624	1,321	2,095	4
$185/Mg				
Mean	1,029	2,192	3,487	6
Minimum	1,017	2,173	3,468	6
Maximum	1,042	2,209	3,505	7
	(iv) Saskatchewan (All Soil Zones)			
$14/Mg				
Mean	424	892	1,406	42
Minimum	418	883	1,396	40
Maximum	431	901	1,414	44
$51/Mg				
Mean	789	1,661	2,621	78
Minimum	777	1,644	2,604	74
Maximum	802	1,678	2,636	82
$76/Mg				
Mean	942	1,985	3,132	93
Minimum	927	1,963	3,112	89
Maximum	957	2,005	3,151	98
$185/Mg				
Mean	1,576	3,323	5,245	156
Minimum	1,552	3,287	5,211	148
Maximum	1,602	3,356	5,276	164

Source: Author's Estimates

TABLE 1G.2: External Social Benefits for a Permanent Change in SOC Stocks 2019
by Counterfactual Scenario, Soil Zone, and Social Cost of Carbon in Saskatchewan
using the Campbell Model

	(1)	(2)	(3)
	External Social Benefit		
	Share of Canola Hectares Reverted to Summer Fallow		
Counterfactual:	25%	50%	75%
	(i) Brown Soil Zone		
Social Cost of Carbon:	*(millions of dollars)*		
$14/Mg	63	128	194
$51/Mg	226	457	692
$76/Mg	334	678	1,027
$185/Mg	724	1,467	2,223
	(ii) Dark Brown Soil Zone		
$14/Mg	202	423	664
$51/Mg	722	1,508	2,371
$76/Mg	1,070	2,236	3,516
$185/Mg	2,317	4,840	7,611
	(iii) Black & Gray Soil Zone		
$14/Mg	405	874	1,413
$51/Mg	1,444	3,120	5,042
$76/Mg	2,142	4,627	7,478
$185/Mg	4,637	10,016	16,188
	(iv) Saskatchewan (All Soil Zones)		
$14/Mg	670	1,425	2,272
$51/Mg	2,392	5,084	8,105
$76/Mg	3,547	7,540	12,020
$185/Mg	7,678	16,323	26,022

Source: Author's Estimates

TABLE 1G.3: Projected External Social Benefits from 2020 to 2169 by Counterfactual Scenario, Soil Zone, and Social Cost of Carbon in Saskatchewan using the Campbell Model

	(1)	(2)	(3)
	External Social Benefit		
	Share of Canola Hectares reverted to Summer Fallow		
Counterfactual:	25%	50%	75%
	(i) Brown Soil Zone		
Social Cost of Carbon:	*(millions of dollars)*		
$14/Mg	40	84	128
$51/Mg	148	312	476
$76/Mg	220	463	707
$185/Mg	470	989	1,509
	(ii) Dark Brown Soil Zone		
$14/Mg	217	439	649
$51/Mg	798	1,619	2,394
$76/Mg	1,183	2,400	3,547
$185/Mg	2,521	5,113	7,556
	(iii) Black & Gray Soil Zone		
$14/Mg	411	825	1,246
$51/Mg	1,512	3,035	4,589
$76/Mg	2,239	4,495	6,796
$185/Mg	4,769	9,573	14,475
	(iv) Saskatchewan (All Soil Zones)		
$14/Mg	667	1,348	2,024
$51/Mg	2,459	4,966	7,458
$76/Mg	3,643	7,358	11,049
$185/Mg	7,760	15,675	23,539

Source: Author's Estimates

136

Chapter 2

The Consequences of Soil Organic Carbon for Crop Yield, Farm Productivity, and Profit

2.1 Introduction

Addressing climate change stands as one of humanity's paramount challenges, representing the pivotal issue of our era. Agricultural soils offer significant potential as carbon sinks, with the expansion of soil organic carbon (SOC) stocks capable of yielding substantial benefits both on-farm and environmentally. Crops with high carbon storage capacities play a vital role in climate regulation, particularly in agricultural systems where soils serve as carbon sinks. Hence, farmer decisions about land use practices that bolster SOC stocks are relevant for governments seeking to offset greenhouse gas (GHG) emissions (Lemma et al., 2021). Minasny et al. (2017) state that if agricultural soils around the world increased SOC by 0.4% each year until SOC saturation in the soil, this could potentially offset 20% to 35% of annual global greenhouse gas emissions from anthropogenic sources.[1] In Canada, increases in SOC stocks on farms from 2013 to 2015 were sufficient to completely offset all agricultural greenhouse gas emissions, translating to an average

---

[1]Achieving this goal depends on many other socioeconomic and environmental factors (Paustian et al., 2016).

net reduction of 16.2 million metric tonnes CO_2-equivalent (Fan et al., 2019). The increase in carbon sequestration in the Canadian prairies is largely credited to increases in crop yield (Lamb et al., 2011; Fan et al., 2019), and the expansion of canola cultivation and less summer fallow hectares (Fan et al., 2019).[2]

In this essay, I examine the long-term effects of carbon sequestration on crop yields using field-level data for all insured farms in Saskatchewan for the years 1998 to 2019. During this time period, farmers eliminated summer fallow , converted a lot of land to zero-tillage and continuous cropping, and consequently sequestered more carbon in the soil. Taking advantage of the resulting variation in SOC over time and across fields, I identify the on-farm shadow value of SOC, which represents the private value to farmers of an additional unit of SOC. I then use dynamic simulations to forecast changes in SOC under different crop rotations, and estimate the resulting long-term changes in on-farm profit. Finally, recognizing that increases in SOC generate a positive externality in the form of reduced atmospheric carbon, I estimate the external social benefits, by crop rotation and soil zone, generated by farmers in Saskatchewan.

Agronomic research suggests that increased SOC stocks can lead to higher crop yields (Lafond et al., 2011; Oldfield et al., 2019; Kane et al., 2021; Rubio et al., 2021; Wu and Congreves, 2021). Cropping choice, tillage practices, and other farm management decisions affect SOC. However, SOC accumulation is a slow process, and it may take several or many years before noticeable differences in SOC are evident among different crop rotations and tillage systems (Lychuk et al., 2019). Previous studies investigating the agronomic and economic factors affecting SOC, farm profitability, and productivity have mainly relied on either aggregated data or data from field trial experiments. Aggregated data fail to address the variation among between fields and cannot incorporate crucial information regarding past cropping patterns and yields for specific land parcels (Hendricks et al., 2014). On the other hand, field trial data might not provide an accurate representation of diverse on-farm responses across the entire province of Saskatchewan. To address these

---

[2]Gaudaré et al. (2023) find that a complete conversion to organic farming has the potential to reduce carbon inputs into SOC by 40%, and hence to reduce the stock of SOC by 9% globally. This illustrates the potential importance of farm management practices and their consequences for changes in the stock of SOC and atmospheric carbon.

limitations, I employ detailed field-level data to analyze the relationship between SOC levels and crop yields.

This essay makes three contributions. First, I show that the shadow value of SOC is not only positive but also exhibits diminishing marginal returns, with significant variations across different crops. In Saskatchewan, the benefit from SOC in terms of average yield increases is greatest for spring wheat and durum wheat, followed by lentils, peas, canola, and barley. Notably, the shadow value of SOC is greatest in the brown soil zone, which has the lowest SOC stock. To arrive at these findings, I employ a dynamic panel fixed effects model that utilizes an exclusive dataset from the Saskatchewan Crop Insurance Corporation (SCIC).[3] This dataset, comprising approximately 800,000 observations, includes detailed information on field-level cropping decisions, yields, soil characteristics, weather conditions, and estimated SOC stocks (the latter provided by Serfas (2024a)), enabling a precise estimation of shadow values for SOC stocks.

Second, this research reveals the potential for farmers to enhance long-term profits through strategic crop rotations: by 28% in the brown soil zone, by 12% in the dark brown soil zone, and by 6% in the black & gray soil zone. This profit boost stems from adopting crop rotations that enhance carbon sequestration over a 32-year period.[4] To quantify these prospective increases in profit over the long term, I conduct a dynamic simulation spanning from 2023 to 2055, analyzing five types of four-year crop rotations for each soil zone (resulting in 8 cycles of four-year crop rotations in the 32-year period).[5] The present value change in on-farm profits with yield response to carbon sequestration (with SOC effects) between the Canola-Spring Wheat-Canola-Spring Wheat rotation to the Lentils-Fallow-Lentils-Peas rotation is equal to 265 CAD per hectare in the brown soil zone, -1 CAD per hectare in the dark brown soil zone, and 322 CAD her hectare in the black & gray soil zone. When comparing the present value of on-farm profits with no yield response to carbon sequestration (without SOC effects) for this scenario, the difference is equal to -430 CAD per hectare

---

[3]This model is similar to the conventional agricultural outcome model as in Deschênes and Greenstone (2007), Schlenker and Roberts (2009), Deschênes and Kolstad (2011), and Blanc (2017).

[4]The change in profits over the 32-year period from 2023 to 2055 in the brown soil zone is computed using the Canola-Spring Wheat-Peas-Spring Wheat rotation and the change in profits in the dark brown and black & gray soil zones is computed using the Canola-Spring Wheat-Canola-Spring Wheat rotation.

[5]The five crop rotations are Canola-Spring Wheat-Canola-Spring Wheat, Canola-Spring Wheat-Peas-Spring Wheat, Spring Wheat-Peas-Spring Wheat-Peas, Spring Wheat-Fallow-Spring Wheat-Fallow, and Lentils-Fallow-Lentils-Peas.

in the brown soil zone, -291 CAD per hectare dark brown soil zone, and 113 CAD per hectare in the black & gray soil zone. The findings emphasize that crop rotations that sequester more SOC yield greater on-farm profits in the long term, whereas rotations leading to SOC emissions actually result in lower future profits.

Third, I calculate the external social benefit (and cost) associated with the sequestration (and release) of SOC on farms across crop rotations and soil zones. This calculation of the external social benefit considers the growth in the stock of SOC and taking into account its dynamic feedback effects of increasing crop yields over time. The estimated external social benefit depends on the counterfactual SOC stock used to reference changes in the stock of SOC, as well as the applied social cost of carbon (SCC). For example, consider a scenario in which all insured hectares in Saskatchewan rotate Canola-Spring Wheat-Peas-Spring Wheat compared to Spring Wheat-Fallow-Spring Wheat-Fallow for 32 years form 2023 to 2055. Using a SCC of 185 USD/Mg of CO_2 from Rennert et al. (2022), this comparison generates external social benefits worth 108 billion CAD as a result of greater accumulated SOC stocks compared with the Spring Wheat-Fallow-Spring Wheat-Fallow rotation. The external social benefit per hectare for this scenario when comparing the Canola-Spring Wheat-Peas-Spring Wheat rotation to the Spring Wheat-Fallow-Spring Wheat-Fallow rotation is equal to 11,067 CAD per hectare in the brown soil zone, 9,445 CAD per hectare in the dark brown soil zone, and 9,394 CAD per hectare in the black & gray soil zone.

Significant public funds are being allocated to carbon sequestration efforts,[6] with a handful of private enterprises beginning to experiment with carbon offset initiatives that compensate farmers for their carbon sequestration activities.[7] It is evident that carbon sequestration offers substantial external social advantages beyond the direct benefits to farmers, such as increased crop yields. This essay provides information on the potential private and social benefits of SOC, and an estimate of external social benefits from sequestering SOC by crop rotation that considers the

---

[6]The United States Government has invested 19.5 billion USD over five years for climate smart agriculture and conservation program through the Inflation Reduction Act (United States Department of Agriculture, 2023). The Government of Canada has invested 3 billion CAD into on-farm environmental stewardship programs Environment and Climate Change Canada (2023a).

[7]Carbon offset programs include Bayer's Carbon Initiative, Nutrien's Carbon Program, Truterra's Farm Carbon Credits, Nori, and Carbon by Indigo Ag.

dynamic feedback effects of SOC on crop yield. A better understanding of the private and public benefits from carbon sequestration is beneficial not only for farmers and agricultural experts in strategizing crop management, but also for policymakers in crafting effective carbon sequestration strategies and in developing carbon offset programs and trading markets.

This essay proceeds as follows; first, I provide the conceptual framework for identifying the shadow value of SOC; second, I provide the empirical framework and identification strategy; third, I explain the data; fourth, I discuss the results of the econometric model; fifth, I perform a dynamic simulation to compute the long-term on-farm and external social benefits from carbon sequestration; finally, I conclude with a discussion of the spatial effects of cropping choice and implications for carbon sequestration policies.

2.2 Conceptual Framework

In this section, I outline the conceptual framework that illustrates the process by which farmers make decisions affecting SOC, under the assumption that their objective is to maximize profits. Given that the majority of decisions regarding on-farm production are made under uncertainty prior to planting, harvesting, and selling the grain, this means that farmers will maximize the profits, production functions, prices, and costs based on expectations held by a farmer. However, in this section, I abstract from uncertainty and treat the problem as if the farmer is omniscient, removing any assumptions made on risk preferences and how they affect production decisions.

Again, I assume that farmers are profit maximizers with respect to their input choices and land allocation. If farmers fully understand and anticipate the dynamic effects of cropping choice and input use, their objective function can be characterized by the following recursive Bellman Equation,

$$
V^{farm}(\mathbf{x_t}, \mathbf{l_t}) = \max_{\mathbf{x_t}, \mathbf{l_t}} \Pi^{farm}(\mathbf{p_t}, \mathbf{w_t}, \mathbf{q_t}(\mathbf{x_t}, \mathbf{l_t}), \mathbf{x_t}) + \beta V^{farm}(\mathbf{x_{t+1}}, \mathbf{l_{t+1}})
$$

$$
\text{s.t.} \ \sum_{c=1}^{C} l_{c,t} \leq L_t \quad \text{and} \quad \{\mathbf{x_{t+1}}, \mathbf{l_{t+1}}\} = f(\mathbf{x_t}, \mathbf{l_t}),
$$

(2.1)

141

where $\mathbf{x_t}$ is a matrix of the use of input $j \in J$, for crop $c \in C$, in year t, and $\mathbf{l_t}$ is a vector of the land allocated to crop c on a farm, L_t is the farmer's total land, $\mathbf{p_t}$ is the price of crop c in year t, and $\mathbf{w_t}$ is the cost of input j in year t. $V(\cdot)$ represents the value function that describes the best possible value with respect to input use and land allocation on a farm starting in year t. The profit function $\Pi^{farm}(\cdot)$ depends on input and output prices, the production function $\mathbf{q_t}(\cdot)$, input use, and land allocation. The land constraint in equation (2.1) ensures a farmer does not allocate more land to crops than she owns each year and the state equation $\{\mathbf{x_{t+1}}, \mathbf{l_{t+1}}\} = f(\mathbf{x_t}, \mathbf{l_t})$ defines how the farmer chooses inputs and land allocation over time (e.g., crop rotations, fertilizer use, and pesticide use).

The solution to equation (2.1) is a set of input use and land allocation that considers dynamic effects from the current choice set and evolving future choice sets. Recursively plugging into the BE (equation (2.1)) for the next period's value function $V^{farm}(\mathbf{x_{t+1}}, \mathbf{l_{t+1}})$ better illustrates the choice set of input use and land allocation over time.[8] Doing so transforms the Bellman Equation into a present value calculation that delineates the dynamic maximization problem of farm-level profits:

$$
\begin{aligned}
\max_{\{\mathbf{x_t}, \mathbf{l_t}\}_{t=0}^{\infty}} PV^{farm} = \max_{\mathbf{x_0}, \mathbf{l_0}} \big\{ & \Pi_0^{farm}(\mathbf{p_0}, \mathbf{w_0}, \mathbf{q_0}(\mathbf{x_0}, \mathbf{l_0}), \mathbf{x_0}) + \\
& \beta \big[\max_{\{\mathbf{x_t}, \mathbf{l_t}\}_{t=1}^{\infty}} \sum_{t=1}^{\infty} \beta^{t-1} \Pi_t^{farm}(\mathbf{p_t}, \mathbf{w_t}, \mathbf{q_t}(\mathbf{x_t}, \mathbf{l_t}), \mathbf{x_t}) \big] \big\} \\
& \text{s.t.} \ \sum_{c=1}^{C} l_{c,t} \leq L_t \quad \text{and} \quad \{\mathbf{x_{t+1}}, \mathbf{l_{t+1}}\} = f(\mathbf{x_t}, \mathbf{l_t}),
\end{aligned}
\tag{2.2}
$$

where PV^{farm} is the present value of the farm-level profits over an infinite-horizon, and β is the discount factor. Equation (2.3) shows a special case of equation (2.2) where farmers do not consider the dynamic effects of the current choice of inputs and land allocation on future profits, implying a discount factor equal to zero. Peters (2023) estimates the discount factor for crop rotation decisions among farmers in Alberta, Canada, by soil zone, employing a dynamic discrete choice modeling. His findings reveal discount factors of 0.65, 0.80, and 0.33 across the black, brown, and dark brown soil zones. This suggests differences in long-term decision-making regarding crop

---

[8]Please refer to Appendix 2A for the derivations that frame equation (2.2) within the context of dynamic programming.

rotations among farmers across soil zones, however, all significantly undervalue future outcomes. Given the unpredictability of commodity prices, input costs, labor availability, and weather conditions, this finding is not unexpected, as these factors contribute to the high-risk nature of farming. If farmers make myopic decisions without consideration of the future, then equation (2.2) reduces to,

$$V_t^{farm} = \max_{\mathbf{x_t}, \mathbf{l_t}} \Pi_t^{farm}(\mathbf{p_t}, \mathbf{w_t}, \mathbf{q_t}(\mathbf{x_t}, \mathbf{l_t}), \mathbf{x_t}) \qquad \text{s.t.} \ \sum_{c=1}^{C} l_{c,t} \leq L_t. \tag{2.3}$$

Throughout the year, some decisions regarding land allocation and input use are made sequentially (Antle, 1983). In this context, I assume that a typical farmer seeks to maximize profits through a two-stage process each year. In the first stage, the farmer chooses the amount of land allocated to specific crops. This decision is made months ahead of seeding to allow time for seed procurement and preparation. In the second stage, the farmer adjusts usage of some (variable) inputs to optimize profits, conditional on the decisions made in the first stage. This two-stage approach enables the farmer to adapt input usage closer to seeding, benefiting from any additional information acquired about expected weather patterns, prices, and costs. The problem is solved through backward induction.

Using a similar the profit function as characterized by Lacroix and Thomas (2011), second-stage crop production decisions at the farm level are defined by equation (2.4), which represents the farm-level profit maximization problem.

$$\max_{x_{j,c,t}} \Pi_t^{farm} = \sum_{c=1}^{C} \left(p_{c,t} q_{c,t}(x_{1,c,t}, ..., x_{J,c,t}, l_{c,t}) - \sum_{j=1}^{J} w_{j,t} x_{j,c,t} \right) \tag{2.4}$$

Let the solutions to equation (2.4) be $q_{c,t}^*(\mathbf{p_t}, \mathbf{w_t}, \mathbf{l_t}, L_t)$ and $x_{j,c,t}^*(\mathbf{p_t}, \mathbf{w_t}, \mathbf{l_t}, L_t)$, where the optimal input use and output depend on vectors of prices, costs, and land allocations for C crops and J inputs.

Equation (2.5) shows the objective function for the first stage where the farmer selects $l_{c,t}$, the amount of land allocated to crop c.

$$\max_{l_{c,t}} \Pi_t^{farm} = \sum_{c=1}^{C} \left(p_{c,t} q_{c,t}^* (\mathbf{p_t}, \mathbf{w_t}, \mathbf{l_t}, L_t) - \sum_{j=1}^{J} w_{j,t} x_{j,c,t}^* (\mathbf{p_t}, \mathbf{w_t}, \mathbf{l_t}, L_t) \right) \text{ s.t. } \sum_{c=1}^{C} l_{c,t} \leq L_t \qquad (2.5)$$

Solving equation (2.5) results in optimal land allocation choices $l_{c,t}^*(\mathbf{p_t}, \mathbf{w_t}, L_t)$, output $q_{c,t}^*(\mathbf{p_t}, \mathbf{w_t}, \mathbf{l_t^*}(\mathbf{p_t}, \mathbf{w_t}, L_t), L_t)$, and input use $x_{j,c,t}^*(\mathbf{p_t}, \mathbf{w_t}, \mathbf{l_t^*}(\mathbf{p_t}, \mathbf{w_t}, L_t), L_t)$.

Now, consider an alternative method where land allocation decisions have already been finalized at both the farm and field levels. In this scenario denoted as the *conditional profit maximization problem*, the farmer focuses on optimizing farm-level profits by adjusting input use conditional on previous cropping decisions. The conditional profit maximization problem, represented by equation (2.6), involves the summation of field-specific profits, contingent upon the preceding cropping choices for each field, denoted as n. When cropping decisions are optimally made by the farmer, the solutions for output and input use align with those obtained from the two-stage problem given by equations (2.4) and (2.5).

$$
\begin{aligned}
\max_{x_{j,c,t}} \Pi_t^{farm} &= \sum_{n=1}^{N} \max_{x_{n,j,c,t}} \left[\Pi_{n,c,t}^{field} \big| c, n \right] \\
&= \sum_{n=1}^{N} \max_{x_{n,j,c,t}} \left[\left(p_{c,t} q_{n,c,t}(x_{n,1,c,t}, ..., x_{n,J,c,t}) - \sum_{j=1}^{J} w_{j,t} x_{n,j,c,t} \right) \bigg| c, n \right]
\end{aligned}
\qquad (2.6)
$$

For a particular crop and field, the profit maximization problem is,

$$\max_{x_{n,j,c,t}} \left[\Pi_{n,c,t}^{field} \big| c, n \right] = \max_{x_{n,j,c,t}} \left[p_{c,t} q_{n,c,t}(x_{n,1,c,t}, ..., x_{n,J,c,t}) - \sum_{j=1}^{J} w_{j,t} x_{n,j,c,t} \bigg| c, n \right]. \qquad (2.7)$$

Crop production by field depends on the stock of SOC per hectare as a quasi-fixed factor, farmer applied inputs per hectare, and weather characteristics. Field-level crop production is equal to

$$\left[q_{n,c,t} \big| c, n \right] = \left[a_{n,t} y_{n,c,t} \left(\frac{x_{n,1,c,t}}{a_{n,t}}, ..., \frac{x_{n,J,c,t}}{a_{n,t}}, SOC_{n,t}, Z_{n,t} \right) \bigg| c, n \right], \qquad (2.8)$$

where $a_{n,t}$ is the hectares per field, $y_{n,c,t}$ is crop yield in kilograms per hectare, $SOC_{n,t}$ is the stock of SOC in kilograms per hectare, and $Z_{n,t}$ is a variable representing weather characteristics.

Applying the envelope theorem and taking the total differential gives the change in field-level profits with respect to SOC and weather,

$$d\left[\Pi_{n,c,t}^{field}|c,n\right] = \left[\left(\frac{\partial p_{c,t}}{\partial q_{n,c,t}}q_{n,c,t} + p_{c,t} - \sum_{j=1}^{J}\frac{\partial w_{j,t}}{\partial q_{n,c,t}}\right)\left(\frac{\partial q_{n,c,t}}{\partial SOC_{n,t}}dSOC_{n,t} + \frac{\partial q_{n,c,t}}{\partial Z_{n,t}}dZ_{n,t}\right) \mid c,n\right].$$
(2.9)

Assuming that farmers in Saskatchewan are price-takers and that a change in SOC or weather on a particular field does not affect the world price for crop c, equation (2.9) simplifies to,

$$d\left[\Pi_{n,c,t}^{field}|c,n\right] = \left[p_{c,t}a_{n,t}\left(\frac{\partial y_{n,c,t}}{\partial SOC_{n,t}}dSOC_{n,t} + \frac{\partial y_{n,c,t}}{\partial Z_{n,t}}dZ_{n,t}\right) \mid c,n\right].$$
(2.10)

The first term of equation (2.10) is the change in crop yield from an increase in the stock of SOC ($\frac{\partial y_{n,c,t}}{\partial SOC_{n,t}}$) multiplied by the hectares in field n ($a_{n,t}$) and commodity price of crop c ($p_{c,t}$). The marginal product of the stock of SOC is equal to $\frac{\partial y_{n,c,t}}{\partial SOC_{n,t}}$. Multiplying the marginal product of SOC by the commodity price gives the shadow value of SOC, which represents the value to farmers from an additional unit of SOC ($p_{c,t}\frac{\partial y_{n,c,t}}{\partial SOC_{n,t}}$).[9] I hypothesize that the shadow value is positive ($p_{c,t}\frac{\partial y_{n,c,t}}{\partial SOC_{n,t}} > 0$) and demonstrates diminishing marginal returns ($p_{c,t}\frac{\partial^2 y_{n,c,t}}{\partial SOC_{n,t}^2} < 0$), implying that its positive effect on field- and farm-level profits decreases as SOC increases. The second component in equation (2.10) accounts for the variation in profits resulting from the influence of weather on crop yield.

The conceptual framework shown in this section illustrates that shocks to either SOC or weather affect field- and farm-level decisions in a comparable manner when optimal decisions regarding cropping choices, output, and inputs are made. Hence, only the direct effects of changes

---

[9]SOC affects many attributes of the soil that influence crop yields such as water retention, nutrients, food for vital soil organisms, and provides soil structure. Fontaine et al. (2003) state: "soil carbon is the driving force of most microbially mediated processes, particularly soil respiration and nitrogen mineralization. The quality of carbon is particularly important because it constrains the supply of energy for enzyme production and growth."

in SOC stocks are considered, whether they influence the profit function indirectly through input use and land allocation decisions. Moving forward, this framework suggests that it is feasible to determine the shadow value of SOC by assessing its effects on yield by field, crop, and year.

2.3 Quantitative Model

In this section, I outline a crop yield regression model for estimating the shadow value of SOC. My methodology closely resembles that of Belcher et al. (2003), in that I employ simulated SOC stocks to estimate the effect of SOC on crop yield.[10] Specifically, I employ SOC stocks derived from the weather version of the Augmented Campbell model, a SOC prediction model developed and simulated by Serfas (2024a).[11]

I employ the Augmented Campbell model to estimate the shadow value of SOC for commonly planted crops in Saskatchewan (spring wheat, durum wheat, canola, barley, lentils, and peas). This model, an extension of the original Campbell model, incorporates an additional SOC pool dedicated to plant residue humification, thus extending the time taken for the predicted SOC stock to reach a steady state. Compared to the Campbell model, the Augmented Campbell model offers greater accuracy in SOC predictions, as the latter tends to underestimate SOC stocks and prematurely reaches a steady state.

Making use of simulated SOC stocks and crop yield data, I employ a dynamic panel regression model to estimate the shadow value of SOC stocks. The model is dynamic because the SOC stock is influenced by previous crop yields. The SOC stock incorporates data on past crop yields, cropping choices, and weather, similar to an autoregressive model which predicts the dependent

---

[10]Belcher et al. (2003) estimate the effect of SOC stocks on crop rotation profit over a 50 year time horizon in western Canada. They employ the STELLA® research modeling software to estimate crop yields, SOC, soil nutrients, and soil water.

[11]The Augmented Campbell model integrates the Plant Biomass Carbon Inputs (PBCI) model to determine carbon inputs based on crop yields. To calculate annual carbon inputs, the PBCI model uses conversion equations that consider plant traits (Bolinder et al., 2007; Maillard et al., 2018; Fan et al., 2019; He et al., 2021; Zhang et al., 2021; Thiagarajan et al., 2022). Measures of carbon inputs reflect changes in yield resulting from changes in weather, cropping choices, and other production practices and decisions. To model changes SOC stocks, the Augmented Campbell model applies first-order kinetics, which uses a set of differential equations to account for the decomposition rates of different SOC "pools", components, or fractions. SOC pools represent the portions of the stock that decompose at varying speeds (either more rapidly or more slowly), influenced by their carbon composition (derived from plant and soil material). Please refer to Serfas (2024a) for an in-depth explanation of the Augmented Campbell model.

variable based on its own past values, with decreasing weights for successive lags. This model is parallel to the conventional agricultural outcome model for crop yield, as employed by Deschênes and Greenstone (2007), Schlenker and Roberts (2009), Deschênes and Kolstad (2011), and Blanc (2017). I estimate this model separately for each soil zone and crop type. The estimating equation is,

$$ y_{n,t} = \lambda SOC_{n,t} + f\left(Z_{n,t},\ \bar{Z}_n\right)\xi + SL_n\delta + X_{n,t}\theta + \alpha_r + \tau_t + \omega_{n,t} + \varepsilon_{n,t}, \qquad (2.11) $$

where, $y_{n,t}$ is crop yield on field n in year t, $SOC_{n,t}$ is the SOC stock, $Z_{n,t}$ is a vector of weather characteristics, $\bar{Z}_n$ is a vector of average weather characteristics that represent climate, SL_n is a vector of soil characteristics that vary across fields, $X_{n,t}$ is a vector of field-level controls that vary across fields and over time, α_r are Rural Municipality (RM) fixed effects that control for unobserved RM-specific time-invariant determinants of crop yield, τ_t are year fixed effects that control for annual differences in crop yield common across fields, $\omega_{n,t}$ are unobserved inputs and farm management characteristics that vary over field and year, and $\varepsilon_{n,t}$ are idiosyncratic errors.

I choose not to use field fixed effects as they exacerbate the Nickell bias often encountered in dynamic panel regression models. Given that a crop might be planted only a few times in the period from 1998 to 2019 on any given field, using field and year fixed effects ends up controlling for too much of the variation in crop yield. In many instances, the time-paths of SOC stocks in a field for a specific crop is fully characterized by the inclusion of field and year fixed effects. In Appendix 2B, through simulation, I demonstrate that when the dynamic independent variable (SOC stocks) exhibits high collinearity with a time trend, the inclusion of field and year fixed effects exacerbates both the Nickell bias and the prediction error bias. I show that employing less-detailed two-way fixed effects (for instance, RM and year) helps to reduce the Nickell bias.

I control for field-level soil characteristics (SL_n) in equation (2.11) using data from the Saskatchewan Detailed Soil Survey and the Canadian National Soils Database (Agriculture and Agri-Food Canada, 2022). These characteristics include the percentage of sand, silt, and clay, the soil

pH, cation exchange capacity, water retention at 33 kilopascals (kP), electrical conductivity, stoni-ness, and slope gradient. Other field-level controls (X_{nt}) include the past four-year crop rotation sequence, with crops grouped into the broad categories of cereal, oilseed, pulse, or fallow. This generates 256 crop rotation dummy variables. Other field-level controls include nitrogen use, total liability of crop insurance by field, and the farm size.[12]

Farmers opt for crops that are expected to perform best on their land, a decision influenced by their investment in physical capital (like farm machinery) or human capital (such as agronomic expertise) to maximize on-farm profits. Acknowledging that crop yields are influenced by the choice of crop, I incorporate a comprehensive set of control variables. First, I employ year fixed effects which control for factors common to all fields such as commodity prices and changes in technology. Second, I factor in the past four-year average yield by crop and crop district, as a farmer is inclined to plant a crop that yields well in their region compared to others.[13] Third, I incorporate controls for crop rotation and RM fixed effects, weather characteristics specific to each field, crop insurance coverage per field (insurance liability), and the size of the farm.

Unobservable time- and field-specific factors such as inputs and farm management charac-teristics are denoted as ω_{nt}. These include managerial ability, equipment quality, and knowledge capital, all of which are understood by the farmer. The majority of attributes encompassed within ω_{nt} are accounted for by factors like crop rotation, RM and year fixed effects, total liability per field, and farm size. However, any remaining variation could bias my results if it correlates with both SOC stocks and crop yields. A potential issue is measurement error in the stock of SOC at-tributed to straw removal, prevalent when crops are used for cow feed and often seen with barley. Predicted SOC stocks assume that straw remains in the field; hence, in crops where significant amounts of straw are removed, predicted SOC stocks may be artificially high. If SOC positively

---

[12]I examine nitrogen use instead of other fertilizers such as phosphorus, potassium, and sulfur. Farmers primarily adjust nitrogen rates to increase crop yields, whereas other macro fertilizers are generally used in fixed proportions with nitrogen to supplement the existing stock of nutrients in the soil. The inclusion of potassium, phosphorus and sulfur fertilizer use in the regression models does not affect the shadow value of SOC stocks. Importantly, most farmers do not apply potassium because Saskatchewan soils are potassium rich, and fertilizers like sulfur are only applied to particular crops such as canola (Government of Saskatchewan, 2023b).

[13]For visual reference, a map of the twenty crop districts in Saskatchewan is provided in Figure 2C.6, located in Appendix 2C.

affects crop yields, this could lead to attenuation bias. Hence, the results should be interpreted conservatively lower-bound estimates.

Weather and climate factors may have a non-linear relationship with crop yield, represented by equation (2.11), which I address using a flexible function $f(.)$. As suggested by Mérel and Gammans (2021), weather variables can be integrated into the model as crop yield penalties for deviating from typical weather or climate patterns. This "climate penalty" is assumed to depend on the squared difference between actual weather conditions and the average climate. The weather variables I include in the model are the average temperature during the growing season (GSAT) from April to September, and total annual precipitation (TAP), along with their squares, their first lags, and their squared differences from their respective long term average or "climate." Here, climate is defined as the average GSAT and TAP during the period 1998–2019 for each field.

Table 2C.1 in Appendix 2C provides a more detailed explanation for each variable included in the dynamic panel regression model represented by equation (2.11).

2.4 Data

To estimate the effects of SOC on crop yield, I combine simulated SOC stock data from Serfas (2024a) with field-specific crop production data sourced from the Saskatchewan Crop Insurance Corporation (SCIC). I also employ data on weather characteristics from Environment and Climate Change Canada (2023b), and data on soil characteristics from the Canadian National Soil Database and Saskatchewan Detailed Soil Survery (Agriculture and Agri-Food Canada, 2022). The SCIC dataset includes information on the legal land description, municipality, soil classification, land use, insurance coverage, seeded acres, type of crop, yield, and fertilizer use. Only farmers that enroll in the Sask Management Plus (SMP) program at SCIC report information on field-level crop yield and fertilizer use. Yields reported by non-SMP farmers are averaged across their fields for each crop annually. Data on nitrogen use for SMP farmers begin in 2004. To control for discrepancies between the comprehensive dataset and the SMP-specific data, I introduce a binary indicator

to denote whether yield data are reported on a field-specific or farm-wide basis. As an additional robustness check, I estimate all models exclusively with data from the SMP sample.

To identify fields, I use the land title dataset from ISC (an exclusive provider of land titles registry information in Saskatchewan) that includes polygons within the dataset for all fields in Saskatchewan (ISC, 2022). This dataset includes detailed geo-referenced information for approximately 311,028 fields. I match weather and soil characteristics to all fields, and link the SCIC data with the legal land description. This yields detailed agricultural production information for 209,021 insured parcels of land. I take a subset of these data to obtain a strongly balanced panel of 36,443 fields with complete information on the time-paths of SOC stocks and cropping choices from 1998 to 2019.

Figure 2.1 shows the field-level map of Saskatchewan categorized by soil zone. I estimate all my models for the brown, dark brown, and black & gray soil zones separately. Farms located within the same soil zone exhibit greater similarity in terms of soil attributes, climate conditions, farm management practices, and cropping choice compared with farms located in different soil zones.

FIGURE 2.1: Field-Level Map of Soil Zones in Saskatchewan
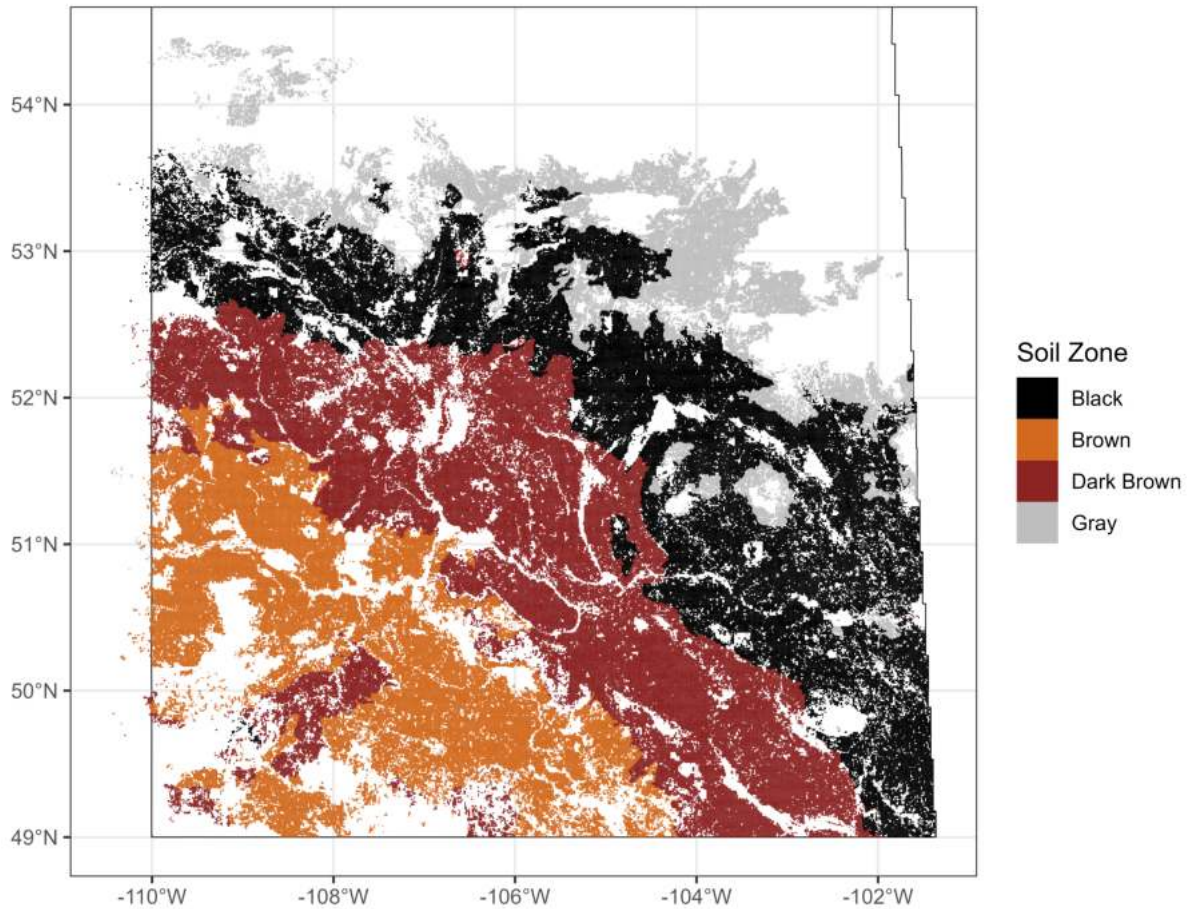
Notes: The y-axis is latitude and the x-axis is longitude.

Figure 2.2 displays various soil attributes for fields, compiled by the Saskatchewan Detailed Soil Survey and the Canadian National Soil Database. The dataset from the Saskatchewan Detailed Soil Survey includes 67,166 geo-referenced soil polygons, each associated with soil attribute data from the Canadian National Soil Database (Agriculture and Agri-Food Canada, 2022). For the purposes of this study, 36,351 polygons from the Saskatchewan Detailed Soil Survey were matched with 36,443 fields documented in the SCIC database. This matching provides detailed field-level data on soil characteristics, enabling the application of RM fixed effects to determine the shadow value of SOC stocks while accounting for the variation in soil characteristics among different fields within an RM.

151

FIGURE 2.2: Field-Level Maps of Soil Characteristics in Saskatchewan
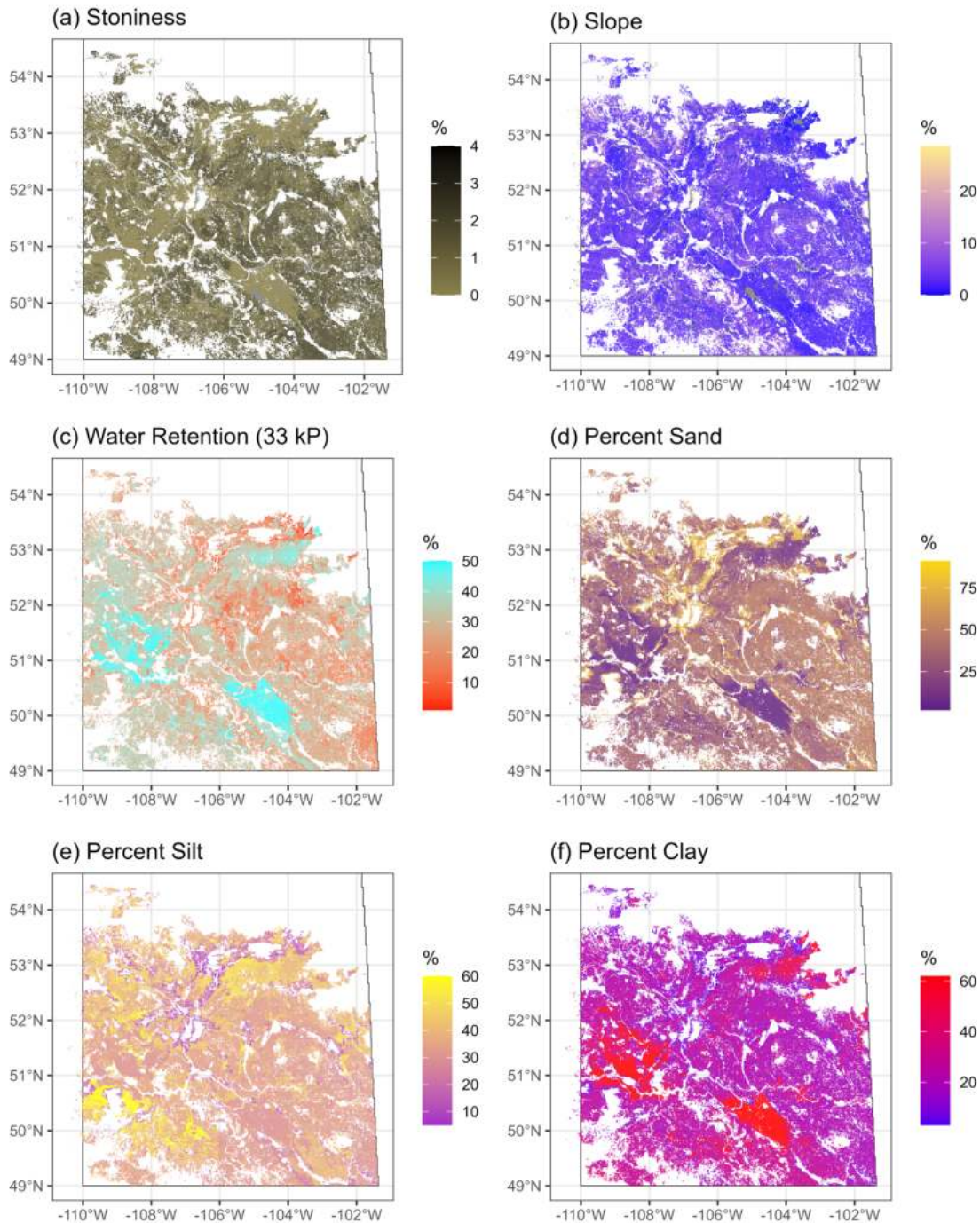
Source: Generated from ISC land titles registry polygons and soil characteristics from the Canadian National Soils Database (Agriculture and Agri-Food Canada, 2022; ISC, 2022).

Notes: The y-axis is latitude and the x-axis is longitude.

I obtained weather information collected by Environment Canada weather stations (Environment and Climate Change Canada, 2023b), and I aggregated temperature and precipitation figures to the month. These data encompasse observations from 56 stations situated throughout the agricultural regions of Saskatchewan, with additional stations near the Saskatchewan border in Alberta and Manitoba. To interpolate the weather data across spatial locations, I applied inverse distance weighting to the spatial pixel based on the nearest five weather stations.[14] The inverse-distance weighting formula for weather $Z_{m,f}$, for month m and pixel n, is shown in Equation (2.12).

$$Z_{m,n} = \frac{\sum_{i=1}^{5} \left(\frac{z_{m,i}}{d_{i,n}} \right)}{\sum_{i=1}^{5} \left(\frac{1}{d_{i,n}} \right)} \tag{2.12}$$

The weather reported at weather station i is weighted by the inverse distance $1/d_{i,n}$ to pixel n such that all weights sum to one. I then take the average of the spatial pixel values that are located within a field.

Figure 2.3 shows the spatial variation in precipitation and temperature across Saskatchewan based on the interpolated weather station data using the five nearest neighbors for June 2007 and June 2009. In any given month of the year, precipitation and temperature may vary considerably across the province of Saskatchewan.

---

[14]I calculate the inverse-distance-weighted weather from the five nearest weather stations employing one million spatial pixels distributed over fields across Saskatchewan. I then take the average of the spatial pixel values that are located within a field. This method significantly enhances the efficiency of generating interpolated spatial weather data compared to the default spatial analysis tools available in R.

FIGURE 2.3: Environment Canada Weather Station interpolated data in Saskatchewan
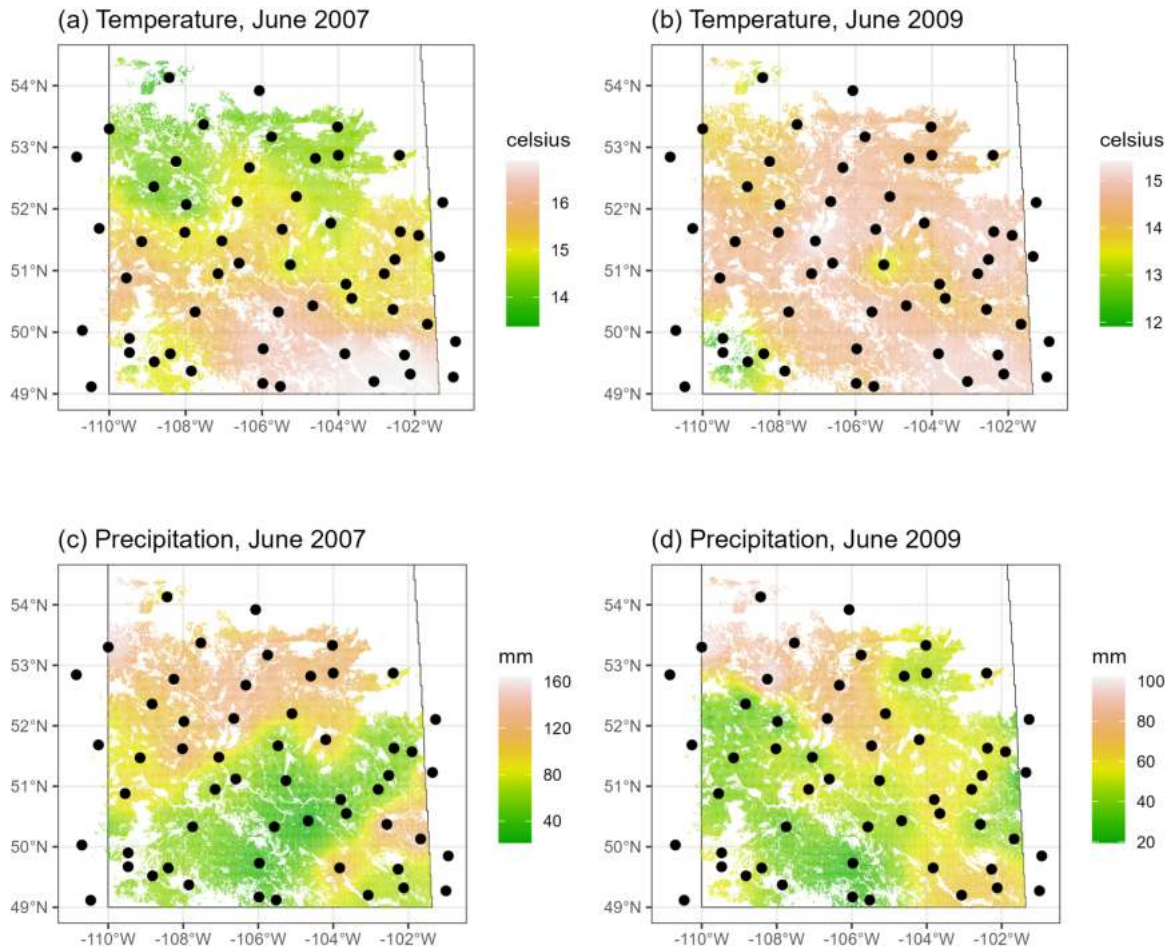
(a) Temperature, June 2007
(b) Temperature, June 2009
(c) Precipitation, June 2007
(d) Precipitation, June 2009

Source: Generated from weather station data collected by Environment and Climate Change Canada (2023b).

Notes: The y-axis is latitude and the x-axis is longitude. A black dot represents the location of a weather station.

Figure 2.4 shows the field-specific stock of SOC in Saskatchewan for 1998 from Serfas (2024a). The SOC stocks for 1998 are computed using soil sampling data from the Saskatchewan Detailed Soil Survey (a survey representing soil conditions in 1971 (Fan et al., 2019)), and from soil samples collected by McConkey et al. (2003) in 1995.

FIGURE 2.4: Saskatchewan Soil Organic Carbon Stock by Field in 1998
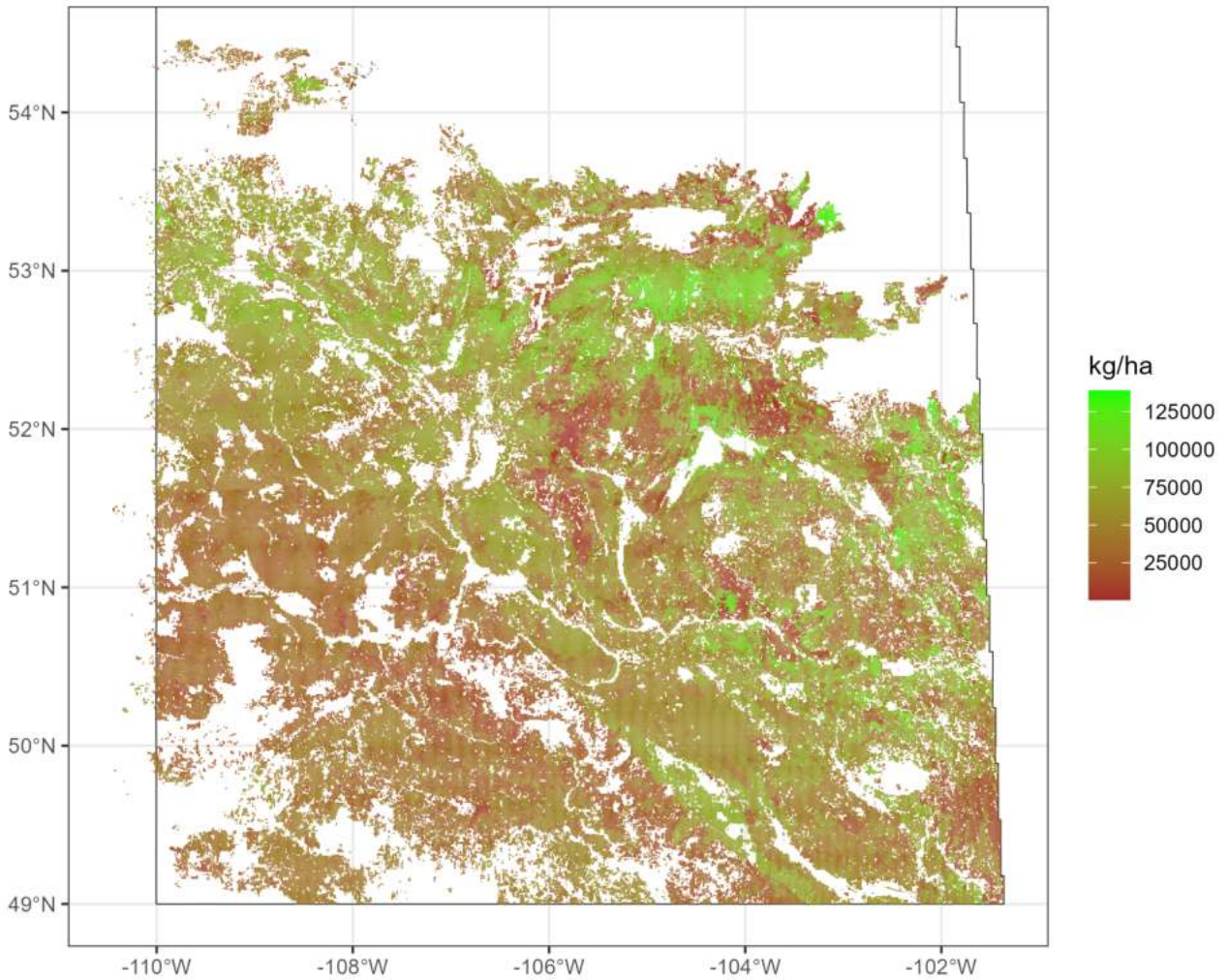
Source: Serfas (2024a).

Notes: The y-axis is latitude and the x-axis is longitude.

Additional summary statistics on the share of hectares by crop, crop yields, nitrogen use, SOC stocks, and weather characteristics by sample are available in Appendix 2C in Figures 2C.1 to 2C.5 and Tables 2C.2 to 2C.6.

155

2.5 The Effects of Soil Organic Carbon on Crop Yield

In this section, I present the findings from dynamic panel regression model used to estimate the marginal product and shadow value of SOC stocks. Unless otherwise stated, this work uses measures of SOC stocks predicted using the Augmented Campbell model (weather version). The analysis for each crop was conducted across different soil zones and for two distinct sets of data: a "Full" sample, which excludes nitrogen use as an explanatory variable, and a narrower "SMP" sample consisting of farmers participating in the SMP program. The SMP subset provides detailed data on nitrogen application and crop yields at the field level. All regression models account for standard errors clustered by farm and weighted according to the size of the field in hectares. First, I estimate the marginal products of SOC for spring wheat, durum wheat, barley, canola, lentils, and peas from the coefficient on SOC stocks. Next, to calculate the shadow value of SOC, I multiplied the derived marginal product of SOC by the prevailing market price of the respective commodity.

Table 2.1 displays the calculated marginal product of SOC stocks for different crops of SOC.[15] All regression models include fixed effects for RM, year, and crop rotation, alongside controls for weather and soil characteristics, historical district-level average yields, farm size, and crop insurance coverage. The Full sample analysis also adjusts for participation in the SMP program using an SMP indicator. The results show that, across all models, the marginal products of SOC for spring wheat, durum wheat, lentils, and peas are greatest in the brown soil zone. For canola and barley, the effects of SOC on yield are not statistically significant in the brown soil zone, but are positive and statistically significant in the dark brown and black & gray soil zones. The marginal product of SOC for lentils is not statistically significance in the black & gray soil zones, and for peas, it is not statistically significant in the dark brown soil zone. In cases with a relatively small sample size, such as for canola and barley in the brown soil zone or durum wheat and lentils in the black & gray soil zone, the estimates of the marginal product of SOC are less precise. Additionally, the variation in coefficients for nitrogen application among the models for spring wheat, durum

---

[15]Table 2D.1 in Appendix D provides comparisons using estimates for spring wheat based on measures of SOC predicted by alternative models. These comparisons reveal that the calculated marginal products for spring wheat are robust across the different SOC prediction models.

wheat, barley, and canola does not display any consistent patterns across different soil zones.[16] Table 2D.6 in Appendix 2D shows the robustness of the marginal product of SOC for spring wheat excluding nitrogen use within the SMP sample, indicating that excluding nitrogen from the model does not introduce bias from omitted variables in the estimation of equation (2.11).

TABLE 2.1: The Marginal Product of Soil Organic Carbon and Nitrogen Use on Crop Yield by Crop, Sample, and Soil Zone in Saskatchewan

	Dependent Variable: Crop Yield					
	(1)	(2)	(3)	(4)	(5)	(6)
Soil Zone:	*Brown*		*Dark Brown*		*Black & Gray*	
Sample:	Full	SMP	Full	SMP	Full	SMP
Spring Wheat:						
Soil Organic Carbon	0.021***	0.024***	0.010***	0.010***	0.004***	0.003***
	(0.006)	(0.009)	(0.001)	(0.002)	(0.001)	(0.001)
Nitrogen Use		2.496		5.750***		9.462***
		(1.581)		(0.827)		(0.86)
Observations	7,425	2,050	33,174	12,245	92,608	36,033
R^2	0.474	0.517	0.577	0.561	0.575	0.532
Canola:						
Soil Organic Carbon	0.005	0.0002	0.003***	0.002**	0.003***	0.002***
	(0.003)	(0.004)	(0.001)	(0.001)	(0.0004)	(0.001)
Nitrogen Use		5.294***		4.601***		5.197***
		(0.757)		(0.304)		(0.372)
Observations	4,085	1,757	40,967	16,761	140,404	55,778
R^2	0.555	0.593	0.520	0.503	0.552	0.539
Barley:						
Soil Organic Carbon	0.012	−0.005	0.010***	0.006	0.003**	0.004**
	(0.011)	(0.019)	(0.003)	(0.004)	(0.001)	(0.002)
Nitrogen Use		13.205***		8.257***		11.964***
		(3.486)		(1.66)		(1.113)
Observations	1,771	616	10,251	3,840	33,213	12,194
R^2	0.583	0.712	0.512	0.489	0.511	0.487
Durum Wheat:						
Soil Organic Carbon	0.020***	0.017***	0.007***	0.015***	0.005	0.010**
	(0.003)	(0.004)	(0.002)	(0.003)	(0.004)	(0.005)
Nitrogen Use		6.177***		6.633***		17.532***
		(0.729)		(0.822)		(2.882)
Observations	18,011	6,619	16,940	6,101	1,899	727
R^2	0.460	0.466	0.564	0.550	0.664	0.748

[16]Minimal to no amount of nitrogen is generally applied to pulse crops relative to others during seeding. For further details on fertilizer application by crop and soil zone in Saskatchewan between 1998 and 2019, see Figure 2C.4 and Table 2C.4 in Appendix 2C.

TABLE 2.1: The Marginal Product of Soil Organic Carbon and Nitrogen Use on Crop
Yield by Crop, Sample, and Soil Zone in Saskatchewan *(continued)*

	Dependent Variable: Crop Yield					
	(1)	(2)	(3)	(4)	(5)	(6)
Soil Zone:	*Brown*		*Dark Brown*		*Black & Gray*	
Sample:	Full	SMP	Full	SMP	Full	SMP
Lentils:						
Soil Organic Carbon	0.006**	0.002	0.004**	−0.003	0.002	0.004
	(0.003)	(0.005)	(0.002)	(0.004)	(0.004)	(0.006)
Nitrogen Use		−3.063*		2.468		−17.311
		(1.734)		(1.927)		(11.499)
Observations	6,342	2,070	12,347	3,129	1,592	405
R^2	0.365	0.451	0.325	0.415	0.618	0.815
Peas:						
Soil Organic Carbon	0.011**	0.004	0.003	0.007	0.004***	−0.001
	(0.004)	(0.009)	(0.002)	(0.004)	(0.001)	(0.003)
Nitrogen Use		−2.033		−3.594		−2.416*
		(4.092)		(2.273)		(1.253)
Observations	3,449	826	11,081	2,168	17,272	3,346
R^2	0.441	0.606	0.414	0.485	0.479	0.470

Source: Authors' Estimates.
Notes: $^*p < 0.1;^{**} p < 0.05;^{***} p < 0.01$. All regression models include Rural Municipality fixed effects, year fixed effects, crop rotation fixed effects, weather characteristics, soil characteristics, past average yields by crop district, farm size, insurance liability, and an SMP indicator. GSAT is Growing Season Average Temperature, TAP is Total Annual Precipitation, and CD is Crop District. Past Average Yield by CD is a rolling average of the past four years of yields for each crop in each CD. There are 256 crop rotation variables for the past four-year crop rotation sequence using the categories: oilseeds, pulses, cereals, and fallow. All regression models account for standard errors clustered by farm and weighted according to the size of the field in hectares. The Full sample includes all fields selected for Soil Organic Carbon (SOC) prediction from the SCIC confidential dataset. The Saskatchewan Management Plus (SMP) sample includes fields that participated in the SMP program and also were selected for SOC prediction. For more information on the variables used as controls, please refer to Table 2C.1 in Appendix 2C.

Table 2.1 shows that the marginal effect of SOC on crop yield is greater in the brown soil zone, which has a lower SOC stock, relative to the dark brown and black & gray soil zones where SOC stocks are higher, consistent with diminishing marginal returns.[17] In Table 2D.2 in Appendix 2D, I estimate all the models using quadratic and logarithmic functional forms for SOC stocks. In Table 2D.2, the coefficients on SOC for the quadratic and logarithmic specifications are statistically

---

[17]These findings align with agronomic research indicating a plateau in yield growth at higher SOC concentrations in the soil (Oldfield et al., 2019).

significant and relatively consistent with the results of the linear model.[18]

Table 2D.4 in Appendix D shows the marginal effect of SOC for each functional form and crop evaluated at the mean stock of SOC and for one standard deviation above and below the mean. These results show that for both quadratic and logarithmic functional forms that the marginal effect is higher for a one standard deviation below the mean stock of SOC within a soil zone relative to the marginal effect evaluated at the mean, and lower for one standard deviation above the mean stock of SOC relative to the mean. All marginal effects for each crop at the mean and by functional form (linear, quadratic, and logarithmic) are greatest in the brown soil zone where the stock of SOC is lower, and the marginal effects are lowest in the black & gray soil zone where the stock of SOC is on average higher across the three soil zones in Saskatchewan. This provides evidence of diminishing marginal returns for crop yield with respect to SOC stocks ($\frac{\partial y_{n,c,t}}{\partial SOC_{n,t}} > 0$ and $\frac{\partial^2 y_{n,c,t}}{\partial SOC_{n,t}^2} < 0$).[19] The relationship of diminishing marginal returns between crop yield and SOC stocks are observed primarily through spatial differences in the stock of SOC rather than changes in the stock within a field.

In Saskatchewan, one standard deviation in the stock of SOC from 1998 to 2019 is approximately equal to 11 Mg/ha in the brown soil zone, 17 Mg/ha in the dark brown soil zone, and 25 Mg/ha in the black & gray soil zone. Hence, the marginal product of SOC within a field will remain relatively constant over time due to the change in the stock of SOC within a field being relatively low compared to the change in SOC observed spatially across fields.[20] This implies that the marginal product of SOC may slowly change within a field, but substantial changes can only be observed over relatively long periods of time ($\geq$30 years).

Table 2.2 presents the elasticity of crop yield with respect to SOC, derived from the "Full"-sample-based estimates of the marginal product of SOC reported in Table 2.1. These elasticities

---

[18]Table 2D.3 in Appendix D outlines the significance in estimates for regressions using the linear, quadratic, and logarithmic functional forms, and also includes the r-squared value for each regression. There are instances in which the marginal product of SOC is statistically significant for a specific functional form and crop. Please refer to Table 2D.3 in Appendix D to see the comparisons in the statistical significance of the marginal products of SOC for each the linear, quadratic, and logarithmic specifications of SOC stocks.

[19]Predictions of crop yield with a linear, quadratic, and logarithmic functional forms for SOC stocks are identical as a result of the r-squared values being very similar across each functional form as shown in Table 2D.3 in Appendix D.

[20]Serfas (2024a) simulates the stock of SOC using the Augmented Campbell model (an SOC prediction model) from 1998 to 2019 and finds that it increased on average by 0.309 Mg/ha/yr across Saskatchewan.

were computed at the respective sample data means, by multiplying the marginal product of SOC by the average SOC stock, then dividing this product by the average yield for each crop and soil zone.

TABLE 2.2: The Elasticity of Crop Yield with respect to Soil Organic Carbon by Soil Zone and Crop Type in Saskatchewan

	(1)	(2)	(3)	(4)	(5)	(6)
Crop Type:	**Spring Wheat**	**Canola**	**Barley**	**Durum Wheat**	**Lentils**	**Peas**
Brown						
$e_{y_c,SOC}$	0.43***	0.11	0.21	0.35***	0.16**	0.22**
	(0.12)	(0.07)	(0.19)	(0.05)	(0.08)	(0.08)
Dark Brown						
$e_{y_c,SOC}$	0.19***	0.09***	0.20***	0.16***	0.15**	0.07
	(0.02)	(0.03)	(0.06)	(0.04)	(0.08)	(0.05)
Black & Gray						
$e_{y_c,SOC}$	0.09***	0.10***	0.06**	0.13	0.10	0.11***
	(0.02)	(0.01)	(0.02)	(0.10)	(0.19)	(0.03)

Source: Authors' Estimates.
Notes: $^*p < 0.1;^{**}p < 0.05;^{***}p < 0.01$. The elasticity of SOC on crop yield is equal to the marginal product of SOC multiplied by the respective average crop yield and SOC stock. All standard errors are calculated by applying the delta method to the standard errors shown in Table 2.1. The marginal products for SOC are estimated using the Full sample of data from the SCIC confidential dataset as shown in Table 2.1. Average crop yields by soil zone are obtained from the confidential SCIC dataset and average SOC stocks are obtained from Serfas (2024a). Brown, Dark Brown, and Black & Gray refer to the three primary soil zones in Saskatchewan. For more information, please refer to the notes in Table 2.1.

In Table 2.2 the estimated elasticities of crop yield with respect to SOC are notably larger for spring wheat and durum wheat, than for barley and pulses, and more so, canola. This variation underscores the crop-specific agronomic effect of SOC on yield. In the brown and dark brown soil zones, the benefits from SOC (i.e., enhanced organic matter, water, and nutrient retention) are smaller for pulses than for cereal crops, which typically are more susceptible to drought conditions. Canola, requiring greater amounts of precipitation, appears to benefit even less than cereals from increased SOC. Nonetheless, these rankings do not apply consistently across different soil

zones, especially the black & gray zone, pointing to the complex interplay of agronomic and scientific factors influencing the effect of SOC on crop yields.

Table 2.3 shows the estimates of the (marginal) shadow value of SOC by crop type and soil zone, equal to the value of the marginal product, computed by multiplying the marginal product of SOC in Table 2.1 by the commodity price from the 2023 Saskatchewan Crop Planning Guide (Government of Saskatchewan, 2023a).

TABLE 2.3: The Shadow Value of Soil Organic Carbon by Soil Zone and Crop Type
in Saskatchewan

	(1)	(2)	(3)	(4)	(5)	(6)
Crop Type:	**Spring Wheat**	**Canola**	**Barley**	**Durum Wheat**	**Lentils**	**Peas**
Brown	*(2023 CAD/ha/yr)/(Mg of SOC/ha)*					
Shadow Value	7.83***	3.88	5.59	8.84***	4.37**	4.85**
	(2.24)	(2.33)	(5.13)	(1.33)	(2.18)	(1.76)
Dark Brown						
Shadow Value	3.73***	2.33***	4.66***	3.09***	2.91**	1.32
	(0.37)	(0.78)	(1.40)	(0.88)	(1.46)	(0.88)
Black & Gray						
Shadow Value	1.49***	2.33***	1.40**	2.21	1.46	1.76***
	(0.37)	(0.31)	(0.47)	(1.77)	(2.91)	(0.44)

Source: Authors' Estimates.
Notes: $^*p < 0.1;^{**} p < 0.05;^{***} p < 0.01$. The shadow value of SOC is equal to the marginal product of SOC (λ) multiplied by the respective commodity price. All standard errors are calculated by applying the delta method to the standard errors shown in Table 2.1. The marginal products for SOC are given by Table 2.1. Commodity prices are from the 2023 Saskatchewan Crop Planning Guide (Government of Saskatchewan, 2023a). Brown, Dark Brown, and Black & Gray refer to the three primary soil zones in Saskatchewan. For more information, please refer to the notes in Table 2.1.

Table 2.3 shows that, among crops, the highest shadow value of SOC is observed for durum wheat in the brown soil zone, barley in the dark brown soil zone, and canola in the black & gray soil zone. However, spring wheat shows the consistently high shadow values of SOC relative to all other crops among the soil zones. The shadow value of SOC is interpreted as, for a one Mg of SOC per hectare increase in the stock of SOC translates into an increase in annual spring wheat profit of 7.83 CAD per hectare in the brown soil zone. This implies that a one Mg per hectare

increase in SOC, the extra annual profit is 2,028 CAD for each section (259 hectares or 640 acres) of land dedicated to spring wheat in the brown soil zone. Similarly, for canola grown in the black & gray soil zone, a one Mg per hectare increase in SOC stocks raises annual profits by 604 CAD per section (259 hectares or 640 acres).

The results presented in this essay diverge from the earlier findings of Belcher et al. (2003), who identified the shadow value of SOC stocks as being higher in the black & gray soil zone than in the brown soil zone. The simulation runs performed by Belcher were based on the environmental and economic conditions of the 1990s and early 2000s, rather than the period analyzed in this essay (1998–2019). In the earlier period, practices in the brown soil zone were dominated by intensive fallowing and tilling, while farmers in the black & gray soil zone had begun transitioning to zero-tillage and continuous cropping practices. These results suggest a temporal shift in the on-farm benefits from SOC stocks, with the increased benefits observed in the brown soil zone likely attributable to the shift towards zero tillage and continuous cropping practices.

2.6   Dynamic Simulation

In this section, first I introduce a conceptual framework to be used to analyze the immediate and long-term effects of carbon sequestration on farm profitability and compare specific alternative crop rotation strategies. Next, I conduct a dynamic simulation across five particular crop rotations, calculating the SOC stock and integrating dynamic crop yield outcomes with the shadow values of SOC. Making use of the results from the dynamic simulation, I compute the on-farm benefits that stem from carbon sequestration from 2023 to 2055, and the benefits relative to different crop rotations. I also compute the present value of on-farm profits and their corresponding external social benefits from 2023 to 2055, as well as the differences between crop rotations. Following this, I analyze the structural effects of weather on crop yields, considering its effects mediated through SOC stocks as well as residual effects that exclude SOC.

SOC accumulates slowly, and therefore the on-farm benefits from carbon sequestration accrue over long periods of time. I illustrate this effect in Figure 2.5, depicting a two period model

where Current (C) represents the profits from a specific crop rotation in the current time period, and Future (F) represents the profits in a future time period. Figure 2.5 shows that when SOC changes over time this affects crop yields and on-farm profits for specific alternative crop rotations. In this specific, contrived example, compared with crop rotation B, rotation A earns lower immediate profits but sequesters more SOC and eventually, as a result, earns higher future profits. In this context, farmers decide which crop rotation to adopt based on the difference in profits between crop rotations in the future time period after SOC and yield growth are realized. In order to calculate the future difference in profit between crop rotations, one must first calculate the change in profit over time (from the current time period to the future time period) that stems from additional SOC accumulated by implementing a specific rotation, represented by the green shaded area in Figure 2.5. This difference in future profit between crop rotations governs how forward-looking farmers make long-term decisions and the decision to adopt a particular crop rotation relative to another.

In Figure 2.5, it is assumed that prices are exogenous. Panel (A) depicts a crop rotation strategy that is highly effective in sequestering SOC, resulting in modest immediate profits (indicated by the shaded blue area), but significantly enhances SOC levels, leading to improved future crop yields and profit. The future yield enhancement is represented as a downward shift in the average total cost curve, such that future profits include both the blue and green shaded areas across both panels. Conversely, Panel (B) illustrates a crop rotation strategy that has higher current profits but is less effective in SOC sequestration, but happens to contribute less to SOC accumulation. This results in a smaller downward shift in the average cost curve. As drawn, current profits are larger for the crop rotation depicted in Panel (B) relative to (A), whereas future profits are larger in Panel (A) relative to (B) owing to the slow, yet more significant, accumulation of SOC for the crop rotation in (A). This scenario illustrates the possibility that a farmer might undervalue the strategy shown in Panel (A) compared to Panel (B) in the current time period, neglecting the future advantages of enhanced soil health and increased crop yields resulting from higher SOC stocks.

163

FIGURE 2.5: Dynamic Effects of Carbon Sequestration on Current and Future Farm Profits

(A) High SOC Sequestering Crop Rotation

Price, p_a

MC_A^C

ATC_A^C

$\square = \pi_a^C$

$\square + \square = \pi_a^F$

e_a^C　e_a^F

$p_a = P_A$　　　　　MR_A

MC_A^F

ATC_A^F

Farm products, q_a

0　　q_a^C　q_a^F

$\Delta \pi_a^{F-C}$

(B) Low SOC Sequestering Crop Rotation

Price, p_b

MC_B^C　MC_B^F

ATC_B^C

$\square = \pi_b^C$

$\square + \square = \pi_b^F$

e_b^C　e_b^F

$p_b = P_B$　　　　　MR_B

ATC_B^F

Farm products, q_b

0　　q_b^C　q_b^F

$\Delta \pi_b^{F-C}$
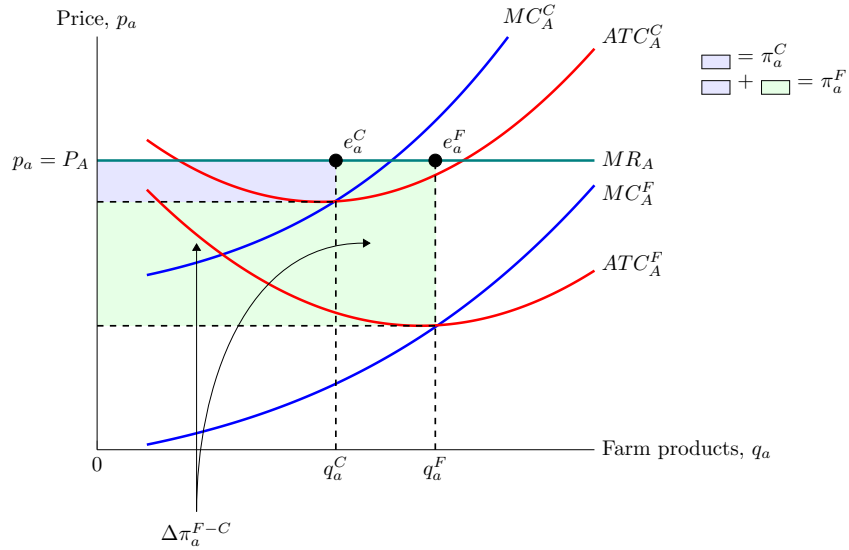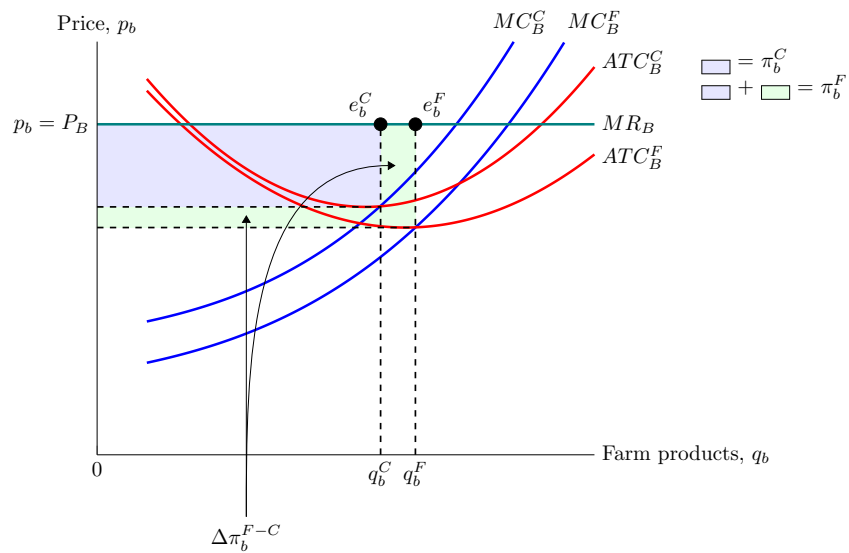
$$\pi_a^C < \pi_b^C \quad \& \quad \pi_a^F > \pi_b^F$$

Source: Author.

Notes: The blue shaded regions indicate the Current (C) profits from each crop rotation. Meanwhile, the green shaded regions show the additional Future (F) profits, the on-farm benefits from having sequestered additional carbon in the soil. In this specific case, current profits are less for crop rotation A than crop rotation B. However, because if sequesters more carbon, crop rotation A generates greater future profits than those of crop rotation B.

164

In what follows, I conduct a dynamic simulation to assess the on-farm benefits for a specific crop rotation that stem only from carbon sequestration from 2023 to 2055. I then calculate the on-farm profitability with and without the benefits from carbon sequestration and calculate the respective external social benefits. The dynamic simulation employs five distinct four-year crop rotation sequences: Canola-Spring Wheat-Canola-Spring Wheat, Canola-Spring Wheat-Peas-Spring Wheat, Spring Wheat-Peas-Spring Wheat-Peas, Spring Wheat-Fallow-Spring Wheat-Fallow, and Lentils-Fallow-Lentils-Peas. Instead of directly applying the Augmented Campbell model, I develop a state equation based on SOC stock data simulated by Serfas (2024a) and crop production data at the field level from SCIC. For each soil zone, I regress the yearly change in SOC stocks on the stock from the previous year, crop yield, and prior cropping patterns represented by dummy variables. This method facilitates dynamic simulation while effectively including the dynamic effects on yield, without having to involve more complex SOC prediction models. All of the data on expected yields, commodity prices, and production costs per hectare are retrieved from the 2023 Saskatchewan Crop Planning Guide (Government of Saskatchewan, 2023a). The initial stock of SOC for 2023 is computed as the weighted average stock for each soil zone weighted by the hectares of a field and simulated by the Augmented Campbell model for the year 2019.[21] The state equation for SOC stocks is characterized as:

$$\Delta SOC_{n,t} = \alpha SOC_{n,t-1} + \mathbf{1}_{c \in C}\{\beta_c Y^c_{n,t-1}\} + \mathbf{1}_{mk \in MK}\{\gamma_{mk}\Theta^{mk}_{n,t}\} + Z_{n,t-1}\delta + v_{n,t}, \qquad (2.13)$$

where, on field n, $\Delta SOC_{n,t}$ is the annual change in SOC between years t and $t-1$, $SOC_{n,t-1}$ is stock of SOC in the previous year, $Y^c_{n,t-1}$ is last year's yield for crop c, $\Theta^{mk}_{n,t}$ is the cropping sequence over the previous two years, $Z_{n,t-1}$ is a vector of weather variables that include GSAT and TAP, and $v_{n,t}$ is the error term. Equation (2.13) is estimated for each soil zone with standard errors clustered at the farm level and observations weighted by the hectares of a field. Index C includes six crops (canola, barley, spring wheat, durum wheat, lentils, peas) and MK includes 49 combinations of

---

[21]I assume that the stock of SOC for the year of 2019 is similar and can be used as a proxy for SOC stocks in the year 2023.

the past two-year cropping sequence, additionally including summer fallow to the set C.[22] The primary function of the state equation is to predict the change in stock of SOC, which then can be used to characterize the dynamic interactions between SOC stocks and crop yield using the shadow value of SOC, which vary across different crop rotations and soil zones.[23]

Figure 2.6 shows the predicted yearly increases in SOC corresponding to each two-year crop rotation within each soil zone. The caption in the top of each column indicates the crop that was planted in the last year, while the label at the bottom of each column indicates the crop that was planted in the year before last. I construct the 95% confidence interval for each prediction, calculated using the variance formula,

$$
\begin{aligned}
Var(\Delta SOC_{n,t}|SOC_{n,t-1}, &\mathbf{1}_{c\in C}\{Y_{n,t-1}^c\}, \mathbf{1}_{mk\in MK}\{\Theta_{n,t}^{mk}\}, Z_{n,t-1}) = \\
& \alpha^2 Var(SOC_{n,t-1}) \\
& + \mathbf{1}_{c\in C}\{\beta_c^2\} Var(\mathbf{1}_{c\in C}\{Y_{n,t-1}^c\}) \\
& + \mathbf{1}_{mk\in MK}\{\gamma_{mk}^2\} Var(\mathbf{1}_{mk\in MK}\{\Theta_{n,t}^{mk}\}) \\
& + \delta^2 Var(Z_{n,t-1}) \\
& + 2\big[\alpha\mathbf{1}_{c\in C}\{\beta_c\} Cov(SOC_{n,t-1}, \mathbf{1}_{c\in C}\{Y_{n,t-1}^c\}) \\
& + \alpha\mathbf{1}_{mk\in MK}\{\gamma_{mk}\} Cov(SOC_{n,t-1}, \mathbf{1}_{mk\in MK}\{\Theta_{n,t}^{mk}\}) \\
& + \alpha\delta Cov(SOC_{n,t-1}, Z_{n,t-1}) \\
& + \mathbf{1}_{c\in C}\{\beta_c\}\mathbf{1}_{mk\in MK}\{\gamma_{mk}\} Cov(\mathbf{1}_{c\in C}\{Y_{n,t-1}^c\}, \mathbf{1}_{mk\in MK}\{\Theta_{n,t}^{mk}\}) \\
& + \mathbf{1}_{c\in C}\{\beta_c\}\delta Cov(\mathbf{1}_{c\in C}\{Y_{n,t-1}^c\}, Z_{n,t-1}) \\
& + \mathbf{1}_{mk\in MK}\{\gamma_{mk}\}\delta Cov(\mathbf{1}_{mk\in MK}\{\Theta_{n,t}^{mk}\}, Z_{n,t-1})\big].
\end{aligned}
\tag{2.14}
$$

---

[22]Adding additional lags of cropping choice slightly improves the prediction of SOC stocks. Table 2E.1 in Appendix 2E shows the ten-fold cross validation results when different cropping sequence lag lengths are tried. I find that the r-squared value increases by 0.04 in the brown soil zone, 0.06 in the dark brown soil zone, and 0.08 in the black & gray soil zone when including four lags relative to two. I employ two lags for past cropping choice in the SOC state equation, which significantly reduces the number of parameters needed for dynamic simulation and does not sacrifice too much predictive performance as shown in Table 2E.1 in Appendix E.

[23]To simulate SOC stocks, I use the forward Euler method. Simulation results using the fourth-order Runge-Kutta method generate identical changes in the stock of SOC to those from the forward Euler method because the state equation for SOC is linear. Hence, non-linear differential equation solvers like the Runge-Kutta method result in similar predictions for changes in SOC stocks.

FIGURE 2.6: Prediction of Annual Change in Soil Organic Carbon by Two-Year Crop Rotation
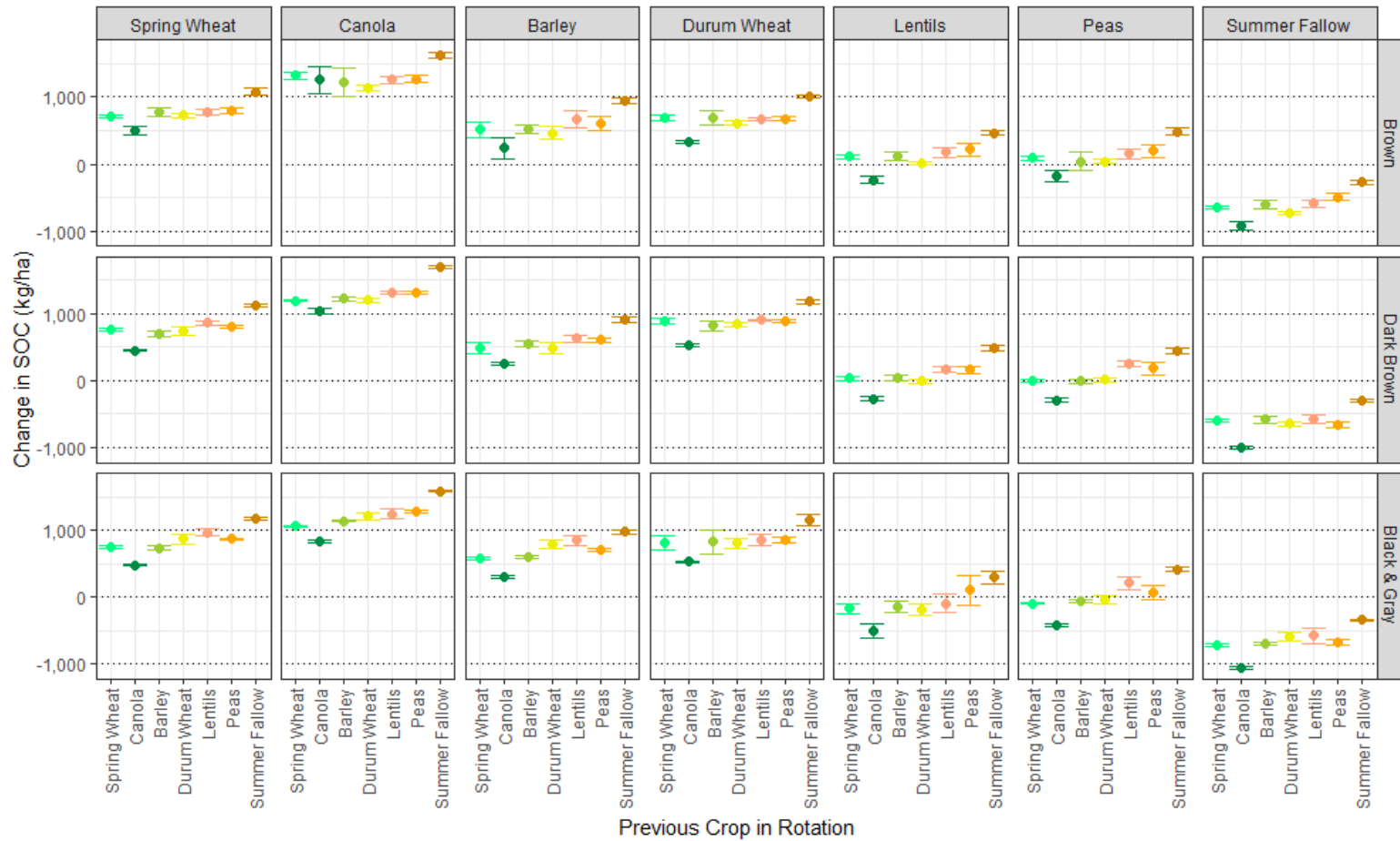
Source: Author's Estimates.

Notes: Crops listed in the top panel refer to the crop seeded last year, whereas crops labeled on the x-axis are preceding year's crop (seeded two-years ago.) Each point represents the predicted annual change in SOC calculated using equation (2.13) and its associated 95% confidence interval calculated using equation (2.14).

In Figure 2.6, for each soil zone, the plots depict the yearly average change in SOC. These predictions were made using the 1998 to 2019 average weather on fields in which SOC is predicted, the 2019 average SOC stock by soil zone, and the expected yield for each crop retrieved from the 2023 Saskatchewan Crop Planning Guide (Government of Saskatchewan, 2023a). The predictions indicate that canola, spring wheat, or durum wheat planted in the preceding year contributed more to annual SOC changes, while lentils, peas, and summer fallow practices contribute less and can result in a decrease in the SOC stock. Additionally, having seeded canola two years ago decreases the increase in SOC for all crops planted in the last year, whereas having opted for summer fallow two years ago increases the increase in SOC change for all crops planted last year.

Figure 2.7 and Table 2.4 display the results from the dynamic simulation for each crop rotation and soil zone. Specific crop rotations were selected for a variety of reasons. Rotations featuring canola are prevalent in the dark brown and black & gray soil zones, while Spring Wheat-Peas-Spring Wheat-Peas is more typical in the brown soil zone. Another common older crop rotation is Spring Wheat-Fallow-Spring Wheat-Fallow, while Lentils-Fallow-Lentils-Peas represents a low carbon sequestering rotation that yields relatively higher profits over the four-year cycle compared to rotations involving cereals and canola.[24]

Figure 2.7 shows the growth in SOC stock in each soil zone for each crop rotation. Across these rotations and soil zones, the Canola-Spring Wheat-Canola-Spring Wheat rotation generates the largest increase in SOC stock from 2023 to 2055 for each soil zone. On average, increases in SOC are greater in the brown and dark brown soil zones than in the black & gray soil zone, likely because of the already higher SOC stock in the latter, necessitating more carbon inputs to be sustained. The smallest increases in SOC stocks are observed in the black & gray soil zone, particularly with the Lentil-Fallow-Lentils-Peas rotation. These simulations are based on expected yields from the 2023 Saskatchewan Crop Planning Guide (Government of Saskatchewan, 2023a), representing an optimistic outlook for future SOC changes. However, we should note that the responses to adopting these crop rotations could vary considerably over time and space due to

---

[24]Fallow is incorporated into this rotation to enable better weed control and reduce disease pressure by exclusively seeding pulse crops.

variation in crop yield, soil characteristics, weather conditions, and farm management practices. Additionally, these predictions are out of sample. As longer time-series data become available, recalibration of the model will be possible and will allow more precise SOC predictions.[25]

FIGURE 2.7: Simulated SOC Stocks by Crop Rotation and Soil Zone
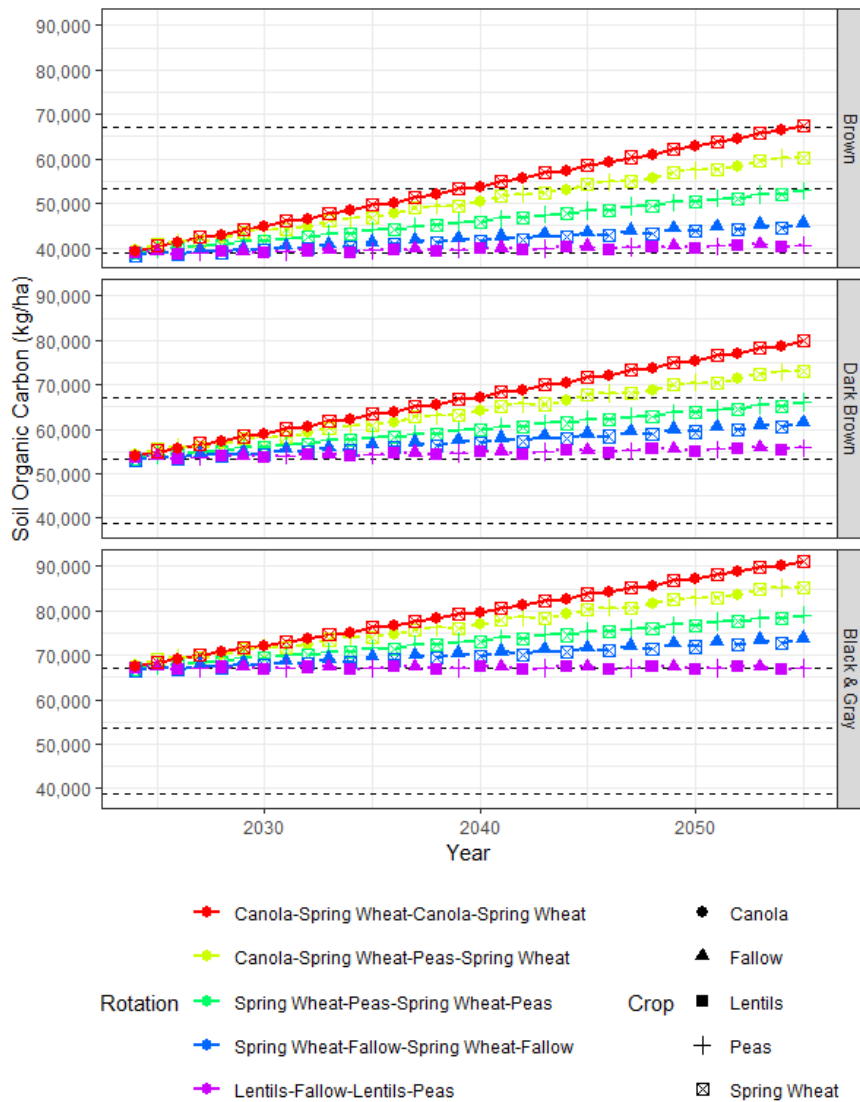
Source: Author's Estimates.

Notes: The time paths for soil organic carbon (SOC) are computed by using equation (2.13) for each soil zone, mean weather conditions from 1998 to 2023, initial SOC stocks in 2019, and the 2023 expected crop yields from the Saskatchewan Crop Planning Guide (Government of Saskatchewan, 2023a).

---

[25]All SOC prediction models are calibrated using historical soil sampling data from the Experimental Research Station operated by Agriculture and Agri-Food Canada located in Swift Current, Saskatchewan.

TABLE 2.4: Percentage Change in On-Farm Profit from Carbon Sequestration by Crop Rotation

	(1)	(2)	(3)	(4)	(5)	(6)	(7)	(8)
Soil Zone:				*Brown*				
Four-Year Rotation Period:	2024–2027	2028–2031	2032–2035	2036–2039	2040–2043	2044–2047	2048–2051	2052–2055
Crop Rotation:				*(% change in profit)*				
Canola-Spring Wheat-Canola-Spring Wheat	2.29	5.33	8.36	11.38	14.39	17.40	20.39	23.38
Canola-Spring Wheat-Peas-Spring Wheat	**3.18**	**6.67**	**10.15**	**13.63**	**17.11**	**20.58**	**24.05**	**27.51**
Spring Wheat-Peas-Spring Wheat-Peas	1.62	5.04	8.48	11.91	15.34	18.78	22.22	25.66
Spring Wheat-Fallow-Spring Wheat-Fallow	-1.30	1.34	3.97	6.60	9.22	11.83	14.43	17.02
Lentils-Fallow-Lentils-Peas	0.05	0.24	0.43	0.61	0.80	0.98	1.16	1.34
Soil Zone:				*Dark Brown*				
Four-Year Rotation Period:	2024–2027	2028–2031	2032–2035	2036–2039	2040–2043	2044–2047	2048–2051	2052–2055
Crop Rotation:								
Canola-Spring Wheat-Canola-Spring Wheat	**0.98**	**2.59**	**4.20**	**5.80**	**7.41**	**9.02**	**10.62**	**12.23**
Canola-Spring Wheat-Peas-Spring Wheat	0.82	1.88	2.94	4.00	5.06	6.11	7.16	8.22
Spring Wheat-Peas-Spring Wheat-Peas	0.15	0.73	1.32	1.91	2.49	3.07	3.65	4.23
Spring Wheat-Fallow-Spring Wheat-Fallow	-0.34	0.63	1.60	2.56	3.52	4.48	5.43	6.38
Lentils-Fallow-Lentils-Peas	0.01	0.08	0.15	0.23	0.30	0.37	0.44	0.51
Soil Zone:				*Black & Gray*				
Four-Year Rotation Period:	2024–2027	2028–2031	2032–2035	2036–2039	2040–2043	2044–2047	2048–2051	2052–2055
Crop Rotation:								
Canola-Spring Wheat-Canola-Spring Wheat	**0.42**	**1.19**	**1.96**	**2.72**	**3.49**	**4.25**	**5.01**	**5.77**
Canola-Spring Wheat-Peas-Spring Wheat	0.45	1.02	1.59	2.17	2.73	3.30	3.86	4.42
Spring Wheat-Peas-Spring Wheat-Peas	0.19	0.57	0.95	1.33	1.71	2.08	2.46	2.83
Spring Wheat-Fallow-Spring Wheat-Fallow	-0.15	0.10	0.35	0.59	0.83	1.08	1.32	1.56
Lentils-Fallow-Lentils-Peas	0.00	0.00	0.00	0.00	0.00	0.00	0.01	0.01

Source: Author's Estimates.

Notes: The percentage change in profit for each four-year crop rotation is relative to the corresponding profit using 2023 prices and costs for each crop rotation from the Saskatchewan Crop Planning Guide (Government of Saskatchewan, 2023a). The entries in bold are for the crop rotation yielding the greatest percentage benefit from SOC sequestration.

In Table 2.4, I summarize the on-farm benefits that stem from cumulative carbon seques-tration calculated as the average percentage increase in profit relative to 2023 for each four-year cycle of crop rotation from 2023 to 2055. These findings indicate that the potential on-farm advan-tages of carbon sequestration are most significant in the brown soil zone, yet still remain beneficial across all of Saskatchewan. The results reveal that, by 2052-55 farmers could accumulate enough SOC to increase their four-year crop rotation profits by 27.51% in the brown soil zone, 12.23% in the dark brown soil zone, and 5.77% in the black & gray soil zone. In the brown soil zone, the Canola-Spring Wheat-Peas-Spring Wheat rotation shows the greatest percentage increase in profit attributable to increased SOC, while in both the dark brown and black & gray soil zones, it is the Canola-Spring Wheat-Canola-Spring Wheat. The results in Table 2.4 show that SOC has a more pronounced affect on rotations including a mix of pulses, cereals, and canola, or just pulses and ce-reals, in the brown soil zone compared to the dark brown and black & gray soil zones. In the dark brown and black & gray soil zone, rotations of spring wheat and canola, excluding pulses, result in notably higher on-farm benefits from carbon sequestration. This dynamic simulation does not fully capture the effects of cropping intensity, and rotations emphasizing substantial canola pro-duction might be more prone to disease. Such susceptibility could significantly decrease on-farm profitability if there is a correlation between disease risk and specific crop rotations.

Using the results from the dynamic simulation, I calculate the change in on-farm profit re-sulting from carbon sequestration over 32 years, depicted as the shaded green region in Figure 2.5.[26] If current profit is denoted as π_i^C for crop rotation i and π_i^F signifies the future profit for the same rotation, then the change in profit attributable to increased SOC after 32 years of dynamic simulation (2023-2055) is,

$$\Delta \pi_i^{F-C} = \pi_i^F - \pi_i^C. \tag{2.15}$$

---

[26]On-farm profit is equal to the return over variable expenses obtained from the 2023 Saskatchewan Crop Planning Guide Government of Saskatchewan (2023a). Variable expenses in the Saskatchewan Crop Planning Guide do not include fixed costs, such as property tax, machinery and building investment and depreciation, or land investment.

Where $\Delta \pi_i^{F-C}$ represents that change in profit from 2023 to 2055 for a four-year crop rotation, as a result of additional SOC, interpreted as the on-farm benefit from carbon sequestration. To compare these benefits between alternative crop rotations, I take the difference. The difference in on-farm benefit from additional SOC yielded by crop rotation i relative to crop rotation j is estimated as,

$$\eta_{ij} = (\pi_i^F - \pi_j^F) - (\pi_i^C - \pi_j^C), \tag{2.16}$$

where η_{ij} is the increase in the on-farm benefits from carbon sequestration obtained by choosing crop rotation i to crop rotation j.

Table 2.5 presents the on-farm benefit from carbon sequestration for each crop rotation as calculated using equation (2.15) (for diagonal elements) and the comparative on-farm benefit from carbon sequestration against a different rotation, calculated using equation (2.16) (for non-diagonal elements). I divide each benefit for the last four years of the four-year crop rotation by four to obtain the yearly average profit increase from the additional SOC accrued after sustaining the respective crop rotation for 32 years. In this case, future profits are valued in 2023 CAD, but are not discounted. Here, I only compute the benefits from carbon sequestration over time and relative to other crop rotations. Following this, I calculate the present value of on-farm profits and their external social benefits for each crop rotation and relative to different rotations.

Table 2.5 shows that the increase in on-farm profit is greatest for the Canola-Spring Wheat-Canola-Spring Wheat rotation. The difference in gains from SOC sequestration between the Canola-Spring Wheat-Peas-Spring Wheat and the Canola-Spring Wheat-Canola-Spring Wheat rotation is minimal (less than 1 CAD per hectare) in the brown soil zone, compared with the dark brown and black & gray soil zones, where the additional gains are 29.78 and 12.46 CAD per hectare, respectively. In the brown soil zone, the difference between Canola-Spring Wheat-Peas-Spring Wheat (or Canola-Spring Wheat-Canola-Spring Wheat) and Spring Wheat-Fallow-Spring Wheat-Fallow is equal to approximately 87 CAD per hectare per year after 32 years of implementation. Meanwhile, the difference in on-farm profits from carbon sequestration between Canola-Spring Wheat-Canola-Spring Wheat and Spring Wheat-Fallow-Spring Wheat-Fallow in the dark brown

172

and black & gray soil zones amount to 63.55 and 39.42 CAD per hectare, after 32 years of rotating Canola-Spring Wheat-Canola-Spring Wheat compared with Spring Wheat-Fallow-Spring Wheat-Fallow.

TABLE 2.5: Matrix of On-Farm Benefits from Carbon Sequestration by Crop Rotation

Formulas:	$Diag\{\Delta\pi_i^{F-C} = \pi_i^F - \pi_i^C\}$	&	$NonDiag\{\eta_{i,j} = (\pi_i^F - \pi_j^F) - (\pi_i^C - \pi_j^C) \; \forall \; i \neq j\}$		
Soil Zone:			*Brown*		
Crop Rotation:	(1)	(2)	(3)	(4)	(5)
			(2023 CAD/ha/yr)		
(1) Canola-Spring Wheat-Canola-Spring Wheat	**109.31**				
(2) Canola-Spring Wheat-Peas-Spring Wheat	0.13	**109.18**			
(3) Spring Wheat-Peas-Spring Wheat-Peas	25.61	25.47	**83.71**		
(4) Spring Wheat-Fallow-Spring Wheat-Fallow	87.44	87.31	61.84	**21.87**	
(5) Lentils-Fallow-Lentils-Peas	103.60	103.47	77.99	16.16	**5.71**
Soil Zone:			*Dark Brown*		
Crop Rotation:	(1)	(2)	(3)	(4)	(5)
(1) Canola-Spring Wheat-Canola-Spring Wheat	**76.00**				
(2) Canola-Spring Wheat-Peas-Spring Wheat	29.78	**46.23**			
(3) Spring Wheat-Peas-Spring Wheat-Peas	54.69	24.91	**21.31**		
(4) Spring Wheat-Fallow-Spring Wheat-Fallow	63.55	33.77	8.86	**12.46**	
(5) Lentils-Fallow-Lentils-Peas	73.00	43.23	18.31	9.46	**3.00**
Soil Zone:			*Black & Gray*		
Crop Rotation:	(1)	(2)	(3)	(4)	(5)
(1) Canola-Spring Wheat-Canola-Spring Wheat	**43.49**				
(2) Canola-Spring Wheat-Peas-Spring Wheat	12.46	**31.03**			
(3) Spring Wheat-Peas-Spring Wheat-Peas	25.16	12.70	**18.33**		
(4) Spring Wheat-Fallow-Spring Wheat-Fallow	39.42	26.95	14.25	**4.08**	
(5) Lentils-Fallow-Lentils-Peas	43.45	30.99	18.28	4.03	**0.04**

Source: Author's Estimates
Notes: Diagonal elements are equal to the on-farm benefit per year derived from carbon sequestration by crop rotation. They signify the difference between current and future profits for a four-year crop rotation applied from 2023 to 2055, measured in 2023 dollars per hectare per year (refer to equation (2.15)). Conversely, non-diagonal elements denote the contrast in on-farm benefits from carbon sequestration across different crop rotations (refer to equation (2.16)). Current profit is computed based on the expected profit outlined in the 2023 Saskatchewan Crop Planning Guide for a four-year crop rotation, while future profit is determined using the 2023 prices and costs from the same guide (Government of Saskatchewan, 2023a), combined with simulated crop yields derived from the last four years of dynamic simulation.

I now compute the present value of on-farm profits and the external social benefit from SOC sequestration from 2023 to 2055, comparing the five alternatve crop rotations across three soil zones in Saskatchewan, as done in Table 2.5.[27] I calculate the present value of on-farm profits with and without yield growth effects attributed to carbon sequestration (with and without SOC effects). The external social benefit is measured as the value of the implied reduction in atmospheric carbon resulting from additional SOC sequestered by a particular crop rotation, compared with the 2023 baseline stock and then relative to an alternative crop rotation. Both the on-farm profits and external social benefits are calculated incorporating the simulated change in SOC stocks from 2023 to 2055. To calculate the external social benefit, I apply a money metric measure of the social cost of carbon (SCC) to the reduction in atmospheric carbon implied by measured changes in the stock of SOC. The computation of the external social benefit involves applying an equivalent annual rental price for SOC, rather than directly employing the SCC.

The present value of on-farm profits and the external social benefit from additional SOC compared with a fixed initial baseline stock of SOC, are characterized as,

$$PV_i = \sum_{t=2024}^{2055} (1+r)^{-(t-2023)} \pi_i, \tag{2.17}$$

and

$$
\begin{aligned}
ESB_i = &\sum_{t=2024}^{2054} (1+\delta)^{-(t-2023)} P(SOC_{i,t}^{Simulated} - SOC_{2023}) \\
&+ \frac{P}{\delta}(1+\delta)^{-(2055-2023)} \left(\frac{\sum_{t=2055-4}^{2055} SOC_{i,t}^{Simulated} - SOC_{2023}}{4} \right),
\end{aligned} \tag{2.18}
$$

where,

$$P = \delta * SCC * \frac{44\ Mg\ CO_2}{12\ Mg\ SOC}.$$

---

[27]It is important to note that since the SOC prediction models are subject to error, so too are the estimates of private and public benefits from changes SOC stocks.

Let r be the real discount rate applied to on-farm profits and evaluated at 5% per year, ESB be the external social benefit per hectare of carbon sequestration by soil zone, $SOC_t^{Simulated}$ is the simulated SOC stock from the dynamic simulation, SOC_{2023} is the 2023 initial stock of SOC,[28] and δ is the discount rate used to calculate the SCC. The annual rental price of SOC is equal to the SCC multiplied by its corresponding discount rate and a conversion factor from CO_2 to SOC from Mikhailova et al. (2019).

In this analysis, I assume after 2055 SOC remains constant. Equation (2.18) therefore has two components: the first captures rising flows of external benefits from additional SOC stored from 2024 to 2054, while the second measures the benefits from the constant flows from 2055 onward, which can be represented as a perpetuity, as the average annual flow across a four-year rotation. I apply a SCC value in this analysis sourced from Rennert et al. (2022) at 185 USD/Mg of CO_2, applying a 2% near-term risk-free discount rate. All external social benefits are converted to 2023 real dollars using the GDP Deflator from the Federal Reserve Bank of St. Louis (U.S. Bureau of Economic Analysis, 2024) and subsequently converted to CAD using the exchange rate from the Bank of Canada (2023a) for 2023.

Figure 2.8 only shows the discounted flow of external social benefits from 2023 to 2055 for each of the five crop rotations and in each of the three soil zones, illustrating the benefits to 2055 (as opposed to the benefits from 2055 and onward in perpetuity), as captured by the first term outlined in equation (2.18). Naturally, the external social benefit is greater for crop rotations with higher SOC sequestration rates and less for those with lower rates of SOC sequestration.[29]

---

[28] As stated earlier in this section, the inital stock of SOC for 2023 is computed as the weighted average stock for each soil zone weighted by the hectares of a field using the Augmented Campbell model provided by Serfas (2024a) for the year 2019 as a proxy for the year 2023.

[29] Please refer to Figure 2.7 to see the change in the SOC stock by crop rotation over time.

FIGURE 2.8: Simulated Stream of Discounted External Social Benefits from Carbon Sequestration by Crop Rotation
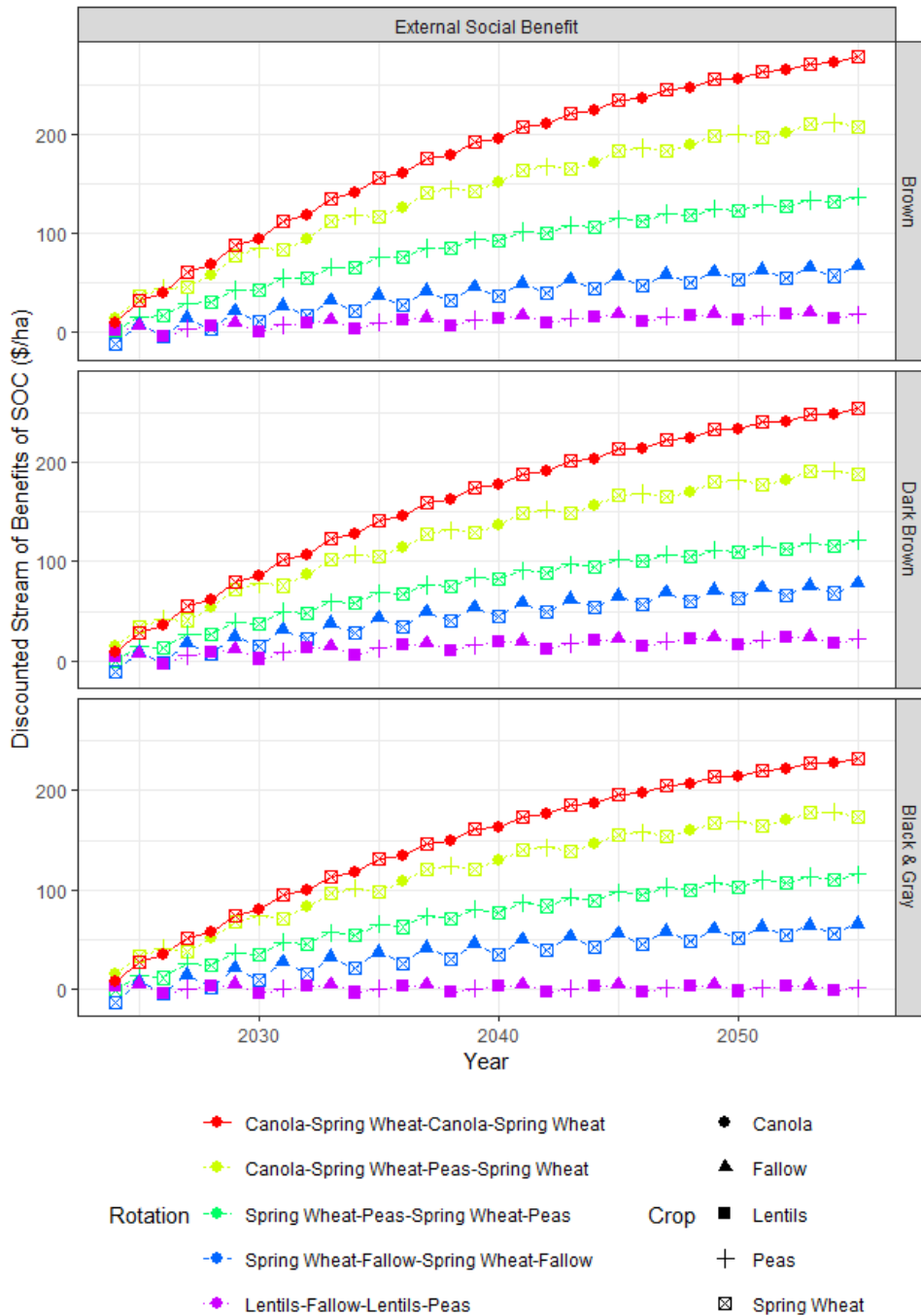
Notes: The external social benefit for each year is calculated using the first term of equation (2.14). All computations are converted to 2023 dollars using the GDP Deflator from the Federal Reserve Bank of St. Louis (U.S. Bureau of Economic Analysis, 2024) and to CAD using the U.S. to Canadian exchange rate from the Bank of Canada (2023a). Here, I employ a social cost of carbon of 185 USD/Mg of CO_2 from Rennert et al. (2022).

The difference in the present value of on-farm profits and the external social benefits between crop rotation i and j are,

$$\Delta PV_{ij} = PV_i - PV_j \qquad (2.19)$$

and

$$\Delta ESB_{ij} = ESB_i - ESB_j. \qquad (2.20)$$

Table 2.6 shows the computed present value of on-farm profits with and without the derived benefits from carbon sequestration by crop rotation and soil zone, evaluated at real discount rate of 5% per year. The present value of on-farm profits without SOC effects over 32 years, for the Canola-Spring Wheat-Peas-Spring Wheat rotation relative to the Lentils-Fallow-Lentils-Peas rotation, is -430 CAD per hectare in the brown soil zone, -291 CAD per hectare in the dark brown soil zone, and 113 CAD per hectare in the black & gray soil zone. For the same comparison with SOC effects, the present value of on-farm profits is 265 CAD per hectare in the brown soil zone, -1 CAD per hectare in the dark brown soil zone, and 322 CAD per hectare in the black & gray soil zone. Hence, the present value of on-farm profits that stems from differences in carbon sequestration between the Canola-Spring Wheat-Peas-Spring Wheat rotation and the Lentils-Fallow-Lentils-Peas rotation on 65 hectares (equivalent a quarter section or field) amounts to 45,175 CAD in the brown soil zone, 18,850 CAD in the dark brown soil zone, and 13,585 CAD in the black & gray soil zone.[30]

As illustrated in Figure 2.5, farmers risk underestimating the long-term present value of crop rotations if they do not consider the long-term effects of SOC on crop yields, and this can affect the comparison of alternative. For example, in Table 2.6, the present value of on-farm profits is lower for the Canola-Spring Wheat-Peas-Spring Wheat rotation relative to the Lentils-Fallow-Lentils-Peas rotation in the brown soil zone when SOC effects are excluded, but this ranking is reversed

---

[30]In the brown soil zone the present value of on-farm profits that stems from carbon sequestration between the Canola-Spring Wheat-Peas-Spring Wheat rotation and the Lentils-Fallow-Lentils-Peas rotation is calculated as 265 CAD per hectare minus -430 CAD per hectare and then multiplied by 65 hectares.

when SOC effects are included. It is important to note that the accuracy of the SOC prediction model is limited for crop rotations with minimal representation in the dataset, especially over extended periods, like the Lentils-Fallow-Lentils-Peas rotation. Farmers typically do not adopt the Lentils-Fallow-Lentils-Peas rotation because it is prone to disease (e.g., aphanomyces). However, this varies by soil zone. For example, because the brown soil zone is drought prone (Marchildon and Sauchyn, 2009), farmers favor rotations with more lentils over canola.

Table 2.6 also shows the external social benefit for each crop rotation, soil zone, and SCC value. For the Canola-Spring Wheat-Peas-Spring Wheat rotation over 32 years relative to the Spring Wheat-Fallow-Spring Wheat-Fallow rotation, and using a SCC of 185 USD/Mg of CO_2, the external social benefit from carbon sequestration is 11,067 CAD per hectare in the brown soil zone, 9,445 CAD per hectare in the dark brown soil zone, and 9,394 CAD per hectare in the black & gray soil zone. The greatest external social benefit from carbon sequestration is for the Canola-Spring Wheat-Canola-Spring Wheat rotation relative to the Lentils-Fallow-Lentils-Peas rotation, amounting to 20,114 CAD per hectare in the brown soil zone, is 17,861 CAD per hectare in the dark brown soil zone, and is 17,884 CAD per hectare in the black & gray soil zone. When comparing rotation (2), which includes canola, spring wheat, and pulses, with rotation (5), which includes lentils, peas, and fallow, it is apparent that the relative private on-farm benefits are much lower compared with the external social benefits attributed to carbon sequestration.

Employing the results from Figure 2.6, suppose every farmer in Saskatchewan who purchases crop insurance opts for the Canola-Spring Wheat-Peas-Spring Wheat rotation compared with the Spring Wheat-Fallow-Spring-Wheat-Fallow, sustained for 32 years. In this scenario, the external social benefit is equal to approximately 108 billion CAD for the entire province of Saskatchewan. Even though the external social benefit per hectare is greater in the brown soil zone in this comparison, approximately 25% of this benefit is attributed to the brown soil zone, 34% to the dark brown soil zone, and 42% to the black & gray soil zone due to differences in the number of hectares in each soil zone.

TABLE 2.6: Matrix of the Present Value of Private On-Farm Profits and External Social Benefits from Carbon Sequestration by Crop Rotation

	Present Value of On-Farm Profits without SOC Effects					Present Value of On-Farm Profits with SOC Effects				
Soil Zone:	Brown					Brown				
Crop Rotation:	(1)	(2)	(3)	(4)	(5)	(1)	(2)	(3)	(4)	(5)
	(2023 CAD/ha)					*(2023 CAD/ha)*				
(1) Canola-Spring Wheat-Canola-Spring Wheat	**7,450**					**8,161**				
(2) Canola-Spring Wheat-Peas-Spring Wheat	1,089	**6,362**				1,070	**7,091**			
(3) Spring Wheat-Peas-Spring Wheat-Peas	2,304	1,215	**5,147**			3,015	1,944	**5,147**		
(4) Spring Wheat-Fallow-Spring Wheat-Fallow	5,352	4,263	3,048	**2,099**		5,953	4,882	2,938	**2,208**	
(5) Lentils-Fallow-Lentils-Peas	659	-430	-1,645	-4,693	**6,791**	1,335	265	-1,680	-4,618	**6,826**
Soil Zone:	Dark Brown					Dark Brown				
Crop Rotation:	(1)	(2)	(3)	(4)	(5)	(1)	(2)	(3)	(4)	(5)
(1) Canola-Spring Wheat-Canola-Spring Wheat	**9,889**					**10,377**				
(2) Canola-Spring Wheat-Peas-Spring Wheat	904	**8,985**				1,084	**9,293**			
(3) Spring Wheat-Peas-Spring Wheat-Peas	1,951	1,046	**7,939**			2,439	1,354	**7,939**		
(4) Spring Wheat-Fallow-Spring Wheat-Fallow	6,711	5,807	4,761	**3,178**		7,134	6,049	4,695	**3,244**	
(5) Lentils-Fallow-Lentils-Peas	614	-291	-1,337	-6,098	**9,276**	1,083	-1	-1,356	-6,051	**9,294**
Soil Zone:	Black & Gray					Black & Gray				
Crop Rotation:	(1)	(2)	(3)	(4)	(5)	(1)	(2)	(3)	(4)	(5)
(1) Canola-Spring Wheat-Canola-Spring Wheat	**11,987**					**12,267**				
(2) Canola-Spring Wheat-Peas-Spring Wheat	814	**11,174**				884	**11,383**			
(3) Spring Wheat-Peas-Spring Wheat-Peas	1,768	954	**10,220**			2,048	1,164	**10,220**		
(4) Spring Wheat-Fallow-Spring Wheat-Fallow	7,727	6,913	5,959	**4,261**		7,987	7,103	5,939	**4,280**	
(5) Lentils-Fallow-Lentils-Peas	926	113	-841	-6,800	**11,061**	1,206	322	-842	-6,781	**11,061**

TABLE 2.6: Matrix of Private On-Farm Benefits and Public External Social Benefits from Carbon Sequestration by Crop Rotation *(continued)*

	External Social Benefits					Total Benefits with SOC Effects				
Soil Zone:	Brown					Brown				
Crop Rotation:	(1)	(2)	(3)	(4)	(5)	(1)	(2)	(3)	(4)	(5)
	(2023 CAD/ha)					*(2023 CAD/ha)*				
(1) Canola-Spring Wheat-Canola-Spring Wheat	**21,500**					**29,661**				
(2) Canola-Spring Wheat-Peas-Spring Wheat	4,911	**16,589**				5,981	**23,680**			
(3) Spring Wheat-Peas-Spring Wheat-Peas	11,067	6,157	**10,432**			14,082	8,101	**15,579**		
(4) Spring Wheat-Fallow-Spring Wheat-Fallow	16,775	11,865	5,708	**4,724**		22,728	16,747	8,646	**6,933**	
(5) Lentils-Fallow-Lentils-Peas	20,114	15,203	9,046	3,338	**1,386**	21,448	15,468	7,367	-1,279	**8,212**
Soil Zone:	Dark Brown					Dark Brown				
Crop Rotation:	(1)	(2)	(3)	(4)	(5)	(1)	(2)	(3)	(4)	(5)
(1) Canola-Spring Wheat-Canola-Spring Wheat	**19,618**					**29,995**				
(2) Canola-Spring Wheat-Peas-Spring Wheat	4,575	**15,042**				5,660	**24,335**			
(3) Spring Wheat-Peas-Spring Wheat-Peas	10,332	5,757	**9,286**			12,771	7,111	**17,225**		
(4) Spring Wheat-Fallow-Spring Wheat-Fallow	14,020	9,445	3,688	**5,598**		21,154	15,494	8,383	**8,841**	
(5) Lentils-Fallow-Lentils-Peas	17,861	13,286	7,529	3,841	**1,757**	18,944	13,284	6,173	-2,210	**11,051**
Soil Zone:	Black & Gray					Black & Gray				
Crop Rotation:	(1)	(2)	(3)	(4)	(5)	(1)	(2)	(3)	(4)	(5)
(1) Canola-Spring Wheat-Canola-Spring Wheat	**18,018**					**30,285**				
(2) Canola-Spring Wheat-Peas-Spring Wheat	3,976	**14,041**				4,860	**25,425**			
(3) Spring Wheat-Peas-Spring Wheat-Peas	9,216	5,239	**8,802**			11,263	6,403	**19,022**		
(4) Spring Wheat-Fallow-Spring Wheat-Fallow	13,370	9,394	4,154	**4,648**		21,357	16,497	10,093	**8,928**	
(5) Lentils-Fallow-Lentils-Peas	17,884	13,907	8,668	4,514	**134**	19,090	14,229	7,826	-2,267	**11,195**

Source: Author's Estimates

Notes: Diagonal elements are equal to the present value of on-farm profits, the external social benefit, or the total benefit derived from carbon sequestration stemming from a four-year crop rotation applied from 2023 to 2055. The total benefits are equal to the sum of the present value of on-farm profits and the external social benefit for each crop rotation. The present value of on-farm profits and the external social benefit are measured in 2023 CAD per hectare per year (refer to equations (2.17) and (2.18)). Non-diagonal elements denote the difference in these benefits from carbon sequestration across different crop rotations (refer to equations (2.19) and (2.20)). On-farm profits are computed based on the expected profits outlined in the 2023 Saskatchewan Crop Planning Guide by crop for a four-year crop rotation using the 2023 prices and costs from the same guide (Government of Saskatchewan, 2023a), combined with simulated crop yields derived from the dynamic simulation.

So far, the influence of SOC on crop yield and profitability has been represented as a consequence of cropping choice and crop rotations. However, given that weather significantly affects crop yields, past weather conditions also dynamically affect SOC, crop yields, and ultimately, on-farm profitability. Figure 2.9 uses the dynamic simulation to show the effects of weather patterns on SOC across different crop rotations, soil zones, and over time (2023–2055) for each of the different crop rotations. In Figure 2.9, I apply equation (2.11) to adjust the expected yields for 2023 from the Saskatchewan Crop Planning Guide to reflect various weather scenarios. Specifically, prolonged drought is modeled as occurring when total annual precipitation (TAP) falls two standard deviations below its average for the entire period 2023–2055, while a prolonged heatwave is represented by growing season average temperature (GSAT) exceeding its average by two standard deviations for the entire period, 2023–2055.

Figure 2.9 shows that weather extremes, specifically prolonged heatwaves or droughts, would have a pronounced affect on lowering SOC stocks relative to the base case from 2023 to 2055, with drought conditions leading to an even larger reduction in SOC than a heatwave. This decline, relative to the base case, is exacerbated if drought coincides with a heatwave, which would result in even lower SOC stocks than those depicted in the worst-case scenarios of Figure 2.9. Adverse weather events can reduce the extent of carbon sequestration and the resulting long-term the benefits. On the other hand, taking a more optimistic view, crop rotations designed to enhance SOC sequestration can mitigate some of the negative effects of volatile weather, maintaining higher SOC stocks and, by extension, yielding greater on-farm benefits from improved SOC management.

181

FIGURE 2.9: Simulated Dynamic Effects of Carbon Sequestration by Weather Scenario
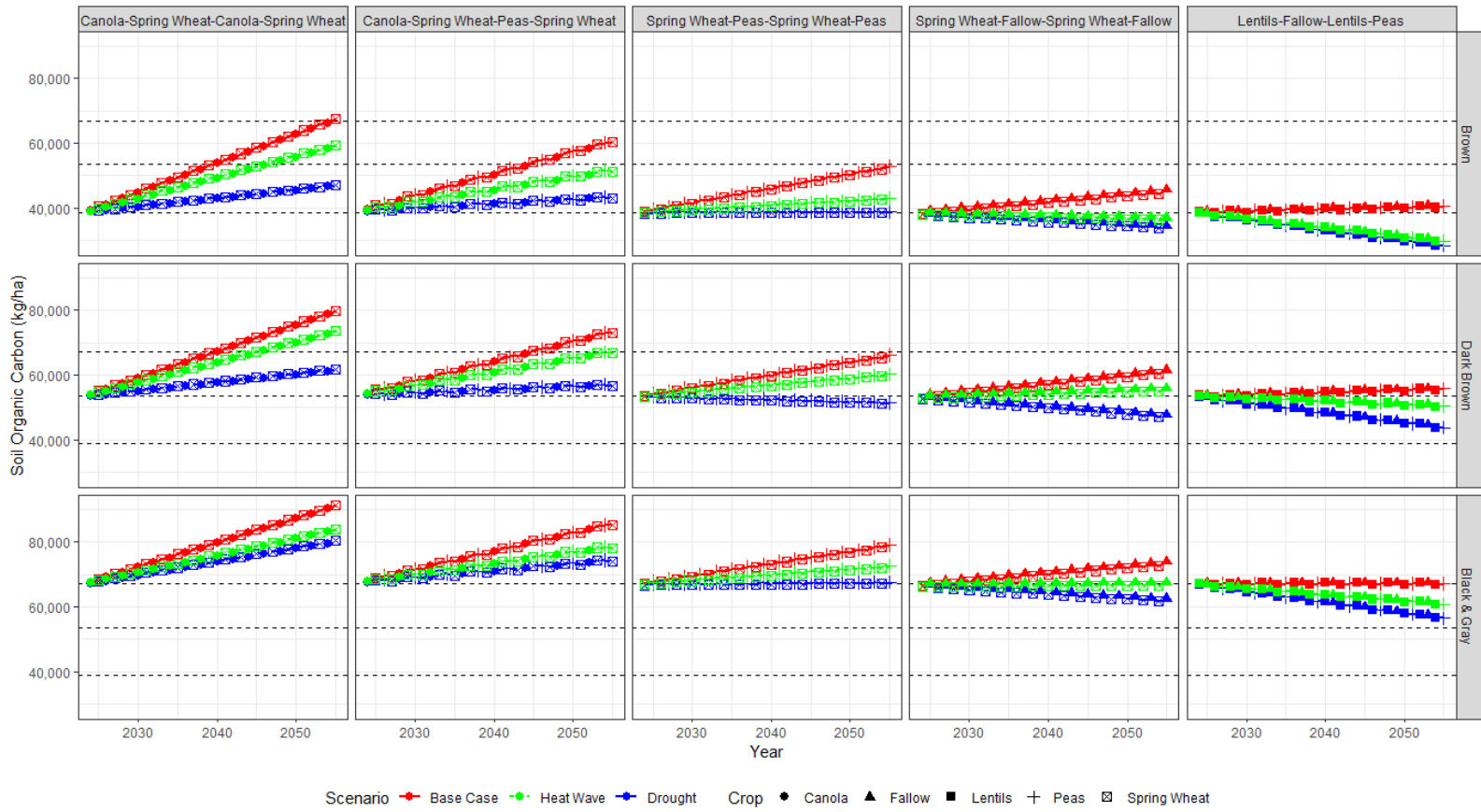
Source: Author's Estimates.

Notes: Please refer to the notes from Figure 2.7. The drought scenario corresponds to two standard deviations below the mean TAP, and the heat wave scenario corresponds to two standard deviations above GSAT.

To compute the structural effects of weather through SOC and other related factors on farm profits, I make use of the coefficients derived from equations (2.11) and (2.13). These coefficients enable the calculation of how weather conditions structurally influence farm profitability. Specifically, the dynamic or marginal effect of weather on current farm profits is calculated as,

$$\frac{\partial \Pi_{n,c,t}}{\partial Z_{n,t-1}} = \underbrace{\frac{\partial \Pi_{n,c,t}}{\partial y_{n,c,t}} \frac{\partial y_{n,c,t}}{\partial \Delta SOC_{n,t}} \frac{\partial \Delta SOC_{n,t}}{\partial Z_{n,t-1}} + \frac{\partial \Pi_{n,c,t}}{\partial y_{n,c,t}} \frac{\partial y_{n,c,t}}{\partial \Delta SOC_{n,t}} \frac{\partial \Delta SOC_{n,t}}{\partial y_{n,c,t-1}} \frac{\partial y_{n,c,t-1}}{\partial Z_{n,t-1}}}_{SOC\ Effect} + \underbrace{\frac{\partial \Pi_{n,c,t}}{\partial y_{n,c,t}} \frac{\partial y_{n,c,t}}{\partial Z_{n,t-1}}}_{Residual\ Effect}$$

(2.21)

$$\Downarrow$$

$$\frac{\partial \Pi_{n,c,t}}{\partial Z_{n,t-1}} = p_{c,t}\left[\lambda_c\left(\delta^{Z_{n,t-1}} + \beta_c\left(\xi_{l(c)}^{Z_{n,t-1}} + 2\left(Z_{n,t-1}\xi_{l(c)}^{Z_{n,t}^2} + (Z_{n,t-1} - \bar{Z}_{n,t-1})\xi_{l(c)}^{(Z_{n,t-1}-\bar{Z}_{n,t-1})^2}\right)\right)\right) + \xi_c^{Z_{n,t-1}}\right].$$

Where c is the current year's crop type, $l(c)$ is the previous year's crop type, and superscripts for coefficients on weather variables correspond to the functional form of the weather variable. The variance of the marginal effect is computed using the delta method, and is computed in three steps.

Step 1:

$$Var(A_1) = Var\left(\xi_{l(c)}^{Z_{n,t-1}} + 2\left(Z_{n,t-1}\xi_{l(c)}^{Z_{n,t}^2} + (Z_{n,t-1} - \bar{Z}_{n,t-1})\xi_{l(c)}^{(Z_{n,t-1}-\bar{Z}_{n,t-1})^2}\right)\right) =$$

$$Var\left(\xi_{l(c)}^{Z_{n,t-1}}\right) + 4\left(Z_{n,t-1}^2 Var\left(\xi_{l(c)}^{Z_{n,t}^2}\right) + (Z_{n,t-1} - \bar{Z}_{n,t-1})^2 Var\left(\xi_{l(c)}^{(Z_{n,t-1}-\bar{Z}_{n,t-1})^2}\right)\right)$$

$$+ 4\left(Z_{n,t-1}Cov\left(\xi_{l(c)}^{Z_{n,t-1}}, \xi_{l(c)}^{Z_{n,t}^2}\right) + (Z_{n,t-1} - \bar{Z}_{n,t-1})Cov\left(\xi_{l(c)}^{Z_{n,t-1}}, \xi_{l(c)}^{(Z_{n,t-1}-\bar{Z}_{n,t-1})^2}\right)\right.$$

$$\left. + 2Z_{n,t-1}(Z_{n,t-1} - \bar{Z}_{n,t-1})Cov\left(\xi_{l(c)}^{Z_{n,t}^2}, \xi_{l(c)}^{(Z_{n,t-1}-\bar{Z}_{n,t-1})^2}\right)\right)$$

(2.22)

Step 2:

$$Var(A_2) = Var\left(\delta^{Z_{n,t-1}} + \beta_c A_1\right) =$$

$$Var\left(\delta^{Z_{n,t-1}}\right) + A_1^2 Var(\beta_c) + \beta_c^2 Var(A_1) + 2A_1 Cov\left(\delta^{Z_{n,t-1}}, \beta_c\right)$$

(2.23)

Step 3:

$$Var\left(\frac{\partial \Pi_{n,c,t}}{\partial Z_{n,t-1}}\right) = Var\left(p_c(\lambda_c A_2 + \xi_c^{Z_{n,t-1}})\right) =$$

$$p_c^2\left(A_2^2 Var(\lambda_c) + \lambda_c^2 Var(A_2) + Var\left(\xi_c^{Z_{n,t-1}}\right) + 2A_2 Cov\left(\lambda_c, \xi_c^{Z_{n,t-1}}\right)\right)$$

(2.24)

Table 2.7 presents the estimates of the marginal effects of last year's weather on the profitability of spring wheat following canola. These total marginal effects can be broken down into two effects based on equation (2.21): the effect through changes in SOC and the residual effect which represents various factors influenced by last year's weather.[31] The marginal effect identifies the structural weather effects on SOC by evaluating them at the average climate condition and at two standard deviations above and below the mean for both GSAT and TAP. I only evaluate the structural effects of last year's weather on SOC for two standard deviations above and below the mean for both GSAT and TAP, rather than additionally providing the same analysis for the residual effect. The nonlinear effects of last year's weather (lag of squared weather variables and their squared deviations from climate) on crop yield are statistically significant, but including these variables does not alter the effect of SOC on crop yield (marginal product of SOC). The effect of weather on profit via its consequences for SOC, while notable, is substantially less than the residual effects. The gain in spring wheat profit of increasing SOC by a Mg per hectare (as shown in Table 2.3) vastly outweighs the implications of a one-degree Celsius increase in GSAT or a one-millimeter increase in TAP (as shown in Table 2.7). This highlights that SOC is not very responsive to year-to-year weather variations, with only minor effects on the profitability of spring wheat following canola.

Because canola stores the most SOC compared to other crops, the influence of weather on both SOC and profitability of spring wheat is the greatest when spring wheat follows canola, rather than other crops. The largest marginal effect is observed when weather conditions are at $\mu_{GSAT} - 2\sigma_{GSAT}$, which pertains to a one-degree Celsius increase in GSAT, a substantial deviation considering that one standard deviation in Saskatchewan is approximately 0.86 degrees Celsius. The smallest marginal effect for GSAT occurs when weather conditions are at $\mu_{GSAT} - 2\sigma_{GSAT}$, representing a heatwave. These results show that when Saskatchewan experiences above average temperatures, crop yield increases when holding precipitation constant. In certain instances, the

---

[31]The residual effect from weather in the previous year affects crop yield through factors such as disease prevalence, soil moisture, nutrient availability (nutrient immobilization), soil compaction, and other weather related factors affecting yield.

added carbon inputs from higher crop yield outweigh the negative effects of GSAT on the decomposition of SOC. This implies that colder weather in Saskatchewan results in lower crop yields, less carbon inputs, and slower decomposition of SOC stocks. When temperature increases, SOC stocks decrease as a result of faster decomposition, but crop yields increase and result in more carbon inputs being added to the soil. The effects of TAP on profit are straightforward, such that the marginal effect is larger when weather conditions are at $\mu_{GSAT} - 2\sigma_{GSAT}$, when additional precipitation is needed for plant growth, and lower at $\mu_{GSAT} + 2\sigma_{GSAT}$ when additional precipitation becomes harmful to plant growth.

TABLE 2.7: Marginal Effect of Previous Year's Weather on Spring Wheat Profit, 2023 CAD/ha

	(1)	(2)	(3)
Soil Zone:	Brown	Dark Brown	Black & Gray
	SOC Effect		
$\mu_{GSAT} + 2\sigma_{GSAT}$	0.67	0.51***	−0.28**
	(1.26)	(0.13)	(0.12)
μ_{GSAT}	−2.09***	−0.68***	−0.27***
	(0.79)	(0.08)	(0.07)
$\mu_{GSAT} - 2\sigma_{GSAT}$	−4.84***	−5.47***	−6.19***
	(1.86)	(0.18)	(0.03)
$\mu_{TAP} + 2\sigma_{TAP}$	0.003	−0.009***	−0.007**
	(0.007)	(0.001)	(0.004)
μ_{TAP}	0.025***	0.007***	0.002
	(0.008)	(0.001)	(0.003)
$\mu_{TAP} - 2\sigma_{TAP}$	0.048***	0.047***	0.043***
	(0.018)	(0.002)	(0.001)
	Residual Effect		
μ_{GSAT}	−3.64	−34.33***	−68.34***
	(21.15)	(10.9)	(9.37)
μ_{TAP}	0.491***	0.276***	0.082***
	(0.107)	(0.048)	(0.032)
	Total Effect		
μ_{GSAT}	−5.72	−35.01***	−68.61***
	(21.17)	(10.9)	(9.37)
μ_{TAP}	0.516***	0.283***	0.084***
	(0.085)	(0.048)	(0.032)

Source: Author's Estimates
Notes: All marginal effects represent the effect of either a one degree Celsius increase in GSAT or a one millimeter increase in TAP on spring wheat profit after canola in the previous year. GSAT is growing season average temperature and TAP is total annual precipitation.

Regarding the residual effects, among zones a one-degree Celsius increase in GSAT has its largest effect on spring wheat profit in the black & gray soil zone, a reduction of 68.34 CAD per hectare. Among the zones, a one-millimeter increase in TAP has its largest effect on spring wheat profit in the brown soil zone, an increase of 0.49 CAD per hectare.

While the immediate effects of weather on SOC may seem negligible, persistent shifts in weather patterns could result in significantly divergent cumulative changes in SOC stocks. For most crop rotations, weather has a more pronounced affect on SOC stocks in the brown soil zone than in the darker brown and black & gray soil zones (see Figure 2.9). This suggests that sequestering SOC in the brown soil zone is more difficult as a result of its prevalence to drought conditions, relative to the dark brown and black & gray soil zones.

2.7   Conclusions

This essay introduces a conceptual framework and a quantitative model for assessing the the on-farm and external benefits from production choices that augment the SOC stock on farms throughout Saskatchewan. Using this model, I estimate the private marginal shadow value of SOC to farmers, differentiated by the type of crop and soil zone. The results from this research can be used to help farmers and agronomists to understand the enduring on-farm effects of enhanced SOC storage, resulting from modifications in production methods, and help government in the design and implementation of effective carbon sequestration policies and carbon markets.

The findings of this essay indicate that the shadow value of SOC is positive and subject to diminishing marginal returns, being notably higher in regions with relatively lower SOC stocks, such as the brown soil zone. Even though the on-farm benefits from marginal changes in the SOC stock in the dark brown and black & gray soil zone are much lower relative to the brown soil zone, they remain to be positive. The shadow value of SOC also varies across crops. In Saskatchewan, spring wheat and durum wheat have the highest average shadow value of SOC across soil zones, followed by peas and lentils, and then canola and barley. Given that noticeable changes in SOC

186

stocks take years to achieve, the associated crop yield improvements resulting from carbon sequestration might not be immediately evident to farmers. However, a dynamic simulation over 32 years with five unique crop rotations reveals that, under average weather conditions, the yield increase from carbon sequestration can lead to substantial on-farm benefits. It is projected that farmers can enhance profits by 28% in the brown soil zone, 12% in the dark brown soil zone, and 6% in the black & gray soil zone over this period as a benefit from additional SOC sequestered by specific crop rotations.[32] Moreover, these rotations offer environmental benefits that exceed the private on-farm gains from carbon sequestration, suggesting that choosing crop rotations with high SOC sequestration potential over those with lower carbon inputs could be worth 108 billion CAD.[33].

Going forward, a better understanding of the incentives and opportunities for farmers to enhance soil carbon storage is essential for developing effective carbon markets and policies aimed at boosting SOC stocks. The motivation for farmers to store more carbon will vary across different regions. It is possible that farmers in regions with a high shadow value for SOC are already adopting practices that increase SOC stocks, though the slow changes in SOC make it challenging to detect and measure the broader social benefits of these practices. On the other hand, some farmers may not fully appreciate the on-farm advantages of carbon sequestration, leading to too little adoption of SOC-enhancing practices. Educating these farmers about the private on-farm benefits of carbon sequestration could be an efficient policy approach to encourage more SOC-enhancing farming practices.

---

[32]These crop rotations include Canola-Spring Wheat-Peas-Spring Wheat in the brown soil zone and Canola-Spring Wheat-Canola-Spring Wheat in the dark brown and black & gray soil zones.

[33]In this scenario, the external social benefit applies to all insured hectares in Saskatchewan assuming that farmers rotate Canola-Spring Wheat-Peas-Spring Wheat compared with Spring Wheat-Fallow-Spring Wheat-Fallow from 2023 to 2055 using a SCC of 185 USD/Mg of CO_2.

Appendix 2A: Derivation of Dynamic Profit Maximization Problem for Farm Profit

In this appendix, I provide the derivation of the dynamic profit maximization problem for farmers with respect to their input choice and land allocation. Let the following Bellman Equation (BE) for maximizing farm-level profits be equal to,

$$
V^{farm}(\mathbf{x_t}, \mathbf{l_t}) = \max_{\mathbf{x_t}, \mathbf{l_t}} \Pi^{farm}(\mathbf{p_t}, \mathbf{w_t}, \mathbf{q_t}(\mathbf{x_t}, \mathbf{l_t}), \mathbf{x_t}) + \beta V(\mathbf{x_{t+1}}, \mathbf{l_{t+1}})
$$

$$
\text{s.t. } \sum_{c=1}^{C} l_{c,t} \leq L_t \quad \text{and} \quad \{\mathbf{x_{t+1}}, \mathbf{l_{t+1}}\} = f(\mathbf{x_t}, \mathbf{l_t}).
$$

(2A.1)

Where $\mathbf{x_t}$ is a matrix of the use of input $j \in J$, for crop $c \in C$, in year t, and $\mathbf{l_t}$ is a vector of the land allocated to crop c on a farm, L_t is the farmer's total land, $\mathbf{p_t}$ is the price of crop c in year t, and $\mathbf{w_t}$ is the cost of input j in year t. $V(\cdot)$ represents the value function that describes the best possible value with respect to input use and land allocation on a farm starting in year t. The profit function $\Pi^{farm}(\cdot)$ depends on input and output prices, the production function $\mathbf{q_t}(\cdot)$, input use, and land allocation. The land constraint in equation (2.1) ensures the farmer does not allocate more land to crops than she owns each year. The state equation $\{\mathbf{x_{t+1}}, \mathbf{l_{t+1}}\} = f(\mathbf{x_t}, \mathbf{l_t})$ defines how producers choose next year's inputs and land allocation based on previous year's inputs and land allocation (e.g., crop rotations and fertilizer use).

I recursively solve for the next period's value function in equation (2A.1), such that the BE for the following periods are:

$$V^{farm}(\mathbf{x_{t+1}}, \mathbf{l_{t+1}}) = \max_{\mathbf{x_{t+1}}, \mathbf{l_{t+1}}} \Pi^{farm}(\mathbf{p_{t+1}}, \mathbf{w_{t+1}}, \mathbf{q_{t+1}}(\mathbf{x_{t+1}}, \mathbf{l_{t+1}}), \mathbf{x_{t+1}}) + \beta V(\mathbf{x_{t+2}}, \mathbf{l_{t+2}})$$

$$\text{s.t.} \quad \sum_{c=1}^{C} l_{c,t+1} \leq L_{t+1} \quad \text{and} \quad \{\mathbf{x_{t+2}}, \mathbf{l_{t+2}}\} = f(\mathbf{x_{t+1}}, \mathbf{l_{t+1}})$$

$$\vdots \tag{2A.2}$$

$$V^{farm}(\mathbf{x_{\infty-1}}, \mathbf{l_{\infty-1}}) = \max_{\mathbf{x_{\infty-1}}, \mathbf{l_{\infty-1}}} \Pi^{farm}(\mathbf{p_{\infty-1}}, \mathbf{w_{\infty-1}}, \mathbf{q_{\infty-1}}(\mathbf{x_{\infty-1}}, \mathbf{l_{\infty-1}}), \mathbf{x_{\infty-1}}) + \beta V(\mathbf{x_{\infty}}, \mathbf{l_{\infty}})$$

$$\text{s.t.} \quad \sum_{c=1}^{C} l_{c,\infty-1} \leq L_{\infty-1} \quad \text{and} \quad \{\mathbf{x_{\infty}}, \mathbf{l_{\infty}}\} = f(\mathbf{x_{\infty-1}}, \mathbf{l_{\infty-1}}).$$

Recursively plugging in equation (2A.2) into (2A.1) leads to,

$$PV^{farm} = \max_{\mathbf{x_t}, \mathbf{l_t}} \{ \Pi_t^{farm}(\mathbf{p_t}, \mathbf{w_t}, \mathbf{q_t}(\mathbf{x_t}, \mathbf{l_t}), \mathbf{x_t}) +$$

$$\max_{\{\mathbf{x_{t+1}}, \mathbf{l_{t+1}}\}} \{ \beta^{t+1} \Pi_{t+1}^{farm}(\mathbf{p_{t+1}}, \mathbf{w_{t+1}}, \mathbf{q_{t+1}}(\mathbf{x_{t+1}}, \mathbf{l_{t+1}}), \mathbf{x_{t+1}}) +$$

$$\cdots + \max_{\{\mathbf{x_{\infty}}, \mathbf{l_{\infty}}\}} \{ \beta^{\infty} \Pi_{\infty}^{farm}(\mathbf{p_{\infty}}, \mathbf{w_{\infty}}, \mathbf{q_{\infty}}(\mathbf{x_{\infty}}, \mathbf{l_{\infty}}), \mathbf{x_{\infty}}) \} \cdots \} \} \tag{2A.3}$$

$$\text{s.t.} \quad \sum_{c=1}^{C} l_{c,t} \leq L_t \quad \text{and} \quad \{\mathbf{x_{t+1}}, \mathbf{l_{t+1}}\} = f(\mathbf{x_t}, \mathbf{l_t}),$$

According to Stockey and Lucas (1989), equation (2A.3) may be characterized as a "sequence problem," which generalizes the BE to an infinite horizon dynamic optimization problem. The sequence problem is denoted as,

$$PV^{farm}(\mathbf{x_t}, \mathbf{l_t}) = \max_{\{\mathbf{x_t}, \mathbf{l_t}\}_{t=0}^{\infty}} \sum_{t=0}^{\infty} \beta^t \Pi^{farm}(\mathbf{p_t}, \mathbf{w_t}, \mathbf{q_t}(\mathbf{x_t}, \mathbf{l_t}), \mathbf{x_t})$$

$$\text{s.t.} \quad \sum_{c=1}^{C} l_{c,t} \leq L_t \quad \text{and} \quad \{\mathbf{x_{t+1}}, \mathbf{l_{t+1}}\} = f(\mathbf{x_t}, \mathbf{l_t}). \tag{2A.4}$$

Incorporating time period zero to equation (2A.4) as done by Bellman (1957) characterizes Bellman's optimality principle,

$$PV^{farm} = \max_{\mathbf{x_0}, \mathbf{l_0}} \left\{ \Pi_0^{farm}(\mathbf{p_0}, \mathbf{w_0}, \mathbf{q_0}(\mathbf{x_0}, \mathbf{l_0}), \mathbf{x_0}) + \right.$$

$$\beta \left[\max_{\{\mathbf{x_t}, \mathbf{l_t}\}_{t=1}^{\infty}} \sum_{t=1}^{\infty} \beta^{t-1} \Pi_t^{farm}(\mathbf{p_t}, \mathbf{w_t}, \mathbf{q_t}(\mathbf{x_t}, \mathbf{l_t}), \mathbf{x_t}) \right] \right\} \tag{2A.5}$$

$$\text{s.t.} \quad \sum_{c=1}^{C} l_{c,t} \leq L_t \quad \text{and} \quad \{\mathbf{x_{t+1}}, \mathbf{l_{t+1}}\} = f(\mathbf{x_t}, \mathbf{l_t}).$$

In equation (2A.5), farmers separate today's input and land allocation decisions from their future decisions. Hence, production decisions are broken into several stages or subproblems, such that decisions made in the current time period lead to optimal future decisions (principle of optimality). If a farmer fully understands all the dynamic linkages over time, they will optimally select inputs and land allocation to maximize the present value of profits taking into consideration all future time periods.

Appendix 2B: Stylized Dynamic Panel Regression with Fixed Effects

In this appendix, I derive the Nickell bias within a stylized dynamic panel regression framework featuring fixed effects, focusing on a specific scenario where the independent variable is soil organic carbon (SOC) derived from lagged crop yields, weather, and cropping choice. Through simulations, I calculate a sample analog of the Nickell bias and contrast it with the actual bias, which is predetermined in the data generating process (DGP). I explore various scenarios, including the incorporation of field and farm fixed effects, as well as the inclusion and exclusion of year fixed effects. Additionally, I investigate the Nickell bias when the SOC stock is simulated with prediction errors.

I find that including field and year fixed effects in simulations leads to overfitting of the data, particularly when the trajectories of SOC stocks closely align with a time trend, thereby exacerbating the Nickell bias. Moreover, the presence of prediction errors further exacerbates this bias. In scenarios where Nickell bias or both Nickell and prediction error biases are present, the estimated shadow value of SOC becomes highly contingent on whether year fixed effects are included or excluded. Hence, a substantial alteration in the estimated coefficient upon the exclusion of year fixed effects signals potential overfitting and biased outcomes when employing field and year fixed effects. Conversely, employing farm fixed effects consistently yields estimations of the shadow value of SOC that remain robust across the inclusion or exclusion of year fixed effects.

Stylized Dynamic Panel Regression Model

Let the stylized dynamic panel regression model for crop yield on SOC stocks be:

$$Y_{n,t} = \Gamma SOC_{n,t} + \alpha_n + u_{n,t}$$

such that:

$$SOC_{n,t} = f\left(\sum_{l=1}^{t-1} Y_{n,t-l}, \sum_{l=1}^{t-1} CT_{n,t-l}, \sum_{l=1}^{t-1} W_{n,t-l}\right).$$

(2B.1)

Where $Y_{n,t}$ is the crop yield on field n in year t, $SOC_{n,t}$ is the soil organic carbon, α_n are field fixed effects, $u_{n,t}$ are idiosyncratic errors, $Y_{n,t-l}$ is the crop yield lagged by l years, $CT_{n,t-l}$ is lagged crop

choice, and $W_{n,t-l}$ is lagged weather.

The demeaned model of equation (2B.1) is equal to,

$$Y_{n,t} - \bar{Y}_n = \Gamma\left(SOC_{n,t} - S\bar{O}C_n\right) + u_{n,t} - \bar{u}_n,$$

such that for any given variable:

(2B.2)

$$\bar{\omega}_n = \frac{1}{T}\sum_{t=1}^{T}\omega_{n,t}.$$

Following the approach of Nickell (1981), the bias of the fixed effects estimator from equation (2B.2) equals

$$\hat{\Gamma}^{FE} - \Gamma = \frac{\sum_{n=1}^{N}\sum_{t=1}^{T}\left(u_{n,t} - \bar{u}_n\right)\left(SOC_{n,t} - S\bar{O}C_n\right)}{\sum_{n=1}^{N}\sum_{t=1}^{T}\left(SOC_{n,t} - S\bar{O}C_n\right)^2}.$$

(2B.3)

Nickell (1981) shows that the probability limit of equation (2B.3) as,

$$\hat{\Gamma}^{FE} - \Gamma \xrightarrow{p} \frac{E\left[\sum_{t=1}^{T}\left(u_{n,t} - \bar{u}_n\right)\left(SOC_{n,t} - S\bar{O}C_n\right)\right]}{E\left[\sum_{t=1}^{T}\left(SOC_{n,t} - S\bar{O}C_n\right)^2\right]}.$$

(2B.4)

Sequential exogeneity implies, [34]

$$E\left[u_{n,t} - \bar{u}_n | SOC_{n,t}, \alpha_n\right] = -\frac{1}{T}\sum_{s=1}^{t-1}u_{n,s}.$$

(2B.5)

Assuming sequential exogeneity, equation (2B.4) reduces to

$$\hat{\Gamma}^{FE} - \Gamma \xrightarrow{p} -\frac{1}{T}\frac{E\left[\sum_{t=1}^{T}SOC_{n,t}\sum_{s=1}^{t-1}u_{n,s}\right]}{E\left[\sum_{t=1}^{T}\left(SOC_{n,t} - S\bar{O}C_n\right)^2\right]}.$$

(2B.6)

To estimate the Nickell bias accurately, it is more suitable to use the sample analog of equation (2B.6) instead of equation (2B.4). This choice is justified by the fact that previous SOC stocks are

---

[34]More specifically, Juodis and Sarafidis (2022) explain weak (sequential) exogeneity as: $E\left[u_{n,s}|x_{n,t}\right] = 0; \ s \geq t$.

orthogonal to the future errors incorporated within $\bar{u}_n$, whereas they are not orthogonal to past errors.

The sample analog formula depicting the Nickell bias is equal to

$$\widehat{Bias} \;=\; \left| -\frac{1}{T} \frac{\sum_{n=1}^{N}\left(\sum_{t=1}^{T} SOC_{n,t}\sum_{s=1}^{t-1}\varepsilon_{n,s}\right)}{\sum_{n=1}^{N}\sum_{t=1}^{T}\left(SOC_{n,t}-S\bar{O}C_n\right)^2} \right|. \tag{2B.7}$$

Equation (2B.7) requires computation with a strongly balanced panel of data. The absolute value is required since the sign frequently does not match the true bias observed in simulations. Nevertheless, the directional change in the magnitude of the analog presented in equation (2B.7) consistently exhibits a positive correlation with variations in the actual bias.

If SOC stocks perfectly follow a trend over time, the Nickell bias from equation (2B.3) is equal to:

$$\hat{\Gamma}^{FE} - \Gamma = \frac{\sum_{n=1}^{N}\sum_{t=1}^{T}\left(u_{n,t}-\bar{u}_n\right)\left(\delta_n\left(\frac{T^2-1}{2}\right)\right)}{\sum_{n=1}^{N}\sum_{t=1}^{T}\left(\delta_n\left(\frac{T^2-1}{2}\right)\right)^2}$$

$$\tag{2B.8}$$

where:

$$\overline{SOC}_n = SOC_{n,0} + \frac{1}{T}\sum_{t=1}^{T} t\delta_{n,t} \;\text{ and }\; SOC_{n,t} = SOC_{n,0} + \sum_{t=1}^{T} t\delta_{n,t}.$$

Equation (2B.8) shows how the bias depends on the relationships between the trend in SOC stocks across fields and the error term. If all covariates influencing the constant annual change in SOC stocks, denoted as δ_n, are accounted for, the errors become orthogonal to the time trend, thus perfectly identifying the true effect of SOC on crop yield. However, in simulations of SOC stocks, the time-paths often follow a linear trajectory with some degree of variability. Introducing time-fixed effects or a time trend leaves only residual variation unrelated to the time trend to discern the effect of SOC stocks on crop yields. This residual variation becomes correlated with the lagged unobserved errors, consequently leading to Nickell bias.

When the regression incorporates multiple covariates, the fixed effects estimator partials out effects that correlate with these variables. Thus, the residual maker matrix, denoted as $\mathbf{M}_X = \mathbf{I} - \mathbf{X}\left(\mathbf{X}'\mathbf{X}\right)^{-1}\mathbf{X}'$, where $\mathbf{X}$ may include time dummies or a time trend, removes the influence of the time trend in SOC stocks on crop yield. This action exacerbates the Nickell Bias, especially when SOC stocks show a strong linear relationship with time. Given that SOC is derived from historical crop yields, it inherently exhibits trends and dynamic relationships, tying it to past errors such as unobserved farm management practices.

In matrix form, the bias in equation (2B.7) when including other covariates such as a time trend or time dummies is,

$$\widehat{Bias} = \left| -\frac{1}{T}\left(\left(\mathbf{SOC} - \overline{SOC}\right)^{*\prime}\left(\mathbf{SOC} - \overline{SOC}\right)^{*} \right)^{-1} SOC^{*\prime}\ddot{\varepsilon} \right|$$

where:

$$\left(SOC - \overline{SOC}\right)^{*} = M_X\left(SOC - \overline{SOC}\right) \tag{2B.9}$$

and

$$\ddot{\varepsilon}' = \begin{bmatrix} 0 & \varepsilon_{1,1} & \sum_{s=1}^{2}\varepsilon_{1,s} & \cdots & \sum_{s=1}^{T-1}\varepsilon_{1,s} & \cdots & 0 & \varepsilon_{N,1} & \sum_{s=1}^{2}\varepsilon_{N,s} & \cdots & \sum_{s=1}^{T-1}\varepsilon_{N,s} \end{bmatrix}.$$

All matrices in equation (2B.9) are $\mathbb{R}^{NT \times 1}$, excluding $\mathbf{X}$ where the column size is equal to the number of independent variables included in the model ($\mathbb{R}^{NT \times T}$ if including time dummies). If the SOC stocks follow a perfect linear trajectory over time, including a time trend in equation (2B.9) removes the biases. However, should there be any deviation from this linear path that correlates with past errors, Nickell bias will appear.

If there is omitted variable bias stemming from the exclusion of a time trend, time-dummies, or year fixed effects, then equation (2B.7) becomes:

$$\hat{\Gamma}^{\text{FE}^*} - \Gamma = \frac{\sum_{n=1}^{N}\sum_{t=1}^{T}\left(u_{n,t} - \bar{u}_n\right)\left(SOC_{n,t} - S\bar{O}C_n\right)}{\sum_{n=1}^{N}\sum_{t=1}^{T}\left(SOC_{n,t} - S\bar{O}C_n\right)^2} + \Gamma_T \underbrace{\frac{\sum_{n=1}^{N}\sum_{t=1}^{T}\left(t - \bar{t}\right)\left(SOC_{n,t} - S\bar{O}C_n\right)}{\sum_{n=1}^{N}\sum_{t=1}^{T}\left(SOC_{n,t} - S\bar{O}C_n\right)^2}}_{=\beta_T}$$

(2B.10)

In equation (2B.10), Γ_T is the effect of the time trend on crop yield and β_T is the effect of the time trend on SOC stocks. I assume that these coefficients represent the effects of omitted variables not directly observed but inferred through the time trend. Should the effects of time on both yield and SOC be positive, this leads to an upward biased in the estimated shadow value of SOC.

Prediction Error Bias

When prediction errors are present in the simulated SOC stocks, there is additional bias, which can accentuate other omitted variable biases, in addition to the Nickell bias.

Let the stylized dynamic panel regression model with prediction error be equal to,

$$\widetilde{Y}_{n,t} = \Gamma\widetilde{SOC}^{o}_{n,t} + \widetilde{u}_{n,t} - \Gamma\widetilde{\xi}_{n,t}$$

where:

$$\widetilde{SOC}_{n,t} = \widetilde{SOC}^{o}_{n,t} + \widetilde{\xi}_{n,t}$$

(2B.11)

such that for any variable:

$$\widetilde{\omega}_{n,t} = \omega_{n,t} - \bar{\omega}_n.$$

In equation (2B.11), $\widetilde{SOC}^{o}_{n,t}$ is the simulated SOC stocks and $\widetilde{\xi}_{n,t}$ is the prediction error. The attenuation bias with Nickell bias from the prediction error may be described as,

$$\hat{\Gamma}^{\text{FE}^{**}} = \Gamma\frac{SS_{\widetilde{SOC}\widetilde{SOC}} + SS_{\widetilde{SOC}\widetilde{\xi}}}{SS_{\widetilde{SOC}\widetilde{SOC}} + 2SS_{\widetilde{SOC}\widetilde{\xi}} + SS_{\widetilde{\xi}\widetilde{\xi}}} + \frac{SS_{\widetilde{SOC}\widetilde{u}} + SS_{\widetilde{\xi}\widetilde{u}}}{SS_{\widetilde{SOC}\widetilde{SOC}} + 2SS_{\widetilde{SOC}\widetilde{\xi}} + SS_{\widetilde{\xi}\widetilde{\xi}}}$$

such that for any given variable:

(2B.12)

$$SS_{\widetilde{\omega}\widetilde{\varphi}} = \sum_{n=1}^{N}\sum_{t=1}^{T}\left(\omega_{n,t} - \bar{\omega}_n\right)\left(\varphi_{n,t} - \bar{\varphi}_n\right).$$

Taking the expectation and applying the central mapping theorem gives,

$$\hat{\Gamma}^{\text{FE}^{**}} \xrightarrow{p} \Gamma \frac{\sigma_{\widetilde{SOC}\widetilde{SOC}} + \sigma_{\widetilde{SOC}\widetilde{\xi}}}{\sigma_{\widetilde{SOC}\widetilde{SOC}} + 2\sigma_{\widetilde{SOC}\widetilde{\xi}} + \sigma_{\widetilde{\xi}\widetilde{\xi}}} + \frac{\sigma_{\widetilde{SOC}\widetilde{u}} + \sigma_{\widetilde{\xi}\widetilde{u}}}{\sigma_{\widetilde{SOC}\widetilde{SOC}} + 2\sigma_{\widetilde{SOC}\widetilde{\xi}} + SS_{\widetilde{\xi}\widetilde{\xi}}}$$

such that for any given variable:

(2B.13)

$$\sigma_{\widetilde{\omega}\widetilde{\varphi}} = E(\omega_{n,t} - E(\omega_n))E(\varphi_{n,t} - E(\varphi_n)).$$

Under the assumption of sequential exogeneity, if there is a correlation between the lagged errors and the prediction errors (as noted in the second term of equation (2B.13)), this correlation exacerbates the Nickell bias. Additionally, an increase in the variability of the prediction error and its covariance with SOC stocks (highlighted in the first term of equation (2B.13)) leads to greater attenuation bias.

For the case where omitted variables are represented by the time trend are included in under-lying DGP and when time-dummies or year fixed effects are not included in the regression model, the bias becomes:

$$\hat{\Gamma}^{\text{FE}^{***}} \xrightarrow{p} \underbrace{\frac{\Gamma\left(\sigma_{\widetilde{SOC}\widetilde{SOC}} + \sigma_{\widetilde{SOC}\widetilde{\xi}}\right)}{\sigma_{\widetilde{SOC}\widetilde{SOC}} + 2\sigma_{\widetilde{SOC}\widetilde{\xi}} + \sigma_{\widetilde{\xi}\widetilde{\xi}}}}_{\text{Prediction Error Bias}} + \underbrace{\frac{\Gamma_T\left(\sigma_{\widetilde{SOC}\widetilde{t}} + \sigma_{\widetilde{\xi}\widetilde{t}}\right)}{\sigma_{\widetilde{SOC}\widetilde{SOC}} + 2\sigma_{\widetilde{SOC}\widetilde{\xi}} + \sigma_{\widetilde{\xi}\widetilde{\xi}}}}_{\text{O.V.B. + Prediction Error Bias}} + \underbrace{\frac{\sigma_{\widetilde{SOC}\widetilde{u}} + \sigma_{\widetilde{\xi}\widetilde{u}}}{\sigma_{\widetilde{SOC}\widetilde{SOC}} + 2\sigma_{\widetilde{SOC}\widetilde{\xi}} + \sigma_{\widetilde{\xi}\widetilde{\xi}}}}_{\text{Nickell + Prediction Error Bias}}.$$

(2B.14)

The bias from the prediction error does not only cause attenuation bias, but worsens the omitted variable bias and the Nickell bias.

In practice, when including and excluding a time trend or year fixed effects from the regression, I expect the estimated coefficient without a time component to be larger due to the positive correlation between yield, SOC, and time, and because the prediction errors increase over time.

Simulation Procedure

In this subsection, I perform a simulation to apply the econometric principles discussed in the preceding section. I illustrate the changes in both the sample analog of the Nickell bias (as per equation (2B.7)) and the true bias when modifying the number of years included in the Data

Generating Process (DGP), introducing year fixed effects, using an unbalanced panel dataset, and incorporating prediction errors in simulated SOC stocks. For this simulation, consider a scenario with 10,000 fields (n), managed by 1,000 farmers (k), across a span of 22 years (t), focusing on a single homogeneous crop.

Let the DGP for crop yield be,

$$Y_{n,t} = \Gamma SOC_{n,t} + e_{n,t} * \Omega_{n \in g}$$

Where:

$$e_{n,t} \sim N(\mu = 0.5,\ \sigma = 0.1)$$

and

$$\Omega_{n \in g} \in \{30,\ 40,\ 50,\ 60\} \mapsto g \in \{1,2,3,4\} \mapsto n \in \{1:250,\ 251:500,\ 501:750,\ 751:1000\}$$

(2B.15)

In all simulations, the true effect of SOC on crop yield remains constant at $\Gamma = 0.5$. As per equation (2B.15), the yield is determined by a fundamental crop yield contingent on the assigned field group. For instance, if a field falls within group 1, the base yield ($\Omega_{n \in g}$) is set at 15 ($30*\mu$), whereas for fields in group 4, the base yield is elevated to 30 ($60*\mu$). Introducing errors with a zero mean and directly incorporating them within the DGP, instead of scaling them by the base yield, does not affect the outcomes because the field fixed effects adequately adjust for variations in base yields across groups. However, scaling the errors by the base yield provides a more realistic representation, especially considering that regions with higher yields might experience more substantial variation in crop yields.

I employ the following first order differential equation to represent the dynamics of SOC stocks. Let SOC be characterized by,

$$SOC_{n,t} = cY_{n,t-1} + (1 - d)\, SOC_{n,t-1}.$$

(2B.16)

Where c is the crop yield to carbon input conversion rate, and d is a parameter for the decay of SOC, such that $(1 - d)$ is the decay rate of SOC stocks. I set c equal to 0.5, and d equal to 0.45, to construct the time-path of SOC (see Panel(A) in Figure 2B.1). The initial SOC stock depends on the group that a field is in, such that $SOC(0)_{n \in g} = \Omega_{n \in g}$. Hence, the initial stock of SOC for a field in group 1 is 30.

Because there is dynamic feedback between SOC and crop yield, the steps used to form the DGP using equations (2B.15) and (2B.16) are:

1. Set all starting measures of SOC for all years to the initial stock value for each field.

2. Calculate the crop yield using equation (2B.15).

3. Recalculate the stock of SOC using (2B.16).

4. Iterate steps 2 and 3 until a stable path is reached.

The approach above vectorizes the dynamic system in R, which substantially increases the computational efficiency and speed.

Simulation Results

The results of the simulation are shown in Tables 2B.1 to 2B.4 and Figure 2B.1. Tables 2B.1 and 2B.2 demonstrate the effect of expanding the number of years in the dynamic panel model with either field or farm fixed effects, effectively mitigating the Nickell bias across all scenarios. Additionally, the influence of an unbalanced panel is examined, yielding results similar to those observed in the strongly balanced panel. Table 2B.1 reveals that the bias computed using the sample analog of the Nickell bias tends to be less precise for panels spanning less than 10 years and when excluding year fixed effects; nevertheless, there exists a positive correlation between the values of the sample analog and the true Nickell bias across panel datasets with different number of years.

In Table 2B.2, the Nickell bias is mitigated when employing farm fixed effects, likely due to reduced overfitting of SOC stock and greater orthogonal residual variation relative to past errors. The shadow value of SOC is predominantly identified across various time periods when using

farmer fixed effects. In this essay, Rural Municipality (RM) fixed effects are employed instead of farmer fixed effects. The rationale behind this choice stems from the fact that over half of farms insure fewer than 10 fields,[35] and approximately 2000 observations insure only one field at the farm level, which will result in overfitting and Nickell bias. I determine farm size using the customer ID from the SCIC dataset, which does consider the possibility of multiple farmers insuring land on the same farming operation. Unlike smaller farms, larger farms or corporations do not encounter this problem as the customer ID pertains to a corporation. In 2019, there were several hundred farms with over 10,000 acres or 4,000 hectares. The median farm size stood at 1,000 acres or 400 hectares, while the average size was 1,700 acres or 690 hectares (with a right-skewed distribution).

Tables 2B.3 and 2B.4 show the effect of prediction error bias alongside Nickell bias, both with and without year fixed effects. The prediction error varies substantially with the degree of prediction error, observed across scenarios with either field or farmer fixed effects. As expected, the inclusion of year fixed effects leads to biased coefficients and exacerbates the Nickell bias. Given the linear trend in SOC stocks, the presence or absence of time-fixed effects serves as a robustness check for both Nickell and prediction error biases. This sensitivity analysis reveals the importance of residual variation in SOC stocks, particularly when they are closely aligned with a time trend.

Incorporating time trends in dynamic panel regressions is essential, though caution is advised to avoid overfitting when using two-way fixed effects. The inclusion of year fixed effects can lead to significant multicollinearity between independent variables, which might enlarge the standard errors but should not bias the estimator. Hence, addressing other biases like omitted variable bias and Nickell bias is crucial for reducing the overall effect of prediction error bias. When prediction errors are random and uncorrelated with unobserved factors influencing crop yield, the bias should be zero.

---

[35]In this simulation each farmer has 10 fields.

TABLE 2B.1: Simulation Results for Nickell Bias in Dynamic Panel Regression Models with Field Fixed Effects

Years	$\hat{\Gamma}^{FE}$	S.E.	T-Value	P-Value	$\widehat{Bias}$	$\|\hat{\Gamma}^{FE} - \Gamma\|$	Observations	Panel	Year FE
A) Number of Years									
1000	0.497	0.000	1200.36	0.000	0.002	0.003	10,000,000	Balanced	No
50	0.445	0.002	239.16	0.000	0.076	0.055	500,000	Balanced	No
22	0.403	0.003	147.76	0.000	0.194	0.097	220,000	Balanced	No
15	0.370	0.003	119.86	0.000	0.283	0.130	150,000	Balanced	No
10	0.318	0.004	79.44	0.000	0.509	0.182	100,000	Balanced	No
5	0.128	0.007	19.39	0.000	1.257	0.372	50,000	Balanced	No
1000	0.497	0.000	1193.54	0.000	0.002	0.003	10,000,000	Balanced	Yes
50	0.418	0.002	185.21	0.000	0.015	0.082	500,000	Balanced	Yes
22	0.304	0.004	80.42	0.000	0.010	0.196	220,000	Balanced	Yes
15	0.172	0.005	36.93	0.000	0.037	0.328	150,000	Balanced	Yes
10	-0.021	0.006	-3.39	0.001	0.038	0.521	100,000	Balanced	Yes
5	-0.501	0.010	-50.14	0.000	0.025	1.001	50,000	Balanced	Yes
B) Unbalanced Panel									
22	0.407	0.006	66.39	0.000	NA	0.093	50,000	Unbalanced	No
22	0.401	0.004	104.09	0.000	NA	0.099	100,000	Unbalanced	No
22	0.319	0.008	38.02	0.000	NA	0.181	50,000	Unbalanced	Yes
22	0.301	0.005	56.70	0.000	NA	0.199	100,000	Unbalanced	Yes

Source: Author's Estimates

Notes: In all cases, c=0.5, and d=0.45 in equation (A.16). Each regression includes field fixed effects and clustering of standard errors at the farm level.

TABLE 2B.2: Simulation Results for Nickell Bias in Dynamic Panel Regression Models with Farmer Fixed Effects

Years	$\hat{\Gamma}^{FE}$	S.E.	T-Value	P-Value	$\widehat{Bias}$	$\lvert \hat{\Gamma}^{FE} - \Gamma \rvert$	Observations	Panel	Year FE
A) Number of Years									
1000	0.500	0.000	1218.05	0.000	0.075	0.000	10,000,000	Balanced	No
50	0.484	0.003	145.66	0.000	0.026	0.016	500,000	Balanced	No
22	0.492	0.003	193.91	0.000	0.113	0.008	220,000	Balanced	No
15	0.489	0.003	188.89	0.000	0.105	0.011	150,000	Balanced	No
10	0.491	0.003	140.93	0.000	0.117	0.009	100,000	Balanced	No
5	0.469	0.006	79.97	0.000	0.240	0.031	50,000	Balanced	No
1000	0.500	0.000	1212.48	0.000	0.070	0.000	10,000,000	Balanced	Yes
50	0.491	0.002	247.89	0.000	0.048	0.009	500,000	Balanced	Yes
22	0.484	0.003	145.66	0.000	0.089	0.016	220,000	Balanced	Yes
15	0.477	0.004	131.71	0.000	0.126	0.023	150,000	Balanced	Yes
10	0.472	0.005	95.70	0.000	0.180	0.028	100,000	Balanced	Yes
5	0.442	0.008	53.58	0.000	0.353	0.058	50,000	Balanced	Yes
B) Unbalanced Panel									
22	0.496	0.005	97.05	0.000	NA	0.004	50,000	Unbalanced	No
22	0.489	0.004	138.99	0.000	NA	0.011	100,000	Unbalanced	No
22	0.497	0.007	73.94	0.000	NA	0.003	50,000	Unbalanced	Yes
22	0.480	0.005	103.93	0.000	NA	0.020	100,000	Unbalanced	Yes

Source: Author's Estimates

Notes: In all cases, c=0.5, and d=0.45 in equation (A.16). Each regression includes farmer fixed effects and clustering of standard errors at the farm level.

TABLE 2B.3: Sensitivity Analysis with respect to Prediction Error with Field Fixed Effects

$\hat{\Gamma}^{FE}$	S.E.	T-Value	c_{true}	d_{true}	c_{error}	d_{error}	R^2	$|\hat{\Gamma}^{FE} - \Gamma|$	Year FE
0.204	0.003	63.07	0.02	0.01	0.5	0.45	0.864	0.296	No
-0.114	0.005	-25.20	0.02	0.01	0.5	0.45	0.874	0.614	Yes
0.414	0.005	77.46	0.5	0.45	0.02	0.01	0.878	0.086	No
0.163	0.020	8.09	0.5	0.45	0.02	0.01	0.882	0.337	Yes
0.290	0.002	130.07	0.02	0.01	0.06	0.04	0.873	0.210	No
-0.040	0.012	-3.43	0.02	0.01	0.06	0.04	0.874	0.540	Yes
0.447	0.002	205.87	0.06	0.04	0.02	0.01	0.871	0.053	No
-0.040	0.005	-8.05	0.06	0.04	0.02	0.01	0.886	0.540	Yes

Source: Author's Estimates

Notes: The time period used is 22 years resulting in 220,000 observations. The underlying DGP in equation (A.16) is defined by parameters c_{true} and d_{true}, where c_{error} and d_{error} represent the parameters used to generate the prediction error in SOC stocks.

TABLE 2B.4: Sensitivity Analysis with respect to Prediction Error with Farmer Fixed Effects

$\hat{\Gamma}^{FE}$	S.E.	T-Value	c_{true}	d_{true}	c_{error}	d_{error}	R^2	$|\hat{\Gamma}^{FE} - \Gamma|$	Year FE
0.266	0.003	85.48	0.02	0.01	0.5	0.45	0.860	0.234	No
0.040	0.004	9.11	0.02	0.01	0.5	0.45	0.867	0.460	Yes
0.470	0.005	86.72	0.5	0.45	0.02	0.01	0.862	0.030	No
0.911	0.021	43.40	0.5	0.45	0.02	0.01	0.866	0.411	Yes
0.309	0.002	137.77	0.02	0.01	0.06	0.04	0.868	0.191	No
0.249	0.008	32.13	0.02	0.01	0.06	0.04	0.868	0.251	Yes
0.840	0.003	244.58	0.06	0.04	0.02	0.01	0.881	0.340	No
0.866	0.013	68.40	0.06	0.04	0.02	0.01	0.881	0.366	Yes

Source: Author's Estimates

Notes: The time period used is 22 years resulting in 220,000 observations. The underlying DGP in equation (A.16) is defined by parameters c_{true} and d_{true}, where c_{error} and d_{error} represent the parameters used to generate the prediction error in SOC stocks.

FIGURE 2B.1: Soil Organic Carbon Stocks by Decomposition Rates, Field, and Group
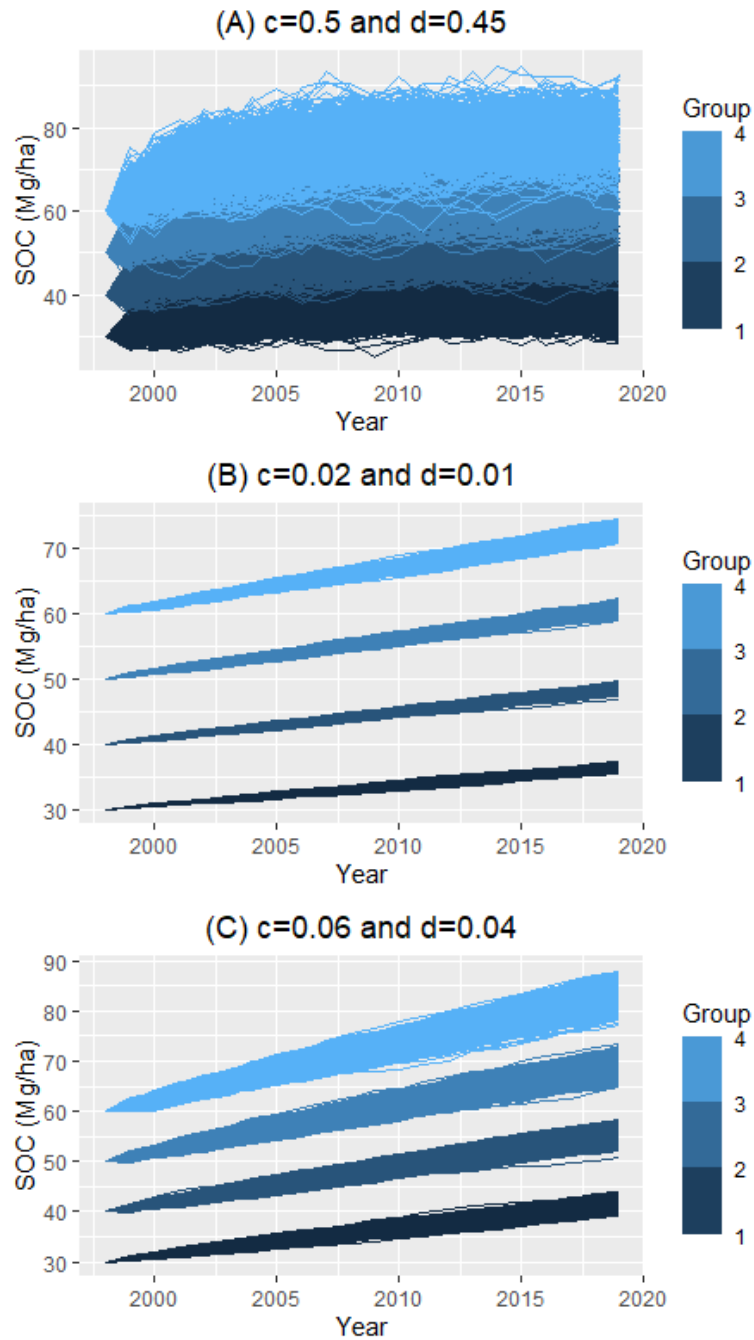
Source: Authors' Estimates

Notes: Panels (A), (B), and (C) include the time-paths of soil organic carbon over time by field and group and are computed using Equations (2B.15) and (2B.16). Each color represents a separate group. Parameter values for c and d correspond to Equation (2B.16).

Appendix 2C: Data and Summary Statistics

TABLE 2C.1: Description of Variables in the Dynamic Panel Regression Model

Primary Variables:	Description:	Source:
Crop Yield	The field-level average yield in kilogram per hectare for the respective crop for farms in the SMP program. The farm-level average yield in kilograms per hectare for fields not included in the SMP program	Saskatchewan Crop Insurance Corporation Confidential Dataset
Soil Organic Carbon	The stock of soil organic carbon on a field in kilograms per hectare.	Serfas (2024a)
Nitrogen Use	The pounds per acre of nitrogen applied on a field.	Saskatchewan Crop Insurance Corporation Confidential Dataset

Weather Variables:		
GSAT	The Growing Season Average Temperature (April to September) in degrees Celsius.	
lag(GSAT)	One year lagged term of Growing Season Average Temperature.	
$GSAT^2$	Squared term of Growing Season Average Temperature.	Environment and Climate Change Canada (2023b)
$(GSAT - \overline{GSAT})^2$	Total Annual Precipitation squared deviation from climate variable for GSAT from 1998 to 1819.	
TAP	Total Annual Precipitation in millimeters.	
lag(TAP)	One year lagged term of Total Annual Precipitation.	
TAP^2	Squared term of Total Annual Precipitation.	
$(TAP - \overline{TAP})^2$	Total Annual Precipitation squared deviation from climate variable for TAP from 1998 to 1819.	

Soil Characteristic Variables:		
Stoniness	Occurrence of stones at the surface of the soil. All values are classified on a discrete scale from 0 to 5, 0 being no stones and 5 being excessively stony.	
Slope	The slope gradient is the slope of the predominant landscape and is measured in percent where a 3 percent slope means that the elevation changes 3 feet for every 100 feet of horizontal distance.	
Percent Sand	Percentage of soil particles that are sand	
Percent Silt	Percentage of soil particles that are silt	
Percent Clay	Percentage of soil particles that are clay	Agriculture and Agri-Food Canada (2022)
pH	Measure for the acidity of the soil.	
Cation Exchange Capacity	Measured in millequivalents per 100 grams of soil. Millequivalents are the number of ions for a particular quantity of electracial charges.	
Water Retention (@33 kilopascals)	The water retention at 33 kilopascals measured as the percentage of the total soil volume.	
Electrical Conductivity	Soil electrical conductivity measured in dS/m or millimhos/centimeter which is inversely proportional to the electrical resistance (Ohms) in the soil.	

TABLE 2C.1: Description of Variables in the Dynamic Panel Regression Model *(continued)*

Primary Variables:	Description:	Source:
Farm Characteristics:		
Liability	The total liability by field or guarantee to a farmer in CAD from the Saskatchewan Crop Insurance Corporation.	Saskatchewan Crop Insurance Corporation Confidential Dataset
Insurer Farm Size	The total hectares in a year for a farmer that are insured by the Saskatchewan Crop Insurance Corporation.	
SMP Indicator	Dummy variable for whether a field is in the Sask Management Plus Program.	
Factors of Cropping Choice:		
Crop Rotation Dummy Variables	There are 256 crop rotation dummy variables for the past four-year crop rotation sequence using the categories: oilseeds, pulses, cereals, and fallow.	Constructed from the Saskatchewan Crop Insurance Corporation Confidential Dataset
Spring Wheat Past CD Average Yield	The past four-year average spring wheat yield in kg/ha by Crop District in Saskatchewan.	
Canola Past Past CD Average Yield	The past four-year average canola yield in kg/ha by Crop District in Saskatchewan.	
Barley Past CD Average Yield	The past four-year average barley yield in kg/ha by Crop District in Saskatchewan.	
Durum Wheat Past CD Average Yield	The past four-year average durum wheat yield in kg/ha by Crop District in Saskatchewan.	
Lentils Past CD Average Yield	The past four-year average lentil yield in kg/ha by Crop District in Saskatchewan.	
Peas Past CD Average Yield	The past four-year average peas yield in kg/ha by Crop District in Saskatchewan.	

FIGURE 2C.1: Share of Hectares in Saskatchewan from 1998 to 2019 by Crop, Dataset, and Soil Zone
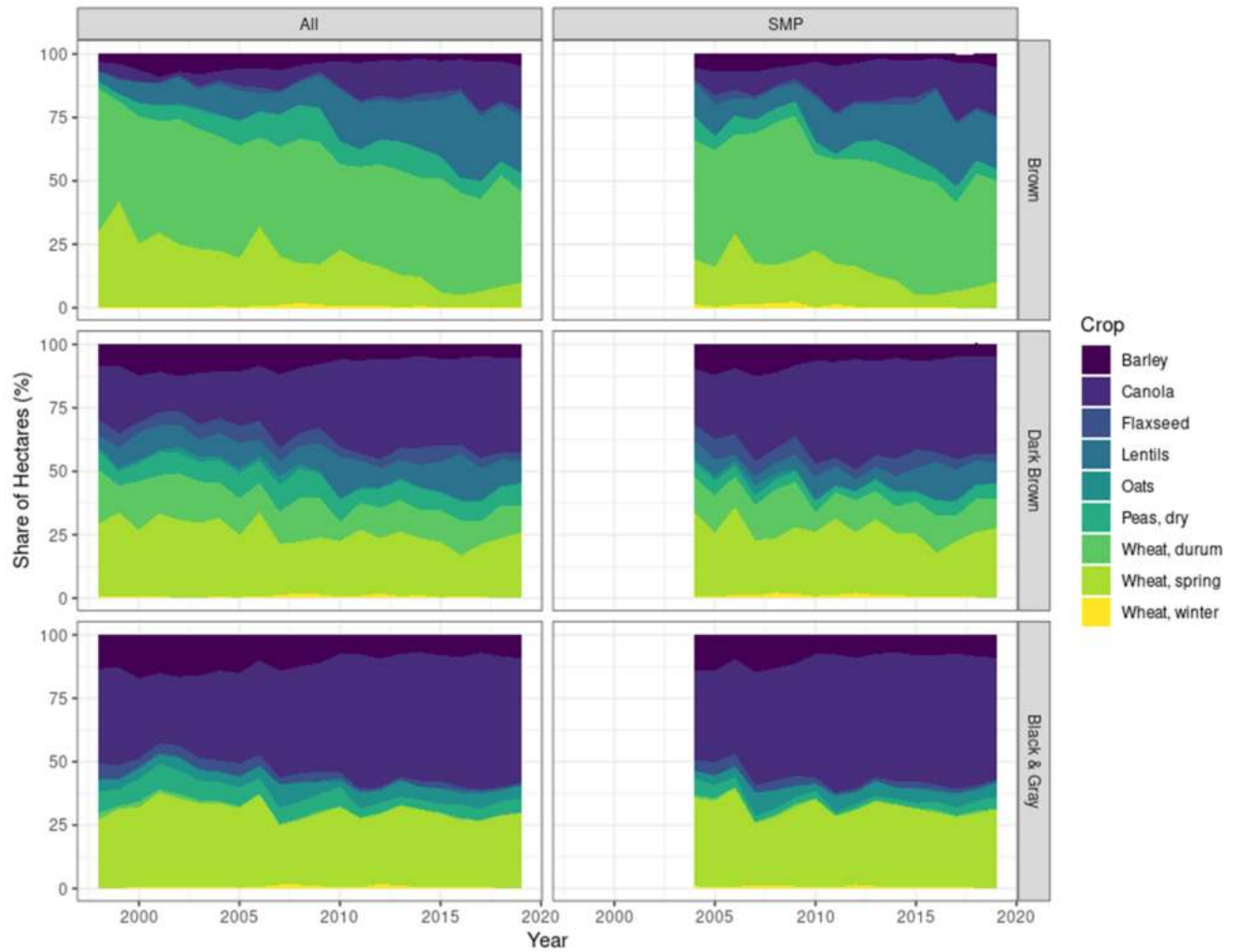
Source: Constructed using SCIC confidential data.
Notes: All data include fields selected for soil organic carbon (SOC) prediction from the SCIC confidential dataset, whereas Saskatchewan Management Plus (SMP) data are a subset of fields that participated in the SMP program.

FIGURE 2C.2: Share of Summer Fallow Hectares in Saskatchewan from 1998 to 2019 by Soil Zone
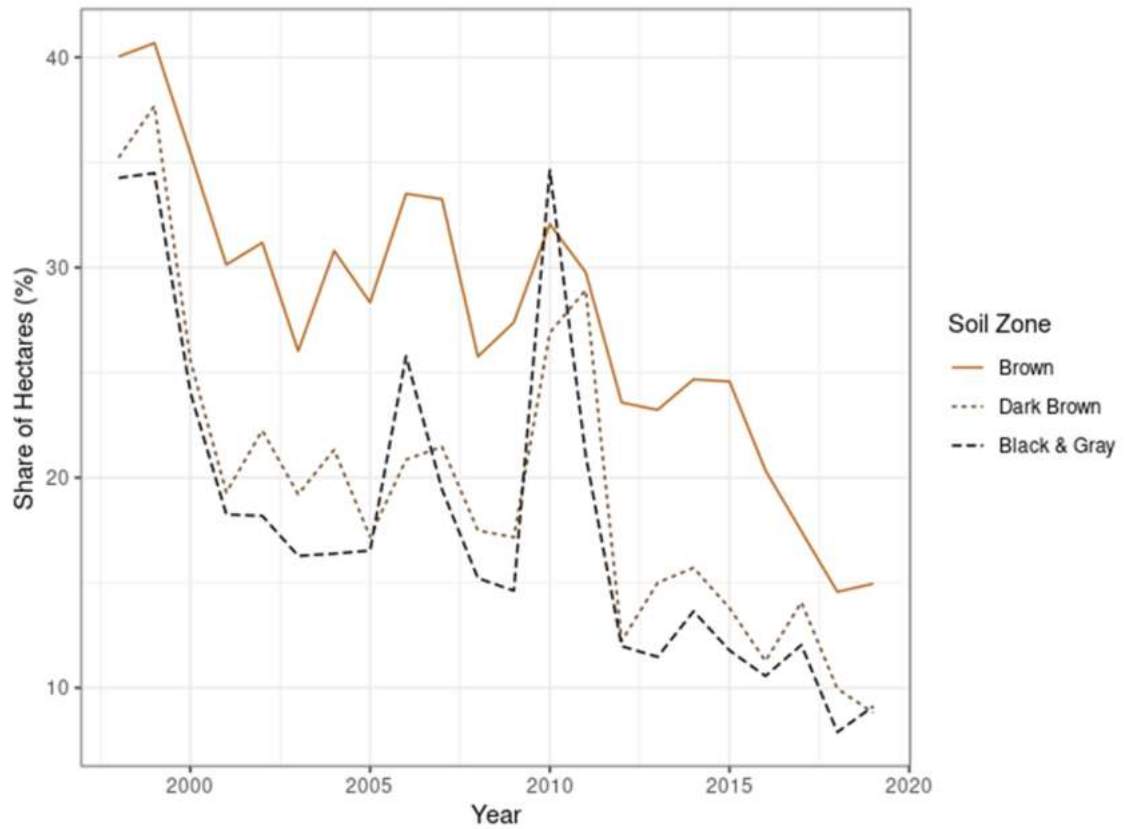
Source: Constructed using SCIC confidential data.
Notes: The share of summer fallow hectares is equal to the summer fallow hectares divided by all cropping hectares and summer fallow hectares for fields selected for SOC prediction.

TABLE 2C.2: Hectares by Crop, Soil Zone and Dataset in Saskatchewan from 1998 to 2019

	(1)	(2)	(3)	(4)
	All Hectares			
Soil Zone:	Brown	Dark Brown	Black & Gray	All
	(thousands of hectares)			
Barley	113	727	2,375	3,216
Canola	257	2,629	9,060	11,947
Flaxseed	38	457	606	1,101
Lentils	402	887	119	1,408
Oats	8	110	1,048	1,166
Peas, dry	215	757	1,304	2,276
Summer Fallow	975	2,231	4,668	7,873
Wheat, durum	1,111	1,243	171	2,524
Wheat, spring	454	2,308	6,354	9,117
Wheat, winter	12	71	150	233
Total	3,584	11,420	25,856	40,860
	SMP Hectares			
	(thousands of hectares)			
Barley	33	213	679	926
Canola	102	946	3,128	4,176
Flaxseed	12	146	170	328
Lentils	123	192	24	339
Oats	1	33	359	392
Peas, dry	48	126	196	370
Wheat, durum	356	361	42	759
Wheat, spring	106	694	2,039	2,839
Wheat, winter	6	31	54	90
Total	788	2,742	6,690	10,220
	SMP Share of All Hectares			
	(%)			
Barley	29.5	29.3	28.6	28.8
Canola	39.8	36.0	34.5	35.0
Flaxseed	32.2	32.0	28.0	29.8
Lentils	30.5	21.7	19.9	24.0
Oats	10.2	29.6	34.2	33.6
Peas, dry	22.5	16.7	15.0	16.3
Wheat, durum	32.0	29.1	24.7	30.1
Wheat, spring	23.4	30.1	32.1	31.1
Wheat, winter	48.0	43.5	35.7	38.7
Total	22.0	24.0	25.9	25.0

Source: Constructed using SCIC confidential data.

Notes: All Hectares include fields selected for SOC prediction and the SMP Hectares include fields that participated in the SMP program and are also selected for SOC prediction.

FIGURE 2C.3: Average Yield in Saskatchewan from 1998 to 2019 by Crop, Dataset, and Soil Zone
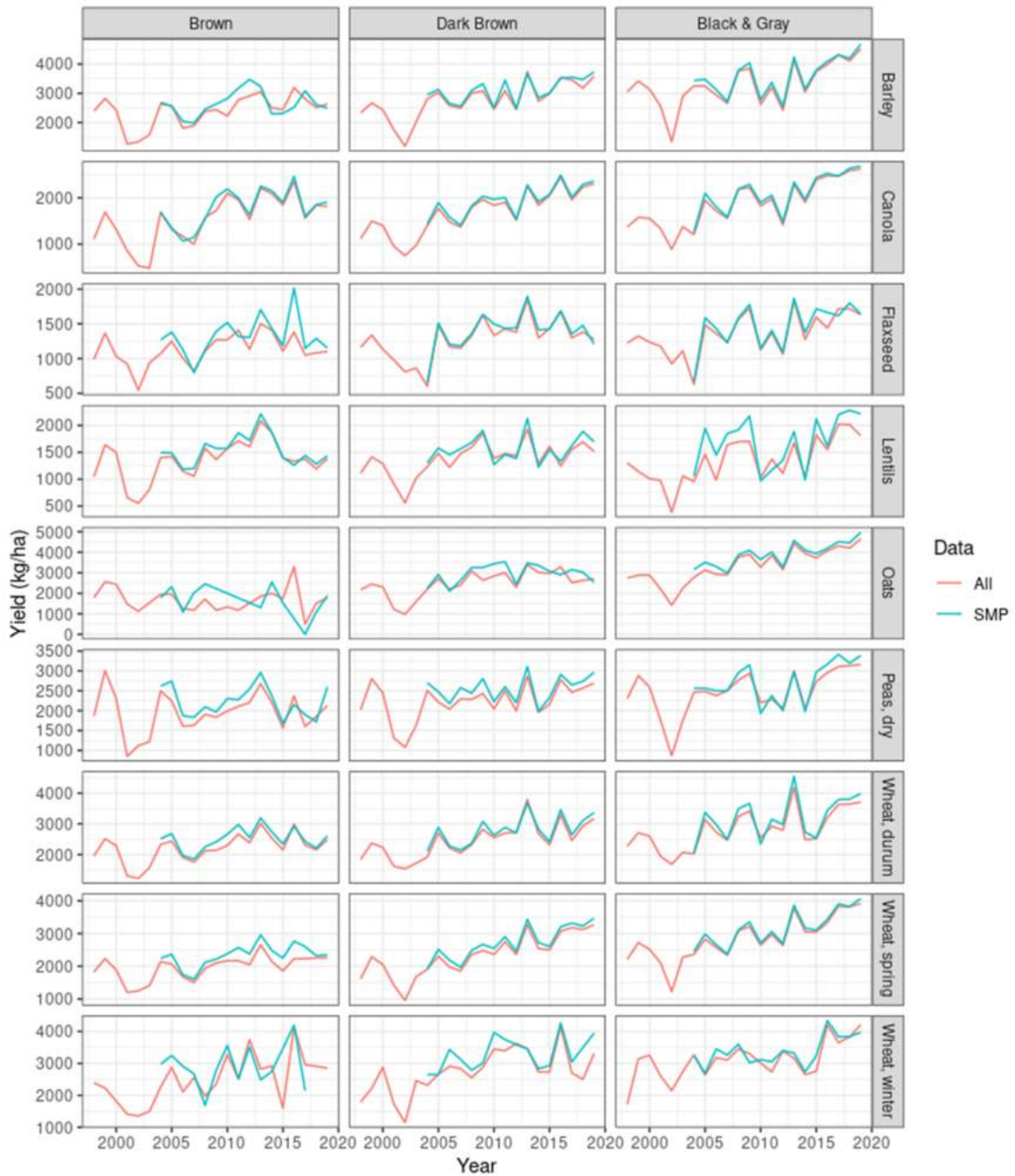
Source: Constructed using SCIC confidential data.

Notes: All data include fields selected for SOC prediction, whereas SMP data are subset of fields that participated in the SMP program.

TABLE 2C.3: Saskatchewan Average Yield by Crop and Soil Zone from 1998 to 2019

	(1)	(2)	(3)	(4)	(5)	(6)
	All Yield					
Soil Zone:	Brown		Dark Brown		Black & Gray	
	Mean	Std. Dev.	Mean	Std. Dev.	Mean	Std. Dev.
	(kg/ha)					
Barley	2,245	1,246	2,647	1,214	3,191	1,309
Canola	1,731	757	1,803	694	1,958	749
Flaxseed	1,160	556	1,267	568	1,294	572
Lentils	1,413	657	1,393	677	1,378	778
Oats	1,624	1,288	2,347	1,225	3,422	1,480
Peas, dry	1,948	937	2,226	949	2,402	1,065
Wheat, durum	2,194	1,001	2,414	1,080	2,617	1,026
Wheat, spring	1,899	846	2,293	1,029	2,839	1,082
Wheat, winter	2,597	1,202	2,878	1,139	3,139	1,108
	SMP Yield					
Soil Zone:	Brown		Dark Brown		Black & Gray	
	Mean	Std. Dev.	Mean	Std. Dev.	Mean	Std. Dev.
	(kg/ha)					
Barley	2,576	1,172	3,051	1,050	3,533	1,146
Canola	1,844	694	1,950	603	2,111	670
Flaxseed	1,296	464	1,379	531	1,439	573
Lentils	1,535	603	1,556	676	1,789	788
Oats	1,734	938	2,881	1,101	3,837	1,286
Peas, dry	2,258	886	2,575	848	2,779	1,012
Wheat, durum	2,499	941	2,742	1,003	3,219	1,006
Wheat, spring	2,261	806	2,700	933	3,146	962
Wheat, winter	2,606	1,068	3,205	957	3,382	945

Source: Constructed using SCIC confidential data.

Notes: All Yield include all fields selected for SOC prediction and the SMP Yield include fields that participated in the SMP program and are also selected for SOC prediction.

FIGURE 2C.4: Average Nitrogen Use in Saskatchewan from 1998 to 2019 by Crop and Soil Zone
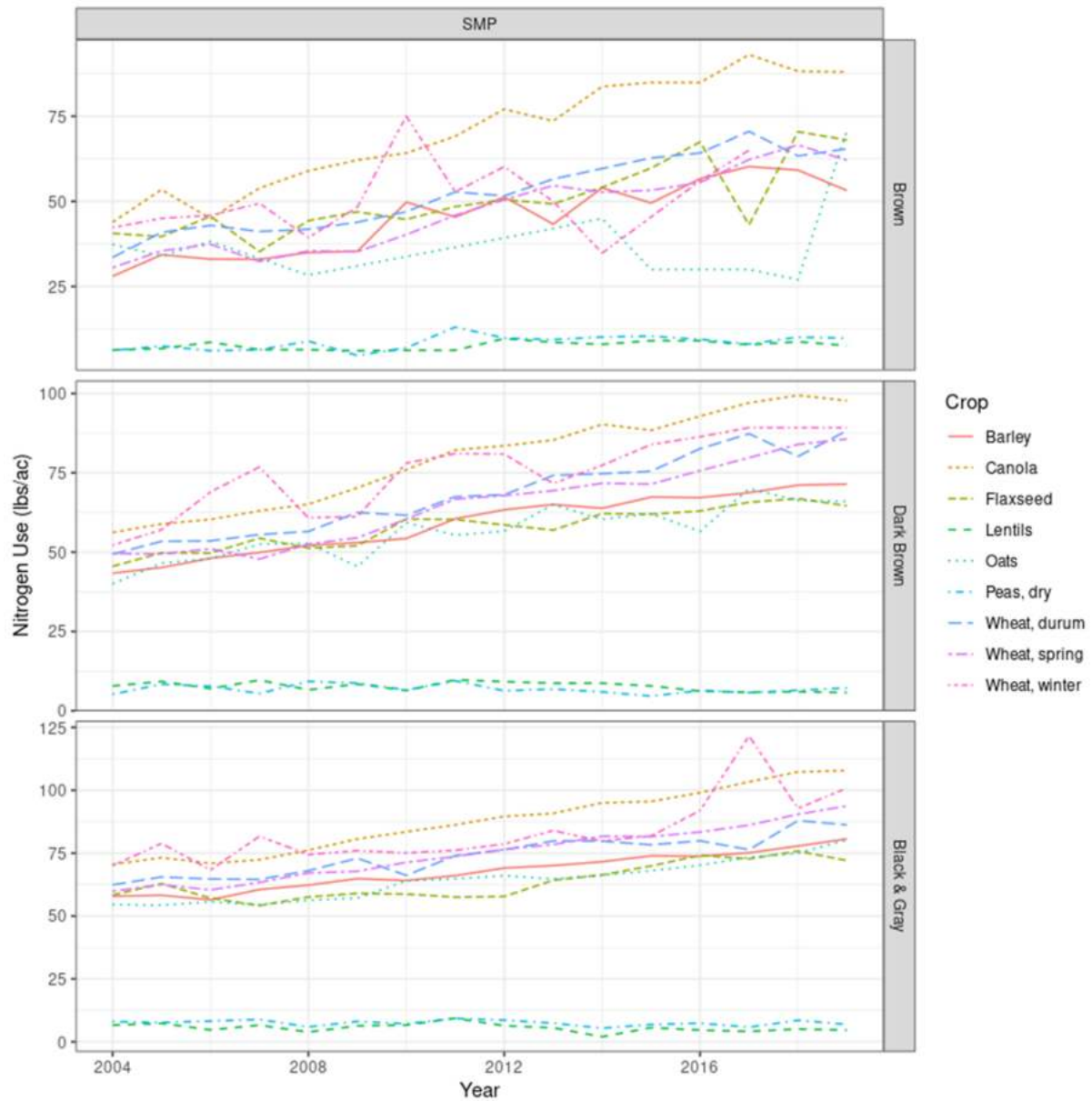
Source: Constructed using SCIC confidential data.
Notes: The SMP data include fields that participated in the SMP program and are selected for SOC prediction.

TABLE 2C.4: Average Nitrogen Use by crop and soil zone in Saskatchewan from 1998 to 2019

	(1)	(2)	(3)	(4)	(5)	(6)
	SMP Nitrogen Use					
Soil Zone:	Brown		Dark Brown		Black & Gray	
	Mean	Std. Dev.	Mean	Std. Dev.	Mean	Std. Dev.
	(lbs/ac)					
Barley	42	21	56	19	66	17
Canola	76	30	81	28	88	27
Flaxseed	50	23	56	18	61	21
Lentils	8	8	7	9	5	6
Oats	38	15	54	19	63	18
Peas, dry	9	9	7	9	8	13
Wheat, durum	52	24	67	26	73	18
Wheat, spring	43	22	64	26	74	22
Wheat, winter	47	19	72	25	81	29

Source: Constructed using SCIC confidential data.

Notes: The SMP data include fields that participated in the SMP program and are selected for SOC prediction.

FIGURE 2C.5: Weighted Average Soil Organic Carbon Stocks in Saskatchewan from 1998 to 2019 by Dataset and Soil Zone
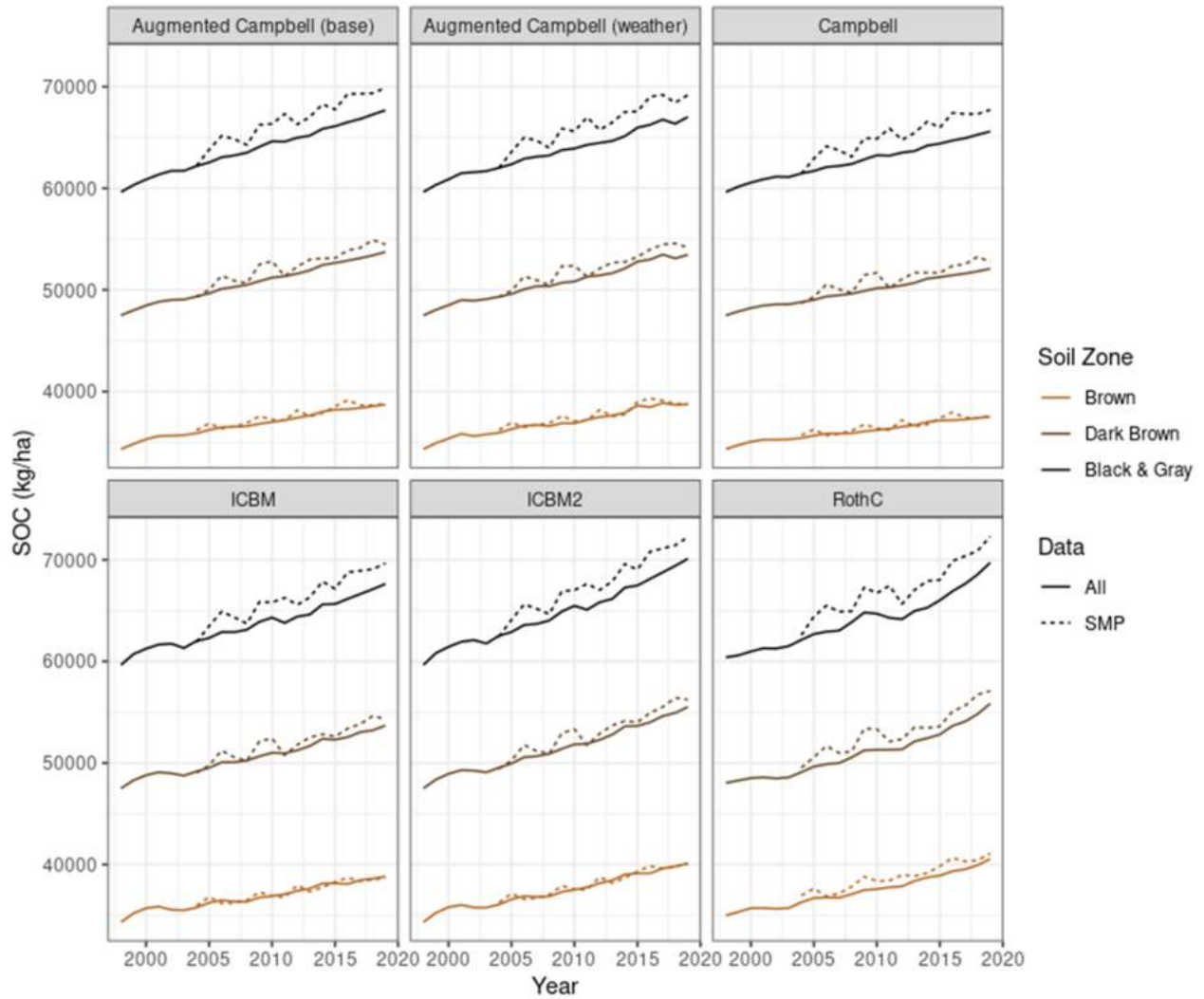
Source: Authors' Estimates.
Notes: All data include fields selected for SOC prediction, whereas SMP data are a subset of fields that participated in the SMP program.

TABLE 2C.5: Weighted Average Simulated Soil Organic Carbon Stocks by soil zone and Prediction Model in Saskatchewan from 1998 to 2019

	(1)	(2)	(3)	(4)	(5)	(6)
Soil Zone:	Brown		Dark Brown		Black & Gray	
Sample:	All	SMP	All	SMP	All	SMP
Augmented Campbell Model (base):			*(kg/ha)*			
Mean	36,790	37,641	50,728	52,331	63,819	66,539
Std. Dev.	10,671	10,785	16,612	16,759	25,322	25,563
Augmented Campbell Model (weather):						
Mean	36,882	37,722	50,669	52,213	63,544	66,147
Std. Dev.	10,693	10,806	16,628	16,784	25,303	25,551
Campbell Model:						
Mean	36,090	36,700	49,834	51,132	62,685	65,075
Std. Dev.	10,593	10,714	16,543	16,707	25,213	25,468
ICBM:						
Mean	36,791	37,382	50,599	51,955	63,605	66,032
Std. Dev.	10,678	10,754	16,583	16,723	25,254	25,493
ICBM/2:						
Mean	37,374	38,185	51,387	53,031	64,679	67,435
Std. Dev.	10,773	10,845	16,690	16,817	25,420	25,647
RothC Model:						
Mean	37,399	38,831	50,934	53,075	63,984	67,024
Std. Dev.	10,303	10,228	15,669	15,563	23,984	23,838

Source: Constructed using SCIC confidential data.
Notes: The All data include fields selected for SOC prediction and the SMP data include fields that participated in the SMP program and are also selected for SOC prediction.

TABLE 2C.6: Summary Statistics for Weather and Climate Variables on Fields from
1998 to 2019 in Saskatchewan

	(1)	(2)	(3)	(4)	(5)	(6)
Sample:		All			SMP	
Soil Zone:	Brown	Dark Brown	Black & Gray	Brown	Dark Brown	Black & Gray
GSAT:			(°C)			
Mean	13.25	13.02	12.56	13.16	12.90	12.42
Std. Dev.	0.82	0.89	0.88	0.70	0.82	0.81
$(GSAT - \overline{GSAT})^2$:						
Mean	0.64	0.60	0.62	0.45	0.49	0.53
Std. Dev.	0.75	0.67	0.73	0.57	0.60	0.71
TAP:			(millimeters)			
Mean	353	382	411	358	385	421
Std. Dev.	90	100	101	88	93	91
$(TAP - \overline{TAP})^2$:						
Mean	7,658	8,697	9,588	7,456	7,871	8,068
Std. Dev.	10,754	13,039	13,892	11,027	13,300	12,477

Source: Created using data from Environment and Climate Change Canada (2023b)
Notes: GSAT is growing season average temperature (April to September) and TAP is total annual precipitation.
The All data include fields selected for SOC prediction and the SMP data include fields that participated in the SMP
program and are also selected for SOC prediction.

FIGURE 2C.6: Crop Districts and Rural Municipalities Map of Saskatchewan
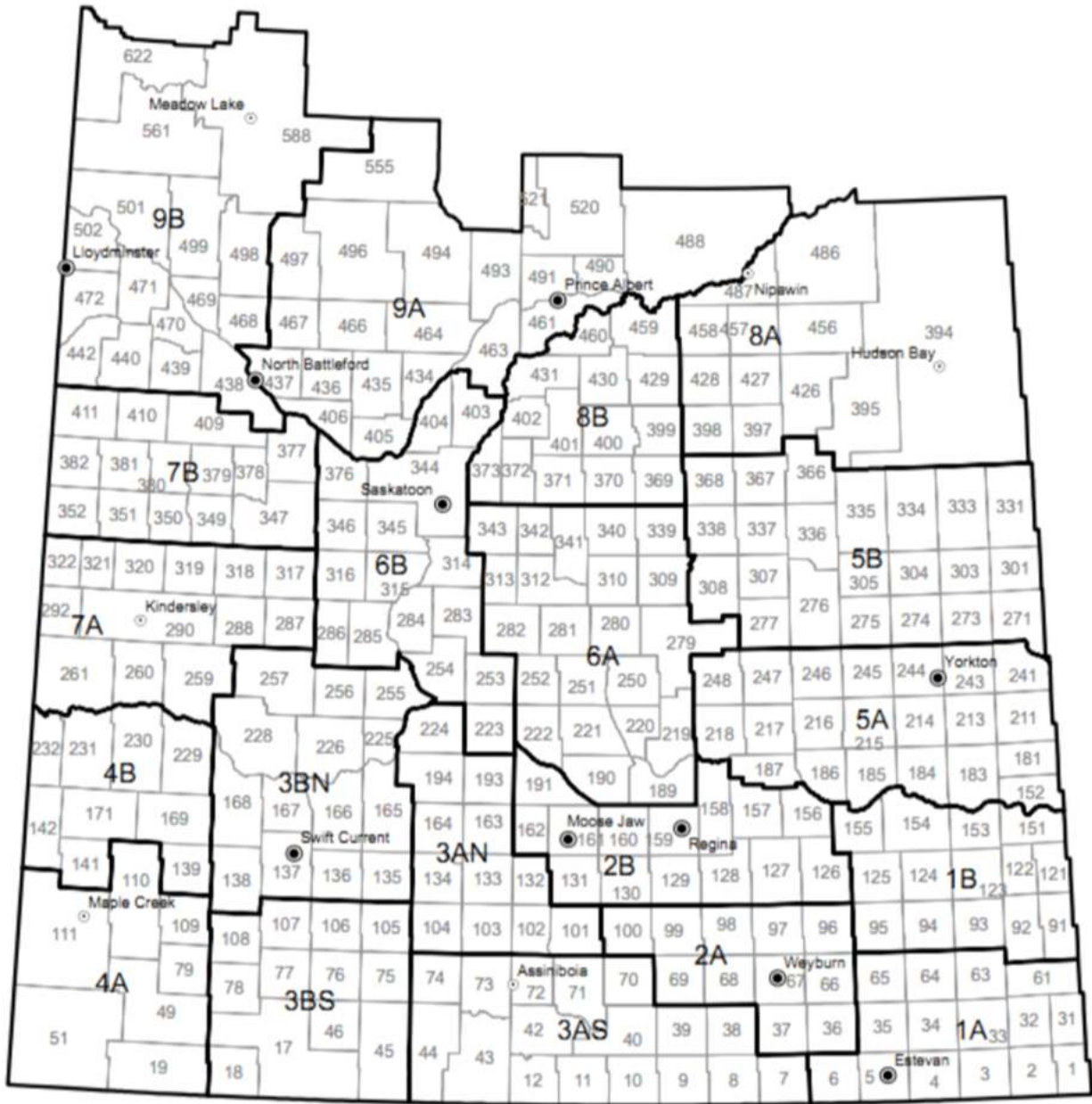
Saskatchewan Crop District Map

Source: Government of Saskatchewan (2017)

Appendix 2D: Supplementary Regressions

TABLE 2D.1: Soil Organic Carbon Marginal Products by SOC Prediction Model, Sample, and Soil Zone in Saskatchewan

	Dependent Variable: Spring Wheat Yield					
	(1)	(2)	(3)	(4)	(5)	(6)
Soil Zone:	*Brown*		*Dark Brown*		*Black & Gray*	
Sample:	Full	SMP	Full	SMP	Full	SMP
Augmented Campbell Model (base):			*(kg/ha)*			
Soil Organic Carbon	0.021***	0.024***	0.011***	0.011***	0.005***	0.003***
	(0.006)	(0.009)	(0.001)	(0.002)	(0.001)	(0.001)
Nitrogen Use		2.502		5.747***		9.459***
		(1.58)		(0.827)		(0.860)
Observations	7,425	2,050	33,174	12,245	92,608	36,033
R^2	0.474	0.517	0.577	0.561	0.575	0.532
Augmented Campbell Model (weather):						
Soil Organic Carbon	0.021***	0.024***	0.010***	0.010***	0.004***	0.003***
	(0.006)	(0.009)	(0.001)	(0.002)	(0.001)	(0.001)
Nitrogen Use		2.496		5.750***		9.462***
		(1.581)		(0.827)		(0.860)
Observations	7,425	2,050	33,174	12,245	92,608	36,033
R^2	0.474	0.517	0.577	0.561	0.575	0.532
Campbell Model						
Soil Organic Carbon	0.017***	0.021**	0.009***	0.009***	0.004***	0.002**
	(0.006)	(0.009)	(0.001)	(0.002)	(0.001)	(0.001)
Nitrogen Use		2.522		5.761***		9.468***
		(1.586)		(0.828)		(0.861)
Observations	7,425	2,050	33,174	12,245	92,608	36,033
R^2	0.473	0.516	0.576	0.56	0.574	0.532
ICBM:						
Soil Organic Carbon	0.020***	0.022**	0.010***	0.010***	0.005***	0.003***
	(0.006)	(0.009)	(0.001)	(0.002)	(0.001)	(0.001)
Nitrogen Use		2.475		5.745***		9.460***
		(1.583)		(0.827)		(0.860)
Observations	7,425	2,050	33,174	12,245	92,608	36,033
R^2	0.474	0.516	0.577	0.56	0.575	0.532
ICBM/2:						
Soil Organic Carbon	0.022***	0.025***	0.012***	0.012***	0.005***	0.003***
	(0.006)	(0.009)	(0.001)	(0.002)	(0.001)	(0.001)
Nitrogen Use		2.467		5.733***		9.452***
		(1.575)		(0.826)		(0.860)
Observations	7,425	2,050	33,174	12,245	92,608	36,033
R^2	0.474	0.517	0.577	0.561	0.575	0.532
RothC Model:						
Soil Organic Carbon	0.030***	0.033***	0.016***	0.015***	0.008***	0.006***
	(0.005)	(0.008)	(0.002)	(0.002)	(0.001)	(0.001)
Nitrogen Use		2.424		5.664***		9.398***
		(1.552)		(0.821)		(0.855)
Observations	7,425	2,050	33,174	12,245	92,608	36,033
R^2	0.479	0.523	0.58	0.563	0.576	0.533

Source: Authors' Estimates.

Notes: $^*p < 0.1;$ $^{**}p < 0.05;$ $^{***}p < 0.01$. For more information, please refer to the notes from Table 2.1.

TABLE 2D.2: Marginal Product of Soil Organic Carbon on Crop Yield by Functional Form of SOC, Crop Type, and Soil Zone in Saskatchewan

	(1)	(2)	(3)	(4)	(5)	(6)
			Dependent Variable: Crop Yield			
Soil Zone:	Brown		Dark Brown		Black & Gray	
Functional Form:	Quadratic	Logarithmic	Quadratic	Logarithmic	Quadratic	Logarithmic
Spring Wheat:			*(kg/ha)*			
SOC	0.051***		0.014***		0.011***	
	(0.015)		(0.004)		(0.002)	
SOC^2	−0.0000004**		−0.00000003		−0.00000003***	
	(0.0000002)		(0.00000002)		(0.000000008)	
ln(SOC)		874.15***		349.57***		344.18***
		(201.11)		(63.21)		(45.62)
Observations	7,425	7,425	33,174	33,174	92,608	92,608
R^2	0.475	0.475	0.577	0.576	0.575	0.575
Canola:						
SOC	0.030***		0.007***		0.008***	
	(0.011)		(0.002)		(0.001)	
SOC^2	−0.0000003***		−0.00000003*		−0.00000003***	
	(0.0000001)		(0.00000002)		(0.000000005)	
ln(SOC)		440.51***		150.03***		125.64***
		(128.48)		(35.39)		(25.19)
Observations	4,085	4,085	40,967	40,967	140,404	140,404
R^2	0.557	0.557	0.520	0.521	0.553	0.552
Barley:						
SOC	0.032		0.004		0.011***	
	(0.031)		(0.007)		(0.003)	
SOC^2	−0.0000002		0.00000005		−0.00000004***	
	(0.0000003)		(0.00000005)		(0.00000002)	
ln(SOC)		469.14		238.90***		260.02***
		(392.02)		(87.59)		(67.67)
Observations	1,771	1,771	10,251	10,251	33,213	33,213
R^2	0.583	0.583	0.512	0.511	0.511	0.511
Durum Wheat:						
SOC	0.054***		0.020***		0.029***	
	(0.010)		(0.006)		(0.011)	
SOC^2	−0.0000004***		−0.00000009**		−0.0000001**	
	(0.00000009)		(0.00000005)		(0.00000005)	
ln(SOC)		858.96***		440.21***		743.60***
		(120.95)		(109.77)		(219.48)
Observations	18,011	18,011	16,940	16,940	1,899	1,899
R^2	0.461	0.460	0.565	0.565	0.666	0.666
Lentils:						
SOC	0.025**		0.007		0.017*	
	(0.010)		(0.005)		(0.010)	
SOC^2	−0.0000002**		−0.00000002		−0.00000008	
	(0.00000009)		(0.00000003)		(0.00000005)	
ln(SOC)		320.76**		158.80**		594.97***
		(124.94)		(74.11)		(215.95)
Observations	6,342	6,342	12,347	12,347	1,592	1,592
R^2	0.366	0.366	0.325	0.325	0.620	0.621
Peas:						
SOC	0.024		0.013**		0.010***	
	(0.015)		(0.006)		(0.004)	
SOC^2	−0.0000001		−0.00000008*		−0.00000003*	
	(0.0000002)		(0.00000004)		(0.00000002)	
ln(SOC)		442.42**		261.063***		117.42
		(192.02)		(96.46)		(78.38)
Observations	3,449	3,449	11,081	11,081	17,272	17,272
R^2	0.441	0.441	0.414	0.414	0.479	0.479

Source: Authors' Estimates.
Notes: $^*p < 0.1$; $^{**}p < 0.05$; $^{***}p < 0.01$. For more information, please refer to the notes from Table 2.1. SOC represents Soil Organic Carbon measured in kilograms per hectare. All models are estimated using the Full sample, which includes all fields selected for soil organic carbon prediction from the SCIC confidential dataset.

TABLE 2D.3: Statistical Significance of the Marginal Product of Soil Organic Carbon by Functional Form, Crop, and Soil Zone in Saskatchewan

				Dependent Variable: Crop Yield					
	(1)	(2)	(3)	(4)	(5)	(6)	(7)	(8)	(9)
Soil Zone:	*Brown*			*Dark Brown*			*Black & Gray*		
Func. Form:	Lin	Quad	Log	Lin	Quad	Log	Lin	Quad	Log
Spring Wheat:									
SOC	***	***		***	***		***	***	
SOC^2		**			-			***	
ln(SOC)			***			***			***
R^2	0.474	0.475	0.475	0.577	0.576	0.575	0.575	0.575	0.575
Canola:									
SOC	-	***		***	***		***	***	
SOC^2		***			*			***	
ln(SOC)			***			***			***
R^2	0.555	0.557	0.557	0.520	0.520	0.521	0.552	0.553	0.552
Barley:									
SOC	-	-		***	-		**	***	
SOC^2		-			-			***	
ln(SOC)			-			***			***
R^2	0.583	0.583	0.583	0.512	0.512	0.511	0.511	0.511	0.511
Durum Wheat:									
SOC	***	***		***	***		-	***	
SOC^2		***			**			**	
ln(SOC)			***			***			***
R^2	0.460	0.461	0.460	0.564	0.565	0.565	0.664	0.666	0.666
Lentils:									
SOC	**	**		**	-		-	*	
SOC^2		**			-			-	
ln(SOC)			**			**			***
R^2	0.365	0.366	0.366	0.325	0.325	0.325	0.618	0.620	0.621
Peas:									
SOC	**	-		-	**		***	***	
SOC^2		-			*			*	
ln(SOC)			**			***			-
R^2	0.441	0.441	0.441	0.414	0.414	0.414	0.479	0.479	0.479

Source: Authors' Estimates.
Notes: $^*p < 0.1$; $^{**}p < 0.05$; $^{***}p < 0.01$; and - is not statistically significant. Lin represents the linear functional form of soil organic carbon stocks, Quad is the quadratic form, and Log is the logarithmic form. All models are estimated using the Full sample of which includes all fields selected for soil organic carbon prediction from the Saskatchewan Crop Insurance Corporation confidential dataset. Please refer to Table 2.1 for information concerning regression results for the linear functional form. For the information on the regression results for the quadratic and logarithmic functional forms, please refer to Table 2D.2 in Appendix D.

TABLE 2D.4: Marginal Effect of Soil Organic Carbon on Crop Yield by Functional Form, Crop, and Soil Zone in Saskatchewan

	(1)	(2)	(3)	(4)	(5)	(6)	(7)	(8)	(9)
	Dependent Variable: Crop Yield								
Soil Zone:	*Brown*			*Dark Brown*			*Black & Gray*		
Func. Form:	Lin	Quad	Log	Lin	Quad (kg/ha)	Log	Lin	Quad	Log
Spring Wheat:									
$\mu_{SOC} + \sigma_{SOC}$		0.018***	0.018***		0.01***	0.005***		0.005***	0.004***
		(0.0061)	(0.0042)		(0.0015)	(0.0009)		(0.0007)	(0.0005)
μ_{SOC}	0.021***	0.025***	0.024***	0.01***	0.011***	0.007***	0.004***	0.007***	0.005***
	(0.006)	(0.0061)	(0.0055)	(0.001)	(0.0016)	(0.0012)	(0.001)	(0.0009)	(0.0007)
$\mu_{SOC} - \sigma_{SOC}$		0.033***	0.033***		0.012***	0.009***		0.008***	0.009***
		(0.0078)	(0.0077)		(0.0021)	(0.0012)		(0.0012)	(0.0012)
Canola:									
$\mu_{SOC} + \sigma_{SOC}$		0.006*	0.009***		0.003***	0.002***		0.003***	0.001***
		(0.0032)	(0.0027)		(0.001)	(0.0005)		(0.0004)	(0.0003)
μ_{SOC}	0.005	0.012***	0.012***	0.003***	0.004***	0.003***	0.003***	0.004***	0.002***
	(0.003)	(0.0043)	(0.0035)	(0.001)	(0.001)	(0.0007)	(0.0004)	(0.0005)	(0.0004)
$\mu_{SOC} - \sigma_{SOC}$		0.017***	0.017***		0.005***	0.004***		0.006***	0.003***
		(0.0059)	(0.0049)		(0.0013)	(0.001)		(0.0007)	(0.0007)
Barley:									
$\mu_{SOC} + \sigma_{SOC}$		0.012	0.01		0.01***	0.004***		0.004***	0.003***
		(0.0105)	(0.0082)		(0.0028)	(0.0013)		(0.0013)	(0.0008)
μ_{SOC}	0.012	0.016	0.013	0.01***	0.009***	0.005***	0.003**	0.006***	0.004***
	(0.011)	(0.0125)	(0.0106)	(0.003)	(0.0028)	(0.0017)	(0.001)	(0.0016)	(0.0011)
$\mu_{SOC} - \sigma_{SOC}$		0.021	0.018		0.007*	0.007***		0.008***	0.007***
		(0.0169)	(0.015)		(0.0038)	(0.0026)		(0.0021)	(0.0018)
Durum Wheat:									
$\mu_{SOC} + \sigma_{SOC}$		0.02***	0.018***		0.007***	0.007***		0.009**	0.008***
		(0.0031)	(0.0025)		(0.0022)	(0.0016)		(0.0037)	(0.0025)
μ_{SOC}	0.02***	0.028***	0.023***	0.007***	0.01**	0.009***	0.005	0.015***	0.012***
	(0.003)	(0.0039)	(0.0033)	(0.002)	(0.0025)	(0.0022)	(0.004)	(0.0052)	(0.0035)
$\mu_{SOC} - \sigma_{SOC}$		0.035***	0.033***		0.013***	0.013***		0.02***	0.019***
		(0.0053)	(0.0046)		(0.0035)	(0.0032)		(0.0073)	(0.0057)
Lentils:									
$\mu_{SOC} + \sigma_{SOC}$		0.006**	0.007**		0.004**	0.002**		0.003	0.007***
		(0.0028)	(0.0026)		(0.0019)	(0.0011)		(0.0036)	(0.0024)
μ_{SOC}	0.006**	0.011***	0.009**	0.004**	0.005**	0.003***	0.002	0.007	0.009***
	(0.003)	(0.0039)	(0.0034)	(0.002)	(0.0022)	(0.0015)	(0.004)	(0.0046)	(0.0034)
$\mu_{SOC} - \sigma_{SOC}$		0.015***	0.012**		0.005*	0.005**		0.011*	0.016***
		(0.0055)	(0.0048)		(0.0028)	(0.0022)		(0.0064)	(0.0056)
Peas:									
$\mu_{SOC} + \sigma_{SOC}$		0.011**	0.009**		0.003	0.004***		0.005***	0.001
		(0.0045)	(0.004)		(0.0022)	(0.0014)		(0.0014)	(0.0009)
μ_{SOC}	0.011**	0.014**	0.012**	0.003	0.006**	0.005***	0.004***	0.006***	0.002
	(0.004)	(0.0059)	(0.0052)	(0.002)	(0.0025)	(0.0019)	(0.001)	(0.0018)	(0.0012)
$\mu_{SOC} - \sigma_{SOC}$		0.017**	0.017**		0.008**	0.008***		0.008***	0.003
		(0.0083)	(0.0073)		(0.0033)	(0.0028)		(0.0024)	(0.0021)

Source: Authors' Estimates.

Notes: $^{*}p < 0.1$; $^{**}p < 0.05$; $^{***}p < 0.01$. Lin represents the linear functional form of soil organic carbon stocks, Quad is the quadratic form, and Log is the logarithmic form. All models are estimated using the Full sample of which includes all fields selected for soil organic carbon prediction from the Saskatchewan Crop Insurance Corporation confidential dataset. Please refer to Table 2.1 for information concerning regression results for the linear functional form. For the information on the regression results for the quadratic and logarithmic functional forms, please refer to Table 2D.2 in Appendix D.

TABLE 2D.5: Shadow Value of Soil Organic Carbon by Functional Form, Crop, and Soil Zone in Saskatchewan

	(1)	(2)	(3)	(4)	(5)	(6)	(7)	(8)	(9)
Soil Zone:		*Brown*			*Dark Brown*			*Black & Gray*	
Func. Form:	Lin	Quad	Log	Lin	Quad	Log	Lin	Quad	Log
					(2023 CAD/ha/yr)/(Mg of SOC/ha)				
Spring Wheat:									
$\mu_{SOC} + \sigma_{SOC}$		6.55***	6.85***		3.84***	1.94***		1.81***	1.44***
		(2.27)	(1.58)		(0.55)	(0.35)		(0.28)	(0.19)
μ_{SOC}	7.83***	9.35***	8.84***	3.73***	4.18***	2.57***	1.49***	2.45***	2.02***
	(2.24)	(2.27)	(2.03)	(0.37)	(0.61)	(0.46)	(0.37)	(0.34)	(0.27)
$\mu_{SOC} - \sigma_{SOC}$		12.15***	12.45***		4.52***	3.36***		3.08***	3.36***
		(2.9)	(2.86)		(0.79)	(0.45)		(0.44)	(0.45)
Canola:									
$\mu_{SOC} + \sigma_{SOC}$		4.79*	7.19***		2.02***	1.73***		2.32***	1.1***
		(2.48)	(2.1)		(0.74)	(0.41)		(0.34)	(0.22)
μ_{SOC}	3.88	9.02***	9.27***	2.33***	2.84***	2.3***	2.33***	3.31***	1.54***
	(2.33)	(3.3)	(2.7)	(0.78)	(0.76)	(0.54)	(0.31)	(0.42)	(0.31)
$\mu_{SOC} - \sigma_{SOC}$		13.25***	13.06***		3.65***	3.42***		4.3***	2.55***
		(4.56)	(3.81)		(1.01)	(0.81)		(0.55)	(0.51)
Barley:									
$\mu_{SOC} + \sigma_{SOC}$		5.48	4.6		4.76***	1.65***		1.74***	1.36***
		(4.88)	(3.84)		(1.31)	(0.61)		(0.58)	(0.36)
μ_{SOC}	5.59	7.6	5.93	4.66***	3.99***	2.2***	1.4**	2.72***	1.91***
	(5.13)	(5.82)	(4.96)	(1.4)	(1.3)	(0.81)	(0.47)	(0.72)	(0.5)
$\mu_{SOC} - \sigma_{SOC}$		9.72	8.35		3.23*	3.27***		3.69***	3.17***
		(7.89)	(6.98)		(1.75)	(1.2)		(0.97)	(0.83)
Durum Wheat:									
$\mu_{SOC} + \sigma_{SOC}$		8.79***	7.98***		3.19***	2.89***		4.09**	3.7***
		(1.38)	(1.12)		(0.97)	(0.72)		(1.63)	(1.09)
μ_{SOC}	8.84***	12.16***	10.29***	3.09***	4.56**	3.84***	2.21	6.57***	5.17***
	(1.33)	(1.72)	(1.45)	(0.88)	(1.11)	(0.96)	(1.77)	(2.28)	(1.53)
$\mu_{SOC} - \sigma_{SOC}$		15.53***	14.5***		5.92***	5.71***		9.06***	8.6***
		(2.34)	(2.04)		(1.55)	(1.42)		(3.21)	(2.54)
Lentils:									
$\mu_{SOC} + \sigma_{SOC}$		4.71**	4.91**		3.2**	1.72**		2.32	4.87***
		(2.04)	(1.91)		(1.37)	(0.8)		(2.65)	(1.77)
μ_{SOC}	4.37**	7.81***	6.33**	2.91**	3.57**	2.28***	1.46	5.22	6.81***
	(2.18)	(2.8)	(2.46)	(1.46)	(1.58)	(1.06)	(2.91)	(3.33)	(2.47)
$\mu_{SOC} - \sigma_{SOC}$		10.91***	8.91**		3.94*	3.39**		8.11*	11.32***
		(3.98)	(3.47)		(2.07)	(1.58)		(4.63)	(4.11)
Peas:									
$\mu_{SOC} + \sigma_{SOC}$		4.95**	4.1**		1.32	1.71***		2.12***	0.58
		(1.99)	(1.78)		(0.99)	(0.63)		(0.63)	(0.39)
μ_{SOC}	4.85**	6.16**	5.29**	1.32	2.43**	2.27***	1.76***	2.78***	0.81
	(1.76)	(2.61)	(2.3)	(0.88)	(1.09)	(0.84)	(0.44)	(0.79)	(0.54)
$\mu_{SOC} - \sigma_{SOC}$		7.38**	7.45**		3.53**	3.38***		3.45***	1.35
		(3.67)	(3.23)		(1.47)	(1.25)		(1.07)	(0.9)

Source: Authors' Estimates.

Notes: $^{*}p < 0.1$; $^{**}p < 0.05$; $^{***}p < 0.01$. Lin represents the linear functional form of soil organic carbon stocks, Quad is the quadratic form, and Log is the logarithmic form. All models are estimated using the Full sample of which includes all fields selected for soil organic carbon prediction from the Saskatchewan Crop Insurance Corporation confidential dataset. Please refer to Table 2.1 for information concerning regression results for the linear functional form. For the information on the regression results for the quadratic and logarithmic functional forms, please refer to Table 2D.2 in Appendix D.

TABLE 2D.6: Marginal Product of Soil Organic Carbon on Spring Wheat Yield by
Soil Zone in Saskatchewan - Fertilizer Use Effects

	Dependent Variable: Crop Yield
	(1)	(2)	(3)	(4)	(5)	(6)
Soil Zone:	*Brown*		*Dark Brown*		*Black & Gray*	
Sample:	SMP	SMP	SMP	SMP	SMP	SMP
Spring Wheat:			*(kg/ha)*			
Soil Organic Carbon	0.024***	0.024***	0.011***	0.010***	0.003***	0.003***
	(0.009)	(0.009)	(0.002)	(0.002)	(0.001)	(0.001)
Nitrogen Use		2.496		5.750***		9.462***
		(1.581)		(0.827)		(0.86)
Observations	2,050	2,050	12,245	12,245	36,033	36,033
R^2	0.515	0.517	0.545	0.561	0.505	0.532

Source: Authors' Estimates.
Notes: $^*p < 0.1;^{**}\ p < 0.05;^{***}\ p < 0.01$. For more information, please refer to the notes from Table 2.1.

TABLE 2D.7: Marginal Product of Soil Organic Carbon on Spring Wheat Yield by
Sample and Soil Zone in Saskatchewan - Field and Year Fixed Effects

	Dependent Variable: Crop Yield					
	(1)	(2)	(3)	(4)	(5)	(6)
Soil Zone:	*Brown*		*Dark Brown*		*Black & Gray*	
Sample:	Full	SMP	Full	SMP	Full	SMP
Spring Wheat:			*(kg/ha)*			
Soil Organic Carbon	−0.022	−0.031	0.052***	−0.032	0.046***	−0.033**
	(0.026)	(0.076)	(0.012)	(0.025)	(0.008)	(0.015)
Nitrogen Use		1.917		3.691***		4.577***
		(3.485)		(1.062)		(0.879)
Observations	8,172	2,356	35,419	13,127	98,233	38,249
R^2	0.703	0.815	0.735	0.794	0.721	0.775

Source: Authors' Estimates.
Notes: $^*p < 0.1$;$^{**}p < 0.05$;$^{***}p < 0.01$. All regression models include field fixed effects. For more information, please refer to the notes from Table 2.1.

TABLE 2D.8: Marginal Product of Soil Organic Carbon on Spring Wheat Yield by Sample and Soil Zone in Saskatchewan - Field and No Year Fixed Effects

	(1)	(2)	(3)	(4)	(5)	(6)
	Dependent Variable: Crop Yield					
Soil Zone:	*Brown*		*Dark Brown*		*Black & Gray*	
Sample:	Full	SMP	Full	SMP	Full	SMP
Spring Wheat:			*(kg/ha)*			
Soil Organic Carbon	0.097***	−0.022	0.124***	0.004	0.157***	0.026
	(0.021)	(0.064)	(0.011)	(0.021)	(0.008)	(0.016)
Nitrogen Use		2.632		4.440***		5.763***
		(3.748)		(1.21)		(0.984)
Observations	8,172	2,356	35,419	13,127	98,233	38,249
R^2	0.658	0.79	0.682	0.757	0.656	0.731

Source: Authors' Estimates.
Notes: $^*p < 0.1$;$^{**} p < 0.05$;$^{***} p < 0.01$. All regression models include field fixed effects and do not include year fixed effects. For more information, please refer to the notes from Table 2.1.

TABLE 2D.9: Linear Trend of Soil Organic Carbon within fields by Crop, Sample, and Soil Zone in Saskatchewan

| | Dependent Variable: Soil Organic Carbon | | |
	(1)	(2)	(3)
Soil Zone:	**Brown**	**Dark Brown**	**Black & Gray**
Sample:	Full	Full	Full
Spring Wheat:		*(kg/ha)*	
Year	215.637***	309.833***	366.940***
	(6.371)	(3.523)	(2.437)
Observations	11,285	43,836	118,151
R^2	0.995	0.997	0.999
Canola:			
Year	279.531***	316.379***	347.823***
	(11.898)	(3.119)	(2.408)
Observations	4,821	48,523	170,163
R^2	0.996	0.997	0.998
Barley:			
Year	232.881***	325.980***	352.431***
	(26.064)	(5.521)	(2.973)
Observations	2,514	13,927	44,528
R^2	0.996	0.998	0.999
Durum Wheat:			
Year	220.233***	286.036***	341.597***
	(4.557)	(5.023)	(21.381)
Observations	24,327	22,742	3,139
R^2	0.992	0.997	0.999
Lentils:			
Year	274.450***	311.599***	332.898***
	(8.88)	(4.939)	(18.64)
Observations	7,455	15,397	2,223
R^2	0.995	0.997	0.999
Peas:			
Year	240.959***	315.323***	358.596***
	(11.589)	(6.318)	(5.011)
Observations	4,220	13,805	23,685
R^2	0.997	0.998	0.999

Source: Authors' Estimates.

Notes: $^*p < 0.1$;$^{**}p < 0.05$;$^{***}p < 0.01$. All regression models include field fixed effects.

TABLE 2D.10: Marginal Product of Soil Organic Carbon on Spring Wheat Yield by
Sample and Soil Zone in Saskatchewan - RM and No Year Fixed Effects

| | Dependent Variable: Crop Yield | | | | | |
	(1)	(2)	(3)	(4)	(5)	(6)
Soil Zone:	*Brown*		*Dark Brown*		*Black & Gray*	
Sample:	Full	SMP	Full	SMP	Full	SMP
Spring Wheat:			*(kg/ha)*			
Soil Organic Carbon	0.030***	0.022**	0.012***	0.010***	0.006***	0.003***
	(0.006)	(0.009)	(0.002)	(0.002)	(0.001)	(0.001)
Nitrogen Use		3.084*		5.846***		9.880***
		(1.628)		(0.842)		(0.889)
Observations	7,425	2,050	33,174	12,245	92,608	36,033
R^2	0.413	0.474	0.511	0.506	0.494	0.472

Source: Authors' Estimates.
Notes: $^*p < 0.1;^{**} p < 0.05;^{***} p < 0.01$. All regression models do not include year fixed effects. For more information, please refer to the notes from Table 2.1.

Appendix 2E: Dynamic Simulation Supplementary Material

TABLE 2E.1: Ten-Fold Cross Validation for the State Equation of Soil Organic Carbon by Soil Zone in Saskatchewan

	(1)	(2)
Cropping Sequence	*Brown Soil Zone*	
Lag Length	RMSE	R^2
1	438	0.66
2	388	0.74
3	375	0.75
4	352	0.78
	Dark Brown Soil Zone	
	RMSE	R^2
1	505	0.58
2	458	0.66
3	439	0.69
4	412	0.72
	Black & Gray Soil Zone	
	RMSE	R^2
1	610	0.50
2	570	0.57
3	544	0.61
4	515	0.65

Source: Authors' Estimates.

Notes: All deviation statistics are computed using the results from the fitted state equation (equation (2.13)) varying by the cropping sequence lag length. RMSE is Root Mean Squared Error. The RMSE and R^2 values are computed as the averages across ten folds from fitting the state equation on a randomly selected "training" dataset and estimating the model on a randomly selected "testing" dataset. All fitted stated equations are estimated using Rural Municipality and year fixed effects, and are weighted by field hectares.

TABLE 2E.2: Top Ten Rotations by Crop and Soil Zone in Saskatchewan from 2015 to 2019

	(1)	(2)
Rotation	Fields	(%)
Brown Soil Zone:		
pulse-cereal-pulse-cereal	1,291	7.1
cereal-cereal-cereal-cereal	1,221	6.7
cereal-pulse-cereal-pulse	1,078	5.9
cereal-fallow-cereal-fallow	655	3.6
fallow-cereal-fallow-cereal	532	2.9
cereal-pulse-cereal-fallow	489	2.7
cereal-pulse-cereal-oilseed	438	2.4
pulse-cereal-fallow-cereal	406	2.2
oilseed-cereal-pulse-cereal	405	2.2
cereal-oilseed-pulse-cereal	382	2.1
Percent of Total		**37.9**
Dark Brown Soil Zone:		
cereal-oilseed-cereal-oilseed	4,267	8.5
oilseed-cereal-oilseed-cereal	4,205	8.4
oilseed-pulse-cereal-oilseed	1,530	3.1
cereal-oilseed-pulse-cereal	1,406	2.8
pulse-cereal-oilseed-cereal	1,354	2.7
oilseed-cereal-pulse-cereal	1,029	2.1
cereal-pulse-cereal-oilseed	1,003	2.0
oilseed-cereal-oilseed-fallow	987	2.0
cereal-oilseed-cereal-pulse	980	2.0
pulse-cereal-oilseed-pulse	857	1.7
Percent of Total		**35.1**
Black & Gray Soil Zone:		
oilseed-cereal-oilseed-cereal	23,030	20.2
cereal-oilseed-cereal-oilseed	22,575	19.8
oilseed-cereal-oilseed-fallow	3,988	3.5
oilseed-oilseed-cereal-oilseed	3,320	2.9
oilseed-cereal-oilseed-oilseed	2,676	2.4
oilseed-fallow-oilseed-fallow	2,632	2.3
oilseed-fallow-oilseed-cereal	2,608	2.3
fallow-oilseed-cereal-oilseed	2,601	2.3
cereal-oilseed-fallow-oilseed	2,571	2.3
fallow-oilseed-fallow-oilseed	2,245	2.0
Percent of Total		**59.9**

Source: Authors' Estimates by construction from the Saskatchewan Crop Insurance database. Percent of Total represents the percent of the top ten crop rotations relative to all crop rotations in that respective soil zone employed from 2015 to 2019.

TABLE 2E.3: Soil Organic Carbon State Equation by Functional Form and Soil Zone in Saskatchewan

	(1)	(2)	(3)	(4)	(5)	(6)	(7)	(8)	(9)
				Dependent Variable: Change in Soil Organic Carbon					
Soil Zone:		*Brown*			*Dark Brown*			*Black & Gray*	
Func. Form:	Lin	Quad	Log	Lin	Quad *(kg/ha)*	Log	Lin	Quad	Log
lag(SOC)	−0.00445*** (0.00026)	−0.00509*** (0.00134)		−0.00207*** (0.00015)	0.00110* (0.00058)		−0.00176*** (0.00007)	−0.00036 (0.00024)	
lag(SOC^2)		0.000000009 (0.00000002)			−0.00000003*** (0.000000006)			−0.00000001*** (0.000000002)	
lag(ln(SOC))			−145.10*** (8.85)			−65.81*** (5.01)			−78.09*** (3.32)
lag(Yield$_{SpringWheat}$)	0.35365*** (0.00790)	0.35366*** (0.00790)	0.35344*** (0.00789)	0.25434*** (0.00441)	0.25481*** (0.00439)	0.25351*** (0.00441)	0.19790*** (0.00305)	0.19833*** (0.00305)	0.19679*** (0.00305)
lag(Yield$_{Canola}$)	0.72550*** (0.02551)	0.72554*** (0.02552)	0.72569*** (0.02557)	0.53419*** (0.00641)	0.53461*** (0.00638)	0.53336*** (0.00642)	0.36516*** (0.00615)	0.36550*** (0.00619)	0.36385*** (0.00612)
lag(Yield$_{Barley}$)	0.24138*** (0.01195)	0.24141*** (0.01196)	0.24151*** (0.01194)	0.17349*** (0.00573)	0.17402*** (0.00575)	0.17298*** (0.00575)	0.14823*** (0.00353)	0.14842*** (0.00353)	0.14773*** (0.00353)
lag(Yield$_{DurumWheat}$)	0.37677*** (0.00557)	0.37682*** (0.00557)	0.37676*** (0.00557)	0.29408*** (0.00472)	0.29354*** (0.00471)	0.29389*** (0.00475)	0.22207*** (0.00976)	0.22179*** (0.00980)	0.22232*** (0.00975)
lag(Yield$_{Lentils}$)	0.32276*** (0.01214)	0.32275*** (0.01214)	0.32245*** (0.01214)	0.18907*** (0.00963)	0.18860*** (0.00963)	0.18875*** (0.00965)	0.02866 (0.02373)	0.02932 (0.02383)	0.02701 (0.02369)
lag(Yield$_{Peas}$)	0.16343*** (0.01179)	0.16347*** (0.01179)	0.16373*** (0.01170)	0.06830*** (0.00686)	0.06835*** (0.00686)	0.06775*** (0.00688)	0.01660*** (0.00522)	0.01661*** (0.00522)	0.01611*** (0.00523)
lag(TAP)	1.38784*** (0.06761)	1.38708*** (0.06749)	1.38446*** (0.06765)	1.71913*** (0.03933)	1.71594*** (0.03924)	1.72364*** (0.03942)	1.67749*** (0.03502)	1.68000*** (0.03512)	1.67732*** (0.03497)
lag(GSAT)	−107.54860*** (4.98508)	−107.63830*** (4.96999)	−108.03570*** (4.98017)	−82.06371*** (2.95836)	−82.10233*** (2.96486)	−81.97311*** (2.93283)	−120.82830*** (2.37296)	−120.59040*** (2.35965)	−120.17900*** (2.37922)
Constant	1,023.131*** (87.619)	1,035.330*** (88.336)	2,385.843*** (133.156)	516.889*** (44.592)	456.178*** (44.741)	1,116.271*** (67.614)	1,122.867*** (29.821)	1,081.502*** (30.228)	1,858.876*** (49.412)
Goodness-of-Fit Statistics:									
Observations	53,837	53,837	53,837	163,246	163,246	163,246	377,593	377,593	377,593
R^2	0.741	0.741	0.741	0.684	0.685	0.684	0.580	0.580	0.579

Source: Authors' Estimates.

Notes: $^*p < 0.1$; $^{**}p < 0.05$; $^{***}p < 0.01$. Lin represents the linear functional form of soil organic carbon stocks, Quad is the quadratic form, and Log is the logarithmic form. All models are estimated using the Full sample of which includes all fields selected for soil organic carbon prediction from the Saskatchewan Crop Insurance Corporation confidential dataset. All models include cropping sequence control variables for the cropping sequence on a field over previous two years. Table 2E.1 in Appendix E includes the ten-fold cross validation results (RMSE and R^2) for the soil organic carbon state equation estimated with various cropping sequence lag lengths.

Chapter 3

Harvesting Benefits: Exploring the Effects of Second-Best Policies on Enhancing Soil Organic Carbon Stocks in Agriculture

3.1 Introduction

In the agricultural sector, policies that incentivize farmers to increase the stock of soil organic carbon (SOC) and reduce atmospheric carbon dioxide are potential instruments for pursuing climate change goals. While carbon emissions from agricultural activities that stem from both crop and livestock farming contribute significantly to climate change, farms can also serve as carbon sinks, sequestering and reducing atmospheric carbon. Incentivizing agricultural practices that enhance the stock of SOC presents a novel avenue for farmers to not only contribute to environmental sustainability, but also economically benefit from their stewardship of the land. Farmers can augment SOC through various farm management techniques, such as increasing carbon inputs through crop selection or slowing SOC decomposition by forgoing tillage practices. Consequently, policies encouraging production methods that foster additional carbon storage are garnering attention

231

from policymakers worldwide.

If the aim is to reduce atmospheric carbon by increasing SOC sequestration on farms, basic economic principles suggest that the first-best policy would involve taxing emissions and providing subsidies for carbon that is sequestered directly. In the agricultural sector, such policies are often disregarded due to the physical challenges and high costs associated with accurately measuring farm emissions, and in most cases require advanced scientific expertise to develop (Weersink et al., 1998; Oldfield et al., 2022).[1] However, second-best policies that subsidize or tax farming practices that produce by-products with external benefits or costs can be economically viable, albeit less efficient than first-best policies (Garnache et al., 2017). Second-best policies for carbon sequestration may include the development of a privately funded carbon offset program for specific farming practices, offering discounts on crop insurance premiums for crops that increase SOC, or public subsidization of agricultural practices that increase SOC.[2] Currently, there are a limited number of programs that pay farmers to adopt management practices specifically to enhance the stock of SOC.[3]

In this essay, I explore the potential effectiveness of theoretical policies aimed at encouraging the adoption of practices that enhance the stock of SOC on Saskatchewan farms. More specifically, I study the effect of a subsidy applied on planting additional hectares of canola and examine how it influences the stock of SOC in Saskatchewan.[4] I focus exclusively on subsidizing additional canola hectares induced by a canola subsidy. This approach aligns with ongoing implementation

[1]The process of accurately measuring specific externalities is often detailed and described as measurement, reporting, and verification (MRV) protocol (Oldfield et al., 2022).

[2]An example of a government-operated carbon trading system is the Emissions Reduction Fund in Australia, managed by the Clean Energy Regulator. This voluntary program encourages the adoption of various practices and technologies across different sectors to reduce net GHG emissions. Specifically, in agriculture, it rewards farmers with Carbon Credit Units for engaging in certain projects, such as applying particular nutrients or planting pasture, aimed at reducing emissions or storing GHGs (Australian Government, 2022).

[3]Notable programs around the world that pay farmers to adopt management practices aimed at enhancing carbon sequestration and soil health include: Indigo Ag and Nori in the United States, the Emissions Reduction Fund in Australia, the Kenya Agriculture Carbon Project, and the Green Low-Carbon Agri-Environmental Scheme (GLAS) in Ireland (Raina et al., 2024).

[4]In this analysis, I do not examine the effects of changing cropping intensity and cropping sequences on yield with respect to increased canola production. Johnston et al. (2005) find that in Melfort, Saskatchewan seeding canola on canola (monoculture) led to lower crop yields relative to rotating other crops such as spring wheat, barley, flax, or peas. Johnston et al. (2005) state that the lower crop yield for monoculture production systems is related to the increase in major pathogens that affect crop productivity.

of policies that subsidize farmers to adopt specific management practices (see Agriculture and Agri-Food Canada (2023), Wongpiyabovorn and Plastina (2023), and Agri-Pulse Communications (2024)). However, this does not mean that subsidizing all hectares of canola is an infeasible policy. Payments made to farmers based on management practices can be awarded on all hectares, but, only providing payments to practices that are not "business-as-usual" (BAU) is essential for a sustainable carbon market (Raina et al., 2024).[5] Limiting payment to additional (not BAU) hectares ensures that payments are only awarded on practices that result in policy-induced atmospheric carbon reductions, rather than providing payments to practices that would have existed without the policy.

There are many studies that examine the effects of carbon credit payments made to producers for sequestering carbon in the soil. Many of these studies focus on how carbon credit payments affect program adoption, contract length, the amount of carbon sequestered, measurement costs, and farm profitability (Antle et al., 2001; Mooney et al., 2004a,b; Gulati and Vercammen, 2005; Mooney et al., 2007; Bangsund and Leistritz, 2008; Antle and Ogle, 2012; Bamière et al., 2021; Mishra et al., 2021). Most of these studies develop an economic simulation model that incorporates acreage responses and SOC dynamics, also known as an integrated assessment model (Antle et al., 2001). They typically rely on carbon sequestration rates based on management practices from the IPCC guidelines, or employ biogeochemical models like Century or DayCent. These studies primarily focus on the effects of carbon payments or credits that subsidize changes in SOC directly (Antle et al., 2001; Mooney et al., 2004a,b, 2007; Bangsund and Leistritz, 2008; Antle and Ogle, 2012; Bamière et al., 2021; Mishra et al., 2021), with little attention on examining the effects of programs that pay per hectare for changes in farm management practices that are additional.[6] Hence, the effectiveness of second-best policies that aim to increase carbon sequestration on agricultural soils is understudied, and filling this gap in the literature is the goal of this essay.

---

[5]Wongpiyabovorn et al. (2024) state that payments for conservation practices that are not additional, or equivalently BAU, run the risk of being cost ineffective.

[6]Mooney et al. (2004a) examine the effects of a subsidy for adopting conservation land management practices, but these payments are not linked to the quantity of carbon stored in the soil. In this essay, I use an SOC prediction model called the Augmented Campbell model, linking subsidy payments from changes in cropping choices to the generated external social benefit from additional sequestered SOC.

This essay seeks to answer three questions about second-best polices for agricultural carbon sequestration: (1) How effective would a canola subsidy be at enhancing SOC stocks throughout Saskatchewan? (2) What would be the net external social benefit (NESB) and change in welfare from carbon sequestration attributable to an optimal subsidy on canola? and (3) What scientific and administrative conditions are necessary in order for carbon sequestration policies to be cost-effective and feasible? Here, the NESB is equal to the external social benefit resulting from carbon sequestration via expanded canola hectares after the policy costs involved have been subtracted. The change in welfare is the NESB plus the change in producer surplus. To answer these questions, I use standard economic theory to determine the optimal canola subsidy for either maximizing the NESB or the change in welfare. I develop a simulation model that employs a novel field-level dataset from the Saskatchewan Crop Insurance Corporation (SCIC) to simulate the effects of implementing a hypothetical canola subsidy for each soil zone in Saskatchewan. The simulation model incorporates acreage responses and SOC dynamics to determine how much carbon is stored as a result of implementing a canola subsidy relative to BAU cropping choices. All simulations start in 2019 and persist indefinitely into the future.

To determine the acreage responses to a canola subsidy, I develop an acreage choice model following the framework developed by Moreno and Sunding (2005), Carpentier and Letort (2014), and Koutchadé et al. (2021).[7] My analysis employs a discrete choice model incorporating both Multinomial Logit (MNL) and Nested Logit (NL) models, leveraging cropping choice data at the field level from the SCIC to estimate the acreage response to expected profits for each crop.[8] To compute how much carbon is stored in the soil as a result of additional canola hectares, I estimate a SOC state equation for each soil zone in Saskatchewan. I employ field-level simulated SOC stock data from Serfas (2024a) spanning 1998–2019. The SOC state equation predicts changes in the stock of SOC using aggregated information on cropping shares by soil zone, where each SOC state equation is a representative field for each soil zone in Saskatchewan. An aggregate approach

---

[7]The acreage choice model in this essay is most similar to the Nested Logit (NL) model devised by Moreno and Sunding (2005), who compute the price elasticity for adopting irrigation technology in California at the field level.

[8]Past studies have typically employed crop shares by farm, allowing for the estimation of MNL or ML models using methods like Ordinary Least Squares (OLS), Instrumental Variables (IV), or General Method of Moments (GMM) (Berry, 1994).

to predicting SOC stocks is preferred as it contains less uncertainty in SOC predictions (Oldfield et al., 2022).[9]

In the simulation model, I compute optimal canola subsidies that maximize NESB in the brown, dark brown, and black & gray soil zones of 324.40 CAD/ha/yr, 205.43 CAD/ha/yr and 226.02 CAD/ha/yr. The optimal canola subsidies that maximize the change in welfare are 648.80 CAD/ha/yr in the brown soil zone, 410.86 CAD/ha/yr in the dark brown soil zone, and 452.05 CAD/ha/yr in the black & gray soil zone. These results are computed using a rental rate for carbon reflecting a social cost of carbon (SCC) of 185 USD/Mg of CO_2 (Rennert et al., 2022), and acreage responses that are estimated from the NL model. When the NESB is maximized, the average policy-induced changes in the stock of SOC compared to BAU practices for all insured hectares are 31.81 kg/ha/yr in the brown soil zone, 52.20 kg/ha/yr in the dark brown soil zone, and 76.49 kg/ha/yr in the black and gray soil zone. These simulated changes in SOC stocks represent approximately 15–20% of the historical average annual change in SOC stocks by soil zone from 1998 to 2019 (Serfas, 2024a). The external social benefit from implementing soil zone-specific optimal canola subsidies that maximizes NESB on all insured hectares in Saskatchewan is 15.2 billion CAD. If the optimal canola subsidies maximize the change in welfare, the external social benefit is 30.4 billion CAD.

I also compute the external cost of the policy from additional nitrous oxide emissions associated with higher fertilizer rates for canola, equal to 666 million CAD when maximizing the NESB and 1.3 billion CAD when maximizing the change in welfare. These costs account for 4.5% of the external social benefits generated from implementing an optimal canola subsidy that maximizes either the NESB or change in welfare for all insured hectares in Saskatchewan.

This essay follows as such: Section 3.2 discusses the current private and public funding for

---

[9]Oldfield et al. (2022) state: "Protocols that use model-based estimates of net-GHG reductions that result from shifts in management practices avoid the need for intensive sampling and can issue credits annually. Process-based biogeochemical models can, in theory, be deployed at different scales from subfield to farm to region. However, limited precision associated with model inputs can increase uncertainty at the site level; thus, process-based models generally do not provide accurate estimates for a single field, especially without detailed site specific data. Uncertainty is inversely related to scale in process-model estimates of SOC changes, with uncertainties of 20% at a US national scale growing to 600 to 700% at the site scale. Thus, models alone are inadequate for soil C estimation at small scales unless there has been considerable calibration in the areas and for the crops over which the model is used."

carbon sequestrated on farms in Canada and the United States; Section 3.3 provides an economic framework used to derive the optimal canola subsidies that maximize the NESB or the change in welfare; Section 3.4 discusses the conceptual framework for the acreage choice model; Section 3.5 and 3.6 derive the MNL and NL estimators for the acreage choice model and the acreage elasticities; Section 3.7 and 3.8 provide a description of the data and estimation results; Sections 3.9 and 3.10 provide the derivation of the simulation model and the simulated results; Section 3.11 provides estimates of nitrous oxide emissions from implementing a canola subsidy; and Section 3.12 concludes.

3.2 Initiatives for Carbon Sequestration Funding in Canada and the United States

In Canada, significant public funds are dedicated to environmental conservation initiatives, as well as policies concerning agricultural carbon sequestration. The Sustainable Canadian Agricultural Partnership allocates 3.5 billion CAD toward on-farm environmental stewardship programs (Environment and Climate Change Canada, 2023a). A component of the Sustainable Canadian Agricultural Partnership is the On-Farm Climate Action Fund (OFCAF) (Agriculture and Agri-Food Canada, 2023), which receives 704.1 million CAD in funding farm management practices that tackle climate change. OFCAF is part of the Government of Canada's Agricultural Climate Smart Solutions initiative, which is part of the broader Natural Climate Solutions Fund with total funding of 4 billion CAD over the coming decade and is managed jointly by Natural Resources Canada, Environment and Climate Change Canada, and Agriculture and Agri-Food Canada (Agriculture and Agri-Food Canada, 2023). OFCAF disburses payments to farmers for the adoption of beneficial management practices, with environmental objectives focused on reducing net GHG emissions through enhanced nitrogen management, the implementation of cover cropping, and the adoption of rotational grazing practices. These payments for beneficial management practices can be facilitated through various entities, including governmental organizations, non-profit organizations, for-profit entities, producer groups, commodity organizations, indigenous groups, and

other non-governmental organizations (Agriculture and Agri-Food Canada, 2023).

In the United States, the Biden administration is exploring ways to compensate farmers for engaging in carbon sequestration efforts (McCauley, 2021). Similarly, private entities are examining the role of agriculture in producing carbon offsets. For instance, Microsoft has secured a deal for 100,000 tonnes of carbon credits for additional carbon stored in the soil with Truterra, a sustainability venture of the Land O'Lakes dairy cooperative (Ellis, 2021). The United States Department of Agriculture (USDA) currently supports programs aimed at improving soil health and addressing resource issues like water and energy conservation. Prominent among these are the Environmental Quality Incentives Program (EQIP) and the Conservation Stewardship Program (CSP), both overseen by the Natural Resource Conservation Service (NRCS) (Wongpiyabovorn and Plastina, 2023). Farmers participating in these programs can receive financial payments for implementing practices such as no-till farming or planting cover crops. Payment rates under these programs vary, with EQIP offering between 7.50 USD/ac/yr (24.83 CAD/ha/yr) and 40.86 USD/ac/yr (135.30 CAD/ha/yr) for cover crop adoption. The average payment for adopting no-till is around 11.06 USD/ac/yr (36.62 CAD/ha/yr) through EQIP and 7.50 USD/ac/yr (24.83 CAD/ha/yr) through CSP. Wongpiyabovorn and Plastina (2023) note that these payments reflect NRCS cost estimates and can vary by region, and in farming practices and expenses.

Emerging initiatives like Farmers for Soil Health are also noteworthy, using DTN's Ecofield farm data platform and satellite imagery to authenticate and remunerate farmers for cover crop adoption (Agri-Pulse Communications, 2024).[10] Additionally, the Alliance to Advance Climate-Smart Agriculture has been granted 80 million USD by the NRCS to fund pilot projects in soil and water conservation districts across Arkansas, Minnesota, North Dakota, and Virginia. These projects are set to directly benefit over 4,000 farmers with payments totaling up to 57 million USD, with the remainder allocated for project management and research. Payments for adopting climate-smart agricultural practices on cropland could reach up to 100 USD/ac/yr, capped

---

[10]More details about Farmers for Soil Health can be found at their website `https://farmersforsoilhealth.com`.

at 160 acres per FSA farm number,[11] and include a climate-smart certification for participating farmers. Eligible practices for these payments include cover cropping, no-till farming, nutrient management, precision nutrient management, conservation crop rotation, and the establishment of pasture and hay.[12]

3.3 Optimal Canola Subsidies

In this essay, I propose to subsidize canola production because each hectare of canola generates an external social benefit from carbon sequestration equal to ESB (2023 CAD/ha/yr). I solve for the optimal subsidy rate, τ (2023 CAD/ha/yr) on policy-induced incremental hectares, that maximize either (1) the benefits from reduced externalities (i.e., the quantity of carbon sequestered) for given subsidy expenditure, or net external social benefits (NESB), or (2) total social benefits or welfare from consumption and production. For convenience, I assume linear supply and a small open economy such that prices are exogenous. In this case, when the subsidy is applied, the change in hectares (ΔA) is equal to the subsidy rate multiplied by the slope of the acreage response function, $\beta : \Delta A = \beta \times \tau$. As a consequence of this change in hectares, the externality costs are reduced by an amount equal to $ESB \times \Delta A = ESB \times \beta \times \tau$. The cost of the subsidy expenditure is equal to: $\tau \times \Delta A = \beta \times \tau^2$. Associated with the policy-induced increase in hectares is an increase in producer surplus equal to $\frac{1}{2}(\tau \times \Delta A) = \frac{1}{2}(\beta \times \tau^2)$.

Net external social benefits are equal to the change in externality cost minus the cost of the subsidy expenditure (i.e., equal to total social surplus or welfare minus the change in producer surplus):

$$NESB = (ESB \times \beta \times \tau) - (\beta \times \tau^2) \tag{3.1}$$

---

[11] Farm Service Agency (FSA) is an agency of the USDA that serves farmers through delivering agricultural programs. A Farm Number is required to obtain access to various USDA programs, as well as be counted in the USDA's Agricultural Census.

[12] For more information on the Alliance to Advance Climate-Smart Agriculture, visit their website at https://www.allianceforcsa.org.

Taking the derivative with respect to τ and setting the result equal to zero yields $\tau^* = \frac{1}{2}ESB$. The optimal subsidy in this case is exactly half the conventional optimal Pigovian subsidy.

Total social benefits or welfare are maximized when the change in welfare is maximized. The change in welfare is equal to the change in externality cost, plus the change in producer surplus, minus the cost of the subsidy expenditure:

$$\Delta W = (ESB \times \beta \times \tau) - (\beta \times \tau^2) + \frac{1}{2}(\beta \times \tau^2) = (ESB \times \beta \times \tau) - \frac{1}{2}(\beta \times \tau^2) \qquad (3.2)$$

Taking the derivative with respect to τ and setting the result equal to zero yields $\tau^{**} = ESB$. This is the standard text-book result for a Pigovian tax (or subsidy) (see Pigou (1920)).

To find the optimal canola subsidies as derived from equations (3.1) and (3.2), estimates of the slope of the acreage response function (β) are needed. In the next section, I develop an acreage choice model to estimate the acreage response with respect to an increase in expected profit for each crop and soil zone in Saskatchewan. I estimate the acreage responses using the confidential field-level SCIC data. Afterwards, I develop a more detailed simulation model that incorporates the estimates of acreage response and a state equation for SOC stocks that depends on the cropping share for each soil zone in Saskatchewan. I use the SOC state equation to determine the external social benefit from additional canola hectares in response to a canola subsidy. Employing the estimates of acreage response and the SOC state equation to determine the external social benefit, I then solve for the optimal canola subsidies via simulation for each objective function ($NESB$ and ΔW), as described in this section.

3.4   Acreage Choice Model

In this section, I outline an acreage choice model based on the premise that farmers select crops to maximize their profits, influenced by variables that are both observable and unobservable to the researcher. Let the profits for field n and crop i to be,

$$\pi_{i,n} = v_{i,n}(z_{i,n}; \theta_0) + u_{i,n}, \tag{3.3}$$

where profit depends on the measure of farmer interest in producing crop i, depending on observed factors, $z_{i,n}$ and unobserved factors $u_{i,n}$ (Carpentier and Letort, 2014). The form of acreage choice is defined for $v_{i,n}$ functions such that θ_0 is a vector of parameters for estimation. As characterized by Seo and Mendelsohn (2009), a farmer will select a crop based on the profit maximization problem,

$$\text{argmax}_{\{1_{i \in C}\}} = [\pi_{1,n}(v_{1,n}(z_{1,n}; \theta_0), u_{1,n}), \ \pi_{2,n}(v_{2,n}(z_{2,n}; \theta_0), u_{2,n}), ..., \pi_{C,n}(v_{C,n}(z_{C,n}; \theta_0), u_{C,n})]. \tag{3.4}$$

This implies that the probability of choosing the *ith* crop relative to the *jth* crop is,

$$Pr_{ij} = Pr(v_{i,n}(z_{i,n}; \theta_0) + u_{i,n} > v_{j,n}(z_{j,n}; \theta_0) + u_{j,n}) \ \forall \ i \neq j, \tag{3.5}$$

which reduces to,

$$Pr_{ij} = Pr(u_{j,n} - u_{i,n} < v_{i,n}(z_{i,n}; \theta_0) - v_{j,n}(z_{j,n}; \theta_0)) \ \forall \ i \neq j. \tag{3.6}$$

If the observed components of the field-level profit for crop i relative to j is greater than the difference in the unobserved components of field-level profit between crop j relative to i, then the farmer is more likely to seed crop i. Because there are unobservable factors within the cropping choice decision, it could also be the case that the field-level profit for crop i is greater than the field-level profit for j, but the farmer chooses to seed crop j due to the unobservable factors.

I assume that farmers choose crops based on profit maximization, such that the profit from choosing a crop is,

$$\pi_{i,n} = v_{i,n}(z_{i,n}; \theta_0) + u_{i,n} = \theta_{i,0} + \theta_{i,1}x_{1,n} + \cdots + \theta_{i,P}x_{P,n} + u_{i,n}. \tag{3.7}$$

As farmers are unable to know the realized profitability of a crop prior to planting, they make crop selections based on expected profits. Therefore,

$$E[\pi_{i,n}] = v_{i,n}(z_{i,n}; \theta_0) + u_{i,n} = \theta_{i,0} + \theta_1 E[\pi_{i,n}^s] + X_n \theta_{i,2} + u_{i,n} \quad \forall \ n \in s. \tag{3.8}$$

where $E[\pi_{i,n}]$ is the expected profit for crop i on field n, $E[\pi_{i,n}^s]$ is the expected profit for soil zone s published by the Saskatchewan Crop Planning Guide before the upcoming growing season, and X_n is a vector of field-level characteristics such as weather, soil, the previous year's crop insurance coverage, the previous year's the size of farm operation in hectares, and the previous year's seeded crop type.

I now use this framework in the following sections 3.5 and 3.6 to derive the standard MNL and NL estimators for the acreage choice model. I provide the standard derivations for the own and cross-acreage elasticities with respect to a change in expected profit for each crop and soil zone.

3.5 Multinomial Logit Model

Employing the profit function outlined in equation (3.8) and the assumption that $u_{i,n}$ follows a Type 1 Extreme Value distribution, the statistical model governing the selection of crop i depends on the following parameters and variables:

$$Pr_{i,n} = \frac{e^{\theta_{i,0} + \theta_1 E[\pi_{i,n}^s] + X_n \theta_{i,2}}}{1 + \sum_{m=1}^{C-1} e^{\theta_{m,0} + \theta_1 E[\pi_{m,n}^s] + X_n \theta_{m,2}}}, \tag{3.9}$$

where $P_{i,n}$ is probability of selecting crop i on field n. The acreage choice depends on the expected profit for a particular crop within a soil zone ($E[\pi_{i,n}^s]$) as well as all other observed factors (X_n). Using the same methodology as developed by Croissant (2012), I estimate the expected profit for

each crop and soil zone with a generic coefficient (θ_1), and all other field-level characteristics with a crop specific coefficient ($\theta_{i,2}$). I assume that the probability of choosing the last crop C is,

$$Pr_{C,n} = \frac{1}{1 + \sum_{m=1}^{C-1} e^{\theta_{m,0} + \theta_1 E[\pi^s_{m,n}] + X_n \theta_{m,2}}}, \tag{3.10}$$

such that $\sum_{i=1}^{C} Pr_{i,n} = 1$. Equation (3.9) represents the closed-form expression of the logit proba-bility for choosing a particular crop, which is solved for by integrating over the cumulative distri-bution of cropping choices by field and assuming that the error terms are independent and iden-tically distributed (i.i.d.) (McFadden, 1974).[13] The derivation used to obtain the logit probabilities is provided in Appendix 3A.

Taking the ratio of the two above probabilities (equations 3.9 and 3.10), and its log, results in,

$$\log\left(\frac{Pr_{i,n}}{Pr_{C,n}}\right) = \theta_{i,0} + \theta_1 E[\pi^s_{i,n}] + X_n \theta_{i,2}. \tag{3.11}$$

Equation (3.11) shows that the coefficients derived from the MNL model correspond to the change in the log-odds ratio of selecting crop i in comparison to crop C. Across all models, spring wheat is chosen as the outside crop.

The likelihood function used to estimate the MNL model is,

$$Pr(x|t) = \prod_{j=1}^{C} \left[\frac{e^{\theta_i' x_n}}{1 + \sum_{m=1}^{C-1} e^{\theta_m' x_n}}\right]^{t_j} \tag{3.12}$$

where $t_j = 1_{i \in C}$ is an encoding vector for cropping choice such that the dataset is represented by $\mathcal{D} = \{(x_1, t_1), \cdots, (x_N, t_N)\}$. The likelihood to observe the dataset is,

$$Pr(x_1, ..., x_N | t_1, ..., t_N) = \prod_{n=1}^{N} \prod_{j=1}^{C} \left[\frac{e^{\theta_i' x_n}}{1 + \sum_{m=1}^{C-1} e^{\theta_m' x_n}}\right]^{t_{nj}}. \tag{3.13}$$

---

[13]The logit formula was originally constructed by Luce (1959) who incorporated assumptions about choice proba-bilities and the independence from irrelevant alternatives property. Following this, Marschak (1960) showed that the logit model produces axioms that are consistent with utility maximization.

Taking the log of the likelihood function provides the solution to the maximization problem:

$$\hat{\theta} = \text{argmax}_{\{\theta \in \Theta\}} \frac{1}{n} \sum_{n=1}^{N} \sum_{j=1}^{C} t_{nj} \log \left[\frac{e^{\theta_i' \mathbf{x}_n}}{1 + \sum_{m=1}^{C-1} e^{\theta_m' \mathbf{x}_n}} \right]. \tag{3.14}$$

Instead of interpreting the coefficient as the change in the log-odds ratio with respect to a change in an independent variable, I derive the marginal effects as done by Train (2009).[14] These effects are applicable to all crops and can be interpreted in the same way as the coefficients in a linear probability model. The marginal effect with respect to expect profit is characterized as,

$$ME_i = \frac{\partial Pr_{i,n}}{\partial E[\pi_{i,n}^s]} = \hat{\theta}_1 \frac{e^{\hat{\theta}_{i,0} + \hat{\theta}_1 E[\pi_{i,n}^s] + X_n \hat{\theta}_{i,2}}}{1 + \sum_{m=1}^{C-1} e^{\hat{\theta}_{m,0} + \hat{\theta}_1 E[\pi_{m,n}^s] + X_n \hat{\theta}_{m,2}}} \times \left(1 - \frac{e^{\hat{\theta}_{i,0} + \hat{\theta}_1 E[\pi_{i,n}^s] + X_n \hat{\theta}_{i,2}}}{1 + \sum_{m=1}^{C-1} e^{\hat{\theta}_{m,0} + \hat{\theta}_1 E[\pi_{m,n}^s] + X_n \hat{\theta}_{m,2}}} \right). \tag{3.15}$$

Using the definition from equation (3.9), the marginal effect reduces to,

$$ME_i = \hat{\theta}_1 Pr_i (1 - Pr_i). \tag{3.16}$$

Multiplying by $E[\pi_{i,n}^s]/Pr_i$ provides the own-acreage elasticity,

$$\varepsilon_i = \hat{\theta}_1 E[\pi_{i,n}^s](1 - Pr_i). \tag{3.17}$$

Deriving the cross marginal effects similarly and multiplying by $E[\pi_{m,n}^s]/Pr_i$ results in the cross-acreage elasticity,

$$\varepsilon_{im} = -\hat{\theta}_1 E[\pi_{m,n}^s] Pr_m. \tag{3.18}$$

---

[14]To see the complete derivations of the marginal effects and elasticities for both the MNL and NL models in a general form, please refer to Appendix 3B.

A limitation of the MNL model is that the ratio of the acreage shares of two different crops will only depend on the payoffs of these crops. As a result, the acreage elasticities of crop i with respect to the gross margins of crop j are equal for all crops $i = 1, ..., C$ for $i \neq j$ (Carpentier and Letort, 2014). Carpentier and Letort (2014) classify this as the "independence of the irrelevant crops" property in the acreage choice MNL model. Hence, there is proportional substitution across alternative crops that depends on the acreage share of a particular crop. It is unlikely that the acreage elasticity of spring wheat with respect to the expected profit of canola and the acreage elasticity of lentils with respect to the expected profit of canola are the same. Because of this, the "independence of the irrelevant crops" (IIC) property is unlikely to hold in practice.[15]

3.6 Nested Logit Model

To avoid imposing restrictive substitution patterns dictated by the IIC assumption, I introduce a Nested Logit (NL) model in this section, which depicts a sequential decision-making framework for crop selection and relaxes the IIC for crops grouped into different nests. While the NL model does not entirely relax the IIC assumption, which is imposed now for crops within the same nest, it allows for more flexible substitution patterns among alternative crops across nests, rendering it a more realistic option compared to the MNL model.[16] Proportional substitution patterns still occurs for crops outside of a nest, and this results in the "independence of irrelevant nests" (IIN) assumption. Compared to the MNL model, the NL model offers greater realism and flexibility regarding substitution patterns between crops.

Let the decision for choosing a nest, which contains multiple crops, be equal to a subset of nests denoted by $B_1, B_2, .., B_K$ for K nests. Assume the cumulative distribution of errors for the NL

---

[15]Train (2009) describes this as the red-bus blue-bus problem in which a traveler has the option to go to work by car or blue bus. If the choice probabilities for taking each transportation mode is 50%, then the ratio of the probabilities between each option is equal to 1. In the example provided by Train (2009), when a red bus is introduced as a new transportation option, the ratio of probabilities for choosing the car and the blue bus must stay the same as a result of the "independence of irrelevant alternatives." One might think that the traveler lowers their probability of taking the blue bus more relative to the car because the red bus is more substitutable with the blue bus. But this is not the case and after introducing the red bus to the choice set, all choice probabilities for the three options lower to $33.\overline{333}$%.

[16]Models that completely relax the IIC assumption, like the Mixed Logit model, pose computational challenges when applied to the very large SCIC field-level dataset and when there is limited variation in the key independent variable (expected profit by year, crop, and soil zone).

model is,

$$F(u) = exp\left(-\sum_{l=1}^{K}\left(\sum_{k\in B_l} e^{-\frac{u_{k,n}}{\lambda_l}}\right)^{\lambda_l}\right).$$ (3.19)

Where the marginal distribution of u is extreme value, $Cov(u_{k,n},\ u_{j,n}) = 0$ if $k \in B_l$ and $j \in B_m$ with $k \neq l$, $Cov(u_{k,n},\ u_{j,n}) \geq 0$ if $k, j \in B_l$, and λ_l is a measure of independence in nest l. If $\lambda_l = 1$ for all l, then the NL model reduces to the MNL model.

Let equation (3.8) represent the profit for choosing any crop and the closed form solution to the distribution of errors shown in equation (3.19) represent the probability of choosing crop i.[17] This choice probability is equal to,

$$Pr_{i,n} = \frac{e^{\frac{\theta_{i,0}+\theta_1 E[\pi^s_{i,n}]+X_n\theta_{i,2}}{\lambda_l}}\left(\sum_{k\in B_l} e^{\frac{\theta_{k,0}+\theta_1 E[\pi^s_{k,n}]+X_n\theta_{k,2}}{\lambda_l}}\right)^{\lambda_l-1}}{\sum_{m=1}^{K}\left(\sum_{k\in B_m} e^{\frac{\theta_{k,0}+\theta_1 E[\pi^s_{k,n}]+X_n\theta_{k,2}}{\lambda_m}}\right)^{\lambda_m}}.$$ (3.20)

The probability of choosing crop i with the nesting structure implies,

$$Pr_{i,n} = Pr_{i,n|k} \times Pr_{k,n}$$ (3.21)

where,

$$Pr_{i,n} = \underbrace{\frac{e^{\frac{\theta_{i,0}+\theta_1 E[\pi^s_{i,n}]+X_n\theta_{i,2}}{\lambda_l}}}{\sum_{k\in B_l} e^{\frac{\theta_{k,0}+\theta_1 E[\pi^s_{k,n}]+X_n\theta_{k,2}}{\lambda_l}}}}_{=Pr_{i,n|k}} \times \underbrace{\frac{\left(\sum_{k\in B_l} e^{\frac{\theta_{k,0}+\theta_1 E[\pi^s_{k,n}]+X_n\theta_{k,2}}{\lambda_l}}\right)^{\lambda_l}}{\sum_{m=1}^{K}\left(\sum_{k\in B_m} e^{\frac{\theta_{k,0}+\theta_1 E[\pi^s_{k,n}]+X_n\theta_{k,2}}{\lambda_m}}\right)^{\lambda_m}}}_{=Pr_{k,n}}.$$ (3.22)

Let the inclusive value from the NL model be equal to,

---

[17]Please refer to Appendix 3A to see the derivation for the closed form solution for this General Extreme Value (GEV) model (Nested Logit).

$$I_{l,n} = \ln \sum_{k \in B_l} e^{\frac{\theta_{k,0} + \theta_1 E[\pi_{k,n}^s] + X_n \theta_{k,2}}{\lambda_l}}. \tag{3.23}$$

Substituting equation (3.23) into (3.22) gives,

$$Pr_{i,n} = \frac{e^{\frac{\theta_{i,0} + \theta_1 E[\pi_{i,n}^s] + X_n \theta_{i,2}}{\lambda_l}}}{\sum_{k \in B_l} e^{\frac{\theta_{k,0} + \theta_1 E[\pi_{k,n}^s] + X_n \theta_{k,2}}{\lambda_l}}} \times \frac{e^{\lambda_l I_{l,n}}}{\sum_{m=1}^{K} e^{\lambda_m I_{m,n}}}. \tag{3.24}$$

In the NL model, under the assumption of profit maximization, the expected profits are determined not by characteristics specific to each nest but by those specific to each crop. Thus, the inclusive value for a given nest represents the expected profits from all cropping choices within that nest, stemming from the second stage of the decision-making process for crop selection. If the inclusive value equals 1 for all nests, the NL model simplifies to the MNL model, indicating the absence of unobserved correlations among crop choices within the same nest (Moreno and Sunding, 2005).

The NL model is estimated by maximum-likelihood estimator employing a similar log-likelihood function as in equation (3.14), but instead maximizes the NL closed form solution for the choice probabilities as shown in equation (3.24). The NL model may alternatively be estimated as a two-step estimator where the first step is the lower model (cropping choice) and the upper model is the choice of the nest (Croissant, 2012). However, estimating the NL model by employing the two-step procedure results in lower standard errors for all estimates and is not as efficient as estimating the nesting and cropping choice simultaneously (Croissant, 2012).

The marginal effect for the NL model with respect to an increase in expected profit is derived as,

$$
ME_i = \frac{\partial Pr_{i,n}}{\partial E[\pi_{i,n}^s]} = \frac{\hat{\theta}_1}{\hat{\lambda}_l} \frac{e^{\frac{\hat{\theta}_{i,0}+\hat{\theta}_1 E[\pi_{i,n}^s]+X_n\hat{\theta}_{i,2}}{\hat{\lambda}_l}} \left(\sum_{k\in B_l} e^{\frac{\hat{\theta}_{k,0}+\hat{\theta}_1 E[\pi_{k,n}^s]+X_n\hat{\theta}_{k,2}}{\hat{\lambda}_l}} \right)^{\hat{\lambda}_l-1}}{\sum_{m=1}^{K} \left(\sum_{k\in B_m} e^{\frac{\hat{\theta}_{k,0}+\hat{\theta}_1 E[\pi_{k,n}^s]+X_n\hat{\theta}_{k,2}}{\hat{\lambda}_m}} \right)^{\hat{\lambda}_m}}
$$

$$
+ \frac{\hat{\theta}_1(\hat{\lambda}_l-1)}{\hat{\lambda}_l} \frac{\left(e^{\frac{\hat{\theta}_{i,0}+\hat{\theta}_1 E[\pi_{i,n}^s]+X_n\hat{\theta}_{i,2}}{\hat{\lambda}_l}} \right)^2 \left(\sum_{k\in B_l} e^{\frac{\hat{\theta}_{k,0}+\hat{\theta}_1 E[\pi_{k,n}^s]+X_n\hat{\theta}_{k,2}}{\hat{\lambda}_l}} \right)^{\hat{\lambda}_l-1}}{\sum_{k\in B_l} e^{\frac{\hat{\theta}_{k,0}+\hat{\theta}_1 E[\pi_{k,n}^s]+X_n\hat{\theta}_{k,2}}{\hat{\lambda}_l}} \sum_{m=1}^{K} \left(\sum_{k\in B_m} e^{\frac{\hat{\theta}_{k,0}+\hat{\theta}_1 E[\pi_{k,n}^s]+X_n\hat{\theta}_{k,2}}{\hat{\lambda}_m}} \right)^{\hat{\lambda}_m}} \tag{3.25}
$$

$$
- \hat{\theta}_1 \left(\frac{e^{\frac{\hat{\theta}_{i,0}+\hat{\theta}_1 E[\pi_{i,n}^s]+X_n\hat{\theta}_{i,2}}{\hat{\lambda}_l}} \left(\sum_{k\in B_l} e^{\frac{\hat{\theta}_{k,0}+\hat{\theta}_1 E[\pi_{k,n}^s]+X_n\hat{\theta}_{k,2}}{\hat{\lambda}_l}} \right)^{\hat{\lambda}_l-1}}{\sum_{m=1}^{K} \left(\sum_{k\in B_m} e^{\frac{\hat{\theta}_{k,0}+\hat{\theta}_1 E[\pi_{k,n}^s]+X_n\hat{\theta}_{k,2}}{\hat{\lambda}_m}} \right)^{\hat{\lambda}_m}} \right)^2 ,
$$

which reduces to

$$
ME_i = \frac{\hat{\theta}_1}{\hat{\lambda}_l} Pr_i + \frac{\hat{\theta}_1(\hat{\lambda}_l-1)}{\hat{\lambda}_l} Pr_i \frac{e^{\frac{\hat{\theta}_{i,0}+\hat{\theta}_1 E[\pi_{i,n}^s]+X_n\hat{\theta}_{i,2}}{\hat{\lambda}_l}}}{\sum_{k\in B_l} e^{\frac{\hat{\theta}_{k,0}+\hat{\theta}_1 E[\pi_{k,n}^s]+X_n\hat{\theta}_{k,2}}{\hat{\lambda}_l}}} - \hat{\theta}_1 Pr_i^2. \tag{3.26}
$$

The own-acreage elasticity with respect to expected profit for the NL choice probabilities is equal to,

$$
\varepsilon_i = \hat{\theta}_1 E[\pi_{i,n}^s] \left(\frac{1}{\hat{\lambda}_l} - \frac{1-\hat{\lambda}_l}{\hat{\lambda}_l} Pr_{i|B_l} - Pr_i \right), \tag{3.27}
$$

and the cross-acreage elasticity with respect to expected profit for the NL model is,

$$
\varepsilon_{im} = \begin{cases} -\hat{\theta}_1 E[\pi_{m,n}^s] Pr_m \left(1 + \frac{1-\hat{\lambda}_l}{\hat{\lambda}_l} \frac{1}{Pr_{B_l}} \right) & if\ m \in B_l \\ -\hat{\theta}_1 E[\pi_{m,n}^s] Pr_m & if\ m \notin B_l \end{cases}. \tag{3.28}
$$

Where,

$$Pr_{i|B_l} = \frac{Pr_i}{\sum_{s \in B_l} Pr_s} = \frac{e^{\frac{\theta_{i,0} + \theta_1 E[\pi_{i,n}^s] + X_n \theta_{i,2}}{\hat{\lambda}_l}}}{\sum_{k \in B_l} e^{\frac{\hat{\theta}_{k,0} + \hat{\theta}_1 E[\pi_{k,n}^s] + X_n \hat{\theta}_{k,2}}{\hat{\lambda}_l}}} \quad \text{and} \quad Pr_{B_l} = \sum_{s \in B_l} Pr_s. \tag{3.29}$$

As depicted in equation (3.28), the cross-acreage elasticity with respect to expected profit for crop m now exhibits variation across nests.[18]

3.7 Data

This section outlines the data used to estimate the acreage choice model using both the MNL and NL estimators. Displayed in Table 3.1 is the dependent variable (Acreage Choice), along with all independent variables incorporated in the analysis. In the MNL and NL models, the acreage choice is represented as $Pr_{i,n,t}$, indicating the likelihood of choosing to plant crop i in the given year on field n in year t. The expected profit, denoted by $E[\pi_{i,n,t}^s]$, is calculated as the difference between revenue and variable costs for each crop i, specific to soil zone s and year t based on information from the Saskatchewan Crop Planning Guides.

I use the expected prices and costs of production published prior to the upcoming growing season from the Saskatchewan Crop Planning Guides for each crop and soil zone from 2001 to 2019 (Government of Saskatchewan, 2023a).[19] Expected profits from the crop planning guide are calculated in 2023 CAD adjusted using the Consumer Price Index (CPI) from the Bank of Canada (2023b). Each year, the Government of Saskatchewan releases a crop planning guide to help farmers make crop production decisions. Prices, costs, and crop yields are expected in that they are forecasted for the upcoming growing season using historical price, cost, and production data and other information or data acquired from producer or industry surveys.

In the Saskatchewan Crop Planning Guides, inputs and returns are associated with obtaining

---

[18]To see the complete derivations of the marginal effects and elasticities in general form, please refer to Appendix 3B.

[19]The Saskatchewan Crop Planning Guides provides consistent and comparable data for on-farm returns and cost of production from 2001 to 2023.

a target yield in the 80th percentile for each soil zone (Government of Saskatchewan, 2023a).[20]

Crop prices reported in the Crop Planning Guides either originate from the average annual farm gate price from Agriculture and Agri-Food Canada's most recent winter farm income forecast, or from reports that retrieve prices from forward contracts or spot prices from local grain buyers (Government of Saskatchewan, 2023a). For more information on the operating costs please refer to the Saskatchewan Crop Planning Guide.[21] Let $x_{i,n,t}$ encompass all additional controls at the field and farm level, such as soil properties, the SOC stock, the average temperature during the previous growing season (GSAT), the total annual precipitation (TAP), the type of crop previously seeded on the field, the previous year's insurance coverage on a field, and the previous year's farm size measured in insured hectares. To account for factors that vary over time but are consistent across all fields within a particular soil zone, all of the models incorporate a linear time trend.[22]

Within this dataset, the simulated SOC stocks originate from Serfas (2024a), who uses field-level information on cropping choices sourced from the SCIC database.[23] The SOC stock variable serves as a proxy for historical yields, cropping decisions, and weather conditions. In the dataset, weather characteristics are interpolated across fields using data from the five nearest neighboring weather stations for each field using daily temperature and precipitation data provided by Environment and Climate Change Canada (2023b). Soil characteristics are from the Canadian National

---

[20]As stated by the Saskatchewan Crop Planning Guide (Government of Saskatchewan, 2023a): "targeted crop yields represent the five-year average of the 80th percentile of production for each crop in each soil zone. That is, for each of the past five years the point where 80 percent of producers would have attained a lower yield for that crop is determined. That value for each of the five years is then averaged. The calculation uses producer data submitted to Saskatchewan Crop Insurance Corporation and released each spring. These target yields reflect a higher level of management, improvements in plant genetics and enhanced nutrient and crop protection management. Producers should adjust the target yield to meet their goals and management style."

[21]In most cases, operating costs are based on retail prices for specific inputs, otherwise obtained from farmers and reviewed by regional crop experts (Government of Saskatchewan, 2023a).

[22]I exclude field or RM fixed effects to avoid the incidental parameters problem (Lancaster, 2000). The incorporation of less granular RM or crop district fixed effects renders the computation of both the MNL and NL models infeasible, as it results in the gradient of the maximum likelihood estimator equal to zero.

[23]Serfas (2024a) introduces an novel SOC prediction model called the Augmented Campbell model, which integrates the Plant Biomass Carbon Inputs (PBCI) model for determining carbon inputs based on crop yields. This model employs conversion formulas that factor in plant traits to compute the annual carbon contributions (Bolinder et al., 2007; Maillard et al., 2018; Fan et al., 2019; He et al., 2021; Zhang et al., 2021; Thiagarajan et al., 2022). These carbon input metrics adjust for yield fluctuations influenced by varying weather conditions, cropping selections, and farming techniques. The Augmented Campbell model utilizes first-order kinetics, a method involving differential equations, to simulate SOC stocks. This approach accounts for the decomposition rates of different SOC pools, where "pools" refer to portions of the SOC that decompose at varying speeds due to their specific carbon content, encompassing both plant and soil material. For a comprehensive explanation of the Augmented Campbell model, please refer to Serfas (2024a).

Soil Database and the Saskatchewan Detailed Soil Survey database and are matched to all fields in Saskatchewan (Agriculture and Agri-Food Canada, 2022). The SCIC dataset includes information on the legal land description, municipality, soil class, land use, insurance coverage, seeded acres, crop type, yield, and fertilizer use.[24]

TABLE 3.1: Acreage Choice Model — Dependent and Indepedent Variables

Variable:	Description:	Source:
Acreage Choice	Binary variable for whether crop i is seeded on field n in year t.	Saskatchewan Crop Insurance Corporation Confidential Dataset
Expected Profit	Expected profit published prior to the upcoming growing season is calculated as forecasted revenue minus the forecasted total variable expenses by crop and soil zone.	2023 Saskatchewan Crop Planning Guide (Government of Saskatchewan, 2023a)
lag(GSAT)	One year lagged term of Growing Season Average Temperature (April to September) in degrees Celsuis.	Environment and Climate Change Canada (2023)
lag(TAP)	One year lagged term of Total Annual Precipitation in millimeters.	
lag(Liability)	One year lagged term for the total liability by field or guarantee to a farmer in CAD from the Saskatchewan Crop Insurance Corportation.	
lag(Insurer Farm Size)	One year lagged term for the total hectares in a year for a farmer that is insured by the Saskatchewan Crop Insurance Corporation.	
lag(Canola)	Lagged cropping choice in the previous year on field n in year $t-1$ is canola.	Saskatchewan Crop Insurance Corporation Confidential Dataset
lag(Cereal)	Lagged cropping choice in the previous year on field n in year $t-1$ is spring wheat, durum wheat, or barley (cereal crop).	
lag(Pulse)	Lagged cropping choice in the previous year on field n in year $t-1$ is peas or lentils (pulse crop).	
lag(Summer Fallow)	Lagged cropping choice in the previous year on field n in year $t-1$ is summer fallow.	
Slope	The slope gradient of the predominant landscape for field n. The slope is measured in percent where a 3 percent slope means that the elevation changes 3 feet for every 100 feet of horizontal distance.	Agriculture and Agri-Food Canada (2022)
Percent Clay	The percentage of soil particles that are clay on field n.	
pH	The measure of acidity of the soil on field n.	
Electrical Conductivity	The soil electrical conductivity measured in dS/m or millimhos/centimeter which is inversely proportional to the electrical resistance (Ohms) in the soil.	
Soil Organic Carbon	The stock of soil organic carbon in kilograms per hectare on field n in year t.	Serfas (2024a)

To identify fields, I use the land title dataset from ISC (an exclusive provider of land titles registry information in Saskatchewan) that identifies all field-level polygons in Saskatchewan (ISC, 2022). This dataset includes detailed geo-referenced information for 311,028 fields. I match weather and soil characteristics to all fields, and link the SCIC data with the legal land description. This procedure yields detailed agricultural production information for 209,021 insured parcels of

---

[24]Only farmers that enroll in the Sask Management Plus (SMP) program at SCIC share field-level crop yield and fertilizer use information.

land. I take a subset of these data to obtain a strongly balanced panel of 36,443 fields with complete information on the time-paths of SOC stocks and cropping choices from 1998 to 2019. Figure 3.1 shows the field-level map of Saskatchewan categorized by soil zone. All my models and results are computed separately for each of the three soil zones: the brown, dark brown, and black & gray soil zones. Farms within a soil zone are more similar in their soil characteristics, climate, farm management practices, and cropping choice than farms in different soil zones.

FIGURE 3.1: Field-level map of soil zones in Saskatchewan
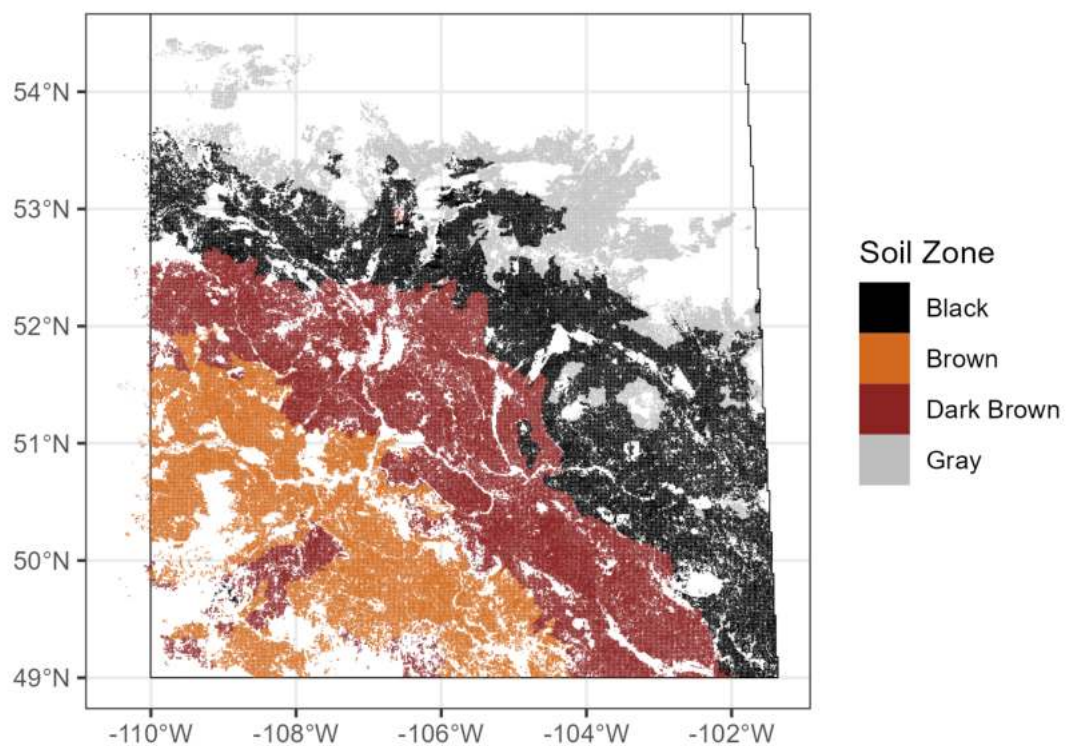
Source: Generated from ISC land titles registry polygons and soil characteristics from the Canadian National Soils Database (Agriculture and Agri-Food Canada, 2022; ISC, 2022).

Notes: The y-axis is latitude and the x-axis is longitude.

251

The identifying assumption in estimating the acreage elasticities is that the expected profits provided by the Saskatchewan Crop Planning Guides for each soil zone do not depend on unobserved attributes specific to individual fields or farms.[25] This means that the expectations of profits or other observed variables at the field level for an individual farmer do not influence the expected profits published by the Saskatchewan Crop Planning Guide.[26]

As the Saskatchewan Crop Planning Guide relies on historical crop production data from farmers in Saskatchewan, using the 80th percentile for targeted crop yield applied to all fields regardless of their specific yield potential, the estimated coefficient for expected profit may be downward biased. This bias arises because variation in expected profits observed in the Saskatchewan Crop Planning Guide is likely to be disproportionately high for seeding a specific type of crop on marginal or less productive land.

3.8   Estimation Results

This section provides the estimation results for the MNL and NL models developed in the previous sections. Table 3.2 presents the Multinomial Logit (MNL) and Nested Logit (NL) estimation results for acreage choice for each soil zone in Saskatchewan. The coefficients for expected profit indicate that for each additional dollar per acre of expected profit, the likelihood of opting any crop over spring wheat increases by a logit log-odds ratio equal to θ_1, holding all other variables in the model constant. These coefficients are often interpreted as the relative risk or odds ratio (Paudel et al., 2013), derived by exponentiating the logit coefficients from the MNL and NL models. A relative risk ratio above one signifies an increase in the relative likelihood of choosing alternative crops over spring wheat for an increase in expected profit. Conversely, a relative risk ratio below one signals a decrease in this likelihood. Given that all coefficients in Table 3.2 are positive, this means that the relative risk ratios across different soil zones exceed one, suggesting a higher propensity to select crops other than spring wheat for an increase in their expected profit.

---

[25]Factors that remain constant over time at the field or farm level also do not affect the expected profits outlined in the Saskatchewan Crop Planning Guides.

[26]Notably, farmers will adjust their expectations on profit using information from the Saskatchewan Crop Planning Guide each year, but discern between the projected profits outlined in the guide and the actual profits anticipated on their farms for upcoming growing season.

TABLE 3.2: Multinomial Logit and Nested Logit Results for Acreage Choice by Soil
Zone in Saskatchewan

	(1)	(2)	(3)	(4)	(5)	(6)
Soil Zone:	Brown		Dark Brown		Black & Gray	
Acreage Choice Model:	MNL	NL	MNL	NL	MNL	NL
Expected Profit	0.0026***	0.0009***	0.0032***	0.0026***	0.0032***	0.0021***
	(0.00011)	(0.00012)	(0.00007)	(0.00009)	(0.00005)	(0.0001)
Inclusive Value 1		0.3244***		0.6696***		0.5547***
		(0.04145)		(0.02559)		(0.02608)
Inclusive Value 2		0.3341***		0.8465***		0.5526***
		(0.04704)		(0.03751)		(0.03575)
Observations	359,485	359,485	990,654	990,654	2,226,294	2,226,294

Source: Authors' Estimates.
Notes: $^*p < 0.1$; $^{**}p < 0.05$; $^{***}p < 0.01$. MNL represents the multinomial logit model and NL represents the nested logit model. The reference crop used in all models is spring wheat. Each coefficient with respect to expected profit represents the likelihood of opting any crop over spring wheat with respect to an increase in expected profit by a logit log-odds ratio equal to θ_1, holding all other variables in the model constant. The coefficient on the inclusive value indicates the degree of independence among the unobserved components of expected profit for alternative crops within a nest. A high coefficient signifies greater independence and less correlation, meaning that the alternative crops within a nest are dissimilar for unobserved reasons. Please refer to Table 3.1 for all other control variables included in the MNL and NL models, as well as the variable description and source.

In Table 3.2, the NL model includes coefficients for the inclusive values across different nests. The nesting configurations that yield coefficients for the inclusive values in the range of 0 to 1 for each soil zone, are provided in Table 3.3. According to Moreno and Sunding (2005), if the coefficient on the inclusive value is significantly different from one, this indicates that there are dissimilarities between alternatives and that the nesting structure is appropriate. Given that all inclusive values significantly differ from one, this evidence strongly supports the chosen nesting structure of crops within each soil zone.[27] The nesting structure is based on crop selection data from 2001 to 2019 in Saskatchewan, meaning that nesting configurations could vary for different subsets of time periods within the SCIC dataset.

---

[27]The 95% confidence intervals for these inclusive values are calculated using the formula $C.I.(\lambda_l) = \lambda_l \pm 1.96 \times S.E.(\lambda_l)$.

TABLE 3.3: Nesting Structure based on Model Specification for Crops and Soil Zones
in Saskatchewan

	(1)	(2)	(3)
Soil Zone:	Brown	Dark Brown	Black & Gray
Nest 1	Spring Wheat Durum Wheat Lentils Peas	Canola Spring Wheat Durum Wheat Barley	Canola Spring Wheat Summer Fallow
Nest 2	Canola Barley Summer Fallow	Lentils Peas Summer Fallow	Barley Durum Wheat Lentils Peas

Source: Author.
Notes: The assignment of crops to nests 1 and 2 follows a unique model specification, ensuring that the inclusive values within the nested logit model for each soil zone in Saskatchewan fall within the 0 to 1 range.

I calculate the own-acreage elasticity for all crops and soil zones using equations (3.17) and (3.27) for both the MNL and NL models, as shown in Table 3.4. Additionally, I calculate the cross-acreage elasticities concerning an increase in expected profit for canola, employing equations (3.18) and (3.28) for each model, presented in Table 3.5.

The own-acreage elasticities across all crops exhibit similar magnitudes between the MNL and NL models, all indicating inelastic response ($\varepsilon_i < 1$). This implies that a one percent rise in expected profit for crop i gives rise to a less than a one percent increase in hectares for that crop. Notably, lentils demonstrate the highest responsiveness to changes in expected profit across all soil zones. Canola and durum wheat also exhibit higher elasticities compared to crops like spring wheat, peas, and barley. Spring wheat has the lowest acreage elasticity among all seeded crops, whereas summer fallow has the lowest compared to all other cropping choices.[28]

---

[28]The expected profit for summer fallow is negative. This means a change in expected profit for summer fallow reflects a cost savings associated with land management when opting for summer fallow.

	(1)	(2)	(3)	(4)	(5)	(6)
Soil Zone:	Brown		Dark Brown		Black & Gray	
Acreage Choice Model:	MNL	NL	MNL	NL	MNL	NL
Canola	0.303***	0.291***	0.370***	0.430***	0.346***	0.395***
	(0.014)	(0.0279)	(0.0086)	(0.0114)	(0.0052)	(0.0077)
Barley	0.151***	0.156***	0.268***	0.328***	0.351***	0.316***
	(0.0068)	(0.0156)	(0.0062)	(0.0094)	(0.0053)	(0.0089)
Spring Wheat	0.148***	0.154***	0.224***	0.266***	0.283***	0.333***
	(0.0067)	(0.0096)	(0.0052)	(0.0073)	(0.0043)	(0.0069)
Durum Wheat	0.180***	0.161***	0.399***	0.486***	0.410***	0.491***
	(0.0081)	(0.0109)	(0.0092)	(0.0138)	(0.0061)	(0.0187)
Lentils	0.450***	0.469***	0.588***	0.562***	0.563***	0.674***
	(0.0203)	(0.0291)	(0.0136)	(0.0127)	(0.0085)	(0.0256)
Peas	0.219***	0.235***	0.310***	0.297***	0.325***	0.343***
	(0.0099)	(0.0144)	(0.0072)	(0.0068)	(0.0049)	(0.0111)
Summer Fallow	0.053***	0.034***	0.076***	0.070***	0.083***	0.098***
	(0.0024)	(0.0029)	(0.0018)	(0.0015)	(0.0012)	(0.0021)

Source: Author's Estimates

Notes: $^{*}p < 0.1$; $^{**}p < 0.05$; $^{***}p < 0.01$. MNL represents the multinomial logit model and NL represents the nested logit model. The own-acreage elasticities with respect to expected profit for the MNL model are calculated using equation (3.17) and for the NL are calculated using equation (3.27) with the mean expected profit and acreage choice. All standard errors are calculated using the nonparametric bootstrap method as outlined by Onukwugha et al. (2015), employing 100 random samples with replacement to estimate the parameters of interest.

Table 3.5 shows the cross-acreage elasticity with respect an increase in expected profit for canola, revealing uniform values across all crops in the MNL model (see equation (3.18)). This uniformity stems from the "IIC" assumption described by Carpentier and Letort (2014). In the NL model, the cross-acreage elasticities with respect to an increase in expected profit for canola demonstrates greater flexibility and realism compared to the MNL model, as these elasticities vary among crops between different nests (see equation (3.28)). For instance, in the brown soil zone the cross-acreage elasticity estimated by the NL model for durum wheat is -0.060, while for barley, it is equal to -0.009.

TABLE 3.5: Cross-Acreage Elasticities with respect to Expected Profit of Canola by Crop and Soil Zone in Saskatchewan

	(1)	(2)	(3)	(4)	(5)	(6)
Soil Zone:	Brown		Dark Brown		Black & Gray	
Acreage Choice Model:	MNL	NL	MNL	NL	MNL	NL
Other Crops	−0.026*** (0.0012)		−0.140*** (0.0032)		−0.249*** (0.0037)	
Crops in Nest 1		−0.060*** (0.0076)		−0.204*** (0.0083)		−0.323*** (0.0082)
Crops in Nest 2		−0.009*** (0.0016)		−0.117*** (0.0043)		−0.167*** (0.0072)

Source: Author's Estimates
Notes: $^*p < 0.1$; $^{**}p < 0.05$; $^{***}p < 0.01$. MNL represents the multinomial logit model and NL represents the nested logit model. Other crops refers to all crops excluding canola. Please see Table 3.3 to see which crops are allocated to nests 1 and 2. The cross-acreage elasticities with respect to canola expected profit for the MNL model are calculated using equation (3.18) and for the NL are calculated using equation (3.28) with the mean expected profit and acreage choice. All standard errors are calculated using the non-parametric bootstrap method as outlined by Onukwugha et al. (2015), employing 100 random samples with replacement to estimate the parameters of interest.

3.9 Simulation Model

In this section, I develop a simulation model to examine the effects of subsidizing canola hectares in Saskatchewan on cropping choice and carbon sequestration. In this model, the canola subsidy is implemented indefinitely into the future, commencing from the year 2019. The model incorporates marginal effects computed using the MNL and NL models.[29] In this model, I assume that farmers in Saskatchewan face exogenous commodity prices when selling their grain at elevator terminals. This assumption is likely to be valid because of competitive arbitrage in the market for

---

[29]An alternative modeling approach to the simulation model could involve constructing a mathematical programming model, which introduces a large degree of realism by optimizing cropping decisions based on economic data and constraints (see Perry et al. (1989) Hoag and Holloway (1991), Garnache et al. (2017), and Cobuloglu and Büyüktahtakın (2017)). The majority of mathematical programming models simulate the decision-making process of a hypothetical farmer who strategically plans for the future by maximizing profits through optimal cropping choices and input use. These models employ data on crop rotation, weather forecasts, commodity prices, and input costs to inform decision-making.

grain, suggesting that Saskatchewan farmers effectively participate in the global grain market.[30] However, if there is any price response to changes in crop production in Saskatchewan, possibly owing to Canada's significant role in the world market for a particular crop, this could limit the effectiveness of the canola subsidy in generating additional canola hectares.

Within the simulation model, I examine two distinct objective functions concerning the implementation of a canola subsidy paid to farmers on policy-induced hectares of canola. First, I examine the effects of maximizing the NESB, which is equal to the external social benefit attributed to the canola subsidy minus the cost. I presume that directing resources towards an environmental policy, whether through private or public funding, involves an opportunity cost. This entails forgoing investments in climate change policies that may offer higher social returns or pose lower risk, where prioritizing cost-effective strategies could potentially result in greater overall environmental or social benefits. With both government and private sectors engaged in climate change mitigation, the management of climate change policy demands meticulous attention from an investment perspective (Pindyck, 2014).

The second objective function I examine is maximizing the change in welfare, which is equal to the NESB plus the change in producer surplus. In this case, when investing in climate change policy, the government would not only consider the environmental benefits generated by implementing a canola subsidy, but also changes in farmer welfare. Because the external social benefit is assessed solely on policy-induced canola hectares, the optimal canola subsidy when maximizing the change in welfare is equal to the external social benefit per policy-induced change in hectares of canola.[31]

Assuming that farmers in Saskatchewan operate as price-takers regarding the pricing and seeding costs of any crop, the market equilibrium for seeded hectares of a crop can be characterized as:

---

[30]There are also implications suggesting that prices for certain commodities are co-integrated with the prices of substitutes, which restricts the price reaction to changes in production. An illustration of this phenomenon is the co-integration observed between the soybean and canola markets (Schaefer et al., 2021).

[31]As stated in section 3.1, implementing a policy that subsidizes all hectares of canola is a feasible policy, and results in a transfer of wealth from the government to producers for all hectares of canola. However, policies that subsidize BAU practices are typically not sustainable and cost ineffective (Raina et al., 2024; Wongpiyabovorn et al., 2024).

$$A_i = \Psi_i + \beta_i E[\pi_i] + \sum_{i \neq m} \beta_{i,m} E[\pi_m], \tag{3.30}$$

where $E[\pi_i]$ is the expected profit of crop i, $E[\pi_m]$ is the expected profit of all other crops not including crop i, and Ψ_i is a constant reflecting all other factors affecting the acreage of crop i that are unrelated to expected profits. Let $\beta_i = ME_i \times \sum_{i=1}^{C} A_i$ so that the marginal effect or change in probability of choosing crop i multiplied by the total hectares of cropland is equal to the change in hectares of crop i with respect to a unit increase in expected profits of crop i.

Taking the derivative with respect to expected profit of crop 1 for C crops in equation (3.30) results in the system of equations,

$$\begin{bmatrix} \frac{\partial A_1}{\partial E[\pi_1]} \\ \frac{\partial A_2}{\partial E[\pi_1]} \\ \vdots \\ \frac{\partial A_C}{\partial E[\pi_1]} \end{bmatrix} = \begin{bmatrix} \beta_1 & 0 & \cdots & 0 \\ \beta_{2,1} & 0 & \cdots & 0 \\ \vdots & \vdots & \ddots & \vdots \\ \beta_{C,1} & 0 & \cdots & 0 \end{bmatrix} \quad \text{subject to:} \quad \beta_1 + \sum_{i=2}^{C} \beta_{i,1} = 0. \tag{3.31}$$

where each marginal effect presented in equation (3.31) is derived from either the MNL or NL models, provided in section 3.8.

The simulation model can be illustrated using a simplified framework as shown in Figure 3.2, with linear marginal net benefit (MNB) curves for canola production and other crops. Additionally, I incorporate into this framework the SOC response to changes in canola hectares and the corresponding external social benefits corresponding to alterations in cropping shares. In Figure 3.2, the marginal net benefit for crop i is denoted as,

$$MNB_i = p_i y_i(A_i) - c_i, \tag{3.32}$$

258

where p_i is the commodity price, c_i is the production cost per hectare, and y_i is yield per hectare for crop i that depends on the total hectares seeded to that crop. The yield per hectare for each crop is assumed to decrease with the increase of cropland for a particular crop. In this case, the implementation of a subsidy on policy-induced canola hectares (crop i) translates to a higher MNB from seeding canola (as depicted in the top panel of Figure 3.2), thereby prompting an increase in canola hectares. The supply of cropland or total hectares of land denoted by L means that with the canola subsidy, farmers substitute from other crops to canola.

The annual change in producer surplus is represented by the green shaded area in the top panel of Figure 3.2. The annual cost of the canola subsidy is not shaded in Figure 3.2, but is equal to twice the area of the change in producer surplus ($\tau(A_i^S - A_i)$). The bottom-left panel of Figure 3.2 illustrates that a permanent increase in canola hectares and a permanent decline in hectares for other crops corresponds to a specific annual increase in SOC stocks relative to BAU practices, given that canola sequesters more carbon in the soil compared to other crops. Assuming a constant rental rate for carbon stored in the soil, the implementation of a canola subsidy enhances the stock of SOC, thereby generating positive external social benefits annually (as outlined by the green shaded area in the bottom-right panel of Figure 3.2).[32]

---

[32]The blue shaded area represents the annual change in producer surplus if all hectares of canola were subsidized, which would result in a transfer of government spending to producers. Because the policy examined in this essay only pays farmers on additional hectares, there is no transfer of spending to producers on all hectares of canola as represented by the blue shaded area in Figure 3.2.

FIGURE 3.2: The Annual Effects of Acreage Response to a Canola Subsidy and the External Social Benefits from Carbon Sequestration
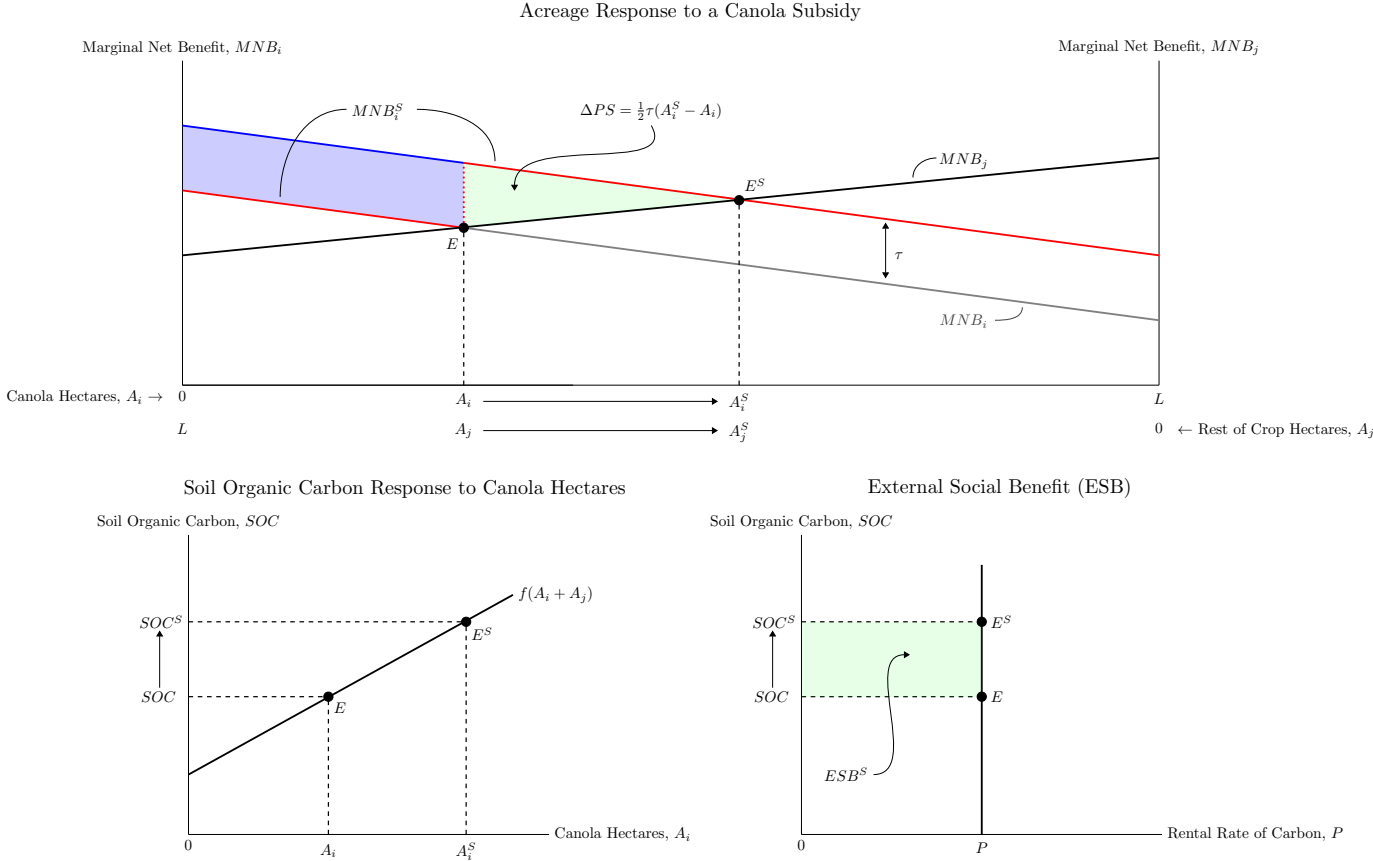
Source: Author.

Notes: The annual effect of a subsidy leads to a permanent increase in canola hectares ($A_i^S - A_i$) and decrease in the hectares allocated to other crops ($A_j^S - A_j$). Because canola stores more SOC relative to other crops, the change in SOC stocks relative to BAU practices is positive due to an increase in canola hectares. The change in annual producer surplus is equal to the one half of the annual canola subsidy per hectare τ multiplied by the permanent policy-induced change in canola hectares ($\Delta PS = (1/2)\tau\Delta A_i = (1/2)\tau(A_i^S - A_i)$). The annual change in the external social benefit is equal to the annual change in SOC from the canola subsidy relative to BAU practices multiplied by the annual rental rate of carbon (P).

The objective function aimed at maximizing the NESB ($NESB_{canola}$) with respect to the subsidy rate for canola starting in 2019 and continuing forever into the future is,[33]

$$\max_{\tau} NESB_{canola} = ESB(\tau, T^*, P, \boldsymbol{\alpha}, \mathbf{A}, \boldsymbol{ME}, E[\pi_{canola}]) - C^{subsidy}(\tau, T^*, \mathbf{A}, ME_{canola}, E[\pi_{canola}]),$$

(3.33)

where,

$$ESB = \sum_{t=1}^{T^*-1}(1+\delta)^{-t}\left\{ tP\Delta SOC \right\} + \frac{1}{\delta}(1+\delta)^{-T^*}\left\{ T^*P\Delta SOC \right\}$$

$$= \sum_{t=1}^{T^*-1}(1+\delta)^{-t}\left\{ tP\Big(\sum_{i=1}^{C}(\Delta A_i + A_i)\Big)\underbrace{\sum_{i=1}^{C}\Big[\alpha_i\Big(\overbrace{\frac{\Delta A_i + A_i}{\sum_{i=1}^{C}(\Delta A_i + A_i)}}^{=s_i^{subsidy}} - \overbrace{\frac{A_i}{\sum_{i=1}^{C} A_i}}^{=s_i}\Big)\Big]}_{=\Delta SOC/\sum_{i=1}^{C}(\Delta A_i + A_i)} \right\}$$

(3.34)

$$+ \frac{1}{\delta}(1+\delta)^{-T^*}\left\{ T^*P\Big(\sum_{i=1}^{C}(\Delta A_i + A_i)\Big)\underbrace{\sum_{i=1}^{C}\Big[\alpha_i\Big(\overbrace{\frac{\Delta A_i + A_i}{\sum_{i=1}^{C}(\Delta A_i + A_i)}}^{=s_i^{subsidy}} - \overbrace{\frac{A_i}{\sum_{i=1}^{C} A_i}}^{=s_i}\Big)\Big]}_{=\Delta SOC/\sum_{i=1}^{C}(\Delta A_i + A_i)} \right\},$$

$$C^{subsidy} = \sum_{t=1}^{T^*-1}(1+\delta)^{-t}\left\{ \tau\Delta A_{canola} \right\} - \frac{1}{\delta}(1+\delta)^{-T^*}\left\{ \tau\Delta A_{canola} \right\},$$

(3.35)

$$\Delta A_i = \tau \times ME_{i,canola} \times \sum_{i=1}^{C} A_i,$$

(3.36)

$$P = \delta * SCC * \frac{44 \text{ Mg CO}_2}{12 \text{ Mg SOC}}, \quad \text{and}$$

(3.37)

---

[33] Bold letters denote the vector of a variable, with each dimension corresponding to the number of crops.

$$\Delta SOC_{n,t} = \gamma SOC_{n,t-1} + \sum_{i=1}^{C} 1_{i \in C} \{ \alpha_i \Theta_{n,t-1}^i \} + Z_{n,t-1} \xi + \nu_{n,t}. \tag{3.38}$$

Let P be the annual rental rate of SOC, which is equal to the SCC multiplied by its corresponding discount rate δ and a conversion factor from CO_2 to SOC (Mikhailova et al., 2019). I employ a SCC equal to 185 USD/Mg of CO_2 at a 2% discount rate per year (Rennert et al., 2022). All monetary values for the SCC are converted to 2023 CAD using the GDP Deflator from the Federal Reserve Bank of St. Louis (U.S. Bureau of Economic Analysis, 2024) and an exchange rate from USD to CAD for 2023 from the Bank of Canada (2023a). The permanent change in the crop share resulting from the canola subsidy is calculated as the difference between $s_i^{subsidy}$ and s_i for crop i. This difference is determined by the permanent policy-induced change in hectares for each crop, where A_i represents the hectares without the canola subsidy, and ΔA_i signifies the permanent policy-induced change in hectares resulting from the canola subsidy. I employ the insured hectares of each crop from the SCIC database for the year 2019. The expected profits for canola by soil zone are computed as the average expected profits derived from the Saskatchewan Crop Planning Guides for the years 2015 to 2019.

Let τ be the per hectare subsidy for canola, expressed in 2023 CAD/ha/yr. The coefficient α_i is estimated from the SOC state equation and quantifies the weighted average annual effect on SOC stocks per hectare for all insured hectares in the following year as a consequence of changing the crop share in the previous year relative to the 2019 crop share. The state-equation shown in equation (3.38) is estimated for each soil zone and is estimated using weighted least squares, weighting by the hectares of a field.[34] Let $\Delta SOC_{n,t}$ denote the SOC change from year $t-1$ to year t, with $SOC_{n,t-1}$ as the SOC stock from the previous year, and $Z_{n,t-1}$ capturing the weather characteristics from the previous year. I include lagged GSAT and TAP in all regressions (refer to Table 3.1 for their descriptions). All standard errors in each regression for the SOC state equation are clustered by farmer. The variable t is used to account for the annual growth in the SOC stock

---

[34]The regression outcomes for equation (3.38) are detailed in Table 3C.1 in Appendix 3C. Different functional forms for the lagged SOC stock are examined and those results are provided in Table 3C.2. Table 3C.2 displays the R^2 values for linear, quadratic, and logarithmic models of lagged SOC stocks, with each model exhibiting very similar predictive performance between change in the SOC stock and the previous year's SOC stock.

relative to the no-policy scenario, whereas T^* is used to signify the time required to achieve a steady state in SOC stocks. I assume it takes approximately 30 years for all soil zones to reach a steady state in SOC stocks.[35] Consequently, shortening the time required to reach a steady state reduces the NESB and the optimal canola subsidy (resulting in less additional SOC stored), while extending this duration leads to a higher change in NESB and the optimal canola subsidy (more additional SOC is stored).[36]

The objective function presented in equation (3.33) does not consider the dynamic effects of yield growth resulting from carbon sequestration. Hence, the optimal subsidies proposed in the simulation model overlook potential yield growth from increased SOC stocks and the subsequent feedback loop between enhanced SOC and crop yields.[37] Including yield response to SOC growth substantially complicates equation (3.33), so much that farmers would additionally respond in their acreage choices over time due to the improved yield productivity from increased SOC, which varies across crop type and soil zone. Appendix 3E provides a sensitivity analysis to examine how the optimal subsidies are affected by an increase in crop yield.[38]

To determine the optimal canola subsidy, I solve the first-order condition from maximizing the NESB in equation (3.33) with respect to the canola subsidy (τ). The first-order condition derived from equation (3.33) is expressed as follows:

---

[35]Serfas (2024a) performs a forward projection of SOC stocks employing the Augmented Campbell model spanning from 2019 to 2169 and discovers that SOC stocks stabilize starting around 2050 in every soil zone, indicating a steady state is attained after approximately 30 years assuming continuous carbon inputs without yield growth. However, for predicting SOC stocks, it is rare to encounter and confirm steady-state equilibria. Hence, the suggested 30-year time period to achieve a steady state should be approached with caution.

[36]Figure 3C.1 in Appendix 3C illustrates how shortening the time it takes to reach a steady state equilibrium in the stock of SOC to 10 and 20 years would affect the NESB.

[37]In Appendix 3C, Table 3C.3 presents results from estimating a SOC state equation that includes control variables for the previous year's crop yield. Despite this inclusion, Table 3C.4 shows the predictive power (R^2) of the state equation when yield control variables are included does not result in sizable changes in the R^2 values for each SOC state equation by soil zone. Table 3C.5 in Appendix 3C also explores the effects of different yield growth effects on the projected change in the SOC stock by crop, considering both a 10% and a 20% increase in crop yields. Depending on the crop yield growth by crop, the resulting changes in the predicted SOC stock could be quite large.

[38]In Appendix E, I examine the robustness of the simulation model and conduct comparative dynamics to examine the effects of yield growth, using simulated rates of yield growth by crop and soil zone provided by Serfas (2024b). Serfas (2024b) finds that canola exhibits varying yield growth rates due to carbon sequestration when subjected to a four-year crop rotation cycle of Canola-Spring Wheat-Canola-Spring Wheat for 32 years, with computed growth rates of 0%, 3.1%, and 2.5% observed across the brown, dark brown, and black & gray soil zones. In comparison, spring wheat yield growth during the same period follows a different trend, showing yield growth of 18.9%, 6.9%, and 2.2% in the respective soil zones after 32 years. The yield growth for peas when subjected to a 32-year rotation of Canola-Spring Wheat-Peas-Spring Wheat is 10.2%, 0%, and 1.5% across the brown, dark brown, and black & gray soil zones.

$$MESB(T^*, P, \boldsymbol{\alpha}, \mathbf{A}, \boldsymbol{ME}, E[\pi_{canola}]) = MC^{subsidy}(\tau, T^*, \boldsymbol{A}, ME_{canola}, E[\pi_{canola}]). \qquad (3.39)$$

Where,[39]

$$
\begin{aligned}
MESB &= \frac{\partial ESB(\tau, T^*, P, \boldsymbol{\alpha}, \mathbf{A}, \boldsymbol{ME}, E[\pi_{canola}])}{\partial \tau} \\
&= \sum_{t=1}^{T^*-1} (1+\delta)^{-t} \left\{ tP \sum_{i=1}^{C} \left[\alpha_i \left(\frac{\Omega_i \sum_{i=1}^{C} A_i + A_i \sum_{i=1}^{C} \Omega_i}{\sum_{i=1}^{C} A_i} \right) \right] \right\} \\
&\quad + \frac{1}{\delta}(1+\delta)^{-T^*} \left\{ T^*P \sum_{i=i}^{C} \left[\alpha_i \left(\frac{\Omega_i \sum_{i=1}^{C} A_i + A_i \sum_{i=1}^{C} \Omega_i}{\sum_{i=1}^{C} A_i} \right) \right] \right\},
\end{aligned}
\qquad (3.40)
$$

$$
\begin{aligned}
MC^{subsidy} &= \frac{\partial C^{subsidy}(\tau, T^*, \boldsymbol{A}, ME_{canola}, E[\pi_{canola}])}{\partial \tau} \\
&= 2\tau \left[\sum_{t=1}^{T^*-1} (1+\delta)^{-t} \Omega_{canola} + \frac{1}{\delta}(1+\delta)^{-T^*} \Omega_{canola} \right],
\end{aligned}
\qquad (3.41)
$$

and

$$\Omega_i = \frac{\partial \Delta A_i}{\partial \tau} = ME_{i,canola} \times \sum_{i=1}^{C} A_i. \qquad (3.42)$$

Solving for τ in equation (3.39) yields the formula for the optimal canola subsidy equal to,

---

[39]Please refer to Appendix 3D for the derivation of the marginal external social benefit formula.

$$\tau^* = \frac{\sum_{t=1}^{T^*-1}(1+\delta)^{-t}\left\{tP\sum_{i=1}^{C}\left[\alpha_i\left(\frac{\Omega_i\sum_{i=1}^{C}A_i+A_i\sum_{i=1}^{C}\Omega_i}{\sum_{i=1}^{C}A_i}\right)\right]\right\}}{2\left[\sum_{t=1}^{T^*-1}(1+\delta)^{-t}\Omega_{canola}+\frac{1}{\delta}(1+\delta)^{-T^*}\Omega_{canola}\right]}$$

$$+ \frac{\frac{1}{\delta}(1+\delta)^{-T^*}\left\{T^*P\sum_{i=1}^{C}\left[\alpha_i\left(\frac{\Omega_i\sum_{i=1}^{C}A_i+A_i\sum_{i=1}^{C}\Omega_i}{\sum_{i=1}^{C}A_i}\right)\right]\right\}}{2\left[\sum_{t=1}^{T^*-1}(1+\delta)^{-t}\Omega_{canola}+\frac{1}{\delta}(1+\delta)^{-T^*}\Omega_{canola}\right]}. \tag{3.43}$$

Equation (3.43) shows that an increase in either the annual rental rate of SOC (P), the total cropland area ($\sum_{i=1}^{C}A_i$), or the time required for SOC stocks to reach a steady state in the stock of SOC (T^*) leads to a corresponding rise in the optimal canola subsidy. Yet, the influence of acreage responses for individual crops or the expected profit for canola on the optimal subsidy remain unknown. Analytical comparative dynamics of the simulation model are necessary to ascertain these relationships.

The objective function to maximize the change in welfare with respect to the canola subsidy is denoted as,

$$\max_{\tau}\Delta W = ESB(\tau, T^*, P, \boldsymbol{\alpha}, \mathbf{A}, \mathbf{ME}, E[\pi_{canola}]) - C^{subsidy}(\tau, T^*, \mathbf{A}, ME_{canola}, E[\pi_{canola}])$$
$$+ \Delta PS^{subsidy}(\tau, T^*, \mathbf{A}, ME_{canola}, E[\pi_{canola}]), \tag{3.44}$$

where,

$$\Delta PS^{subsidy} = \sum_{t=1}^{T^*-1}(1+\delta)^{-t}\left\{\frac{1}{2}\tau\Delta A_{canola}\right\} + \frac{1}{\delta}(1+\delta)^{-T^*}\left\{\frac{1}{2}\tau\Delta A_{canola}\right\}. \tag{3.45}$$

The first-order condition of equation (3.44) with respect to the canola subsidy is,

$$MESB(T^*, P, \boldsymbol{\alpha}, \mathbf{A}, \boldsymbol{ME}, E[\pi_{canola}]) = MC^{subsidy}(\tau, T^*, \boldsymbol{A}, ME_{canola}, E[\pi_{canola}])$$
$$- \partial \Delta PS^{subsidy}(\tau, T^*, \boldsymbol{A}, ME_{canola}, E[\pi_{canola}])/\partial \tau. \tag{3.46}$$

Where,

$$\frac{\partial \Delta PS^{subsidy}}{\partial \tau} = \tau \left[\sum_{t=1}^{T^*-1} (1+\delta)^{-t} \Omega_{canola} + \frac{1}{\delta}(1+\delta)^{-T^*} \Omega_{canola} \right]. \tag{3.47}$$

Solving for τ in equation (3.46) provides the solution for the optimal canola subsidy that maximizes the change in welfare:

$$\tau^{**} = \frac{\sum_{t=1}^{T^*-1}(1+\delta)^{-t} \left\{ tP \sum_{i=1}^{C} \left[\alpha_i \left(\frac{\Omega_i \sum_{i=1}^{C} A_i + A_i \sum_{i=1}^{C} \Omega_i}{\sum_{i=1}^{C} A_i} \right) \right] \right\}}{\sum_{t=1}^{T^*-1}(1+\delta)^{-t} \Omega_{canola} + \frac{1}{\delta}(1+\delta)^{-T^*} \Omega_{canola}}$$
$$+ \frac{\frac{1}{\delta}(1+\delta)^{-T^*} \left\{ T^* P \sum_{i=1}^{C} \left[\alpha_i \left(\frac{\Omega_i \sum_{i=1}^{C} A_i + A_i \sum_{i=1}^{C} \Omega_i}{\sum_{i=1}^{C} A_i} \right) \right] \right\}}{\sum_{t=1}^{T^*-1}(1+\delta)^{-t} \Omega_{canola} + \frac{1}{\delta}(1+\delta)^{-T^*} \Omega_{canola}}. \tag{3.48}$$

The optimal canola subsidy described in equation (3.48) leads to a NESB of zero. This indicates that the external social benefit per policy-induced hectare of canola equals the optimal canola subsidy required to maximize the change in welfare. Solving for the optimal canola subsidy that maximizes the change in welfare can also be achieved by equating the external social benefit to the cost of the subsidy, satisfying condition that NESB is zero. Setting the external social benefit equal to the subsidy cost yields,

$$ESB(\tau^{**}, T^*, P, \pmb{\alpha}, \pmb{A}, \pmb{ME}, E[\pi_{canola}]) = C^{subsidy}(\tau^{**}, T^*, \pmb{A}, ME_{canola}, E[\pi_{canola}])$$

$$\Downarrow$$ (3.49)

$$ESB = \tau^{**}\left[\sum_{t=1}^{T^*-1}(1+\delta)^{-t}\left\{\Delta A_{canola}(\tau^{**})\right\} - \frac{1}{\delta}(1+\delta)^{-T^*}\left\{\Delta A_{canola}(\tau^{**})\right\}\right].$$

Solving for τ in equation (3.49) provides the optimal canola subsidy as derived in equation (3.48),

$$\tau^{**} = \frac{ESB(\tau^{**}, T^*, P, \pmb{\alpha}, \pmb{A}, \pmb{ME}, E[\pi_{canola}])}{\sum_{t=1}^{T^*-1}(1+\delta)^{-t}\left\{\Delta A_{canola}(\tau^{**})\right\} - \frac{1}{\delta}(1+\delta)^{-T^*}\left\{\Delta A_{canola}(\tau^{**})\right\}}$$

$$= \frac{MESB(T^*, P, \pmb{\alpha}, \pmb{A}, \pmb{ME}, E[\pi_{canola}])}{\sum_{t=1}^{T^*-1}(1+\delta)^{-t}\left\{\Omega_{canola}\right\} - \frac{1}{\delta}(1+\delta)^{-T^*}\left\{\Omega_{canola}\right\}}.$$ (3.50)

Where,[40]

$$ESB(\tau, T^*, P, \pmb{\alpha}, \pmb{A}, \pmb{ME}, E[\pi_{canola}]) = \tau MESB(T^*, P, \pmb{\alpha}, \pmb{A}, \pmb{ME}, E[\pi_{canola}]).$$ (3.51)

Equation (3.50) reveals that when maximizing the change in welfare, the optimal canola subsidy equals the external social benefit per policy-induced hectare of canola. I can also be shown that the optimal canola subsidy in equation (3.43) that maximizes the NESB is equal to half of the optimal canola subsidy that maximizes the change in welfare as given in equation (3.48). This suggests,

---

[40]Please refer to Appendix 3D to see the derivation of equation (3.51).

$$\tau^* = \frac{ESB(\tau^*, T^*, P, \boldsymbol{\alpha}, \mathbf{A}, \mathbf{ME}, E[\pi_{canola}])}{2\left[\sum_{t=1}^{T^*-1}(1+\delta)^{-t}\left\{\Delta A_{canola}(\tau^*)\right\} - \frac{1}{\delta}(1+\delta)^{-T^*}\left\{\Delta A_{canola}(\tau^*)\right\}\right]}$$

$$= \frac{MESB(T^*, P, \boldsymbol{\alpha}, \mathbf{A}, \mathbf{ME}, E[\pi_{canola}])}{2\left[\sum_{t=1}^{T^*-1}(1+\delta)^{-t}\left\{\Omega_{canola}\right\} - \frac{1}{\delta}(1+\delta)^{-T^*}\left\{\Omega_{canola}\right\}\right]}.$$

(3.52)

Equation (3.52) aligns with the optimal subsidy shown in equation (3.43), which is derived from the NESB maximization problem.

For solving the simulation model, I employ the Newton-Raphson method as the search algorithm to numerically solve both the optimal canola subsidy from maximizing NESB in equation (3.33) and the subsidy maximizing the change in welfare in equation (3.44). The Newton-Raphson method is a root-finding algorithm that yields approximations of roots for real-valued functions. The root that satisfies the maximization problem for welfare change, as given in equation (3.44), corresponds to $NESB = 0$, meeting the first-order condition outlined in equation (3.50). Similarly, the root for the NESB maximization problem in equation (3.33) is $ESB - 2C^{subsidy} = 0$, satisfying the first-order condition provided by equation (3.52).

3.10   The Effects of a Canola Subsidy on Soil Organic Carbon Stocks

This section presents the results of the simulation model for the two cases outlined in the previous section: (1) the case where the canola subsidy is set to maximize the NESB, and (2) the case where the canola subsidy is set to maximize the change in welfare. Table 3.6 shows the outcomes for the NESB maximization, focusing on the acreage choice model (MNL and NL models) across various soil zones in Saskatchewan, using an annual rental rate for carbon computed with a SCC valued at 185 USD/Mg of CO_2. Table 3.7 shows the results for simulation model that maximizes the change in welfare. Tables 3.6 and 3.7 both show the calculated optimal canola subsidy, policy-induced changes in hectares for each crop, average annual change in the SOC stock per hectare for all

insured hectares from additional canola hectares relative to the change for BAU practices, external social benefit, targeted policy cost, net external social benefit, change in producer surplus, and change in welfare for all insured hectares by soil zone in Saskatchewan.

The optimal subsidies indicated in Table 3.6, as per the MNL and NL models, equal 241.24 and 324.40 CAD/ha/yr in the brown soil zone, 229.73 and 205.43 CAD/ha/yr in the dark brown soil zone, and 220.03 and 226.02 CAD/ha/yr in the black & gray soil zone.[41] In Table 3.7, as anticipated from the derivation of equations (3.2) and (3.50), the optimal canola subsidy when maximizing the change in welfare is twice as large as the optimal canola subsidy when maximizing the NESB. For the MNL and NL models, in the brown soil zone, the optimal canola subsidy for maximizing the change in welfare is 482.49 and 648.80 CAD/ha/yr, while for the dark brown soil zone, it is 459.45 and 410.86 CAD/ha/yr, and for the black & gray soil zone, it is 440.07 and 452.05 CAD/ha/yr.

In both Tables 3.6 and 3.7, the optimal canola subsidy for the brown soil zone surpasses those for the dark brown and black & gray soil zones. This relationship arises because the acreage response and the change in SOC stocks within the brown soil zone are lower than those in the dark brown and black & gray soil zones. Consequently, to incentivize a comparable change in canola hectares, farmers in the brown soil zone require a larger canola subsidy compared to their counterparts in the dark brown and black & gray zones, where canola already constitutes a larger crop share.

In all instances, the policy-induced change in hectares is positive for canola, accompanied by reductions in hectares for all other crops. In Table 3.6, subsidizing farmers to grow canola leads to an increase in canola hectares in percentage terms equal to 15.51% in the brown soil zone, 17.31% in the dark brown soil zone, and 17.27% in the black & gray soil zone for the NL model. In this case, canola hectares increase a total of 677 thousand hectares (17.13%) in Saskatchewan as a result

---

[41]Payments to farmers for adopting no-till practices under EQIP average 11.06 USD/ac (36.62 CAD/ha/yr), while under CSP, they average 7.50 USD/ac/yr (24.83 CAD/ha/yr). For cover crops, EQIP payments can reach up to 40.86 USD/ac/yr (135.30 CAD/ha/yr), whereas CSP payments remain at 7.50 USD/ac/yr (24.83 CAD/ha/yr) (Wong-piyabovorn and Plastina, 2023). The canola subsidies in this analysis are expected to be much lower after discounting for the environmental risks and impermanence of carbon sequestration.

of the subsidy. Table 3C.6 in Appendix C shows the change in hectares and the percentage change for all cases examined in the simulation model.

The results from the simulation model also show how the canola subsidy affects the average annual change in the stock of SOC on all insured hectares. The change in SOC stocks from the canola subsidy is greater in the black & gray soil zone compared to the brown and dark brown soil zones. This is attributable to higher yields of canola in the black & gray soil zone, leading to the larger policy-induced increase in the average stock of SOC stock relative to BAU practices for the same increase in canola hectares in other soil zones. According to Tables 3.6 and 3.7, the MNL model indicates a smaller change in SOC stock across all policy scenarios compared to the NL model, except in the dark brown soil zone. This highlights the differences in estimated substitution patterns resulting from the application of the IIC assumption across crops between the MNL and NL models.

Serfas (2024a) predicts SOC stock changes in each soil zone from 1998 to 2019 in Saskatchewan equal to an increase of 201 kg/ha/yr in the brown soil zone, 288 kg/ha/yr in the dark brown soil zone, and 371 kg/ha/yr in the black & gray soil zone. Table 3.6 indicates that the average annual change in the SOC stock per hectare for all insured hectares from optimal policy induced additional canola hectares is equal to approximately 15–20% of the historical annual change in SOC stocks as simulated by Serfas (2024a). Conversely, in Table 3.7, the change in SOC stocks across all soil zones corresponds to approximately 30 to 40% of the historical annual change in SOC stocks simulated by Serfas (2024a). These observations imply that subsidizing canola hectares in Saskatchewan could lead to a sizable increase in the average stock of SOC across all insured hectares depending on objectives compared to scenarios without such subsidies.

TABLE 3.6: Simulation Model Results for the Net External Social Benefit Maximization Problem over an Infinite Time Horizon starting in 2019

	(1)		(2)		(3)		(4)	
Soil Zone:	Brown		Dark Brown		Black & Gray		All	
Acreage Choice Model:	MNL	NL	MNL	NL	MNL	NL	MNL	NL
Optimal Canola Subsidy (2023 CAD/ha/yr)	241.24	324.40	229.73	205.43	220.03	226.02	226.36	226.54
Change in Hectares:					*(ha)*			
Canola	40,854	52,800	226,675	235,259	217,112	389,415	484,641	677,474
Barley	−1,358	−4,231	−20,055	−26,103	−19,209	−35,131	−40,622	−65,464
Spring Wheat	−5,617	−2,697	−66,373	−86,389	−63,573	−199,151	−135,563	−288,237
Durum Wheat	−14,286	−6,859	−33,155	−43,153	−31,756	−1,819	−79,196	−51,831
Lentils	−5,395	−2,590	−26,210	−19,485	−25,104	−1,949	−56,709	−24,024
Peas	−2,961	−1,422	−22,851	−16,987	−21,887	−18,412	−47,698	−36,821
Summer Fallow	−11,236	−35,002	−58,032	−43,142	−55,584	−132,951	−124,853	−211,095
Total	0	0	0	0	0	0	0	0
Policy Induced Change in SOC (kg/ha/yr)	18.30	31.81	56.25	52.20	63.48	76.49	51.61	58.69
Welfare:					*(millions of 2023 CAD)*			
External Social Benefit	975	1,694	5,150	4,780	7,223	8,705	13,348	15,178
Targeted Cost of Subsidy	487	847	2,575	2,390	3,612	4,352	6,674	7,589
Net External Social Benefit	487	847	2,575	2,390	3,612	4,352	6,674	7,589
Change in Producer Surplus	244	423	1,287	1,195	1,806	2,176	3,337	3,795
Change in Welfare	731	1,270	3,862	3,585	5,417	6,528	10,011	11,384

Source: Author's Estimates

Notes: MNL represents the multinomial logit model and NL represents the nested logit model. The optimal subsidy, policy-induced change in hectares, weighted average annual change in the SOC stock per hectare for all insured hectares from additional canola hectares relative to the weighted average annual change in SOC stock without the canola subsidy, external social benefits, subsidy costs, change in producer surplus, and change in welfare are calculated by maximizing the net external social benefit (NESB) as shown in equation (3.33). All external social benefits are calculated using a rental rate for carbon storage compute with the social cost of carbon equal to 185 USD/Mg of CO_2.

TABLE 3.7: Simulation Model Results for the Change in Welfare Maximization Problem over an Infinite Time Horizon starting in 2019

	(1)		(2)		(3)		(4)	
Soil Zone:	Brown		Dark Brown		Black & Gray		All	
Acreage Choice Model:	MNL	NL	MNL	NL	MNL	NL	MNL	NL
Optimal Canola Subsidy *(2023 CAD/ha/yr)*	482.49	648.80	459.45	410.86	440.07	452.05	450.29	453.08
Change in Hectares:					*(ha)*			
Canola	81,708	105,600	453,351	470,517	663,882	778,830	1,198,941	1,354,947
Barley	−2,716	−8,462	−40,110	−52,205	−102,063	−70,262	−144,889	−130,929
Spring Wheat	−11,235	−5,394	−132,746	−172,778	−298,262	−398,303	−442,243	−576,475
Durum Wheat	−28,571	−13,717	−66,309	−86,306	−5,286	−3,639	−100,166	−103,662
Lentils	−10,791	−5,181	−52,420	−38,969	−5,664	−3,899	−68,874	−48,049
Peas	−5,922	−2,843	−45,702	−33,975	−53,492	−36,825	−105,116	−73,643
Summer Fallow	−22,473	−70,003	−116,065	−86,283	−199,116	−265,903	−337,654	−422,189
Total	0	0	0	0	0	0	0	0
Policy Induced Change in SOC *(kg/ha/yr)*	36.60	63.61	112.50	104.41	126.95	152.99	103.23	117.38
Welfare:					*(millions of 2023 CAD)*			
External Social Benefit	1,949	3,388	10,300	9,559	14,446	17,409	26,695	30,356
Targeted Cost of Subsidy	1,949	3,388	10,300	9,559	14,446	17,409	26,695	30,356
Net External Social Benefit	0	0	0	0	0	0	0	0
Change in Producer Surplus	975	1,694	5,150	4,780	7,223	8,705	13,348	15,178
Change in Welfare	975	1,694	5,150	4,780	7,223	8,705	13,348	15,178

Source: Author's Estimates

Notes: MNL represents the multinomial logit model and NL represents the nested logit model. The optimal canola subsidy, policy-induced change in hectares, weighted average annual change in the SOC stock per hectare for all insured hectares from additional canola hectares relative to the weighted average annual change in SOC stock without the canola subsidy, external social benefits, subsidy costs, change in producer surplus, and change in welfare are calculated by maximizing the change in welfare as shown in equation (3.42). All external social benefits are calculated using a rental rate for carbon storage compute with the social cost of carbon equal to 185 USD/Mg of CO_2.

Tables 3.6 and 3.7 also provide the calculated external social benefits resulting from the policy-induced increase in SOC stock across all insured hectares in Saskatchewan starting from the year 2019 and extending indefinitely into the future. Table 3.6 outline the external social benefits, ranging from 975 to 1,694 million CAD in the brown soil zone, 4,780 to 5,510 million CAD in the dark brown soil zone, and 7,223 to 8,705 million CAD in the black & gray soil zone depending on the acreage choice model.[42] Consequently, the NESB for all insured hectares in Saskatchewan, upon applying a different canola subsidy for each soil zone, amounts to 7.6 billion CAD. This calculation employs the acreage responses derived from the NL model, and using a rental rate for carbon compute with the SCC of 185 USD/Mg of CO_2.

When maximizing the change in welfare, the results in Table 3.7 show that all the external social benefits, optimal canola subsidy, and the policy-induced change in the average annual change in the stock of SOC are twice as large as their counterparts in Table 3.6. In Table 3.7, the external social benefit is equal to the targeted cost of the policy, which results in NESB equal to zero. Hence, the change in producer surplus in Table 3.7 is equal to the change in welfare. When employing the NL model, the change in welfare is equal to 1,694 million CAD in the brown soil zone, 4,780 million CAD in the dark brown soil zone, and 8,705 million CAD in the black & gray soil zone. In Table 3.7, when applying a soil zone specific optimal canola subsidies that maximizes the change in welfare, the change in welfare amounts to 15.2 billion CAD in Saskatchewan.

3.11 Nitrous Oxide Emissions

In this section, I estimate the change in nitrous oxide emissions from the implementation of an optimal canola subsidy. Nitrous oxide emissions are expected to increase as canola hectares increase due to the higher rates of fertilizer that are applied relative to all other crops. Fertilizer application rates in the black & gray soil zone are typically higher than the rates applied in the brown and dark brown soil zones, whereas fertilizer rates are the lowest in the brown soil zone for all crops. In 2019, the average nitrogen rate was approximately 100 kg/ha in the brown soil zone for canola,

---

[42]In Table 3.6, the targeted cost of the policy and the NESB are equal to half of the external social benefit, and the change in producer surplus is equal to a quarter of the external social benefit.

110 kg/ha in the dark brown soil zone, and 120 kg/ha in the black & gray soil zone. In 2019, the nitrogen rate for spring wheat was approximately 70 kg/ha in the brown soil zone, 96 kg/ha in the dark brown soil zone, and 105 kg/ha in the black & gray soil zone. All nitrogen fertilizer application rates are obtained from the SCIC database and apply only to farmers who participate in the Saskatchewan Management Plus (SMP) program and provide information on fertilizer, seed, and herbicide use. It is important to note that farmers who participate in the SMP program could apply a different rate of nitrogen fertilizer relative to farmers who do not participate in the program. Hence, there a potential for selection bias when computing nitrous oxide emissions based on fertilizer application rates for only farmers who participate in the SMP program.

To calculate the nitrous oxide emissions from increased fertilizer use, I employ emission factors (EFs) with respect to synthetic nitrogen use. The EFs are used to estimate nitrous oxide emissions with respect to a unit of synthetic nitrogen fertilizer applied. I obtain EFs with respect to synthetic nitrogen use for each soil zone in Saskatchewan from Rochette et al. (2018). They estimate the EFs using the IPCC Teir II methodology for direct nitrous oxide emissions for agricultural soils across Canada.[43] Using this framework, they estimate an average EF with respect to synthetic nitrogen fertilizer use for the Canadian prairies region equal to 0.0019 ± 0.00064 kg N_2O-N/kg N, which is 6.9 times lower than the estimated EF for Eastern Canada (0.013 ± 0.0064 kg N_2O-N/kg N). They also estimate the EFs by soil zone across the Canadian prairies. Table 3.8 shows the EFs from Rochette et al. (2018) by soil zone in the Canadian prairies, which are equal to 0.0033 kg N_2O-N/kg N in the black & gray soil zone, and 0.0033 kg N_2O-N/kg N in the brown and dark brown soil zones. The EFs estimated by Rochette et al. (2018) do not include indirect emissions linked to the application of synthetic nitrogen, such as leaching, volatilization, and nitrogen run-off. Furthermore, these EFs overlook the complete carbon footprint stemming from the production and distribution of nitrogen fertilizers.

---

[43]Rochette et al. (2018) employ data from 50 peer-reviewed papers and 4 unpublished studies in their analysis. This dataset encompasses 1,026 treatment-years for various cropping systems, soil types, climatic regions, nitrogen fertilizer types, and nitrogen fertilizer rates. Rochette et al. (2018) estimate the EFs using a stepwise regression analysis selecting eight variables to predict cumulative nitrous oxide emissions. These variables include growing season precipitation, synthetic nitrogen application, soil sand content, mean annual air temperature, soil pH, crop type(annual or perennial), soil C:N ratio, and the two month precipitation following the nitrogen application

TABLE 3.8: Nitrous Oxide Emission Factors with respect to Synthetic Nitrogen Fertilizer Use by Soil Zone in Saskatchewan

	Nitrous Oxide Emission Factor	
Soil Zone	kg N_2O-N/kg N	kg CO_2-eq/kg N
Brown and Dark Brown	0.0016	0.749
Black & Gray	0.0033	1.545

Source: Rochette et al. (2018)

Notes: Nitrous oxide emission factors (EFs) with respect to synthetic nitrogen fertilizer are computed in CO_2-eq by first converting N_2O-N to N_2O with the conversion rate of 44/28 and then converting N_2O to CO_2-eq with a conversion rate of 298 (Environment and Climate Change Canada, 2022). The EFs from Rochette et al. (2018) do not account for indirect emissions associated with synthetic nitrogen use, such as leaching, volatilization, and run-off from nitrogen. This also does not encompass the full carbon footprint associated with nitrogen fertilizer production and distribution.

In Table 3.9, the change in nitrous oxide emissions are determined by using the EFs from Table 3.8. I compute the change in aggregate nitrogen fertilizer use for each soil zone and crop in 2019 using the confidential field-level SCIC dataset. I calculate the change in nitrous oxide emissions as a result of implementing a canola subsidy that either maximizes the NESB or change in welfare (refer to equations (3.33) and (3.44)). The change in nitrous oxide emissions for each soil zone from implementing a canola subsidy is calculated as,

$$\Delta N_2O = EF \times \sum_{i=1}^{C} (\overline{N}_i \times \Delta A_i). \tag{3.53}$$

Where ΔA_i is the permanent change in hectares as a result of the canola subsidy, $\overline{N}_i$ is the average nitrogen fertilizer use per hectare for each crop and soil zone, and EF is the emission factor by soil zone for nitrous oxide emissions with respect to nitrogen fertilizer use.

In Table 3.9, the change in SOC stocks for each soil zone are computed by converting the policy-induced change in SOC to units of CO_2-eq with a conversion ratio of 44/12 from SOC to CO_2-eq (Mikhailova et al., 2019). The change in SOC stocks occurs for only 30 years until a steady state equilibrium in SOC stocks is reached, whereas nitrous oxide emissions are assumed to occur forever into the future.

In Table 3.10, the external cost from the change in nitrogen use is equal to the change in nitrous oxide emissions for all insured hectares in Saskatchewan multiplied by the SCC of 185 USD/Mg of CO_2, and converted to 2023 CAD (Bank of Canada, 2023a; U.S. Bureau of Economic Analysis, 2024). Following this, I value the stream of external costs indefinitely into the future, employing a real discount rate of 2% per year. This valuation assumes that the change in nitrogen fertilizer application resulting from the canola subsidy stays constant over time.

TABLE 3.9: Change in Soil Organic Carbon and Nitrous Oxide Emissions from Implementing a Hypothetical Canola Subsidy

	(1)	(2)	(3)	(4)
	Change in SOC		Change in Nitrous Oxide Emissions	
Objective Function:	Net External Social Benefit	Change in Welfare	Net External Social Benefit	Change in Welfare
	(kg of CO_2-eq/ha/yr)			
Brown	116.62	233.24	1.41	2.82
Dark Brown	191.42	382.83	2.11	4.22
Black & Gray	280.47	560.95	7.30	14.60

Source: Author's Estimates.

Notes: The change in nitrous oxide emissions are calculated using the nitrous oxide EFs in Table 3.8 from Rochette et al. (2018) and the change in average fertilizer use by soil zone and crop obtained from the SCIC database for the year 2019. Please refer to equation (3.53) to see how the change in nitrous oxide emissions are calculated as a result of a canola subsidy. This is done for each objective function for a canola subsidy that maximizes the NESB or the change in welfare (see equations (3.33) and (3.44)). The policy-induced change in SOC stocks per hectare per year from Tables 3.6 and 3.7 are converted to CO_2-eq using the conversion ratio from SOC to CO_2 equal to 44/12 (Mikhailova et al., 2019). This annual change in kg of CO_2-eq/ha/yr for SOC only happens for 30 years until a steady state equilibrium is obtained in SOC stocks, whereas the change in nitrous oxide emissions is assumed to occur indefinitely into the future.

Using the results in Table 3.10, I compute an external cost from a change in nitrous oxide emissions as a result of the optimal canola subsidy of 2.72% of the external social benefit from carbon sequestration in the brown soil zone, 2.47% in the dark brown soil zone, and 5.93 in the black & gray soil zone. Here, the external cost is the same percent of external social benefits for when the optimal canola subsidy maximizes NESB or the change in welfare. This percentage is greatest in the black & gray soil zone because the EF for nitrogen fertilizer use is greater relative to the EFs for the brown and dark brown soil zones. In Saskatchewan, the external cost from nitrous oxide emissions for all insured hectares is 4.47 percent of the external social benefits from carbon sequestration. When the optimal canola subsidy is set to maximize the NESB, the external cost

for all of Saskatchewan is equal to 0.6 billion CAD, and when it is set to maximize the change in welfare the external cost is equal to 1.3 billion CAD.

TABLE 3.10: External Costs from a Change in Nitrous Oxide Emissions from Implementing a Hypothetical Canola Subsidy

	(1)	(2)
	Change in External Costs from Policy-Induced Nitrous Oxide Emissions	
Objective Function:	Net External Social Benefit	Change in Welfare
	(millions of 2023 CAD)	
Brown	46	91
Dark Brown	117	234
Black & Gray	503	1,006
Total	666	1,331

Source: Author's Estimates

Notes: The external cost from the change in nitrogen use as a result of implementing a canola subsidy that either maximizes the NESB or change in welfare is equal to the change in nitrous oxide emissions for all insured hectares in Saskatchewan (see equation (3.53)) multiplied by a SCC of 185 USD/Mg of CO_2 (Rennert et al., 2022). I then convert this external cost to 2023 CAD (Bank of Canada, 2023a; U.S. Bureau of Economic Analysis, 2024) and use a real discount rate of 2% per year to value the stream of external costs indefinitely into the future. Please refer to Tables 3.8 and 3.9 for more information on the how to compute the change in nitrous oxide emissions as a result of the canola subsidy.

In this analysis, most of the nitrous oxide emissions stem from the nitrogen fertilizer use applied to all cereals and oilseeds, instead of from substitution effects between crops as a result of the canola subsidy.[44] Hence, most of the external costs from a change in nitrous oxide emissions caused by the canola subsidy are from substituting away from seeding pulse crops or fallowing to seeding more canola.

---

[44]It is important to note that the reduction nitrogen fertilizer use not only contains external social benefits, but also external costs. Reducing nitrogen use lowers nitrous oxide emissions, but it also has a negative effect on crop productivity. Lower nitrogen use applied leads to less carbon inputs, lowering SOC stocks. As stated by Guenet et al. (2021), "the use of mineral nitrogen to increase crop productivity may induce an increase of carbon inputs into the soil but a complex balance must be found to avoid excessive nitrous oxide emissions and nitrogen leaching."

3.12 Conclusions

Agricultural carbon sequestration offers a promising avenue for both policymakers and the private sector to combat climate change on a global scale. The results of this research highlight that identifying policy-driven changes in soil organic carbon (SOC) stocks could yield positive net external social benefits (NESB) or change in welfare, rendering subsidies on canola hectares a feasible investment option for either public or private entities. The NESB is calculated as the external social benefit minus the subsidy cost, whereas the change in welfare is equal to the NESB plus the change in producer surplus. Assuming efficient administration of payments to farmers and minimal overall policy costs, incentivizing farmers to expand canola hectares could be overseen by various entities such as crop insurance agencies, private firms, or government bodies armed with comprehensive farming data. To optimize policy execution, payments might be targeted toward canola hectares surpassing the farm- or region-specific average crop share for canola. The policy in this essay is hypothetical, meaning that efforts to incentivize farming practices that promote enhancing SOC stocks, through the development and execution of a carbon sequestration policy, would first need to undergo rigorous evaluation by economists, scientists, policymakers, and contract specialists alike.

The results from the analysis in this essay reveal sizable hypothetical optimal canola subsidies. Utilizing acreage responses from the nested logit (NL) model, I compute an optimal canola subsidy that would maximize NESB of 324.40 CAD/ha/yr in the brown soil zone, 205.43 CAD/ha/yr in the dark brown soil zone, and 226.02 CAD/ha/yr in the black & gray soil zone. If such a policy were implemented, a farmer who opted to increase canola production by 65 hectares in the brown soil zone would receive payments at the rate of 324.40 CAD/ha/yr, totaling 21,086 CAD annually, and indefinitely. Table 3E.3 in Appendix 3E shows that for such a policy implemented for only 10 (20, 30) years would pay a farmer who opted to increase canola production by 65 hectares in the brown soil zone at a rate of 76.05 (140.27, 199.86) CAD/ha/yr , totaling 4,943 (9,118, 12,991) CAD annually. In comparison, under EQIP, farmers can receive 4,156 USD/yr (equivalent to 5,569 CAD/yr) per 65 hectare field for the initial five years of the contract and 5,982 USD/yr (equivalent to 8,016 CAD/yr) for years 6–10 for adopting cereal rye as a cover crop and maintaining no-till

practices. Therefore, a canola subsidy acts as a compelling incentive for farmers, particularly those previously cultivating fewer canola hectares and especially in the brown soil zone, by offering enhanced payments, thus encouraging expanded canola adoption to increase SOC stocks and their environmental benefits.

The Government of Canada has invested 4 billion CAD into the Natural Climate Solution Fund aimed at supporting diverse policies across various industries and environments to mitigate the effects of climate change,[45] and 3.5 billion CAD as part of the Sustainable Canadian Agricultural Partnership toward on-farm environmental stewardship programs (Agriculture and Agri-Food Canada, 2023; Environment and Climate Change Canada, 2023a, 2024). Similarly, in the United States, the Inflation Reduction Act (IRA) allocates 19.5 billion USD over a five-year period to climate-smart agriculture and conservation programs overseen by the NRCS (United States Department of Agriculture, 2023).[46] The findings from this essay demonstrate the potential for achieving environmental benefits from carbon sequestration efforts on the Canadian prairies by implementing a hypothetical canola subsidy. Additionally, these results highlight the possibility of harvesting similar benefits from soils in comparable agricultural regions worldwide through analogous second-best policies. These policies would involve compensating farmers to adopt specific farm management practices that provide external social benefits, validated by scientific research for each particular region.

---

[45]The Natural Climate Solution Fund encompasses initiatives within the Environmental and Climate Change programs, covering sectors such as agricultural production, flood risk management, clean fuel regulations, waste management, wetlands preservation, climate-resilient rural and indigenous communities, among others (Environment and Climate Change Canada, 2024).

[46]Within the IRA, specific provisions include 8.45 billion USD for the Environmental Quality Incentives Program (EQIP), 4.95 billion USD for the Regional Conservation Partnership Program (RCPP), 3.45 billion USD for the Conservation Stewardship Program (CSP), and 1.4 billion USD for the Agricultural Conservation Easement Program (ACEP) (United States Department of Agriculture, 2023).

Appendix 3A: Derivation of the Closed Form Choice Probabilities for the Multinomial Logit and Nested Logit Models

This section presents the derivation of the closed-form choice probabilities that are used in estimating acreage choice within the multinomial and nested logit models. These derivations are adapted from Train (2009), with the inclusion of the complete derivation of the choice probabilities. Specifically, I introduce the additional step of u-substitution required to integrate over the probability density function for the Gumbel or Type 1 Extreme Value distribution.

Let the distribution of u_{cf} follow an independent and identical Gumbel distribution or a Type 1 Extreme Value distribution be

$$f(u_{cf}) = e^{-u_{cf}} e^{-e^{-u_{cf}}}, \tag{3A.1}$$

and the cumulative distribution be,

$$F(u_{cf}) = e^{-e^{-u_{cf}}}. \tag{3A.2}$$

Let the probability of choosing crop j over crop c be equal to

$$Pr_{c,f} = Prob(v_c(z_f;\theta_0) + u_{cf} > v_j(z_f;\theta_0) + u_{jf}) \quad \forall \, j \neq c, \text{ and}$$
$$Pr_{c,f} = Prob(u_{jf} < u_{cf} + v_c(z_f;\theta_0) - v_j(z_f;\theta_0)) \quad \forall \, j \neq c. \tag{3A.3}$$

Then the cumulative distribution is equal to

$$Pr_{cf}|u_{cf} = \prod_{j \neq c} e^{-e^{-(u_{cf} + v_c(z_f;\theta_0) - v_j(z_f;\theta_0))}}. \tag{3A.4}$$

280

Because u_{cf} is unknown, the choice probability is the integral of $Pr_{cf}|u_{cf}$ over all values u_{cf} weighted by its density Train (2009). Let $u_{cf} = s$, such that integrating over the probability distribution is represented as

$$Pr_{cf}|u_{cf} = \int_{s=-\infty}^{\infty} \left(\prod_{j \neq c} e^{-e^{-(s+v_c(z_f;\theta_0)-v_j(z_f;\theta_0))}} \right) e^{-s} e^{-e^{-s}} ds. \tag{3A.5}$$

Collecting terms gives

$$
\begin{aligned}
Pr_{cf}|u_{cf} &= \int_{s=-\infty}^{\infty} \left(\prod_{j} e^{-e^{-(s+v_c(z_f;\theta_0)-v_j(z_f;\theta_0))}} \right) e^{-s} ds \\
&= \int_{s=-\infty}^{\infty} exp\left(-\sum_{j} e^{-(s+v_c(z_f;\theta_0)-v_j(z_f;\theta_0))}\right) e^{-s} ds \\
&= \int_{s=-\infty}^{\infty} exp\left(-e^{-s} \sum_{j} e^{-(v_c(z_f;\theta_0)-v_j(z_f;\theta_0))}\right) e^{-s} ds.
\end{aligned}
\tag{3A.6}
$$

With u-substitution, let $x = exp(-s)$ and $-exp(-s)ds = dx$. Where $\lim_{s \to \infty} exp(-s) = 0$ and $\lim_{s \to -\infty} exp(-s) = \infty$. Integrating by u-substitution provides

$$
\begin{aligned}
Pr_{cf}|u_{cf} &= \int_{\infty}^{0} exp\left(-t \sum_{j} e^{-(v_c(z_f;\theta_0)-v_j(z_f;\theta_0))}\right)(-dt) \\
&= \int_{0}^{\infty} exp\left(-t \sum_{j} e^{-(v_c(z_f;\theta_0)-v_j(z_f;\theta_0))}\right) dt \\
&= \left. \frac{exp\left(-t \sum_{j} e^{-(v_c(z_f;\theta_0)-v_j(z_f;\theta_0))}\right)}{-\sum_{j} e^{-(v_c(z_f;\theta_0)-v_j(z_f;\theta_0))}} \right|_{0}^{\infty} \\
&= \frac{1}{\sum_{j} e^{-(v_c(z_f;\theta_0)-v_j(z_f;\theta_0))}} \\
&= \frac{e^{v_c(z_f;\theta_0)}}{\sum_{j} e^{v_j(z_f;\theta_0)}}.
\end{aligned}
\tag{3A.7}
$$

General Extreme Value models

To find the closed form solution for the nested logit model, I employ the assumptions from the general extreme value (GEV) models as done by Train (2009). Provided the GEV conditions hold, the closed form solution for any extreme value function can be solved (McFadden, 1978).

Consider a function G that depends on Y_j and let $Y_j = e^{V_j}$ for all j. Assume the derivative of G is equal to $G_i = \frac{\partial G}{\partial Y_i}$. A discrete choice model can be used if G satisfies the following criteria:

1. $G > 0$ for all positive values of Y_j for all j.

2. G is homogeneous of degree one. That is, if each Y_j is scaled by the value of ρ, then G rises by the same proportion $(G(\rho Y_1, ..., \rho Y_J) = \rho G(Y_1, ..., Y_J))$.

3. If $G \to \infty$ then $Y_j \to \infty$ for any j.

4. The cross partial derivatives of G change signs in a particular way such that $G_i \geq 0$ for all i, $G_{ij} = \frac{\partial G_i}{\partial Y_j} \leq 0$ for all $j \neq i$, $G_{ijk} = \frac{\partial G_{ij}}{\partial Y_k} \geq 0$ for any distinct i, j, and k, and so on for higher-order cross partials.

Assume that $G = \sum_{j=1}^{J} Y_j$ and that $G_i = 1$. All the conditions from (1) to (4) are satisfied based on the functional form of G. For the standard logit formula, the probability of choosing crop i is denoted as,

$$Pr_i = \frac{Y_i G_i}{G} = \frac{Y_i}{\sum_{j=1}^{J} Y_j} = \frac{e^{V_i}}{\sum_{j=1}^{J} e^{V_j}}. \tag{3A.8}$$

For the Nested Logit model, let there be J alternatives partitioned into K nests labeled as $B_1, ..., B_K$. Assume now that,

$$G = \sum_{k=1}^{K} \left(\sum_{s \in B_k} Y_s^{\frac{1}{\lambda_k}} \right)^{\lambda_k}, \tag{3A.9}$$

where λ_k is between 0 and 1 for all k. Based on the functional form of G, it is apparent that G is positive for all values of Y_i for all i, homogeneous degree one, and converges to infinity

282

when Y_i converges to infinity for any i. The fourth property is that the partial derivatives must be alternating, and the first partial derivative must be non-negative with respect to Y_i. The first partial derivative of G with respect to Y_i is,

$$G_i = \lambda_k \left(\sum_{s \in B_k} Y_s^{\frac{1}{\lambda_k}} \right)^{\lambda_k - 1} \frac{1}{\lambda_k} Y_i^{\frac{1}{\lambda_k} - 1} = Y_i^{\frac{1}{\lambda_k} - 1} \left(\sum_{s \in B_k} Y_s^{\frac{1}{\lambda_k}} \right)^{\lambda_k - 1} \quad \forall \, i \in B_k. \tag{3A.10}$$

Because $Y_i \geq 0$ for all i, the condition that $G_i \geq 0$ holds. The second cross-partial derivative is equal to

$$
\begin{aligned}
G_{ij} = \frac{\partial G_i}{\partial Y_j} &= (\lambda_k - 1) Y_i^{\left(\frac{1}{\lambda_k}\right) - 1} \left(\sum_{s \in B_k} Y_s^{\frac{1}{\lambda_k}} \right)^{\lambda_k - 2} \frac{1}{\lambda_k} Y_j^{\frac{1}{\lambda_k} - 1} \\
&= \frac{\lambda_k - 1}{\lambda_k} (Y_i Y_j)^{\frac{1}{\lambda_k} - 1} \left(\sum_{s \in B_k} Y_s^{\frac{1}{\lambda_k}} \right)^{\lambda_k - 2} \quad \forall \, j \in B_k, \text{ and } i \neq j.
\end{aligned}
\tag{3A.11}
$$

Because $0 \leq \lambda_k \leq 1$, then $G_{ij} \leq 0$. For higher order cross partials, the result is such,

$$
\begin{aligned}
G_{ijm} = \frac{\partial G_{ij}}{\partial Y_{jm}} &= (\lambda_k - 2) \frac{\lambda_k - 1}{\lambda_k} (Y_i Y_j)^{\frac{1}{\lambda_k} - 1} \left(\sum_{s \in B_k} Y_s^{\frac{1}{\lambda_k}} \right)^{\lambda_k - 3} \frac{1}{\lambda_k} Y_m^{\frac{1}{\lambda_k} - 1} \\
&= \frac{(\lambda_k - 1)(\lambda_k - 2)}{\lambda_k^2} (Y_i Y_j Y_m)^{\frac{1}{\lambda_k} - 1} \left(\sum_{s \in B_k} Y_s^{\frac{1}{\lambda_k}} \right)^{\lambda_k - 3} \quad \forall \, m \in B_k, \text{ and } i \neq j \neq m
\end{aligned}
\tag{3A.12}
$$

Because $0 \leq \lambda_k^2 - 3\lambda_k + 2 \leq 2$ for $0 \leq \lambda_k \leq 1$, then $G_{ijm} \geq 0$. Given that conditions (1) to (4) are satisfied, the choice probability for choosing crop i in the nested logit is,

$$Pr_i = \frac{Y_i G_i}{G} = \frac{Y_i Y_i^{\frac{1}{\lambda_k} - 1} \left(\sum_{s \in B_k} Y_s^{\frac{1}{\lambda_k}} \right)^{\lambda_k - 1}}{\sum_{k=1}^{K} \left(\sum_{s \in B_k} Y_s^{\frac{1}{\lambda_k}} \right)^{\lambda_k}} = \frac{Y_i^{\frac{1}{\lambda_k}} \left(\sum_{s \in B_k} Y_s^{\frac{1}{\lambda_k}} \right)^{\lambda_k - 1}}{\sum_{k=1}^{K} \left(\sum_{s \in B_k} Y_s^{\frac{1}{\lambda_k}} \right)^{\lambda_k}}. \tag{3A.13}$$

If $Y_j = e^{V_j}$, then the nest logit acreage/cropping choice probability becomes,

$$Pr_i = \frac{e^{\frac{V_i}{\lambda_k}} \left(\sum_{s \in B_k} e^{\frac{V_s}{\lambda_k}} \right)^{\lambda_k - 1}}{\sum_{k=1}^{K} \left(\sum_{s \in B_k} e^{\frac{V_s}{\lambda_k}} \right)^{\lambda_k}}. \tag{3A.14}$$

Appendix 3B: Derivation of Multinomial Logit and Nested Logit Marginal Effects and Elasticities

Multinomial Logit Model

Let the choice probability be,

$$Pr_{i,n} = \frac{e^{\theta_{i,0}+\theta_1 x_{i,1,n}+\cdots+\theta_{i,P} x_{i,P,n}}}{1+\sum_{m=1}^{C-1} e^{\theta_{m,0}+\theta_1 x_{m,1,n}+\cdots+\theta_{m,P} x_{m,P,n}}}. \tag{3B.1}$$

The marginal effect is equal to,

$$ME_i = \frac{\partial Pr_{i,n}}{\partial x_{1,n}} = \hat{\theta}_1 \frac{e^{\hat{\theta}_{i,0}+\hat{\theta}_1 x_{i,1,n}+\cdots+\hat{\theta}_{i,P} x_{i,P,n}}}{1+\sum_{m=1}^{C-1} e^{\hat{\theta}_{m,0}+\hat{\theta}_1 x_{m,1,n}+\cdots+\hat{\theta}_{m,P} x_{m,P,n}}} \times \left(1 - \frac{e^{\hat{\theta}_{i,0}+\hat{\theta}_1 x_{i,1,n}+\cdots+\hat{\theta}_{i,P} x_{P,n}}}{1+\sum_{m=1}^{C-1} e^{\hat{\theta}_{m,0}+\hat{\theta}_1 x_{m,1,n}+\cdots+\hat{\theta}_{m,P} x_{m,P,n}}} \right) \tag{3B.2}$$

Substituting equation (3B.1) into (3B.2), the marginal effect reduces to

$$ME_i = \hat{\theta}_1 Pr_i(1 - Pr_i). \tag{3B.3}$$

Multiplying by $x_{i,1}/Pr_i$, the own elasticity is equal to

$$\varepsilon_i = \hat{\theta}_1 x_{i,1}(1 - Pr_i), \tag{3B.4}$$

The cross marginal effect is equal to,

$$ME_{ij} = \frac{\partial Pr_{i,n}}{\partial x_{j,n}} = -\hat{\theta}_1 \frac{e^{\hat{\theta}_{i,0}+\hat{\theta}_1 x_{i,1,n}+\cdots+\hat{\theta}_{i,P} x_{i,P,n}}}{(1+\sum_{m=1}^{C-1} e^{\hat{\theta}_{m,0}+\hat{\theta}_1 x_{m,1,n}+\cdots+\hat{\theta}_{m,P} x_{m,P,n}})^2} e^{\hat{\theta}_{j,0}+\hat{\theta}_1 x_{j,1,n}+\cdots+\hat{\theta}_{j,P} x_{j,P,n}}$$

$$= -\hat{\theta}_1 Pr_i Pr_j. \tag{3B.5}$$

By multiplying equation (3B.5) by $x_{j,1}/Pr_i$ the cross-acreage elasticity is

$$\varepsilon_{ij} = -\hat{\theta}_1 x_{j,1} Pr_j. \tag{3B.6}$$

Nested Logit Model

Let the general form choice probability for the nested logit model be,

$$Pr_{i,n} = \frac{e^{\frac{(\theta_{i,0}+\theta_1 x_{i,1,n}+\cdots+\theta_{i,P}x_{i,P,n})}{\lambda_l}} \left(\sum_{k\in B_l} e^{\frac{(\theta_{k,0}+\theta_1 x_{k,1,n}+\cdots+\theta_{k,P}x_{k,P,n})}{\lambda_l}} \right)^{\lambda_l-1}}{\sum_{m=1}^{K} \left(\sum_{k\in B_m} e^{\frac{(\theta_{k,0}+\theta_1 x_{k,1,n}+\cdots+\theta_{k,P}x_{k,P,n})}{\lambda_m}} \right)^{\lambda_m}}. \tag{3B.7}$$

Taking the derivative with respect to the first independent variable in equation (3B.7) is the marginal effect and is equal to,

$$
\begin{aligned}
ME_i = \frac{\partial Pr_{i,n}}{\partial x_{i,1,n}} = {} & \frac{\hat{\theta}_1}{\hat{\lambda}_l} \frac{e^{\frac{(\hat{\theta}_{i,0}+\hat{\theta}_1 x_{i,1,n}+\cdots+\hat{\theta}_{i,P}x_{i,P,n})}{\hat{\lambda}_l}} \left(\sum_{k\in B_l} e^{\frac{(\hat{\theta}_{k,0}+\hat{\theta}_1 x_{k,1,n}+\cdots+\hat{\theta}_{k,P}x_{P,n})}{\hat{\lambda}_l}} \right)^{\hat{\lambda}_l-1}}{\sum_{m=1}^{K} \left(\sum_{k\in B_m} e^{\frac{(\hat{\theta}_{k,0}+\hat{\theta}_1 x_{1,n}+\cdots+\hat{\theta}_{k,P}x_{P,n})}{\hat{\lambda}_m}} \right)^{\hat{\lambda}_m}} \\
& + \frac{\hat{\theta}_1(\hat{\lambda}_l-1)}{\hat{\lambda}_l} \frac{\left(e^{\frac{(\hat{\theta}_{i,0}+\hat{\theta}_1 x_{i,1,n}+\cdots+\hat{\theta}_{i,P}x_{i,P,n})}{\hat{\lambda}_l}} \right)^2 \left(\sum_{k\in B_l} e^{\frac{(\hat{\theta}_{k,0}+\hat{\theta}_1 x_{k,1,n}+\cdots+\hat{\theta}_{k,P}x_{k,P,n})}{\hat{\lambda}_l}} \right)^{\hat{\lambda}_l-1}}{\sum_{k\in B_l} e^{\frac{(\hat{\theta}_{k,0}+\hat{\theta}_1 x_{k,1,n}+\cdots+\hat{\theta}_{k,P}x_{k,P,n})}{\hat{\lambda}_l}} \sum_{m=1}^{K} \left(\sum_{k\in B_m} e^{\frac{(\hat{\theta}_{k,0}+\hat{\theta}_1 x_{k,1,n}+\cdots+\hat{\theta}_{k,P}x_{k,P,n})}{\hat{\lambda}_m}} \right)^{\hat{\lambda}_m}} \\
& - \hat{\theta}_1 \left(\frac{e^{\frac{(\hat{\theta}_{i,0}+\hat{\theta}_1 x_{i,1,n}+\cdots+\hat{\theta}_{i,P}x_{i,P,n})}{\hat{\lambda}_l}} \left(\sum_{k\in B_l} e^{\frac{(\hat{\theta}_{k,0}+\hat{\theta}_1 x_{k,1,n}+\cdots+\hat{\theta}_{k,P}x_{k,P,n})}{\hat{\lambda}_l}} \right)^{\hat{\lambda}_l-1}}{\sum_{m=1}^{K} \left(\sum_{k\in B_m} e^{\frac{(\hat{\theta}_{k,0}+\hat{\theta}_1 x_{k,1,n}+\cdots+\hat{\theta}_{k,P}x_{k,P,n})}{\hat{\lambda}_m}} \right)^{\hat{\lambda}_m}} \right)^2.
\end{aligned}
\tag{3B.8}
$$

The marginal effect reduces to

$$ME_i = \frac{\partial Pr_{i,n}}{\partial x_{i,1,n}} = \frac{\hat{\theta}_1}{\hat{\lambda}_l} Pr_i$$

$$+ \frac{\hat{\theta}_1(\hat{\lambda}_l - 1)}{\hat{\lambda}_l} Pr_i \frac{e^{\frac{(\hat{\theta}_{i,0} + \hat{\theta}_1 x_{i,1,n} + \cdots + \hat{\theta}_{i,P} x_{i,P,n})}{\hat{\lambda}_l}}}{\sum_{k \in B_l} e^{\frac{(\hat{\theta}_{k,0} + \hat{\theta}_1 x_{k,1,n} + \cdots + \hat{\theta}_{k,P} x_{k,P,n})}{\hat{\lambda}_l}}} \cdot \tag{3B.9}$$

$$- \hat{\theta}_1 Pr_i^2.$$

The own elasticity with respect to profit for the NL choice probabilities is equal to

$$\varepsilon_i = \hat{\theta}_1 x_{i,1} \left(\frac{1}{\hat{\lambda}_l} - \frac{1 - \hat{\lambda}_l}{\hat{\lambda}_l} Pr_{i|B_l} - Pr_i \right). \tag{3B.10}$$

The cross marginal effect for a variable within the same nest as variable $i \in l$ is,

$$ME_{ij} = \frac{\hat{\theta}_1(\hat{\lambda}_l - 1)}{\hat{\lambda}_l} \frac{e^{\frac{(\hat{\theta}_{j,0} + \hat{\theta}_1 x_{j,1,n} + \cdots + \hat{\theta}_{j,P} x_{j,P,n})}{\hat{\lambda}_l}} e^{\frac{(\hat{\theta}_{i,0} + \hat{\theta}_1 x_{i,1,n} + \cdots + \hat{\theta}_{i,P} x_{i,P,n})}{\hat{\lambda}_l}} \left(\sum_{k \in B_l} e^{\frac{(\hat{\theta}_{k,0} + \hat{\theta}_1 x_{k,1,n} + \cdots + \hat{\theta}_{k,P} x_{k,P,n})}{\hat{\lambda}_l}} \right)^{\hat{\lambda}_l - 1}}{\sum_{k \in B_l} e^{\frac{(\hat{\theta}_{k,0} + \hat{\theta}_1 x_{k,1,n} + \cdots + \hat{\theta}_{k,P} x_{k,P,n})}{\hat{\lambda}_l}} \sum_{m=1}^{K} \left(\sum_{k \in B_m} e^{\frac{(\hat{\theta}_{k,0} + \hat{\theta}_1 x_{k,1,n} + \cdots + \hat{\theta}_{k,P} x_{k,P,n})}{\hat{\lambda}_m}} \right)^{\hat{\lambda}_m}}$$

$$- \hat{\theta}_1 \frac{e^{\frac{(\hat{\theta}_{j,0} + \hat{\theta}_1 x_{j,1,n} + \cdots + \hat{\theta}_{j,P} x_{j,P,n})}{\hat{\lambda}_l}} e^{\frac{(\hat{\theta}_{i,0} + \hat{\theta}_1 x_{i,1,n} + \cdots + \hat{\theta}_{i,P} x_{i,P,n})}{\hat{\lambda}_l}} \left(\left(\sum_{k \in B_l} e^{\frac{(\hat{\theta}_{k,0} + \hat{\theta}_1 x_{k,1,n} + \cdots + \hat{\theta}_{k,P} x_{k,P,n})}{\hat{\lambda}_l}} \right)^{\hat{\lambda}_l - 1} \right)^2}{\left(\sum_{m=1}^{K} \left(\sum_{k \in B_m} e^{\frac{(\hat{\theta}_{k,0} + \hat{\theta}_1 x_{k,1,n} + \cdots + \hat{\theta}_{k,P} x_{k,P,n})}{\hat{\lambda}_m}} \right)^{\hat{\lambda}_m} \right)^2} \cdot$$

$$\tag{3B.11}$$

This reduces to

$$ME_{ij} = -\frac{\hat{\theta}_1(1 - \hat{\lambda}_l)}{\hat{\lambda}_l} Pr_{j|B_l} Pr_i - \hat{\theta}_1 Pr_j Pr_i \tag{3B.12}$$

The cross elasticity within the nest is,

$$\varepsilon_{ij} = -\frac{\hat{\theta}_1(1-\hat{\lambda}_l)}{\hat{\lambda}_l}Pr_{j|B_l}x_{j,1} - \hat{\theta}_1x_{j,1}Pr_j$$

$$= -\hat{\theta}_1x_{j,1}Pr_j\left(1 + \frac{1-\hat{\lambda}_l}{\hat{\lambda}_l}\frac{Pr_{j|B_l}}{Pr_j}\right) \qquad (3B.13)$$

$$= -\hat{\theta}_1x_{j,1}Pr_j\left(1 + \frac{1-\hat{\lambda}_l}{\hat{\lambda}_l}\frac{1}{Pr_{B_l}}\right).$$

The cross marginal effect for a variable outside nest of variable $i \notin l$ is,

$$ME_{ij} = -\hat{\theta}_1 e^{\frac{(\hat{\theta}_{j,0}+\hat{\theta}_1 x_{j,1,n}+\cdots+\hat{\theta}_{j,P}x_{j,P,n})}{\hat{\lambda}_s}}\left(\sum_{k\in B_s} e^{\frac{(\hat{\theta}_{k,0}+\hat{\theta}_1 x_{k,1,n}+\cdots+\hat{\theta}_{k,P}x_{k,P,n})}{\hat{\lambda}_s}}\right)^{\hat{\lambda}_s-1} \times$$

$$\frac{e^{\frac{(\hat{\theta}_{i,0}+\hat{\theta}_1 x_{i,1,n}+\cdots+\hat{\theta}_{i,P}x_{i,P,n})}{\hat{\lambda}_l}}\left(\sum_{k\in B_l} e^{\frac{(\hat{\theta}_{k,0}+\hat{\theta}_1 x_{k,1,n}+\cdots+\hat{\theta}_{k,P}x_{k,P,n})}{\hat{\lambda}_l}}\right)^{\hat{\lambda}_l-1}}{\left(\sum_{m=1}^{K}\left(\sum_{k\in B_m} e^{\frac{(\hat{\theta}_{k,0}+\hat{\theta}_1 x_{k,1,n}+\cdots+\hat{\theta}_{k,P}x_{k,P,n})}{\hat{\lambda}_m}}\right)^{\hat{\lambda}_m}\right)^2}. \qquad (3B.14)$$

This reduces to

$$ME_{ij} = -\hat{\theta}_1 Pr_j Pr_i. \qquad (3B.15)$$

The cross elasticity outside the nest is,

$$\varepsilon_{ij} = -\hat{\theta}_1 x_{j,1}Pr_j. \qquad (3B.16)$$

Hence, the cross elasticity with respect to profit for the NL model is,

$$\varepsilon_{ij} = \begin{cases} -\hat{\theta}_1 x_{j,1}Pr_j\left(1 + \frac{1-\hat{\lambda}_l}{\hat{\lambda}_l}\frac{1}{Pr_{B_l}}\right) & if\ j \in B_l \\ -\hat{\theta}_1 x_{j,1}Pr_j & if\ j \notin B_l \end{cases}. \qquad (3B.17)$$

Where,

$$Pr_{i|B_l} = \frac{Pr_i}{\sum_{s \in B_l} Pr_s} = \frac{e^{\frac{(\hat{\theta}_{i,0} + \hat{\theta}_1 x_{i,1,n} + \cdots + \hat{\theta}_{i,P} x_{i,P,n})}{\hat{\lambda}_l}}}{\sum_{k \in B_l} e^{\frac{(\hat{\theta}_{k,0} + \hat{\theta}_1 x_{k,1,n} + \cdots + \hat{\theta}_{k,P} x_{k,P,n})}{\hat{\lambda}_l}}} \quad \text{and} \quad Pr_{B_l} = \sum_{s \in B_l} Pr_s. \qquad (3B.18)$$

Appendix 3C: Supplementary Tables and Figures

TABLE 3C.1: Regression Results for Soil Organic Carbon State Equation by Soil Zone
in Saskatchewan

	(1)	(2)	(3)
	Dependent variable: ΔSOC		
Soil Zone:	**Brown**	**Dark Brown**	**Black & Gray**
	(kg/ha)		
lag(SOC)	−0.004***	−0.001***	−0.001***
	(0.0003)	(0.0002)	(0.0001)
lag(Canola)	906.019***	832.786***	499.892***
	(39.596)	(12.236)	(8.241)
lag(Barley)	214.283***	114.884***	−109.667***
	(37.846)	(12.971)	(9.224)
lag(Spring Wheat)	261.624***	223.619***	−41.599***
	(28.352)	(11.506)	(7.967)
lag(Durum Wheat)	303.113***	321.440***	143.089***
	(29.119)	(13.728)	(17.752)
lag(Lentils)	−221.466***	−271.892***	−642.737***
	(28.563)	(12.787)	(26.977)
lag(Peas)	−155.800***	−199.121***	−472.620***
	(29.175)	(12.449)	(9.885)
lag(Summer Fallow)	−754.763***	−763.389***	−1,129.714***
	(29.015)	(13.937)	(11.231)
lag(GSAT)	−31.6279***	−35.335***	−15.539***
	(2.257)	(1.319)	(1.395)
lag(TAP)	2.205***	1.881***	1.693***
	(0.067)	(0.040)	(0.036)
Goodness-of-Fit Statistics:			
Observations	56,107	169,546	392,417
R^2	0.528	0.523	0.453

Source: Author's Estimates

Notes: *p<0.1; **p<0.05; ***p<0.01. Each regression is estimated by weighted least squares, weighted by the hectares of a field. All standard errors are clustered by farm.

TABLE 3C.2: R-Squared Values for the Soil Organic Carbon State Equation by Functional Form and Soil Zone in Saskatchewan

	(1)	(2)	(3)
State Equation:	$\Delta SOC = f(SOC) + X + v$		
Soil Zone:	*Brown*	*Dark Brown*	*Black & Gray*
Functional Form: ($f(SOC)$)	*Goodness-of-Fit Statistic: R^2*		
Linear	0.528	0.523	0.453
Quadratic	0.529	0.524	0.454
Logarithmic	0.525	0.522	0.452
Observations	56,107	169,546	392,417

Source: Author's Estimates

Notes: *p<0.1; **p<0.05; ***p<0.01. Each regression is estimated by weighted least squares, weighted by the hectares of a field. All standard errors are clustered by farm.

TABLE 3C.3: Regression Results for Soil Organic Carbon State Equation with Crop Yield Effects by Soil Zone in Saskatchewan

	(1)	(2)	(3)
	Dependent variable: ΔSOC		
Soil Zone:	**Brown**	**Dark Brown**	**Black & Gray**
	(kg/ha)		
lag(SOC)	−0.005***	−0.003***	−0.002***
	(0.0003)	(0.0002)	(0.0001)
lag(yield$_{Canola}$)	0.740***	0.506***	0.356***
	(0.029)	(0.009)	(0.007)
lag(yield$_{Barley}$)	0.229***	0.151***	0.163***
	(0.017)	(0.008)	(0.005)
lag(yield$_{SpringWheat}$)	0.358***	0.217***	0.176***
	(0.010)	(0.006)	(0.004)
lag(yield$_{DurumWheat}$)	0.377***	0.281***	0.222***
	(0.006)	(0.007)	(0.015)
lag(yield$_{Lentils}$)	0.311***	0.205***	−0.0002
	(0.014)	(0.010)	(0.034)
lag(yield$_{Peas}$)	0.180***	0.093***	0.058***
	(0.012)	(0.007)	(0.007)
lag(Canola)	−378.223***	−75.714***	−189.052***
	(49.572)	(17.539)	(13.823)
lag(Barley)	−338.650***	−311.693***	−629.442***
	(34.142)	(22.619)	(16.107)
lag(Spring Wheat)	−444.299***	−297.217***	−536.790***
	(30.223)	(15.238)	(13.207)
lag(Durum Wheat)	−548.235***	−390.796***	−446.510***
	(30.442)	(18.791)	(37.312)
lag(Lentils)	−668.244***	−568.176***	−637.384***
	(31.594)	(17.927)	(37.428)
lag(Peas)	−512.879***	−412.552***	−605.774***
	(34.717)	(18.182)	(17.853)
lag(Summer Fallow)	−758.317***	−771.585***	−1,128.748***
	(27.341)	(13.661)	(11.222)
lag(GSAT)	−14.483***	−27.262***	−13.233***
	(2.279)	(1.383)	(1.371)
lag(TAP)	1.730***	1.800***	1.727***
	(0.060)	(0.040)	(0.036)
Goodness-of-Fit Statistics:			
Observations	56,107	169,546	392,417
R^2	0.674	0.607	0.505

Source: Author's Estimates
Notes: *p<0.1; **p<0.05; ***p<0.01. Each regression is estimated by weighted least squares, weighted by the hectares of a field. All standard errors are clustered by farm. Lagged weather variables include the first lags of growing season average temperature (GSAT) and total annual precipitation (TAP).

TABLE 3C.4: Comparison of SOC Stock Predictions by SOC State Equation With and Without Yield Controls

	(1)	(2)	(3)	(4)	(5)	(6)
	Dependent Variable: ΔSOC					
Soil Zone:	Brown		Dark Brown		Black & Gray	
Coefficient:	α_i	$\alpha_i + \beta_i * \bar{y}_i$	α_i	$\alpha_i + \beta_i * \bar{y}_i$	α_i	$\alpha_i + \beta_i * \bar{y}_i$
			(kg/ha)			
Canola	906.019	942.209	832.786	839.167	499.892	509.005
Barley	214.283	205.796	114.884	100.246	-109.667	-101.604
Spring Wheat	261.624	256.473	223.619	204.105	-41.599	-37.105
Durum Wheat	303.113	313.672	321.440	299.127	143.089	141.999
Lentils	-221.466	-208.412	-271.892	-271.412	-642.737	-640.211
Peas	-155.800	-147.672	-199.121	-201.222	-472.620	-464.870
Summer Fallow	-754.763	-758.317	-763.389	-771.585	-1129.714	-1128.748

Source: Author's Estimates

Notes: All change in SOC stocks with respect to land use are computed using estimates from Tables 3C.1 and 3C.3. More specifically, the change in SOC stocks for columns (1), (3), and (5) are from estimated coefficients for the past year's land use (α_i for crop i) given in Table 3C.1, and columns (2), (4), and (6) consider yield effects at the mean yield in addition to land use ($\alpha_i + \beta_i * \bar{y}_i$), where the coefficients are provided in Table 3C.3.

TABLE 3C.5: Comparison of SOC Stock Effects for the SOC State-Equation with respect to Yield Growth

	(1)	(2)	(3)	(4)	(5)	(6)	(7)	(8)	(9)
					Dependent Variable: ΔSOC				
Soil Zone:		Brown			Dark Brown			Black & Gray	
Coefficient:	$\alpha_i + \beta_i * \bar{y}_i$	$\alpha_i + \beta_i * 1.1\bar{y}_i$	$\alpha_i + \beta_i * 1.2\bar{y}_i$	$\alpha_i + \beta_i * \bar{y}_i$	$\alpha_i + \beta_i * 1.1\bar{y}_i$	$\alpha_i + \beta_i * 1.2\bar{y}_i$	$\alpha_i + \beta_i * \bar{y}_i$	$\alpha_i + \beta_i * 1.1\bar{y}_i$	$\alpha_i + \beta_i * 1.2\bar{y}_i$
Crop:					*(kg/ha)*				
Canola	942.209	1074.252	1206.295	839.167	930.656	1022.144	509.005	578.811	648.616
Barley	205.796	260.241	314.686	100.246	162.036	182.633	−101.604	−48.820	3.964
Spring Wheat	256.473	326.550	396.628	204.105	279.303	304.369	−37.105	12.864	62.833
Durum Wheat	313.672	399.863	486.054	299.127	402.615	437.112	141.999	200.850	259.700
Lentils	−208.412	−162.428	−116.445	−271.412	−226.897	−212.059	−640.211	−640.494	−640.776
Peas	−147.672	−111.152	−74.631	−201.222	−169.523	−158.957	−464.870	−450.780	−436.689
Summer Fallow	−758.317	−758.317	−758.317	−771.585	−771.585	−771.585	−1128.748	−1128.748	−1128.748

Source: Author's Estimates
Notes: All change in SOC stocks with respect to land use are computed using estimates from Table 3C.3. The change in SOC stocks for columns (1), (4), and (7) are from estimated coefficients for past year's land use and yield effects at the mean yield ($\alpha_i + \beta_i * \bar{y}_i$). Columns (2), (5), and (8) compute the change in SOC stocks with a 10% yield growth, and columns (3), (6), and (9) employs a 20% yield growth.

FIGURE 3C.1: The Effects of the Steady State Equilibrium in Soil Organic Stocks on the Net External Social Benefit
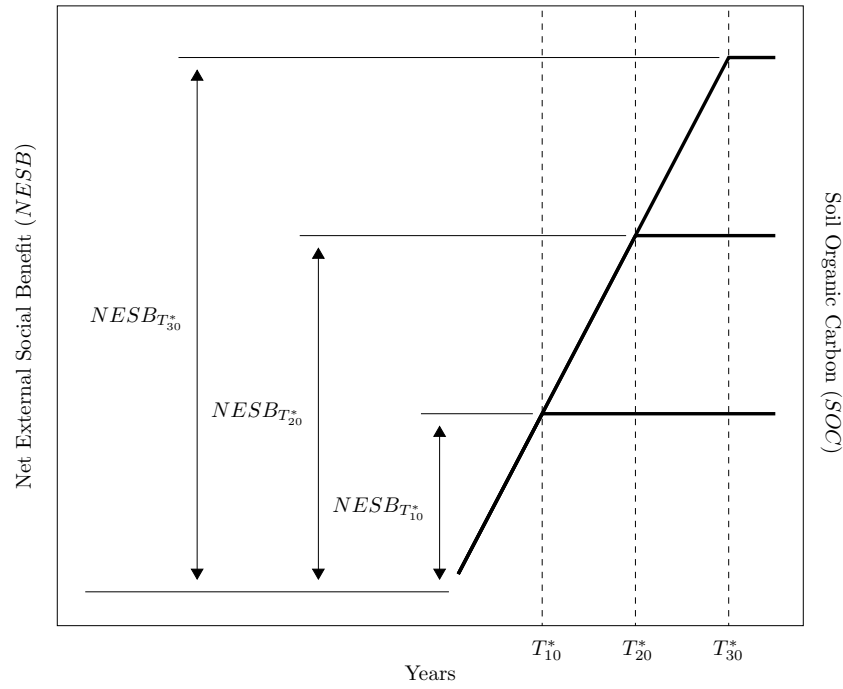
Source: Author.
Notes: T^* represents the number of years it takes to reach a steady state equilibrium in the stock of soil organic carbon.

TABLE 3C.6: Simulation Model Results for a Change in Hectares from Implementing an Optimal Canola Subsidy over an Infinite Time Horizon starting in 2019

	(1)		(2)		(3)		(4)		(5)		(6)		(7)		(8)	
Objective Function:	*Net External Social Benefit*															
Soil Zone:	Brown				Dark Brown				Black & Gray				All			
Model:	MNL		NL		MNL		NL		MNL		NL		MNL		NL	
Change in Hectares:	*(ha)*	*(%)*	*(ha)*	*(%)*	*(ha)*	*(%)*	*(ha)*	*(%)*	*(ha)*	*(%)*	*(ha)*	*(%)*	*(ha)*	*(%)*	*(ha)*	*(%)*
Canola	40,854	12.00	52,800	15.51	226,675	16.68	235,259	17.31	217,112	9.63	389,415	17.27	484,641	12.26	677,474	17.13
Barley	-1,358	-1.50	-4,231	-4.67	-20,055	-10.32	-26,103	-13.43	-19,209	-4.55	-35,131	-8.32	-40,622	-5.74	-65,464	-9.26
Spring Wheat	-5,617	-2.96	-2,697	-1.42	-66,373	-7.06	-86,389	-9.19	-63,573	-4.68	-199,151	-14.65	-135,563	-5.45	-288,237	-11.58
Durum Wheat	-14,286	-2.02	-6,859	-0.97	-33,155	-8.68	-43,153	-11.30	-31,756	-195.71	-1,819	-11.21	-79,196	-7.18	-51,831	-4.70
Lentils	-5,395	-1.25	-2,590	-0.60	-26,210	-8.31	-19,485	-6.18	-25,104	-79.43	-1,949	-6.17	-56,709	-7.28	-24,024	-3.08
Peas	-2,961	-2.11	-1,422	-1.01	-22,851	-7.27	-16,987	-5.40	-21,887	-8.81	-18,412	-7.41	-47,698	-6.78	-36,821	-5.23
Summer Fallow	-11,236	-3.26	-35,002	-10.15	-58,032	-16.47	-43,142	-12.24	-55,584	-12.05	-132,951	-28.83	-124,853	-10.78	-211,095	-18.23
Total	0	0.00	0	0.00	0	0.00	0	0.00	0	0.00	0	0.00	0	0.00	0	0.00
Objective Function:	*Change in Welfare*															
Soil Zone:	Brown				Dark Brown				Black & Gray				All			
Model:	MNL		NL		MNL		NL		MNL		NL		MNL		NL	
Change in Hectares:	*(ha)*	*(%)*	*(ha)*	*(%)*	*(ha)*	*(%)*	*(ha)*	*(%)*	*(ha)*	*(%)*	*(ha)*	*(%)*	*(ha)*	*(%)*	*(ha)*	*(%)*
Canola	81,708	24.01	105,600	31.03	453,351	33.37	470,517	34.63	663,882	29.44	778,830	34.53	1,198,941	30.32	1,354,947	34.27
Barley	-2,716	-3.00	-8,462	-9.33	-40,110	-20.63	-52,205	-26.85	-102,063	-24.17	-70,262	-16.64	-144,889	-20.49	-130,929	-18.51
Spring Wheat	-11,235	-5.92	-5,394	-2.84	-132,746	-14.12	-172,778	-18.38	-298,262	-21.95	-398,303	-29.31	-442,243	-17.77	-576,475	-23.17
Durum Wheat	-28,571	-4.05	-13,717	-1.94	-66,309	-17.37	-86,306	-22.61	-5,286	-32.58	-3,639	-22.43	-100,166	-9.08	-103,662	-9.39
Lentils	-10,791	-2.50	-5,181	-1.20	-52,420	-16.63	-38,969	-12.36	-5,664	-17.92	-3,899	-12.34	-68,874	-8.84	-48,049	-6.17
Peas	-5,922	-4.21	-2,843	-2.02	-45,702	-14.54	-33,975	-10.81	-53,492	-21.52	-36,825	-14.82	-105,116	-14.94	-73,643	-10.47
Summer Fallow	-22,473	-6.52	-70,003	-20.31	-116,065	-32.94	-86,283	-24.49	-199,116	-43.18	-265,903	-57.67	-337,654	-29.15	-422,189	-36.45
Total	0	0.00	0	0.00	0	0.00	0	0.00	0	0.00	0	0.00	0	0.00	0	0.00

Source: Author's Estimates

Notes: MNL represents the multinomial logit model and NL represents the nested logit model. The change in hectares with respect to the optimal canola subsidy are calculated by maximizing either the net external social benefit as shown in equation (3.33) or the change in welfare as shown in equation (3.42). Please refer to Tables 3.6 and 3.7 for more information.

Appendix 3D: Derivation of the Marginal External Social Benefit from Carbon Sequestration

In this section, I provide the derivation for equation (3.51), showing the relationship between the external social benefit and the marginal external social benefit. Using the definition from equation (3.34), the external social benefit is,

$$
\begin{aligned}
ESB = {} & \sum_{t=1}^{T^*-1} (1+\delta)^{-t} \left\{ tP\Big(\sum_{i=1}^{C}(\Delta A_i + A_i) \Big) \sum_{i=1}^{C} \left[\alpha_i \Big(\frac{\Delta A_i + A_i}{\sum_{i=1}^{C}(\Delta A_i + A_i)} - \frac{A_i}{\sum_{i=1}^{C} A_i} \Big) \right] \right\} \\
& + \frac{1}{\delta}(1+\delta)^{-T^*} \left\{ T^*P\Big(\sum_{i=1}^{C}(\Delta A_i + A_i) \Big) \sum_{i=1}^{C} \left[\alpha_i \Big(\frac{\Delta A_i + A_i}{\sum_{i=1}^{C}(\Delta A_i + A_i)} - \frac{A_i}{\sum_{i=1}^{C} A_i} \Big) \right] \right\}.
\end{aligned}
\tag{3D.1}
$$

Equation (3D.1) reduces to,

$$
\begin{aligned}
ESB = {} & \sum_{t=1}^{T^*-1} (1+\delta)^{-t} \left\{ tP \sum_{i=1}^{C} \left[\alpha_i \Big(\frac{\Delta A_i \sum_{i=1}^{C} A_i + A_i \sum_{i=1}^{C} \Delta A_i}{\sum_{i=1}^{C} A_i} \Big) \right] \right\} \\
& + \frac{1}{\delta}(1+\delta)^{-T^*} \left\{ T^*P \sum_{i=1}^{C} \left[\alpha_i \Big(\frac{\Delta A_i \sum_{i=1}^{C} A_i + A_i \sum_{i=1}^{C} \Delta A_i}{\sum_{i=1}^{C} A_i} \Big) \right] \right\}.
\end{aligned}
\tag{3D.2}
$$

Taking the derivative of the external social benefit with respect to τ provides the marginal external social benefit,

$$
\begin{aligned}
MESB = {} & \sum_{t=1}^{T^*-1} (1+\delta)^{-t} \left\{ tP \sum_{i=1}^{C} \left[\alpha_i \Big(\frac{\Omega_i \sum_{i=1}^{C} A_i + A_i \sum_{i=1}^{C} \Omega_i}{\sum_{i=1}^{C} A_i} \Big) \right] \right\} \\
& + \frac{1}{\delta}(1+\delta)^{-T^*} \left\{ T^*P \sum_{i=1}^{C} \left[\alpha_i \Big(\frac{\Omega_i \sum_{i=1}^{C} A_i + A_i \sum_{i=1}^{C} \Omega_i}{\sum_{i=1}^{C} A_i} \Big) \right] \right\}.
\end{aligned}
\tag{3D.3}
$$

Where,

$$\Omega_i = \frac{\partial \Delta A_i}{\partial \tau} = ME_{i,canola} \times \sum_{i=1}^{C} A_i. \qquad (3D.4)$$

Multiplying Ω_i by τ provides the change in canola hectares ΔA_i ($\tau\Omega_i = \Delta A_i$), as shown in equation (3.36). Given this relationship, it is now apparent that,

$$\tau MESB = \sum_{t=1}^{T^*-1} (1+\delta)^{-t} \left\{ tP \sum_{i=1}^{C} \left[\alpha_i \left(\frac{\Delta A_i \sum_{i=1}^{C} A_i + A_i \sum_{i=1}^{C} \Delta A_i}{\sum_{i=1}^{C} A_i} \right) \right] \right\}$$

$$+ \frac{1}{\delta}(1+\delta)^{-T^*} \left\{ T^*P \sum_{i=1}^{C} \left[\alpha_i \left(\frac{\Delta A_i \sum_{i=1}^{C} A_i + A_i \sum_{i=1}^{C} \Delta A_i}{\sum_{i=1}^{C} A_i} \right) \right] \right\} \qquad (3D.5)$$

$$= ESB.$$

Appendix 3E: Sensitivity Analysis

In this section, I examine the sensitivity by employing comparative dynamics with the simulation model and the objective that maximizes the NESB as presented in equation (3.33). First, I examine the effects of increasing crop yields, second, I examine the effects of scaling down the acreage responses, and third, I examine the effect of shortening the time horizon of the hypothetical policy to 10, 20, and 30 years on the optimal canola subsidy.

By excluding the dynamic feedback effects between crop yields and SOC stocks from the optimization procedure and using comparative dynamics, I employ a hypothetical increase in crop yields, applying the outcomes across different crop categories as computed by Serfas (2024b). These yield growth rates are 0% (3.1%, 2.5%) for oilseeds, 18.9% (6.9%, 2.2%) for cereals, and 10.2% (0%, 1.5%) for pulses in the brown (dark brown, black & gray) soil zone. Table 3E.1 shows the results for the base case as shown in Table 3.6, as well as the case for when the SOC state equation includes crop yield control variables (please see Table 3C.3 in Appendix 3C).

In Table 3E.1, the calculated optimal canola subsidy rates using the mean crop yields are 360.88 CAD/ha/yr, 235.71 CAD/ha/yr, and 254.71 CAD/ha/yr for the brown, dark brown, and black & gray soil zones. The policy-induced annual change in weighted average SOC stocks for all insured hectares equal 39.36 kg/ha/yr, 68.73 kg/ha/yr, and 91.17 kg/ha/yr for the brown, dark brown, and black & gray soil zones. After increasing the crop yields at the rates provided by Serfas (2024b), this results in optimal subsidies equal to 348.59 CAD/ha/yr, 235.89 CAD/ha/yr, and 258.09 CAD/ha/yr for the brown, dark brown, and black & gray soil zones. With re-optimization of the canola subsidies including higher crop yields, this slightly adjusts the predicted annual change in the weighted average stock of SOC, equaling 36.73 kg/ha/yr, 68.83 kg/ha/yr, and 99.73 kg/ha/yr for the brown, dark brown, and black & gray soil zones.[47]

---

[47]All calculations in Table 3E.1 are based on acreage responses estimated by the NL model and using a rental rate calculated from the SCC of 185 USD/Mg of CO_2.

	(1)	(2)	(3)
Soil Zone:		*Brown*	
Crop Yield Scenario:	Base	Mean Yield	High Yield
Optimal Canola Subsidy *(2023 CAD/ha/yr)*	324.40	360.88	348.59
Policy Induced Change in SOC *(kg/ha/yr)*	31.81	39.36	36.73
Net External Social Benefit *(2023 CAD)*	847	1,048	978
Soil Zone:		*Dark Brown*	
Crop Yield Scenario:	Base	Mean Yield	High Yield
Optimal Canola Subsidy *(2023 CAD/ha/yr)*	205.43	235.71	235.89
Policy Induced Change in SOC *(kg/ha/yr)*	52.20	68.73	68.83
Net External Social Benefit *(2023 CAD)*	2,390	3,146	3,150
Soil Zone:		*Black & Gray*	
Crop Yield Scenario:	Base	Mean Yield	High Yield
Optimal Canola Subsidy *(2023 CAD/ha/yr)*	226.02	254.74	258.09
Policy Induced Change in SOC *(kg/ha/yr)*	76.49	91.17	99.73
Net External Social Benefit *(2023 CAD)*	4,352	5,528	5,675

Source: Author's Estimates

Notes: The optimal subsidy, policy-induced change in hectares, external social benefits, and costs for the base case are calculated by maximizing the net external social benefit (NESB) as shown in equation (3.33). For the mean yield and high yield cases, instead of employing the SOC state equation given by equation (3.38), I predict changes in SOC stocks using the regression results that include crop yield control variables as shown in Table 3C.3 in Appendix 3C. The high crop yield scenario refers to the growth rates simulated by Serfas (2024b) under various crop rotations. These increases in crop yields are 0%, 3.1%, and 2.5% for oilseeds, 18.9%, 6.9%, and 2.2% for cereals, and 10.2%, 0%, and 1.5% for pulses in the brown, dark brown, black & gray soil zones.

Table 3E.1 shows that increases in crop yield result in reduced optimal canola subsidies in the brown and dark brown soil zones, and an increase in the optimal canola subsidy for the black & gray soil zone. This pattern can be attributed to the smaller yield growth for cereals in the black & gray zone relative to canola, coupled with a higher rate of substitution between canola and spring wheat compared to the other soil zones.[48] Hence, if yield growth from SOC enhancements favor canola over spring wheat in the black & gray zone—unlike in the brown and dark brown

---

[48]Table 3.5 shows that for the NL model the cross-acreage elasticity for spring wheat with respect to expected profit of canola is larger in the black & gray soil zone in comparison to the brown and dark brown soil zones.

zones—raising the canola subsidy incentivizes a greater amount of substitution in hectares from spring wheat to canola, thereby increasing the NESB.

The simulation model presented in this essay also does not consider another important aspect: the dynamics of crop supply in response to increased on-farm profits. According to the theory proposed by Eckstein (1984), who developed a land allocation model, the productivity of a crop is influenced by whether more land was allocated to a different crop in the preceding year, indicating the effects of rotating crops. This suggests that the acreage response may be higher in the short term compared to the long term, as demonstrated by Hendricks et al. (2014) in their study of corn and soybean rotations in Iowa, Illinois, and Indiana at the field level. If the long-term elasticity of cropping choices decreases following the implementation of the canola subsidy over a prolonged period of time, the outcomes depicted in the simulation model could be inflated.

TABLE 3E.2: The Effects of Reduced Marginal Effects on the Results of the Simulation Model with respect to a Canola Subsidy

	(1)	(2)
Soil Zone:	*Brown*	
Acreage Response Scenario:	Base	30% Reduction
Optimal Canola Subsidy *(2023 CAD/ha/yr)*	324.40	324.40
Policy Induced Change in SOC *(kg/ha/yr)*	31.81	22.26
Net External Social Benefit *(millions of 2023 CAD)*	847	593
Soil Zone:	*Dark Brown*	
Acreage Response Scenario:	Base	30% Reduction
Optimal Canola Subsidy *(2023 CAD/ha/yr)*	205.43	205.43
Policy Induced Change in SOC *(kg/ha/yr)*	52.20	36.54
Net External Social Benefit *(millions of 2023 CAD)*	2,390	1,673
Soil Zone:	*Black & Gray*	
Acreage Response Scenario:	Base	30% Reduction
Optimal Canola Subsidy *(2023 CAD/ha/yr)*	226.02	226.02
Policy Induced Change in SOC *(kg/ha/yr)*	76.49	53.54
Net External Social Benefit *(millions of 2023 CAD)*	4,352	3,047

Source: Author's Estimates

Notes: The optimal subsidy, policy-induced change in hectares, external social benefits, and costs are calculated by maximizing the net external social benefit (NESB) as shown in equation (3.33). A 30% reduction is applied to all the marginal effects for that specific scenario.

To measure the effects of long term adjustments in cropping hectares, I lower all acreage response estimates (marginal effects estimated by the NL model) by 30%. Table 3E.2 shows that for each soil zone the downward scaling of all the acreage responses does not alter the optimal canola subsidies. However, this substantially reduces the NESB across all soil zones, such that the NESB is equal to 593 million CAD, 1,673 million CAD, and 3,047 million CAD in the brown, dark brown, and black & gray soil zones. This decrease in acreage responses leads to a reduction in the NESB, equal to -254 million CAD in the brown soil zone, -717 million CAD in the dark brown soil zone, and -1,305 million CAD in the black & gray soil zone.

The larger effect is anticipated in the black & gray soil zone, which has a higher proportion of canola planted compared to the brown and dark brown soil zones. This examination highlights the importance of crop supply dynamics, which may diminish the long-term acreage response to a subsidy and, consequently, the expected NESB from incentivizing farmers to incorporate more canola into their crop rotations. Therefore, the NESB figures derived from the simulation model should be viewed as optimistic estimates concerning long term acreage response.

In the simulation model, I consider the effects of reducing the time-horizon examined to subsidize farmers to seed additional hectares of canola. Contracts that pay producers to adopt a particular management practice provide payments for a specific number of years for when the practice is implemented. Table 3E.3 shows the effects on the optimal canola subsidy when only the external social benefit from carbon sequestration is valued for a definite time horizon, specifically 10, 20, and 30 years. In Table 3E.3, the optimal canola subsidy maximizes the NESB or change in welfare where the external social benefit is calculated using a rental rate for carbon computed with the SCC of 185 USD/Mg of CO_2.

TABLE 3E.3: Optimal Canola Subsidy with respect to the Time Horizon of the Simulation Model by Soil Zone in Saskatchewan

	(1)	(2)	(3)	(4)	(5)	(6)
	Optimal Canola Subsidy:					
Soil Zone:	Brown		Dark Brown		Black & Gray	
Objective Function	*NESB*	ΔW	*NESB*	ΔW	*NESB*	ΔW
	(2023 CAD/ha/yr)					
10 Years	76.05	152.10	48.16	96.32	52.99	105.98
20 Years	140.27	280.54	88.83	177.65	97.73	195.46
30 Years	199.86	399.73	126.56	253.13	139.25	278.51

Source: Author's Estimates

Notes: *NESB* represents the net external social benefit and ΔW represents the change in welfare. All simulation scenarios employ an annual rental rate of carbon based on a social cost of carbon of 185 USD/Mg of CO_2 and employ marginal effects from the nested logit model to compute the optimal canola subsidy for each objective function (net external social benefit and change in welfare). Please refer to Tables 3.6 and 3.7 for more information.

Table 3E.3 shows that shortening the time horizon reduces the optimal canola subsidy. This is due to the fact that the external social benefit is lower if sequestered SOC is valued for a shorter time period, and less SOC is sequestered for years prior to the steady state equilibrium in SOC stocks. When examining the optimal canola subsidies that maximize the NESB for a 20 year time horizon, this results in an optimal subsidy equal to 140.25 CAD/ha/yr (42.36 USD/ac/yr) in the brown soil zone, 88.83 CAD/ha/yr (26.83 USD/ac/yr) in the dark brown soil zone, and 97.73 CAD/ha/yr (29.51 USD/ac/yr) in the black & gray soil zone.

Bibliography

Agri-Pulse Communications (2024). Beyond Cover Crops and Tillage: How Can We Really Calculate Farm Carbon Emissions? Webinar hosted by Agri-Pulse Communications. January. https://www.agri-pulse.com/media/videos/play/1050?utm_source=DTN+webinar+1%2F8%2F24+attendees&utm_campaign=9fc17caa72-EMAIL_CAMPAIGN_2017_02_23_COPY_01&utm_medium=email&utm_term=0_948412f46e-9fc17caa72-50940693.

Agriculture and Agri-Food Canada (2022). National Soil Database. Agriculture and Agri-Food Canada, Government of Canada. https://sis.agr.gc.ca/cansis/nsdb/index.html.

Agriculture and Agri-Food Canada (2023). Agricultural Climate Solutions – On-Farm Climate Action Fund. Government of Canada. https://agriculture.canada.ca/en/programs/agricultural-climate-solutions-farm-climate-action-fund.

Andrén, O. and T. Kätterer (1997). ICBM: the introductory carbon balance model for exploration of soil carbon balances. *Ecological Applications 7*(4), 1226–1236.

Antle, J. M. (1983). Sequential decision making in production models. *American Journal of Agricultural Economics 65*(2), 282–290.

Antle, J. M., S. M. Capalbo, S. Mooney, E. T. Elliott, and K. H. Paustian (2001). Economic analysis of agricultural soil carbon sequestration: an integrated assessment approach. *Journal of agricultural and resource economics*, 344–367.

Antle, J. M. and S. M. Ogle (2012). Influence of soil c, n2o and fuel use on ghg mitigation with no-till adoption. *Climatic Change 111*, 609–625.

Attia, A., N. Rajan, Q. Xue, S. Nair, A. Ibrahim, and D. Hays (2016). Application of DSSAT-CERES-Wheat model to simulate winter wheat response to irrigation management in the Texas High Plains. *Agricultural Water Management 165*, 50–60.

Australian Government (2022). Carbon Credits (Carbon Farming Initiative) Act 2011. Department of Industry, Science, Energy and Resources, Australian Government . `https://www.legislation.gov.au/Details/C2020C00281`.

Awada, L., R. S. Gray, and C. Nagy (2016). The benefits and costs of zero tillage RD&E on the Canadian prairies. *Canadian Journal of Agricultural Economics 64*(3), 417–438.

Bamière, L., P. Jayet, S. Kahindo, and E. Martin (2021). Carbon sequestration in french agricultural soils: A spatial economic evaluation. *Agricultural Economics 52*(2), 301–316.

Banger, K., E. Nafziger, J. Wang, and C. Pittelkow (2019). Modeling inorganic soil nitrogen status in maize agroecosystems. *Soil Science Society of America Journal 83*(5), 1564–1574.

Bangsund, D. A. and F. L. Leistritz (2008). Producer responses to carbon sequestration incentives in the northern great plains. *Great Plains Research*, 165–176.

Bank of Canada (2023a). Annual Average Exchange Rates. `https://www.bankofcanada.ca/rates/exchange/annual-average-exchange-rates/`.

Bank of Canada (2023b). Inlfation Calculator - Consumer Price Indexes for Canada, Monthly (V41690973 series). Statistics Canada. `https://www.bankofcanada.ca/rates/related/inflation-calculator/`.

Belcher, K. W., M. M. Boehm, and R. P. Zentner (2003). The economic value of soil quality under alternative management in the Canadian prairies. *Canadian Journal of Agricultural Economics 51*(2), 175–196.

Bellman, R. (1957). Dynamic Programming, Princeton, N.J.: Princeton University Press.

Berry, S. T. (1994). Estimating discrete-choice models of product differentiation. *The RAND Journal of Economics 25*(2), 242–262.

Bista, P., S. Machado, R. Ghimire, S. J. Del Grosso, and M. Reyes-Fox (2016). Simulating soil organic carbon in a wheat–fallow system using the DayCent model. *Agronomy Journal 108*(6), 2554–2565.

Blanc, É. (2017). Statistical emulators of maize, rice, soybean and wheat yields from global gridded crop models. *Agricultural and Forest Meteorology 236*, 145–161.

Bolinder, M. A. abd Janzen, H. H., E. G. Gregorich, D. A. Angers, and A. J. VandenBygaart (2007). An approach for estimating net primary productivity and annual carbon inputs to soil for common agricultural crops in Canada. *Agriculture, Ecosystems & Environment 118*(1-4), 29–42.

Bolinder, M. A., A. J. VangenBygaart, E. G. Gregorich, D. A. Angers, and H. H. Janzen (2006). Modelling soil organic carbon stock change for estimating whole-farm greenhouse gas emissions. *Canadian Journal of Soil Science 86*(3), 419–429.

Brierley, J. A., H. B. Stonehouse, and R. Mermut (2011). Vertisolic soils of Canada: Genesis, distribution, and classification. *Canadian Journal of Soil Science 91*(5), 903–916.

Cai, J., Y. Liu, T. Lei, and L. S. Pereira (2007). Estimating reference evapotranspiration with the FAO Penman–Monteith equation using daily weather forecast messages. *Agricultural and Forest Meteorology 145*(1-2), 22–35.

Campbell, C. A., H. H. Janzen, K. Paustian, E. G. Gregorich, L. Sherrod, B. C. Liang, and R. P. Zentner (2005). Carbon storage in soils of the North American Great Plains: Effect of cropping frequency. *Agronomy Journal 97*(2), 349–363.

Campbell, C. A., F. Selles, G. P. Lafond, and R. P. Zentner (2001). Adopting zero tillage management: Impact on soil C and N under long-term crop rotations in a thin Black Chernozem. *Canadian Journal of Soil Science 81*(2), 139–148.

Campbell, C. A., A. J. VandenBygaart, B. Grant, R. P. Zentner, B. G. McConkey, R. Lemke, E. G. Gregorich, and M. R. Fernandez (2007a). Quantifying carbon sequestration in a conventionally tilled crop rotation study in southwestern Saskatchewan. *Canadian Journal of Soil Science 87*(1), 23–38.

Campbell, C. A., A. J. VandenBygaart, R. P. Zentner, B. G. McConkey, W. Smith, R. Lemke, ..., and P. G. Jefferson (2007b). Quantifying carbon sequestration in a minimum tillage crop rotation study in semiarid southwestern Saskatchewan. *Canadian Journal of Soil Science 87*(3), 235–250.

Campbell, C. A., R. P. Zentner, B. C. Liang, G. Roloff, E. C. Gregorich, and B. Blomert (2000). Organic C accumulation in soil over 30 years in semiarid southwestern Saskatchewan - Effect of crop rotations and fertilizers. *Canadian Journal of Soil Science 80*(1), 179–192.

Carpentier, A. and E. Letort (2014). Multicrop production models with multinomial logit acreage shares. *Environmental and Resource Economics 59*, 537–559.

Chang, K. H., J. Warland, P. Voroney, P. Bartlett, and W.-R. C. (2013). Using DayCENT to simulate carbon dynamics in conventional and no-till agriculture. *Soil Science Society of America Journal 77*(3), 941–950.

Cobuloglu, H. I. and I. E. Büyüktahtakın (2017). A two-stage stochastic mixed-integer programming approach to the competition of biofuel and food production. *Computers & Industrial Engineering 107*, 251–263.

Coleman, K. and D. S. Jenkinson (1996). RothC-26.3-A Model for the turnover of carbon in soil. In Evaluation of soil organic matter models (pp. 237-246). Springer, Berlin, Heidelberg.

Congreves, K. A., B. B. Grant, S. W. N. Campbell, C. A., A. J. VandenBygaart, R. Kröbel, ..., and R. L. Desjardins (2015). Measuring and modeling the long-term impact of crop management on soil carbon sequestration in the semiarid Canadian prairies. *Agronomy Journal 107*(3), 1141–1154.

Croissant, Y. (2012). Estimation of multinomial logit models in R: The mlogit Packages. R package version 0.2-2. http://cran.r-project.org/web/packages/mlogit/vignettes/mlogit.pdf.

Deschênes, O. and M. Greenstone (2007). The economic impacts of climate change: evidence from agricultural output and random fluctuations in weather. *American Economic Review 97*(1), 354–385.

Deschênes, O. and C. Kolstad (2011). Economic impacts of climate change on California agriculture. *Climatic Change 109*(1), 365–386.

Diele, F., C. Marangi, and A. Martiradonna (2021). Non-Standard Discrete RothC Models for Soil Carbon Dynamics. *Axiomsl 10*(2), 56.

Eckstein, Z. (1984). A rational expectations model of agricultural supply. *Journal of Political Economy 92*(1), 1–19.

Ellert, B. H. and J. R. Bettany (1995). Calculation of organic matter and nutrients stored in soils under contrasting management regimes. *Canadian Journal of Soil Science 75*(4), 529–538.

Ellert, B. H., H. H. Janzen, B. G. McConkey, and R. Lal (1995). Measuring and comparing soil carbon storage. *Assessment Methods for Soil Carbon*, 131–146.

Ellis, J. (2021). Microsoft to Purchase up to \$2m in Carbon Credits from Land O'Lakes. AgFunderNews (AFN), February. https://agfundernews.com.

Environment and Climate Change Canada (2022). National Inventory Report 1990 – 2020: Greenhouse Gas Sources and Sinks in Canada. Canada's Submission to the United Nations Framework Convention on Climate Change. Part 2, Table A3.5-8. Government of Canada.

Environment and Climate Change Canada (2023a). 2030 Emissions Reduction Plan: Agriculture. Reported in the 2030 Emissions Reduction Plan – Sector-by-sector overview. Government of Canada. https://www.canada.ca/content/dam/eccc/documents/pdf/climate-change/erp/factsheet-07-agriculture.pdf.

Environment and Climate Change Canada (2023b). Historical Climate Data. Weather, Climate and Hazard, Environment and Natural Resources. Government of Canada. https://climate.weather.gc.ca/index_e.html.

Environment and Climate Change Canada (2024). Environment and Climate Change Canada funding programs. Government of Canada. https://www.canada.ca/en/environment-climate-change/services/environmental-funding.html.

Environmental Protection Agency (2016). The Social Cost of Carbon. In EPA Fact Sheet. United States Environmental Protection Agency. United States Environmental Protection Agency. https://19january2017snapshot.epa.gov/climatechange/social-cost-carbon_.html.

Falloon, P. D., P. Smith, J. U. Smith, J. Szabo, K. Coleman, and S. Marshall (1998). Regional estimates of carbon sequestration potential: linking the Rothamsted carbon model to GIS databases. *Biology and Fertility of Soils 27*(3), 236–241.

Fan, J., B. G. McConkey, H. Janzen, L. Townley-Smith, and H. Wang (2017). Harvest index–yield relationship for estimating crop residue in cold continental climates. *Field Crops Research 204*, 153–157.

Fan, J., B. G. McConkey, B. C. Liang, D. A. Angers, H. H. Janzen, R. Kröbel, ..., and W. N. Smith (2019). Increasing crop yields and root input make Canadian farmland a large carbon sink. *Geoderma 136*, 49–58.

Farina, R., R. Sándor, M. Abdalla, J. Álvaro-Fuentes, L. Bechini, M. A. Bolinder, ..., and G. Bellocchi (2021). Ensemble modelling, uncertainty and robust predictions of organic carbon in long-term bare-fallow soils. *Global Change Biology 27*(4), 904–928.

Fontaine, S., A. Mariotti, and L. Abbadie (2003). The priming effect of organic matter: a question of microbial competition? *Soil Biology and Biochemistry 35*(6), 837–843.

Food and Agricultural Organization (2020). Technical Specifications and Country Guidelines for Global Soil Organic Carbon Sequestration Potential Map. . https://www.fao.org/3/cb9002en/cb9002en.pdf.

Fortin, J. G., M. A. Bolinder, F. Anctil, T. Kätterer, O. Andrén, and L. E. Parent (2011). Effects of climatic data low-pass filtering on the ICBM temperature-and moisture-based soil biological activity factors in a cool and humid climate. *Ecological Modelling 222*(17), 3050–3060.

Gan, Y. T., C. A. Campbell, H. H. Janzen, R. L. Lemke, P. Basnyat, and C. L. McDonald (2009). Carbon input to soil from oilseed and pulse crops on the Canadian prairies. *Ecosystems & Environment 132*(3-4), 290–297.

Garnache, C., P. R. Mérel, J. Lee, and J. Six (2017). The social costs of second-best policies: Evidence from agricultural GHG mitigation. *Journal of Environmental Economics and Management 82*, 39–73.

Gaudaré, U., M. Kuhnert, P. Smith, M. Martin, P. Barbieri, S. Pellerin, and T. Nesme (2023). Soil organic carbon stocks potentially at risk of decline with organic farming expansion. *Nature Climate Change*, 1–7.

Gill, R. A., R. H. Kelly, W. J. Parton, K. A. Day, R. B. Jackson, J. A. Morgan, ..., and X. S. Zhang (2002). Using simple environmental variables to estimate below-ground productivity in grasslands. *Global Ecology and Biogeography 11*(1), 79–86.

Government of Saskatchewan (2017). Saskatchewan Ministry of Agriculture Land Lease Survey. A report prepared by Insightrix Research Incorporated and the Saskatchewan Ministry of Agriculture. January.

Government of Saskatchewan (2020). Comprehensive Natural-Air-Grain-Drying (NAD) Factsheet. Saskatchewan Agriculture, Government of Saskatchewan. `https://pubsaskdev.blob.core.windows.net/pubsask-prod/119546/NAD%252BFactsheet_FINAL_2020-08-24.pdf`.

Government of Saskatchewan (2022). Saskatchewan: A Global Leader in Agricultural Trade. Ministry of Agriculture, Government of Saskatchewan. . `https://pubsaskdev.blob.core.windows.net/pubsask-prod/110626/Endless%252BOpportunities%252B-%252BNovember%252B2022.pdf`.

Government of Saskatchewan (2023a). Crop Planning Guide and Crop Planner. Saskatchewan Agriculture, Government of Saskatchewan. `https://www.saskatchewan.ca/business/agriculture-natural-resources-and-industry/agribusiness-farmers-and-ranchers/farm-business-management/crop-planning-guide-and-crop-planner`.

Government of Saskatchewan (2023b). Soils, Fertilizer and Nutrients. Saskatchewan Agriculture, Government of Saskatchewan. `https://www.saskatchewan.ca/business/agriculture-natural-resources-and-industry/agribusiness-farmers-and-ranchers/crops-and-irrigation/soils-fertility-and-nutrients`.

Greenestone, M., E. Kopits, and A. Wolverton (2013). Developing a social cost of carbon for US regulatory analysis: A methodology and interpretation. Review of Environmental Economics

and Policy.

Guenet, B., B. Gabrielle, C. Chenu, D. Arrouays, J. Balesdent, M. Bernoux, E. Bruni, J. P. Caliman, R. Cardinael, S. Chen, ..., and F. Zhou (2021). Can n2o emissions offset the benefits from soil organic carbon storage? *Global Change Biology 27*(2), 237–256.

Gulati, S. and J. Vercammen (2005). The optimal length of an agricultural carbon contract. *Canadian Journal of Agricultural Economics 53*(4), 359–373.

He, W., B. B. Grant, Q. Jing, R. Lemke, M. S. Luce, R. Jiang, . . . , and W. N. Smith (2021). Measuring and modeling soil carbon sequestration under diverse cropping systems in the semiarid prairies of western Canada. *Journal of Cleaner Production 328*, 129614.

Hendricks, N. P., A. Smith, and D. A. Sumner (2014). Crop supply dynamics and the illusion of partial adjustment. *American Journal of Agricultural Economics 96*(5), 1469–1491.

Hoag, D. L. and H. A. Holloway (1991). Farm production decisions under cross and conservation compliance. *American Journal of Agricultural Economics 73*(1), 184–193.

Interagency Working Group on Social Cost of Greenhouse Gases (2021). Technical support document: social cost of carbon, methane, and nitrous oxide interim estimates under executive order 13990. Technical Report, White House. Interagency Working Group on Social Cost of Greenhouse Gases, United States Government. https://www.whitehouse.gov/wp-content/uploads/2021/02/TechnicalSupportDocument_SocialCostofCarbonMethaneNitrousOxide.pdf.

ISC (2022). SaskGrid Township Fabric Map. Land Titles Registry, Land Surveys Directory, Personal Property Registry and Corporate Registry. ISC, Saskatchewan. https://www.isc.ca/MapsandPhotos/GISData/Pages/SaskGridTownshipFabricMap.aspx.

Janzen, H. H., K. J. van Groenigen, D. S. Powlson, T. Schwinghamer, and J. W. van Groenigen (2022). Photosynthetic limits on carbon sequestration in croplands. *Geoderma 416*, 115810.

Johnston, A. M., H. R. Kutcher, and K. L. Bailey (2005). Impact of crop sequence decisions in the saskatchewan parkland. *Canadian Journal of Plant Science 85*(1), 95–102.

Juodis, A. and V. Sarafidis (2022). An incidental parameters free inference approach for panels with common shocks. *Journal of Econometrics 229*(1), 19–54.

Kane, D. A., M. A. Bradford, E. Fuller, E. E. Oldfield, and S. A. Wood (2021). Soil organic matter protects US maize yields and lowers crop insurance payouts under drought. *Environmental Research Letters 16*(4), 044018.

Kätterer, T. and O. Andrén (2001). The ICBM family of analytically solved models of soil carbon, nitrogen and microbial biomass dynamics—descriptions and application examples. *Ecological Modelling 136*(2-3), 191–207.

Koutchadé, O. P., A. Carpentier, and F. Femenia (2021). Modeling Corners, Kinks, and Jumps in Crop Acreage Choices: Impacts of the EU Support to Protein Crops. *American Journal of Agricultural Economics 103*(4), 1502–1524.

Kröbel, R., M. A. Bolinder, H. H. Janzen, S. M. Little, A. J. VandenBygaart, and T. Kätterer (2016). Canadian farm-level soil carbon change assessment by merging the greenhouse gas model Holos with the Introductory Carbon Balance Model (ICBM). *Agricultural Systems 143*, 76–85.

Lacroix, A. and A. Thomas (2011). Estimating the environmental impact of land and production decisions with multivariate selection rules and panel data. *American Journal of Agricultural Economics 93*(3), 784–802.

Lafond, G. P., R. Geremia, D. A. Derksen, and R. P. Zentner (1993). The effects of tillage systems on the economic performance of spring wheat, winter wheat, flax and field pea production in east-central Saskatchewan. *Canadian Journal of Plant Science 73*(1), 47–54.

Lafond, G. P., F. Walley, W. E. May, and C. B. Holzapfel (2011). Long term impact of no-till on soil properties and crop productivity on the Canadian prairies. *Soil and Tillage Research 117*, 110–123.

Lamb, A., R. Green, I. Bateman, M. Broadmeadow, T. Bruce, J. Burney, ..., and A. Balmford (2011). The potential for land sparing to offset greenhouse gas emissions from agriculture. *Nature Climate Change 6*(5), 488–492.

Lancaster, T. (2000). The incidental parameter problem since 1948. *Journal of Econometrics 95*(2), 391–413.

Le Noë, J., S. Manzoni, R. Abramoff, T. Bölscher, E. Bruni, R. Cardinael, P. Ciais, ..., and B. Guenet (2023). Soil organic carbon models need independent time-series validation for reliable prediction. *Communications Earth & Environment 4*, 158.

Lemke, R. L., A. J. VandenBygaart, C. A. Campbell, G. P. Lafond, and B. Grant (2010). Crop residue removal and fertilizer N: effects on soil organic carbon in a long-term crop rotation experiment on a Udic Boroll. *Agriculture, Ecosystems & Environment 135*(1-2), 42–51.

Lemma, B., S. Williams, and K. Paustian (2021). Long term soil carbon sequestration potential of smallholder croplands in southern Ethiopia with DAYCENT model. *Journal of Environmental Management 294*, 112893.

Liang, B. C., A. J. VandenBygaart, J. D. MacDonald, D. Cerkowniak, B. G. McConkey, R. L. Desjardins, and D. A. Angers (2020). Revisiting no-till's impact on soil organic carbon storage in Canada. *Soil and Tillage Research 198*, 104529.

Liu, J., R. L. Desjardins, S. Wang, D. E. Worth, B. Qian, and J. Shang (2022). Climate impact from agricultural management practices in the Canadian Prairies: Carbon equivalence due to albedo change. *Journal of Environmental Management 302*(A), 113938.

Luce, D. (1959). Individual Choice Behavior. John Wiley and Sons, New York.

Lychuk, T. E., A. P. Moulin, R. L. Lemke, R. C. Izaurralde, E. N. Johnson, O. O. Olfert, and S. A. Brandt (2019). Climate change, agricultural inputs, cropping diversity, and environment affect soil carbon and respiration: A case study in Saskatchewan. *Geoderma 337*, 664–678.

Maillard, É., B. G. McConkey, M. S. Luce, D. A. Angers, and J. Fan (2018). Crop rotation, tillage system, and precipitation regime effects on soil carbon stocks over 1 to 30 years in Saskatchewan. *Canada. Soil and Tillage Research 117*, 97–104.

Marchildon, G. P. abd Pittman, J. and D. J. Sauchyn (2009). The dry belt and changing aridity in the Palliser Triangle 1895–2000. *In Prairie Forum 34*(1), 31–44.

313

Marschak, J. (1960). Binary choice constraints on random utility indications. In K. Arrow, ed., Stanford Symposium on Mathematical Methods in the Social Sciences. Stanford University Press, Stanford, CA. pp. 312–329.

Martin, M. P., S. Cordier, J. Balesdent, and D. Arrouays (2009). Periodic solutions for soil carbon dynamics equilibriums with time-varying forcing variables. *Ecological modelling 204*(3-4), 523–530.

McCauley, D. J. (2021). Offsets, Insets, Carbon Markets: Incentivizing Farmers to Improve Soil Health, Sequester Carbon. *Crops & Soils 54*(5), 14–21.

McConkey, B., M. St. Luce, R. Hangs, J. Schoenau, A. Anderson, B. Grant, W. Smith, G. Padbury, K. Brandt, and D. Cerkowniak (2020). Prairie Soil Carbon Balance Project: Monitoring SOC Change Across Saskatchewan Farms from 1996 to 2018. Report prepared for the Saskatchewan Soil Conservation Association.

McConkey, B. G., B. C. Liang, C. A. Campbell, D. Curtin, A. Moulin, S. A. Brandt, and G. P. Lafond (2003). Crop rotation and tillage impact on carbon sequestration in Canadian prairie soils. *Soil and Tillage Research 74*(1), 81–90.

McFadden, D. (1974). McFadden, D. (1974), 'Conditional logit analysis of qualitative choice behavior', in P. Zarembka, ed., Frontiers in Econometrics, Academic Press, New York, pp. 105-142.

McFadden, D. (1978). Modeling the choice of residential location, in A. Karlqvist, L. Lundqvist, F. Snickars, and J. Weibull, eds., Spatial Interaction Theory and Planning Models, North-Holland, Amsterdam, pp. 75–96.

Mérel, P. and M. Gammans (2021). Climate Econometrics: Can the Panel Approach Account for Long-Run Adaptation? *American Journal of Agricultural Economics 103*(4), 1207–1238.

Mikhailova, E. A., G. R. Groshans, C. J. Post, M. A. Schlautman, and G. C. Post (2019). Valuation of soil organic carbon stocks in the contiguous United States based on the avoided social cost of carbon emissions. *Resources 8*(3), 153.

Minasny, B., B. P. Malone, A. B. McBratney, D. A. Angers, D. Arrouays, A. Chambers, ..., and L. Winowiecki (2017). Soil carbon 4 per mille. *Geoderma 292*, 59–86.

Mishra, S. K., S. Gautam, U. Mishra, and C. D. Scown (2021). Performance-based payments for soil carbon sequestration can enable a low-carbon bioeconomy. *Environmental science & technology 55*(8), 5180–5188.

Mooney, S., J. Antle, S. Capalbo, and K. Paustian (2004a). Design and costs of a measurement protocol for trades in soil carbon credits. *Canadian Journal of Agricultural Economics 52*(3), 257–287.

Mooney, S., J. Antle, S. Capalbo, and K. Paustian (2004b). Influence of project scale and carbon variability on the costs of measuring soil carbon credits. *Environmental Management 33*, S252–S263.

Mooney, S., K. Gerow, J. Antle, S. Capalbo, and K. Paustian (2007). Reducing standard errors by incorporating spatial autocorrelation into a measurement scheme for soil carbon credits. *Climatic Change 80*, 55–72.

Moreno, G. and D. L. Sunding (2005). Joint estimation of technology adoption and land allocation with implications for the design of conservation policy. *American Journal of Agricultural Economics 87*(4), 1009–1019.

Necpálová, M., R. P. Anex, M. N. Fienen, S. J. Del Grosso, M. J. Castellano, J. E. Sawyer, ..., and D. W. Barker (2015). Understanding the DayCent model: Calibration, sensitivity, and identifiability through inverse modeling. *Environmental Modelling & Software 66*, 110–130.

Nickell, S. (1981). Biases in dynamic models with fixed effects. *Econometrica: Journal of the Econometric Society*, 1417–1426.

Oldfield, E. E., M. A. Bradford, and S. Wood (2019). Global meta-analysis of the relationship between soil organic matter and crop yields. *Soil 5*(1), 15–32.

Oldfield, E. E., A. J. Eagle, R. L. Rubin, J. Rudek, J. Sanderman, and D. R. Gordon (2022). Crediting agricultural soil carbon sequestration. *Science 375*(6586), 1222–1225.

Onukwugha, E., J. Bergtold, and R. Jain (2015). A primer on marginal effects—Part I: Theory and formulae. *PharmacoEconomics 33*, 25–30.

Parshotam, A. (1996). The Rothamsted soil-carbon turnover model—discrete to continuous form. *Ecological Modelling 86*(2-3), 283–289.

Parshotam, A. (2001). Inert Organic Matter (IOM) in the Rothamsted Soil-Carbon Turnover Model: Analytical Solutions. In Conference: MODSIM01. International Congress of Modelling and Simulation (pp. 1079-1084).

Paudel, K. P., M. Pandit, and M. A. Dunn (2013). Using spectral analysis and multinomial logit regression to explain households' choice patterns. *Empirical Economics 44*, 739–760.

Paustian, K., S. Collier, J. Baldock, R. Burgess, J. Creque, M. DeLonge, ..., and M. Jahn (2019). Quantifying carbon for agricultural soil management: from the current status toward a global soil information system. *Carbon Management 10*(6), 567–587.

Paustian, K., J. Lehmann, S. Ogle, D. Reay, G. P. Robertson, and P. Smith (2016). Climate-smart soils. *Nature 532*(7597), 49–57.

Pearce, D. (2003). The social cost of carbon and its policy implications. *Oxford Review of Economic Policy 19*(3), 362–384.

Perry, G. M., B. A. McCarl, M. E. Rister, and J. W. Richardson (1989). Modeling government program participation decisions at the farm level. *American Journal of Agricultural Economics 71*(4), 1011–1020.

Peters, A. (2023). Estimating Time Preferences with Structure: Crop Rotations in Agriculture. Vancouver School of Economics, University of British Columbia. *Working Paper*. `https://alpeters.github.io/assets/pdf/Peters_Estimating_Time_Preferences_with_Structure-WP.pdf`.

Pigou, A. C. (1920). The Economics of Welfare. London: Macmillan, 1924.

Pindyck, R. S. (2014). Risk and return in the design of environmental policy. *Journal of the Association of Environmental and Resource Economists 1*(3), 395–418.

Poeplau, C., T. Kätterer, M. A. Bolinder, G. Börjesson, A. Berti, and E. Lugato (2015). Low stabilization of aboveground crop residue carbon in sandy soils of Swedish long-term experiments. *Geoderma 237*, 246–255.

Porker, K., M. Straight, and J. R. Hunt (2020). Evaluation of G×E×M interactions to increase harvest index and yield of early sown wheat. *Frontiers in Plant Science 11*(994).

Raina, N., M. Zavalloni, and D. Viaggi (2024). Incentive mechanisms of carbon farming contracts: A systematic mapping study. *Journal of Environmental Management 352*, 120126.

Rennert, K., F. Errickson, B. C. Prest, L. Rennels, R. G. Newell, W. Pizer, ..., and D. Anthoff (2022). Comprehensive evidence implies a higher social cost of CO2. *Nature 610*(7933), 687–692.

Riggers, C., C. Poeplau, A. Don, C. Bamminger, H. Höper, and R. Dechow (2019). Multi-model ensemble improved the prediction of trends in soil organic carbon stocks in German croplands. *Geoderma 345*, 17–30.

Rochette, P., C. Liang, D. Pelster, O. Bergeron, R. Lemke, R. Kroebel, D. MacDonald, W. Yan, and C. Flemming (2018). Soil nitrous oxide emissions from agricultural soils in canada: Exploring relationships with soil, crop and climatic variables. *Agriculture, Ecosystems & Environment 254*, 69–81.

Rovira, P., T. Sauras-Yera, and J. Romanyá (2022). Equivalent-mass versus fixed-depth as criteria for quantifying soil carbon sequestration: How relevant is the difference? *Catena 214*, 106283.

Rubio, V., R. Diaz-Rossello, J. A. Quincke, and H. M. van Es (2021). Quantifying soil organic carbon's critical role in cereal productivity losses under annualized crop rotations. *Agriculture, Ecosystems & Environment 321*, 107607.

Russell, A. R., G. C. van Kooten, J. G. Izett, and M. E. Eisweth (2022). Damage functions and the social cost of carbon: addressing uncertainty in estimating the economic consequences of mitigating climate change. *Environmental Management 69*(5), 919–936.

Schaefer, A. K., R. J. Myers, S. R. Johnson, M. D. Helmar, and T. Radich (2021). How have oilseed relative price relationships changed over time? *AgBioForum 23*(1), 72–83.

Schlenker, W. and M. J. Roberts (2009). Nonlinear temperature effects indicate severe damages to US crop yields under climate change. *Proceedings of the National Academy of Sciences 106*(37), 15594–15598.

Seo, S. N. and R. Mendelsohn (2009). An analysis of crop choice: Adapting to climate change in South American farms. *Ecological Economics 67*(1), 109–116.

Serfas, D. A. (2024a). A New Field-Level Measure of the Stock of Soil Organic Carbon and Value of Carbon Sequestration. University of California, Davis, Department of Agricultural and Resource Economics. *Working Paper*.

Serfas, D. A. (2024b). The Consequences of Soil Organic Carbon for Crop Yield, Farm Productivity, and Profit. University of California, Davis, Department of Agricultural and Resource Economics. *Working Paper*.

Smith, J. O., P. Smith, M. Wattenbach, M. Zaehle, R. Hiederer, R. J. Jones, ..., and F. Ewert (2005). Projected changes in mineral soil carbon of European croplands and grasslands, 1990–2080. *Global Change Biology 11*(12), 2141–2152.

Smith, W. N., B. B. Grant, C. A. Campbell, B. G. McConkey, R. L. Desjardins, R. Kröbel, and S. S. Malhi (2012). Crop residue removal effects on soil carbon: Measured and inter-model comparisons. *Agriculture, Ecosystems & Environment 161*, 27–38.

Sothe, C., A. Gonsamo, J. Arabian, W. A. Kurz, S. A. Finkelstein, and J. Snider (2022). Large soil carbon storage in terrestrial ecosystems of Canada. *Global Biogeochemical Cycles 36*(3), e2021GB007213.

St. Luce, M., N. Ziadi, and R. A. V. Rossel (2022). A new approach for local predictions of soil organic carbon content using large soil spectral libraries. *Geoderma 425*, 116048.

Statistics Canada (2021). Estimated areas, yield, production, average farm price and total farm value of principal field crops, in metric and imperial units (Table 32-10-0359-01). Statistics

Canada. Government of Canada. `https://www150.statcan.gc.ca/t1/tbl1/en/tv.action?pid=3210035901`.

Statistics Canada (2022). Estimated areas, yield, production, average farm price and total farm value of principal field crops, in metric and imperial units (Table 32-10-0359-01). Statistics Canada. Government of Canada. `https://www150.statcan.gc.ca/t1/tbl1/en/tv.action?pid=3210035901`.

Stockey, N. and R. Lucas (1989). Recursive Methods in Economic Dynamics, Cambridge, Mass.: Harvard University Press.

Taneja, P., H. B. Vasava, S. Fathololoumi, P. Daggupati, and A. Biswas (2022). Predicting soil organic matter and soil moisture content from digital camera images: comparison of regression and machine learning approaches. *Canadian Journal of Soil Science 102*(3), 767–784.

Thiagarajan, A., J. Fan, B. G. McConkey, H. H. Janzen, , and C. A. Campbel (2018). Dry matter partitioning and residue N content for 11 major field crops in Canada adjusted for rooting depth and yield. *Canadian Journal of Soil Science 98*(3), 574–579.

Thiagarajan, A., C. Liang, J. D. MacDonald, W. Smith, A. J. VandenBygaart, B. Grant, ..., and F. J. (2022). Prospects and challenges in the use of models to estimate the influence of crop residue input on soil organic carbon in long-term experiments in Canada. *Geoderma Regional 30*, e00534.

Thornthwaite, C. W. and J. R. Mather (1955). The Water Balance. Publications in Climatology, Vol 8, No. 1, Centerton, N.J., Laboratory of Climatology.

Train, K. E. (2009). Discrete choice methods with simulation. Cambridge University Press.

Tukey, J. W. (1970). Exploratory Data Analysis. Vol. 3. Limited Preliminary Edition. Reading: Addison-Wesley.

United States Department of Agriculture (2023). Biden-Harris Administration Announces Availability of Inflation Reduction Act Funding for Climate-Smart Agriculture Nationwide. United States Department of Agriculture. `https://www.usda.gov/media/press-releases/2023/02/`

13/biden-harris-administration-announces-availability-inflation#:~:text=The%20I
nflation%20Reduction%20Act%20(IRA,Conservation%20Service%20(NRCS)%20implements.

University of Saskatchewan (2023). Saskatchewan Soil Information System. University of Saskatchewan. https://www.sksis.ca/map.

U.S. Bureau of Economic Analysis (2024). Gross Domestic Product: Implicit Price Deflator [GDPDEF], retrieved from FRED, Federal Reserve Bank of St. Louis. February 2. https://fred.stlouisfed.org/series/GDPDEF.

VandenBygaart, A. J., E. G. Gregorich, and D. A. Angers (2003). Influence of agricultural management on soil organic carbon: A compendium and assessment of Canadian studies. *Canadian Journal of Soil Science 83*(4), 363–380.

VandenBygaart, A. J., B. G. McConkey, D. A. Angers, W. Smith, H. De Gooijer, M. Bentham, and T. Martin (2008). Soil carbon change factors for the Canadian agriculture national greenhouse gas inventory. *Canadian Journal of Soil Science 88*(5), 671–680.

Voroney, R. P., E. A. Paul, and A. D. W. (1989). Decomposition of wheat straw and stabilization of microbial products. *Canadian Journal of Soil Science 69*(1), 63–77.

Weersink, A., N. Bannon, J. Riddle, and M. Turland (2019). Canada's Supply of Agricultural Land. Working Paper Series, Institute for the Advanced Study of Food and Agriculture Policy. Department of Food, Agricultural and Resource Economics (FARE), Ontario Agricultural College, University of Guelph.

Weersink, A., J. Livernois, J. F. Shogren, and S. J. S. (1998). Economic instruments and environmental policy in agriculture. *Canadian Public Policy 24*(3), 309–327.

Weihermüller, L., A. Graf, M. Herbst, and H. Vereecken (2013). Simple pedotransfer functions to initialize reactive carbon pools of the RothC model. *European Journal of Soil Science 64*(5), 567–575.

White, A. C., H. M. Darby, B. T. Dube, B. Sands, J. W. Faulkner, M. Albers, and M. Payne (2021). Measuring ecosystem services from soil health. Vermont Payment for Ecosystem Services Technical Research Report #1.

Willmott, C. J. (1981). On the validation of models. *Physical Geography* 2(2), 181–194.

Willmott, C. J., C. M. Rowe, and Y. Mintz (1985). Climatology of the terrestrial seasonal water cycle. *Journal of Climatology* 5(6), 589–606.

Wongpiyabovorn, O. and A. Plastina (2023). Financial Support for Conservation Practices: EQIP and CSP. Extensions and Outreach, Iowa State University. July. `https://www.extension.iastate.edu/agdm/crops/pdf/a1-39.pdf`.

Wongpiyabovorn, O., A. Plastina, and J. Crespi (2024). Challenges to voluntary ag carbon markets. *Applied Economic Perspectives and Policy* 45(2), 1154–1167.

Woodruff, C. M. (1950). Estimating the nitrogen delivery of soil from the organic matter determination as reflected by Sanborn Field. *Proceedings. Soil Science Society of America 14*, 208–212.

Wu, Q. and K. Congreves (2021). A soil health scoring framework for arable cropping systems in Saskatchewan, Canada. *Canadian Journal of Soil Science* 102(2), 341–358.

Zentner, R. P., J. Stephenson, C. A. Campbell, K. Bowren, A. Moulin, and L. Townley-Smith (1990). Effects of rotation and fertilization on economics of crop production in the Black soil zone of north-central Saskatchewan. *Canadian Journal of Plant Science* 70(3), 837–851.

Zhang, X., S. Lu, C. Wang, A. Zhang, and X. Wang (2021). Optimization of tillage rotation and fertilization increased the soil organic carbon pool and crop yield in a semiarid regio. *Land Degradation & Development* 32(18), 5241–5252.

Zhongming, Z., L. Linong, Y. Xiaona, Z. Wangqiang, and L. Wei (2019). 2019 Refinement to the 2006 IPCC Guidelines for National Greenhouse Gas Inventories. `https://www.ipcc-nggip.iges.or.jp/public/2019rf/pdf/4_Volume4/19R_V4_Ch05_Cropland.pdf`.